University of Kent

# Kent Academic Repository

**Tarrant, Daniel.S.J (2015) *Investigating the effects of increased levels of the translation elongation factor eEF1A within eukaryotic cells.* Doctor of Philosophy (PhD) thesis, University of Kent,.**

## Downloaded from

https://kar.kent.ac.uk/48089/ The University of Kent's Academic Repository KAR

## The version of record is available from

## This document version

UNSPECIFIED

## DOI for this version

## Licence for this version

UNSPECIFIED

## Additional information

## Versions of research works

### Versions of Record

If this version is the version of record, it is the same as the published version available on the publisher's web site. Cite as the published version.

### Author Accepted Manuscripts

If this document is identified as the Author Accepted Manuscript it is the version after peer review but before type setting, copy editing or publisher branding. Cite as Surname, Initial. (Year) 'Title of article'. To be published in *Title of Journal* , Volume and issue numbers [peer-reviewed accepted version]. Available at: DOI or URL (Accessed: date).

## Enquiries

If you have questions about this document contact ResearchSupport@kent.ac.uk. Please include the URL of the record in KAR. If you believe that your, or a third party's rights have been compromised through this document please see our Take Down policy (available from https://www.kent.ac.uk/guides/kar-the-kent-academic-repository#policies).

# Investigating the effects of increased levels of the translation elongation factor eEF1A within eukaryotic cells

Daniel.S.J.Tarrant

A thesis submitted to the University of Kent for the degree of PhD in Cellular Biology

**Declaration**

No part of this thesis has been submitted in support of any other application for a degree or qualification of the University of Kent or any other University or institution of learning. Furthermore, all work contained within this thesis is based on my own research conducted over the period of my PhD.

Daniel Tarrant

September 2014

**Acknowledgements**

First I would like to thank my supervisors Dr. Campbell Gourlay and Dr. Tobias von der Haar for opening my eyes to the world of academic research. For all their support and guidance during this study, and for giving me the opportunity to carry out the research detailed in this thesis.

I would like to thank everyone in the Kent Fungal Group. You have made the last four years an enjoyable experience, and I have cherished your friendship and support. Also thank you for the highly entertaining conversations at tea time.

Thank you to all my family and friends. To Rachael Hutton, for the regular drinking sessions during the writing of this thesis, allowing me to briefly forget the task awaiting me at home. Thank you to my siblings Hannah, Amy, Ben, Thomas and Henry you have all had your own positive effects on my life, but there are just too many of you to thank individually. Thank you to my parents Amanda and Stephen Tarrant for the love and support that you have given me throughout my life, for always being proud of my achievements and for allowing me to grow into the person I am today.

Finally, but by no means least, thank you to Annabel, your support throughout the past four years, and particularly the last few months of this PhD have proved vital. Thank you for *mostly* knowing what to say, and when to say it, and for tolerating my seemingly bi-polar moods during writing. Thank you to my son Oliver for making me realise that sleep is a luxury and without it we can achieve much more with our day, and thank you to my daughter, Erin, whose imminent arrival gave me the motivation to get this thesis written as quickly as possible.

## Contents

## ***Abbreviations***

| | |
|---|---|
| **aa-tRNA** | Aminoacyl transfer RNA |
| **ADP** | Adenosine diphosphate |
| **ATP** | Adenosine triphosphate |
| **CAP-Gly** | Cytoskelton-associated protein Glycine-rich domain |
| **CI** | Cell index |
| **CMV** | Cytomegalovirus |
| **DSS** | 4,4-dimethyl-4-silapentant-1-sufonic acid |
| **ECL** | Enhanced chemiluminescence |
| **eEF** | Eukaryotic elongation factor |
| **EF-Tu** | Bacterial elongation factor 1 |
| **eIF** | Eukaryotic initiation factor |
| **eRF** | Eukaryotic release factor |
| **FACS** | Fluorescence-activated cell sorting |
| **FRT** | Flippase recognition target |
| **GDP** | Guanosine diphosphate |
| **GFP** | Green fluorescent protein |
| **GO** | Gene ontology |
| **GTP** | Guanosine Triphosphate |
| **HEK293** | Human embryonic kidney cells |
| **kDa** | Kilo Dalton |
| **mRNA** | Messenger RNA |
| **NMR** | Nuclear magnetic resonance |
| **NUSE** | Normalised unscaled standard error |
| **$OD_{600}$** | Optical density measured at 600 nm |
| **PABP1** | Poly A binding protein |
| **PCR** | Polymerase chain reaction |
| **PIC** | Preinitiation complex |
| **RFP** | Red fluorescent protein |
| **RLE** | Relative log expression |
| **RMA** | Robust multi-array average |
| **TEF** | Translation elongation factor |
| **TF** | Transcription factor |
| **TOR** | Target of rapamycin |
| **tRNA** | Transfer RNA |
| **VHL** | Von Hippel-Lindau |

## ***Abstract***

The highly conserved eukaryotic elongation factor 1A (eEF1A) plays a canonical role in translation elongation, where it is responsible for delivering the aminoacylated tRNA to the A-site of the 80S ribosome. Further to this essential role it is reported to be involved in a plethora of moonlighting functions that are not fully characterised or understood. One of the human isoforms, eEF1A2, is known to induce cancer when expressed in non-native tissues, although the mechanism by which it promotes tumour growth is not yet known.

In this study we have characterised eEF1A overexpression in yeast and provided evidence to suggest that elevated levels of eEF1A result spindle defects which lead to chromosomal abnormalities that have the potential to induce uncontrolled cell growth in human cells. Moreover, we have confirmed conservation of this chromosomal abnormality in human cell lines suggesting that the mechanism that eEF1A utilises to induce these effects are highly conserved. We have also observed that in yeast, eEF1A overexpression results in increased metabolic activity, a hallmark of cancer cells.

We hypothesise that eEF1A interacts with the dynactin complex, a regulator of spindle dynamics, resulting in aberrant spindle formation. This in turn leads to chromosomal abnormalities that appear toxic to the cell. Cells appear to overcome the toxicity induced by eEF1A by suppressing plasmid copy number to the lowest levels possible. This however, brings its own problems and appears to result in synthetic effects together with eEF1A overexpression.

“Science, my lad, is made up of mistakes, but they are mistakes which it is useful to make, because they lead little by little to the truth.”

*-Jules Verne, A Journey to the Centre of the Earth*


A word cloud in the shape of yeast eEF1A generated from the contents of this thesis

# Chapter 1: Introduction

## 1.1 Translation in eukaryotes

The process of protein synthesis, translation, is a highly conserved mechanism throughout the living world.

Following gene transcription, the mRNA exits the nucleus to undergo translation in the cytoplasm. The primary translation complex is the eukaryotic 80S ribosome. The 80S ribosome consists of two subunits, the large 60S and the small 40S. Translation can be divided into four stages; initiation, elongation, termination and recycling. Beginning with initiation, the 80S ribosome along with a methionyl $tRNA_i$ bound in its petidyl (P) site is assembled at the AUG start codon of the mRNA. During elongation, the aminoacyl tRNAs enter the acceptor (A) site allowing decoding to take place. Cognate tRNAs form a peptide bond whilst non-cognate tRNAs are ejected from the ribosome. Following translocation of the tRNA to the P site, and shifting of the mRNA codons, the process is repeated. Termination occurs when a stop codon is encountered resulting in the completed peptide being released from the ribosome. The final stage is recycling, this is when the ribosomal subunits dissociate, resulting in the release of the mRNA and the deacylated tRNA ready for another further rounds of the process.

### *1.1.1 Translation Initiation*

The majority of the mRNAs in the cell undergo translation in a cap-dependent manner. The process of translating an mRNA transcript in this manner begins with the initiation step of translation.

A pool of small 40S subunits associate with eIF3, and bind to the ternary complex (eIF2·GTP·Met-tRNAi) resulting in the 43S pre-initiation complex (PIC). eIF4F binds at the 5'-cap of the mRNA and ATP-dependent activation of the mRNA allows for loading on to the 43S

PIC. The 43S PIC then scans the mRNA in a 5' to 3' direction until it reaches the initiation codon. Once the start codon is positioned in the P site the ternary complex is hydrolysed resulting in the release of the initiation factors facilitating binding of the 60s ribosomal subunit.

### *1.1.2 Translation elongation*

Translation elongation (see Figure 1.1) is a highly conserved stage of translation across all three domains of life, eukaryotes, bacteria and archaea, making it an excellent process to understand using model systems.

Peptide chain elongation starts upon translocation of the $tRNA_i$ to the P site leaving the A site vacant. A ternary complex consisting of eEF1A, GTP and an aminoacyl tRNA (aa-tRNA), delivers the aa-tRNA to the A site, where, if cognate, enters the next step of elongation. The interaction between the mRNA and cognate tRNA in the A site induces a conformational change of the 40s ribosomal subunit allowing for interrogation between cognate and near cognate pairs. This activity in turn activates eEF1A's GTPase activity, resulting in the liberation of the aminoacyl tRNA from eEF1A·GDP to the A site to continue its peptide bond formation.

The peptide bond between the incoming amino acid and the peptidyl tRNA is then catalysed by the ribosomal peptidyl transfer centre (Moore and Steitz, 2003), resulting in both the deacylated tRNA and the peptidyl-tRNA being in hybrid states, spanning multiple sites across both the large and small ribosomal subunits (Green and Noller, 1997). Eukaryotic elongation factor 2 (eEF2) facilitates complete movement of the deacylated tRNA to the E site, translocation of the peptidyl tRNA to the P site and movement of the mRNA by three nucleotides thus placing the next codon in the A site, hydrolysing GTP in the process

(Wintermeyer et al., 2001). This process is repeated until a stop codon is encountered at which point termination commences.

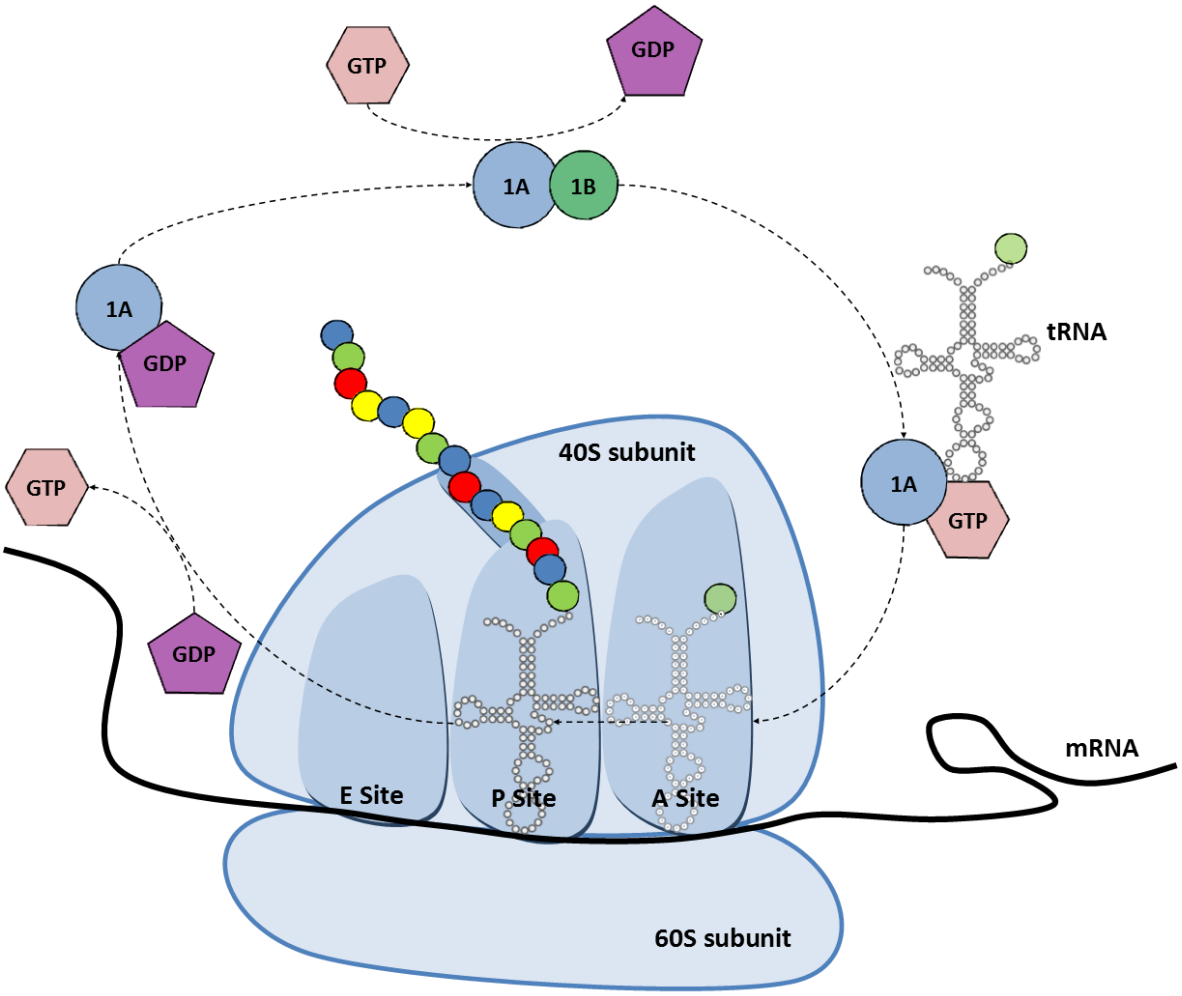


***Figure 1.1 A schematic view of translation elongation in yeast.*** *A cyclical view of the elongation step, showing entry, and translocation of the tRNA in the ribosome. Also illustrated is the cycling of the active and inactive eEF1A whose activation state is dependent on GDP exchange catalysed by the eEF1B complex.*

## *1.1.3 Translation termination*

Upon recognition of a stop codon in the ribosomal A-site, formation of a quaternary complex comprising of the ribosome, release factors 1 (eRF1) and 3 (eRF3),and GTP, triggers peptidyl-tRNA hydrolysis releasing the nascent peptide (Drugeon *et al.*, 1997).

## 1.2 Eukaryotic elongation factor 1A

The highly characterised eukaryotic translation elongation factor 1A (eEF1A), previously known as eEF-1α (Thornton *et al.*, 2003), is one of the most abundant cytoplasmic proteins in the cell, accounting for between 3 and 10% of all soluble protein (Merrick, 1992). It is encoded for by highly conserved genes resulting in near identical proteins across all three domains of life. It is a 50 kDa G-protein whose canonical role is in the delivery of aminoacylated tRNA to the A site of the ribosome during translation elongation. However, further roles have been well characterised for this moonlighting protein, from actin bundling and nuclear export, to induction of tumour growth (Grosshans *et al.*, 2000; Munshi *et al.*, 2001; Thornton *et al.*, 2003).

### *1.2.1 Genes encoding eEF1A*

eEF1A is encoded by highly conserved genes from prokaryotes to eukaryotes, with many species possessing two or more genes encoding identical or similar proteins. *Escherichia coli* has two genes encoding the eEF1A equivalent EF-Tu (Jaskunas *et al.*, 1975), the yeasts *Saccharomyces cerevisiae* and *Candida albicans* both possess two genes *Tef1* and *TEF2* (Schirmaier and Philippsen, 1984; Sundstrom *et al.*, 1990), and *Schizosaccharomyces pombe* is known to have three genes *Tef101*, *Tef102* and *Tef103* (Mita *et al.*, 1997). In mammals there are two actively transcribed genes *eEF1A1* and *eEF1A2* which share a 75% similarity in coding regions (see figure 1.2).

```
eEF1A1-H.sapiens      ATGGGAAAGGAAAAGACTCATATCAACATTGTCGTCATTGGACACGTAGATTCGGGCAAG 60
eEF1A2-H.sapiens      ATGGGCAAGGAGAAGACCCACATCAACATCGTGGTCATCGGCCACGTGGACTCCGGAAAG 60
Tef1                  ATGGGTAAAGAGAAGTCTCACATTAACGTTGTCGTTATCGGTCATGTCGATTCTGGTAAG 60
TEF2                  ATGGGTAAAGAGAAGTCTCACATTAACGTTGTCGTTATCGGTCATGTCGATTCTGGTAAG 60
                      ***** ** ** *** * ** ** *** * ** ** ** ** ** ** ** ** ** ***

eEF1A1-H.sapiens      TCCACCACTACTGGCCATCTGATCTATAAATGCGGTGGCATCGACAAAAGAACCATTGAA 120
eEF1A2-H.sapiens      TCCACCACCACGGGCCACCTCATCTACAAATGCGGAGGTATTGACAAAAGGACCATTGAG 120
Tef1                  TCTACCACTACCGGTCATTTGATTTACAAGTGTGGTGGTATTGACAAGAGAACCATCGAA 120
TEF2                  TCTACCACTACCGGTCATTTGATTTACAAGTGTGGTGGTATTGACAAGAGAACCATCGAA 120
                      ** ***** ** ** **  * ** ** ** ** ** ** ** ***** ** ***** **

eEF1A1-H.sapiens      AAATTTGAGAAGGAGGCTGCTGAGATGGGAAAGGGCTCCTTCAAGTATGCCTGGGTCTTG 180
eEF1A2-H.sapiens      AAGTTCGAGAAGGAGGCGGCTGAGATGGGGAAGGGATCCTTCAAGTATGCCTGGGTGCTG 180
Tef1                  AAGTTCGAAAAGGAAGCCGCTGAATTAGGTAAGGGTTCTTTCAAGTACGCTTGGGTTTTG 180
TEF2                  AAGTTCGAAAAGGAAGCCGCTGAATTAGGTAAGGGTTCTTTCAAGTACGCTTGGGTTTTG 180
                      ** ** ** ***** ** *****  * ** ***** ** ******** ** *****  **

eEF1A1-H.sapiens      GATAAACTGAAAGCTGAGCGTGAACGTGGTATCACCATTGATATCTCCTTGTGGAAATTT 240
eEF1A2-H.sapiens      GACAAGCTGAAGGCGGAGCGTGAGCGCGGCATCACCATCGACATCTCCCTCTGGAAGTTC 240
Tef1                  GACAAGTTAAAGGCTGAAAGAGAAAGAGGTATCACTATCGATATTGCTTTGTGGAAGTTC 240
TEF2                  GACAAGTTAAAGGCTGAAAGAGAAAGAGGTATCACTATCGATATTGCTTTGTGGAAGTTC 240
                      ** **  * ** ** **  * **  * ** ***** ** ** **  *  * ***** **

eEF1A1-H.sapiens      GAGACCAGCAAGTACTATGTGACTATCATTGATGCCCCAGGACACAGAGACTTTATCAAA 300
eEF1A2-H.sapiens      GAGACCACCAAGTACTACATCACCATCATCGATGCCCCCGGCCACCGCGACTTCATCAAG 300
TEF1                  GAAACTCCAAAGTACCAAGTTACCGTTATTGATGCTCCAGGTCACAGAGATTTCATCAAG 300
TEF2                  GAAACTCCAAAGTACCAAGTTACCGTTATTGATGCTCCAGGTCACAGAGATTTCATCAAG 300
                      ** **    ****** *  * **  * ** ***** ** ** *** * ** ** *****

eEF1A1-H.sapiens      AACATGATTACAGGGACATCTCAGGCTGACTGTGCTGTCCTGATTGTTGCTGCTGGTGTT 360
eEF1A2-H.sapiens      AACATGATCACGGGTACATCCCAGGCGGACTGCGCAGTGCTGATCGTGGCGGCGGGCGTG 360
TEF1                  AACATGATTACTGGTACTTCTCAAGCTGACTGTGCTATCTTGATTATTGCTGGTGGTGTC 360
TEF2                  AACATGATTACTGGTACTTCTCAAGCTGACTGTGCTATCTTGATTATTGCTGGTGGTGTC 360
                      ******** ** ** ** ** ** ** ***** **  *  ****  * ** *  ** **

eEF1A1-H.sapiens      GGTGAATTTGAAGCTGGTATCTCCAAGAATGGGCAGACCCGAGAGCATGCCCTTCTGGCT 420
eEF1A2-H.sapiens      GGCGAGTTCGAGGCGGGCATCTCCAAGAATGGGCAGACGCGGGAGCATGCCCTGCTGGCC 420
TEF1                  GGTGAATTCGAAGCCGGTATCTCTAAGGATGGTCAAACCAGAGAACACGCTTTGTTGGCT 420
TEF2                  GGTGAATTCGAAGCCGGTATCTCTAAGGATGGTCAAACCAGAGAACACGCTTTGTTGGCT 420
                      ** ** ** ** ** ** ***** *** **** ** **  * ** ** **  *  ****

eEF1A1-H.sapiens      TACACACTGGGTGTGAAACAACTAATTGTCGGTGTTAACAAAATGGATTCCACTGAGCCA 480
eEF1A2-H.sapiens      TACACGCTGGGTGTGAAGCAGCTCATCGTGGGCGTGAACAAAATGGACTCCACAGAGCCG 480
TEF1                  TTCACCTTGGGTGTTAGACAATTGATTGTTGCTGTCAACAAGATGGACTCCGTCAAATGG 480
TEF2                  TTCACCTTGGGTGTTAGACAATTGATTGTTGCTGTCAACAAGATGGACTCCGTCAAATGG 480
                      * ***  ******* *  **  * ** ** *  ** ***** ***** ***    *

eEF1A1-H.sapiens      CCCTACAGCCAGAAGAGATATGAGGAAATTGTTAAGGAAGTCAGCACTTACATTAAGAAA 540
eEF1A2-H.sapiens      GCCTACAGCGAGAAGCGCTACGACGAGATCGTCAAGGAAGTCAGCGCCTACATCAAGAAG 540
TEF1                  GACGA-ATCCAGA-----TTCCAAGAAATTGTCAAGGAAACCTCCAACTTTATCAAGAAG 534
TEF2                  GACGA-ATCCAGA-----TTCCAAGAAATTGTCAAGGAAACCTCCAACTTTATCAAGAAG 534
                        * * * * ***     *   * ** ** ** ******  *  *   *  ** *****

eEF1A1-H.sapiens      ATTGGCTACAACCCCGACACAGTAGCATTTGTGCCAATTTCTGGTTGGAATGGTGACAAC 600
eEF1A2-H.sapiens      ATCGGCTACAACCCGGCCACCGTGCCCTTTGTGCCCATCTCCGGCTGGCACGGTGACAAC 600
TEF1                  GTTGGTTACAACCCAAAGACTGTTCCATTCGTCCCAATCTCTGGTTGGAACGGTGACAAC 594
TEF2                  GTTGGTTACAACCCAAAGACTGTTCCATTCGTCCCAATCTCTGGTTGGAACGGTGACAAC 594
                       * ** ********    ** **  * ** ** ** ** ** ** *** * *********

eEF1A1-H.sapiens      ATGCTGGAGCCAAGTGCTAACATGCCTTGGTTCAAGGGATGGAAAGTCACCCGTAAGGAT 660
eEF1A2-H.sapiens      ATGCTGGAGCCCTCCCCCAACATGCCGTGGTTCAAGGGCTGGAAGGTGGAGCGTAAGGAG 660
TEF1                  ATGATTGAAGCTACCACCAACGCTCCATGGTACAAGGGTTGGGAAAAGGAAACCAAGGCC 654
TEF2                  ATGATTGAAGCTACCACCAACGCTCCATGGTACAAGGGTTGGGAAAAGGAAACCAAGGCC 654
                      *** * **  *     * ***   ** **** ****** *** *          ****

eEF1A1-H.sapiens      GGCAATGCCAGTGGAACCACGCTGCTTGAGGCTCTGGACTGCATCCTACCACCAACTCGT 720
eEF1A2-H.sapiens      GGCAACGCAAGCGGCGTGTCCCTGCTGGAGGCCCTGGACACCATCCTGCCCCCCCACGCGC 720
TEF1                  GGTGTCGTCAAGGGTAAGACTTTGTTGGAAGCCATTGACGCCATTGAACAACCATCTAGA 714
TEF2                  GGTGTCGTCAAGGGTAAGACTTTGTTGGAAGCCATTGACGCCATTGAACAACCATCTAGA 714
                      **    *  *  **     *  ** * ** **  * ***  ***    *  **  *  *

eEF1A1-H.sapiens      CCAACTGACAAGCCCTTGCGCCTGCCTCTCCAGGATGTCTACAAAATTGGTGGTATTGGT 780
eEF1A2-H.sapiens      CCCACGGACAAGCCCCTGCGCCTGCCGCTGCAGGACGTGTACAAGATTGGCGGCATTGGC 780
TEF1                  CCAACTGACAAGCCATTGAGATTGCCATTGCAAGATGTTTACAAGATTGGTGGTATTGGT 774
TEF2                  CCAACTGACAAGCCATTGAGATTGCCATTGCAAGATGTTTACAAGATCGGTGGTATTGGT 774
                      ** ** ********  ** *  ****  * ** ** ** ***** ** ** ** *****
eEF1A1-H.sapiens      ACTGTTCCTGTTGGCCGAGTGGAGACTGGTGTTCTCAAACCCGGTATGGTGGTCACCTTT 840
eEF1A2-H.sapiens      ACGGTGCCCGTGGGCCGGGTGGAGACCGGCATCCTGCGGCCGGGCATGGTGGTGACCTTT 840
TEF1                  ACTGTGCCAGTCGGTAGAGTTGAAACCGGTGTCATCAAGCCAGGTATGGTTGTTACTTTT 834
TEF2                  ACTGTGCCAGTCGGTAGAGTTGAAACCGGTGTCATCAAGCCAGGTATGGTTGTTACTTTC 834
```

```
                    ** ** ** ** **  * ** ** ** **  *  *    ** ** ***** ** ** **

eEF1A1-H.sapiens    GCTCCAGTCAACGTTACAACGGAAGTAAAATCTGTCGAAATGCACCATGAAGCTTTGAGT 900
eEF1A2-H.sapiens    GCGCCAGTGAACATCACCACTGAGGTGAAGTCAGTGGAGATGCACCACGAGGCTCTGAGC 900
TEF1                GCCCCAGCTGGTGTTACCACTGAAGTCAAGTCCGTTGAAATGCATCACGAACAATTGGAA 894
TEF2                GCCCCAGCTGGTGTTACCACTGAAGTCAAGTCCGTTGAAATGCATCACGAACAATTGGAA 894
                    ** ****      * ** ** ** ** ** ** ** ** ***** ** **     **

eEF1A1-H.sapiens    GAAGCTCTTCCTGGGGACAATGTGGGCTTCAATGTCAAGAATGTGTCTGTCAAGGATGTT 960
eEF1A2-H.sapiens    GAAGCTCTGCCCGGCGACAACGTCGGCTTCAATGTGAAGAACGTGTCGGTGAAGGACATC 960
TEF1                CAAGGTGTTCCAGGTGACAACGTTGGTTTCAACGTCAAGAACGTTTCCGTTAAGGAAATC 954
TEF2                CAAGGTGTTCCAGGTGACAACGTTGGTTTCAACGTCAAGAACGTTTCCGTTAAGGAAATC 954
                     *** * * ** ** ***** ** ** ***** ** ***** ** ** ** *****  *

eEF1A1-H.sapiens    CGTCGTGGCAACGTTGCTGGTGACAGCAAAAATGACCCACCAATGGAAGCAGCTGGCTTC 1020
eEF1A2-H.sapiens    CGGCGGGGCAACGTGTGTGGGGACAGCAAGTCTGACCCGCCGCAGGAGGCTGCTCAGTTC 1020
TEF1                AGAAGAGGTAACGTCTGTGGTGACGCTAAGAACGATCCACCAAAGGGTTGCGCTTCTTTC 1014
TEF2                AGAAGAGGTAACGTCTGTGGTGACGCTAAGAACGATCCACCAAAGGGTTGCGCTTCTTTC 1014
                     *  * ** *****   *** ***   **    ** ** **   **     ***   ***

eEF1A1-H.sapiens    ACTGCTCAGGTGATTATCCTGAACCATCCAGGCCAAATAAGCGCCGGCTATGCCCCTGTA 1080
eEF1A2-H.sapiens    ACCTCCCAGGTCATCATCCTGAACCACCCGGGGCAGATTAGCGCCGGCTACTCCCCGGTC 1080
TEF1                AACGCTACCGTCATTGTTTTGAACCATCCAGGTCAAATCTCTGCTGGTTACTCTCCAGTT 1074
TEF2                AACGCTACCGTCATTGTTTTGAACCATCCAGGTCAAATCTCTGCTGGTTACTCTCCAGTT 1074
                    *   *    ** **  *  ******* ** ** ** **    ** ** **  * ** **

eEF1A1-H.sapiens    TTGGATTGCCACACGGCTCACATTGCATGCAAGTTTGCTGAGCTGAAGGAAAAGATTGAT 1140
eEF1A2-H.sapiens    ATCGACTGCCACACAGCCCACATCGCCTGCAAGTTTGCGGAGCTGAAGGAGAAGATTGAC 1140
TEF1                TTGGATTGTCACACTGCTCACATTGCTTGTAGATTCGACGAATTGTTGGAAAAGAACGAC 1134
TEF2                TTGGATTGTCACACTGCTCACATTGCTTGTAGATTCGACGAATTGTTGGAAAAGAACGAC 1134
                     * ** ** ***** ** ***** ** ** *  ** *  **  **  *** ****  **

eEF1A1-H.sapiens    CGCCGTTCTGGTAAAAAGCTGGAAGATGGCCCTAAATTCTTGAAGTCTGGTGATGCTGCC 1200
eEF1A2-H.sapiens    CGGCGCTCTGGCAAGAAGCTGGAGGACAACCCCAAGTCCCTGAAGTCTGGAGACGCGGCC 1200
TEF1                AGAAGATCTGGTAAGAAGTTGGAAGACCATCCAAAGTTCTTGAAGTCCGGTGACGCTGCT 1194
TEF2                AGAAGATCTGGTAAGAAGTTGGAAGACCATCCAAAGTTCTTGAAGTCCGGTGACGCTGCT 1194
                     *  * ***** ** *** **** **    ** ** * * ******* ** ** ** **

eEF1A1-H.sapiens    ATTGTTGATATGGTTCCTGGCAAGCCCATGTGTGTTGAGAGCTTCTCAGACTATCCACCT 1260
eEF1A2-H.sapiens    ATCGTGGAGATGGTGCCGGGAAAGCCCATGTGTGTGGAGAGCTTCTCCCAGTACCCGCCT 1260
TEF1                TTGGTCAAGTTCGTTCCATCTAAGCCAATGTGTGTTGAAGCTTTCAGTGAATACCCACCA 1254
TEF2                TTGGTCAAGTTCGTTCCATCTAAGCCAATGTGTGTTGAAGCTTTCAGTGAATACCCACCA 1254
                     * **  *  * ** **    ***** ******** **    ***    * ** ** **

eEF1A1-H.sapiens    TTGGGTCGCTTTGCTGTTCGTGATATGAGACAGACAGTTGCGGTGGGTGTCATCAAAGCA 1320
eEF1A2-H.sapiens    CTCGGCCGCTTCGCCGTGCGCGACATGAGGCAGACGGTGGCCGTAGGCGTCATCAAGAAC 1320
TEF1                TTAGGTAGATTCGCTGTCAGAGACATGAGACAAACTGTCGCTGTCGGTGTTATCAAGTCT 1314
TEF2                TTAGGTAGATTCGCTGTCAGAGACATGAGACAAACTGTCGCTGTCGGTGTTATCAAGTCT 1314
                     * **  * ** ** **  * ** ***** ** ** ** ** ** ** ** *****

eEF1A1-H.sapiens    GTGGACAAGAAGGCTGCTGGAGCTGGCAAGGTCACCAAGTCTGCCCAGAAAGCTCAGAAG 1380
eEF1A2-H.sapiens    GTGGAGAAGAAGAGCGGCGGCGCCGGCAAGGTCACCAAGTCGGCGCAGAAGGCGCAGAAG 1380
TEF1                GTTGACAAGA---CTGAAAAGGCCGCTAAGGTTACCAAGGCTGCTCAAAAGGCTGCTAAG 1371
TEF2                GTTGACAAGA---CTGAAAAGGCCGCTAAGGTTACCAAGGCTGCTCAAAAGGCTGCTAAG 1371
                    ** ** ****     *     ** *  ***** ****** * ** ** ** **    ***

eEF1A1-H.sapiens    GC---TAAATGA 1389
eEF1A2-H.sapiens    GCGGGCAAGTGA 1392
TEF1                ------AAATAA 1377
TEF2                ------AAATAA 1377
                          ** * *
```

***Figure 1.2 ORF alignment between human eEF1A1 and eEF1A2, and S.cerevisiae TEF1 and TEF2.*** *eEF1A1 is more similar to both TEF1 and TEF2, however conservation across the species is highly conserved. eEF1A1 shares 70.5% identity to TEF1 and 70.4% identity to TEF2, and eEF1A2 shares 66.8% identity with TEF1 and 66.6% identity with TEF1.*

Despite the similarity between *eEF1A1* and *eEF1A2* these genes have different expression patterns throughout the body. In higher eukaryotes *eEF1A1* is expressed in all tissues during development, but is no longer present at detectable levels in the muscles and heart tissue of

adults (Lee *et al.*, 1992; Chambers *et al.*, 1998). Instead high level expression of *eEF1A2* is switched on in these tissues, as well as in motor neurons of the medulla. Lower levels of *eEF1A2* expression is also detectable in the islet cells of the pancreas, and endocrine cells of the digestive tract (Newbery *et al.*, 2007).

Strict regulation of differential *eEF1A* gene expression has been observed during developmental stages. In mice, *eEF1A1* is downregulated during the first two weeks of life to undetectable levels in muscular tissues by 25 days (Khalyfa *et al.*, 2001), with *eEF1A2* gradually being upregulated. Ablation of *eEF1A2* by deletion of the locus results in mice exhibiting the mutant wasted phenotype (*wst*)(Chambers *et al.*, 1998). These mice present wasting and neurological and immunological abnormalities at 21 days old, and mortality occurs by 28 days (Shultz *et al.*, 1982).

### *1.2.2 eEF1A Proteins*

eEF1A exists as two variant, tissue-specific, isoforms, eEF1A1 and eEF1A2, in all higher vertebrates. In humans these proteins share 92% identity and 98% similarity (Tomlinson *et al.*, 2005)(see figure 1.4). It is not however only human eEF1A isoforms that show considerable similarity with eEF1A in other mammals, including mice and rats, differing by only one amino acid compared to that of humans, and rabbits share 100% identity with humans (Lee *et al.*, 1994; Kahns *et al.*, 1998).

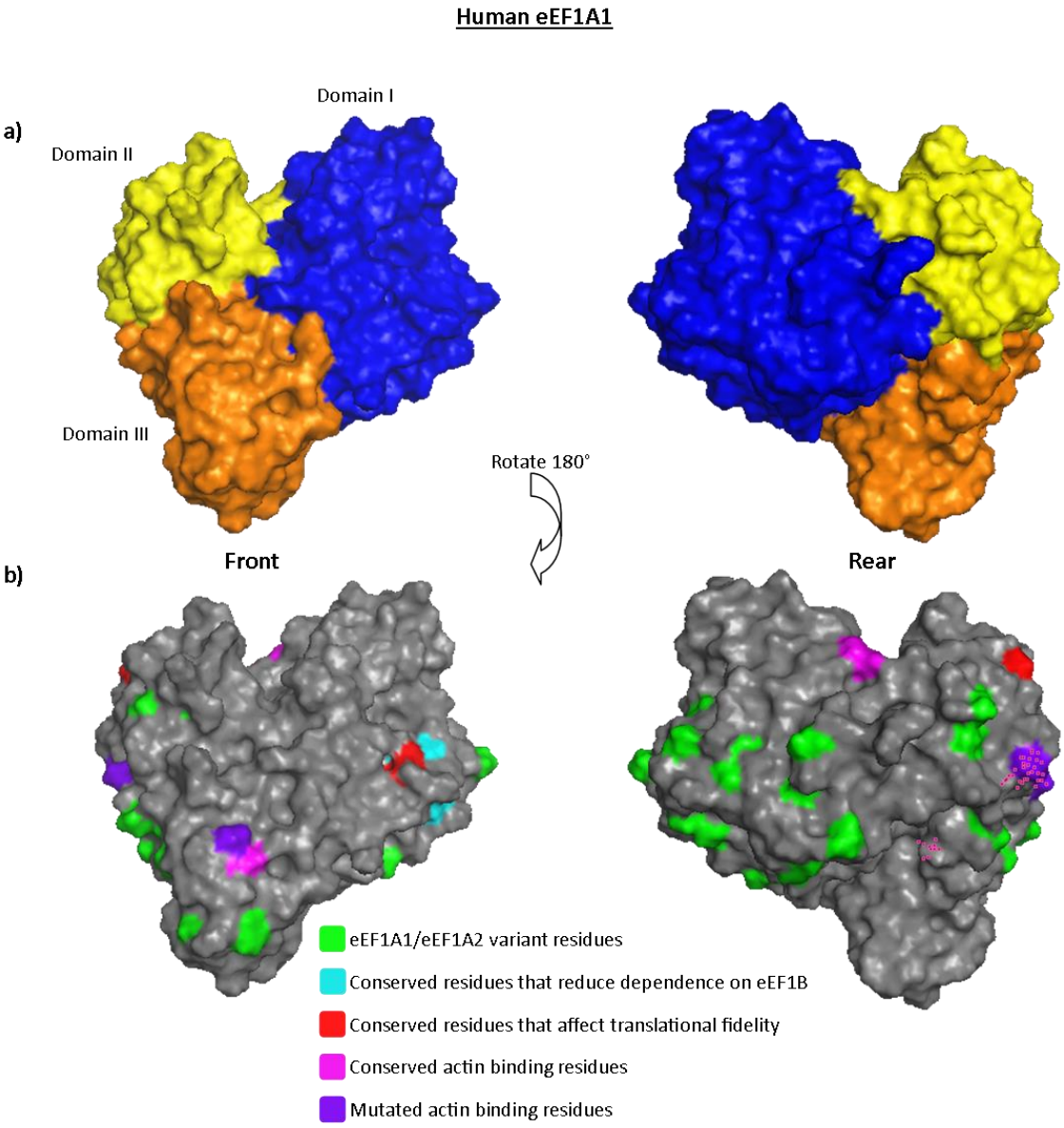


***Figure 1.3 Four structural surface renditions of human eEF1A1.*** *Models are rotated 180° about the y-axis 1a) shows the three domain boundaries, domain I is blue, domain II is yellow and domain III is orange. 1b) shows some of the conserved and mutated residues from yeast eEF1A, to human eEF1A1 and eEF1A2. Green shows the variant residues between eEF1A1 and eEF1A2, cyan shows conserved residues from yeast to humans that have been shown to reduce eEF1A dependence on eEF1Bp, red shows conserved residues from yeast to humans that have been shown to affect translational fidelity, magenta shows conserved residues from yeast to humans that have been shown to affect actin binding, and purple shows residues that have been shown to affect actin binding in yeast, are not conserved through to humans, and are also mutated from human eEF1A1 to eEF1A2.*

The amino acids that differ between isoforms however, may give us insight into the differing functional profiles of eEF1A proteins. A high degree of conservation between the varying

amino acids exists across species (see figure 1.3) indicating unique functions of both eEF1A isoforms, probably arising through evolutionary selection (Lee *et al.*, 1994).

When compared, the human eEF1A1 and eEF1A2 variant residues to the residues of known function in yeast eEF1A it is interesting to note that several of the variations are in actin binding domains (see table 1.1 and figure 1.3). This is compelling evidence to suggest that at least the actin binding function of eEF1A isoforms is altered as yN329, yK333 and yY355 are all known to affect the growth of cells and eEF1As ability to bundle actin (Gross and Kinzy, 2007).

**Table 1.1 - Actin binding residues in yeast that are not conserved in human eEF1A isoforms**

| Human eEF1A1 | Human eEF1A2 | Yeast eEF1A |
|---|---|---|
| N331 | S331 | N329 |
| M335 | Q335 | K333 |
| A358 | S358 | Y355 |

*Residues listed are known actin binding residues in yeast eEF1A but are not conserved in human isoforms.*

### *1.2.3 Phosphorylation states of eEF1A*

Once it has hydrolysed GTP and released its aminoacyl tRNA to the A site of the ribosome, eEF1A·GDP is released to be recycled to its GTP bound, active form allowing it to participate in further rounds of elongation. Nucleotide exchange on eEF1A is catalysed by its guanine-nucleotide exchange factor (GEF) eEF1B. In yeast, eEF1B is a multifactor complex composed of eEF1Bα and eEF1Bγ, with eEF1Bβ in plants, and eEF1Bδ in metazoans. Despite significant sequence identity eEF1A1 and eEF1A2 exhibit differences in their relative affinities for GTP and GDP (Kahns *et al.*, 1998). eEF1A1 binds GTP more strongly than GDP, with the opposite

being true for eEF1A2. This suggests there should be a greater reliance of eEF1A2 on its GEF, the eEF1B complex, the opposite however, is true. eEF1A2 shows very little affinity with any component of the eEF1B complex (Mansilla *et al.*, 2002), indicating a primary role for eEF1A2 that differs to its canonical function. However, it is important to note that in neurons and muscle where eEF1A2 is the only form of eEF1A it must still have the ability to carry out its canonical GTP bound roles, with evidence from both the Abbott and Zhang labs that eEF1B does still act as the GTP exchange factor for eEF1A2 (Cao et al., 2009; Soares et al., 2009).

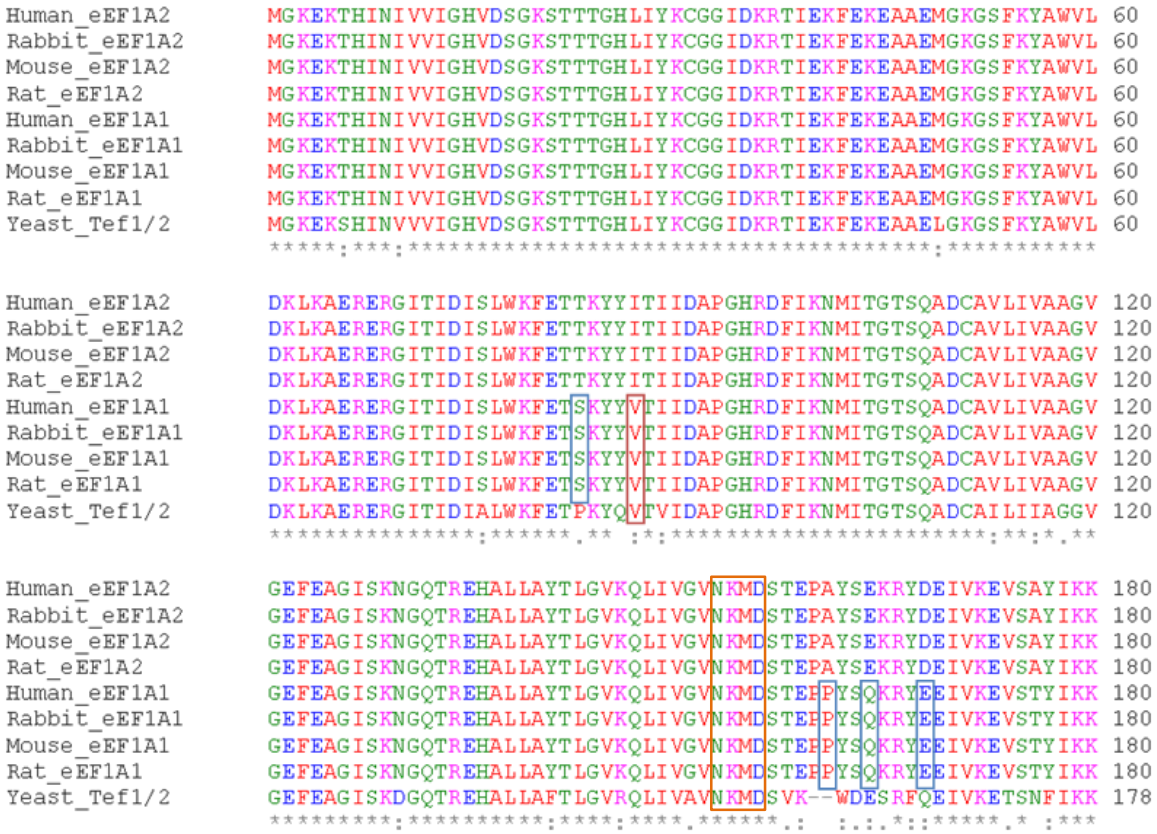

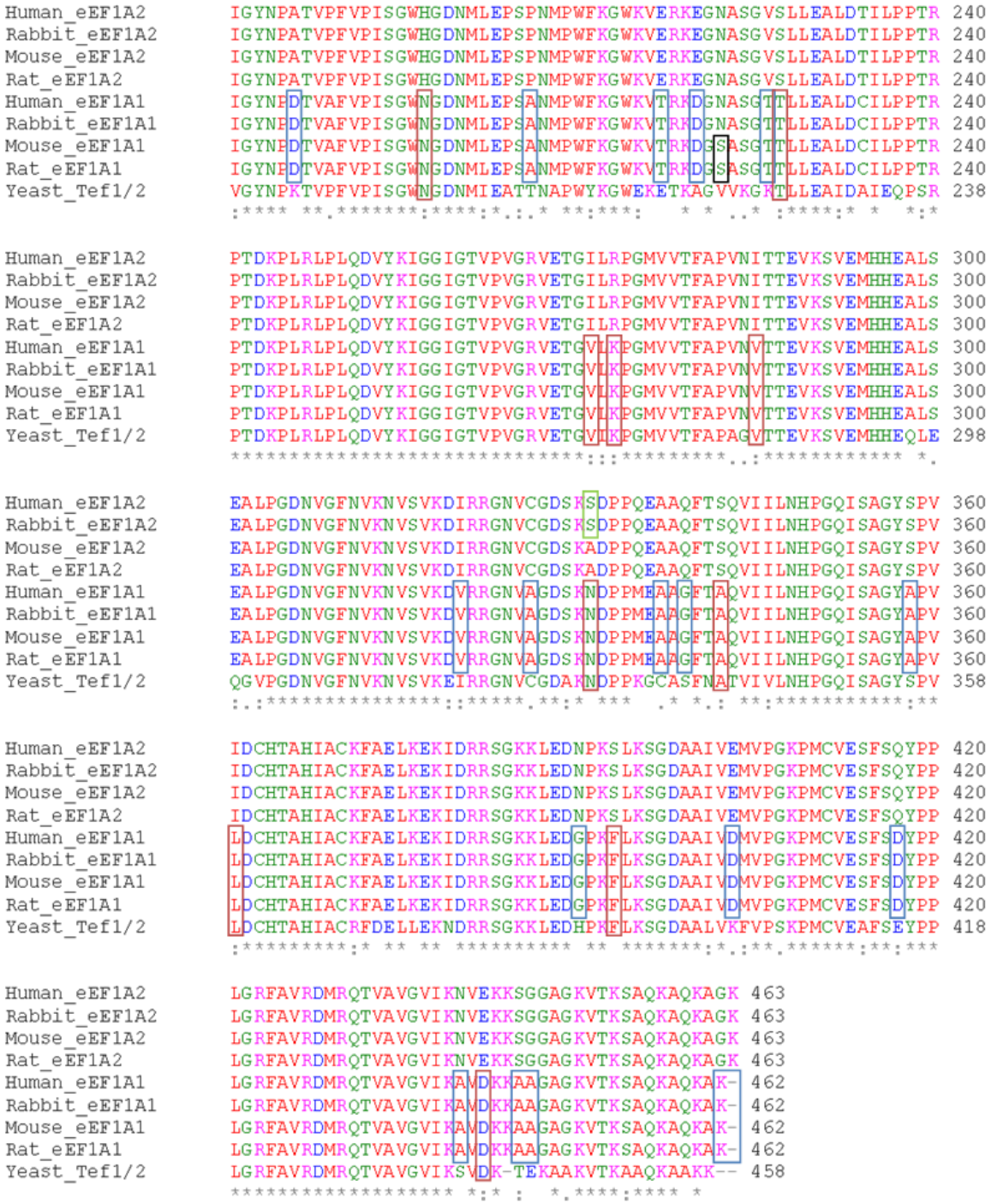


***Figure 1.4 Polypeptide alignment of human, rabbit, mouse, rat and yeast eEF1A isoforms***. *Red boxes show conserved differences between eEF1A1 and eEF1A2 from yeast to human. Blue boxes show conserved differences between eEF1A1 to eEF1A2 from mouse to human. The black box shows the single amino acid variation between human and rabbit, and mouse and rat eEF1A1. The green box shows the single amino acid variation between human and rabbit, and mouse and rat eEF1A2. The highly conserved GTP binding motif NKMD is outlined in orange, residues 152-156.*

## *1.2.4 Non-canonical functions of eEF1A*

As discussed in the abstract eEF1A is a multifunctional protein and performs a wide variety of roles with in the cell. In addition to its canonical role in translation, eEF1A has several other roles, some well characterised, others not so well which appear to be conserved across species. Understanding the functional differences between eEF1A1 and eEF1A2 could assist in our understanding of differential tissue expression of these proteins and how eEF1A2 induces tumour growth.

### *1.2.4.1 eEF1A as a nuclear exporter*

One of the more contentious roles that eEF1A is reported to be involved in, is that of nuclear export. There have been separate studies that have linked eEF1A to nuclear export during both protein synthesis and transcription. Reported by both the Kutay and Görlich labs, eEF1A is actively exported from the nucleus when it is recruited to the exportin-5/RanGTP complex via aa-tRNA. Although it is not understood how eEF1A could be trapped in the nucleus as no nuclear transporter has yet been characterised, and under normal conditions eEF1A is excluded from the nucleus (Bohnsack *et al.*, 2002; Calado *et al.*, 2002). However, in Exp5 depleted cells, and in mutant *Δmsn5* (orthologue of Exp5) yeast cells, it is known that eEF1A does enter the nucleus (Lund *et al.*, 2004; Murthi *et al.*, 2010). Another study into the mammalian nuclear export signal, transcription dependant nuclear export mechanism (TD-NEM), suggested that eEF1A mediated export of a range of proteins including, the von Hippel-Lindau (VHL) tumour suppressor and the poly(A)-binding protein (PABP1). They suggested that eEF1A mediated export was stimulated from the cytoplasmic side of the nuclear envelope, without eEF1A physically entering the nucleus (Khacho et al., 2008).

### *1.2.4.2 eEF1A, protein degradation and aggresome formation*

Thinking of eEF1A as a component in protein degradation initially seems counterintuitive. However, when considering the abundance of eEF1A in close proximity to the ribosome, and so, the nascent polypeptide, this function seems plausible. eEF1A is also proposed to be an excellent candidate to recognise damaged proteins and shuttle them to the proteasome, due to its central role in translation elongation (Sasikumar *et al.*, 2012). A role for eEF1A in protein degradation was initially identified for ubiquitin-dependent degradation of certain $N^{\alpha}$-acetylated proteins (Gonen *et al.*, 1994). Further *in vitro* studies showed eEF1A can interact with nascent polypeptides whilst they are still undergoing synthesis (Hotokezaka *et al.*, 2002). eEF1A can also interact with the unfolded protein once released from the ribosome and act as a chaperone to help mediate protein folding. *In vivo* evidence for eEF1A acting on protein degradation came from the Madura lab in 2005. They demonstrated high-copy number eEF1A rescued the slow growth phenotype observed upon deletion of the *RAD53* and *RPN10* genes that are involved in the proteolytic pathway (Chuang et al., 2005). eEF1A was shown to interact with Rpt1p, a subunit of the proteasome 19S regulatory particle, with the *Δrpt1* mutant showing a reduction in the interaction between eEF1A and the proteasome. A more recent study highlights a further role for eEF1A in aggresome formation. It was demonstrated that upon accumulation of newly synthesised aberrant proteins, eEF1A would bind with them, with a reduction of eEF1A resulting in reduced aggresome formation (Meriin *et al.*, 2012).

When taken together these data suggest a role for eEF1A in not only detecting and chaperoning damaged or misfolded proteins from the ribosome to the proteasome, but also in sensing the accumulation of defective products upon decreased proteasomal activity, and signalling to activate the heat shock response and a putative aggresome formation pathway.

### *1.2.4.3 eEF1A has both pro- and anti-apoptotic effects.*

eEF1A has been reported to have both pro- and anti-apoptotic effects. A correlation was initially observed between the levels of eEF1A and the rate of apoptosis, followed by an observation made during a cDNA screen, that elevated levels of eEF1A result in resistance to apoptosis (Duttaroy *et al.*, 1998; Talapatra *et al.*, 2002). The explanation for these contrasting results may be that eEF1A is present in higher eukaryotes in two isoforms, eEF1A1 and eEF1A2. During muscle differentiation eEF1A1 was revealed as pro-apoptotic, whereas eEF1A2 was anti-apoptotic (Ruest *et al.*, 2002). Further studies have found that increased levels of eEF1A2 or decreased levels of eEF1A1 correlates to ER stress-induced apoptosis (Talapatra *et al.*, 2002).

Findings from a recent medical study have found that the expression level of eEF1A2 in prostate cancer tissues was significantly higher than in healthy tissue (Sun *et al.*, 2014). Reduction of eEF1A2 expression was coupled to a large inhibition of proliferation and elevated levels of apoptosis. Further analysis revealed that suppression of eEF1A2 led to an increase of apoptosis pathway proteins caspase3, BAD, BAX and PUMA, with levels of eEF1A2 being inversely correlated to caspase3 levels in prostate cancer tissues.

### *1.2.4.4 eEF1A and viral propagation*

For a virus to thrive it needs to not only synthesise its own proteins, but it must also rely on host proteins to replicate. It makes sense that many studies suggest an interaction between viruses and eEF1A, as eEF1A is one of the most abundant cellular proteins and the fact the some viruses have evolved to utilise it is unsurprising. eEF1A·GTP interacts with aa-tRNA as well as other mammalian RNA species, so, it is also unsurprising that eEF1A is able to bind

some RNA structures of in the untranslated regions of viral genomes (Mateyak and Kinzy, 2010; Li *et al.*, 2013).

## *1.2.5 The role of eEF1A in cancer*

Despite recent medical advances using traditional cytotoxic treatments, the global burden of cancer has continued to increase, and it remains the leading cause of morbidity and mortality (Siegel *et al.*, 2013). Understanding of translation, and the many translation factors involved, is considered as being an important step in elucidating cancer progression (Scheper *et al.*, 2007). eEF1A is a translation elongation factor whose roles have been studied extensively, but although eEF1A1 and eEF1A2 share a high degree of structural and functional similarity, only one of the isoforms has been directly implicated as being an oncogene.

### *1.2.5.1 eEF1A1 is not an oncogene*

There is no evidence to implicate eEF1A1 as an oncogene. It maps to chromosome 6q14 and this region is frequently lost in many cancers (Kobayashi *et al.*, 2008; Siddiq *et al.*, 2012). This had led to speculation that 6q14 may contain a tumour suppressor gene (Thornton *et al.*, 2003) with several studies suggesting U50 snuRNA could be a primary candidate (Williams and Farzaneh, 2012).

Induction of eEF1A1 overexpression has been observed in some cancer cell lines that have been treated with pharmacological compounds indicating it as a potential therapeutic target. Greater than two-fold changes in expression levels were seen in erythroblastic leukaemia, osteosarcoma, and pancreatic cancer cell lines that are resistant to methotrexate, relative to the methotrexate sensitive lines (Selga *et al.*, 2009). Increased levels of eEF1A1 mRNA has been identified in a cisplatin resistant, head and neck carcinoma cell line (UMSCC 10b/Pt-S15) (Johnsson *et al.*, 2000). Increased expression of eEF1A1 RNA has also been detected in various

tumours and cancer cell lines without treatment, such as, primary glioblastoma, prostate cancer and hepatocellular carcinoma (Mohler *et al.*, 2002; Grassi *et al.*, 2007; Scrideli *et al.*, 2008).

#### *1.2.5.2 eEF1A2 is a true oncogene*

Although it seems that eEF1A1 possesses little or no oncogenic properties, there is strong evidence implicating eEF1A2 as a true oncogene (Anand *et al.*, 2002). eEF1A2 exhibits the true hallmarks of an oncogene, it is not only detected at elevated levels in breast, ovarian and lung cancers, to name a few, but it is also able to transform mammalian cells (Kallioniemi *et al.*, 1994; Anand *et al.*, 2002; Lam *et al.*, 2006).

eEF1A2 is located at loci 20q13.3, a region which is subject to chromosomal amplification in 5-10% of breast cancers (Hodgson *et al.*, 2003). There are several putative oncogenes located in the region 20q13, and dependent upon the loci amplified, the prognosis varies (Kallioniemi *et al.*, 1994; Ginestier *et al.*, 2006).

eEF1A2 is overexpressed in approximately 30% of ovarian cancers and ectopic expression in NIH3T3 cells results in enhanced growth rate, anchorage-independent growth, and induced tumour formation when xenografted in nude mice (Anand *et al.*, 2002). Further studies have revealed overexpression of eEF1A2 in more than 85% of serus and endometroid cancers (Pinke *et al.*, 2008). eEF1A2 has been shown to be an independent prognostic marker for survival in serous cancers, with patients with elevated levels of eEF1A2 expected to have an increased probability of 20 year survival (Pinke *et al.*, 2008).

20q13 amplification is used as a marker for breast cancer and is linked to a poor prognosis and enhanced tumour aggressiveness (Kallioniemi *et al.*, 1994; Courjal *et al.*, 1996). The

eEF1A2 locus (loci 20q13.3) is some 10 Mb away from the 20q13 amplification used to predict prognosis, however surprisingly eEF1A2 mRNA and protein are detectable in breast cancers (Gonçalves and Malta-Vacas, 2005; Kulkarni *et al.*, 2007). It is also surprising is that eEF1A2 levels indicate a good prognosis for patients, contrary to amplification of the 20q13 locus (Kulkarni *et al.*, 2007). Levels of eEF1A2 in malignant tumours is 30 times higher than healthy breast tissue, and benign breast tumours (Tomlinson *et al.*, 2005).

Comparative genomic hybridisation studies have identified eEF1A2 as playing a role in lung cancer (Li *et al.*, 2006; Zhu *et al.*, 2007). eEF1A2 gene, mRNA and protein are all found to be elevated in lung adenocarcinomas, and are correlated to disease progression, decreased lifespan of the patient, and a poor prognosis (Li *et al.*, 2006).

It is interesting that eEF1A2 appears to confer different effects dependent on the tissue it is expressed in. It has been observed as an oncogene in ovary, breast and lung cancer, but appears as a good prognostic marker in some cases, and a bad prognostic marker in others. It is also interesting that ablation of eEF1A2 in lung cancer, using short-interfering RNA reduces cell proliferation and promotes apoptosis. However, in ovarian cancer, eEF1A2 overexpression increases cell proliferation, but has no effect on drug-induced cell death or anoikis (Pinke *et al.*, 2008). These data suggest that the tissue that eEF1A2 is expressed in has a dramatic effect on its interactions and its functions.

### *1.2.6 The role of eEF1A in other diseases*

As previously discussed in section 1.2.5 eEF1A2 is involved in the progression of several cancers when expressed at elevated levels, but studies have also revealed that deletion and mutations in eEF1A2 also result in various disease states.

### *1.2.6.1 Deletion of a 15.6 kb region causes the inactivation of eEF1A2 resulting in the wasted mouse*

Spontaneous deletion of a 15.6 kb region upstream of *eEF1A2* results in the removal of all promoter regions and its first non-coding exon causing complete inactivation of the gene (Chambers *et al.*, 1998). Loss of eEF1A2 in this fashion results in the wasted mouse phenotype. Mice with this mutation grow normally to approximately 21 days, at this point eEF1A2 should be expressed at sufficient levels to counter the decline in eEF1A1 expression. However, in the *wst* mouse a lack of *eEF1A2* expression results in the mouse losing weight, as well as developing tremors and progressive atrophy of the spleen and thymus, resulting in mortality by 28 days (Shultz *et al.*, 1982).

Initially identified as neuron degeneration by the Moses lab in 1989, the "wasted" mutation was originally associated with hindlimb paralysis and tremors (Lutsep et al., 1989). Lutsep et al. observed vacuolar degeneration within the neurons of wst/wst mice and the accumulation of neurofilaments. They suggested that it may be the phosphorylation of the neurofilaments that is important in the onset of the observed neuron degeneration.

### *1.2.6.2 De novo mutations in eEF1A2 are recorded to cause neurological abnormalities*

Three unique *de novo* mutations have been observed in four patients each exhibiting neurological afflictions. The first mutation characterised c.208G>A resulted in the substitution of glycine 70 for serine. Two patients have been recorded as possessing this mutation, the first exhibited severe intellectual disability and myoclonic seizures, and the second had epileptic encephalopathy (de Ligt *et al.*, 2012; Veeramah *et al.*, 2013). Two further mutations were characterised in 2014, c.754G>C, p.D252H and c.364G>A p.E122K. These two patients

exhibited similar facial features including a depressed nasal bridge, tented upper lip, everted lower lip, and downturned corners of the mouth. All patients exhibited severe intellectual disability, autistic behaviour, absent speech, neonatal hypotonia, epilepsy and progressive microcephaly (Nakajima *et al.*, 2014). Nakajima et al recommend that based on the characterisation of these mutations a new neurological syndrome be classified.

## 1.3 The yeast actin cytoskeleton

Part of the main cellular machinery, actin is involved in a range of cellular functions. Both the yeast protein and gene *ACT1* were discovered over 30 years ago and have been highly characterised (Water *et al.*, 1980; Shortle *et al.*, 1982). Within the yeast cell actin can exist in one of three ultra-structures, patches, cables, and in the contractile ring (Moseley and Goode, 2006).

Similar to eEF1A, actin is a highly conserved, abundant protein essential for the survival of the cell (Pollard, 2000). It exists as both globular monomeric (G-actin) and filamentous polymeric (F-actin) forms. G-actin is a 42kDa protein encoded for by *ACT1* and consists of two large domains, that are each composed of two subdomains (Water *et al.*, 1980; Shortle *et al.*, 1982; Kabsch *et al.*, 1990). The large domains form a hinged molecule with a deep cleft which provides a nucleotide binding site. F-actin forms a right-handed double helix in a polar manner. These two forms of actin co-exist in a dynamic cycle, making and breaking filaments as required.

Polymerisation of actin is limited by the initial nucleation event, the binding of three G-actin monomers. Once the hurdle of nucleation is overcome, polymerisation rapidly progresses. Preferential addition of ATP bound actin to the barbed end results in polarised growth. This is followed by the hydrolysis of the ATP subunit resulting in ADP+Pi (inorganic phosphate)

bound actin and a conformational change in the monomers structure (Pollard, 1986; Kudryashov *et al.*, 2010). Pi is then liberated, to leave ADP-bound actin (Pollard, 2000). Once dissociated from the pointed end the ADP-actin monomers are free to exchange ADP for ATP and commence the cycle once more (see figure 1.5).

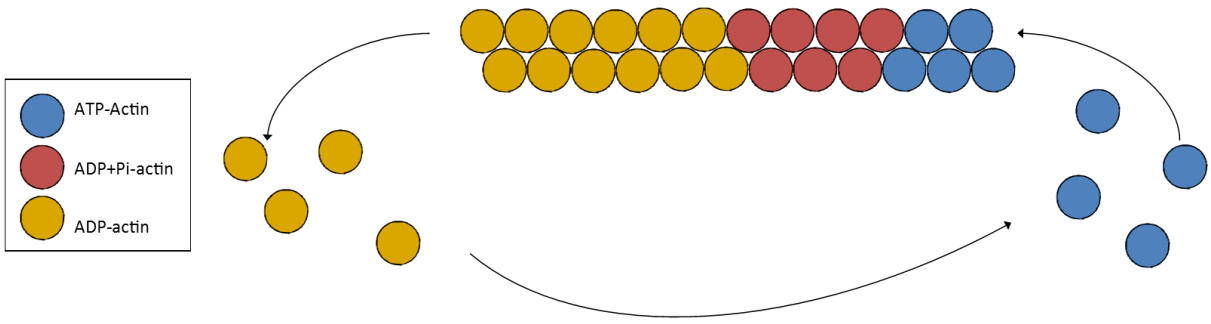


***Figure 1.5 A schematic view of actin treadmilling.*** *ATP-actin is shown in blue, ADP+Pi-actin is red, and ADP-actin is yellow.*

## 1.4 The actin cytoskeleton and translation

Research from the Gourlay lab and previously published in the literature has established significant functional links between the protein translational machinery and the cytoskeleton. The cytoskeleton regulates the spacial and temporal organisation of the translational apparatus including ribosomes and polysomes (Wolosewick and Porter, 1976; Ramaekers *et al.*, 1983). It has also been shown that disruption of F-actin, by latrunculin, reduces translation levels whilst disruption of microtubules does not (Stapulionis *et al.*, 1997). The effects of the translational machinery on the actin cytoskeleton are discussed below.

### *1.4.1 Initiation factors and the actin cytoskeleton*

A lot remains to be discovered regarding the localisation of translation initiation factors, as they play intrinsic roles in development, cell polarity and cell migration. The translation

initiation factor eIF3 is known associate with the actin binding protein Sla2p and with membranes via actin filaments, although nothing is understood about the functional significance of this (Palecek *et al.*, 2001; Pincheira *et al.*, 2001).

The double mutant *ΔeIF2A/ΔeIF4E* has been demonstrated to disrupt actin organisation. Cells exhibited an almost total loss of actin filaments and cables, resulting in severely retarded growth and 85% of cells stalling at the G2/M transition (Komar *et al.*, 2005). The single *ΔeIF2A* and *ΔeIF4E* mutants had a reduced effect on actin polymerisation and growth relative to the double mutant. However, contrary to the authors' hypothesis, both the double and the single mutants showed increased levels of actin. It was expected that the mutants would exhibit reduced translation and so, a lower abundance of actin. The increased levels were explained by eIF2A acting as a suppressor of cap-independent translation processes. This indicated that no direct link existed between actin and the translation initiation machinery, but that actin levels were changed due to altered expression of regulatory proteins (Komar *et al.*, 2005).

The eIF4F complex is found in the non-soluble fraction of lysed fibroblasts that suggests an association with the cytoskeleton, although no association was observed in intact cells visualized by fluorescence microscopy (Willett *et al.*, 2006). Functional domains of eIF4G, a subunit of eIF4F, was overexpressed in *S.pombe* resulting in aberrant cytokinesis, and causing a loss of cell polarity and disruption of actin patches (Hashemzadeh-Bonehi *et al.*, 2003).

### *1.4.2 Elongation factors and the actin cytoskeleton*

Other than eEF1A, to be discussed later in section 1.4.4, little evidence exists for interactions between other translation elongation factors and the actin cytoskeleton. eEF2 has been observed to co-localise with actin in fibroblasts, but there is no evidence of a strong association between the two. It was suggested that the interaction is likely to be indirect, and

rather due to association of the entire translational machinery and the mRNA anchored to actin (Shestakova et al. 1991).

### *1.4.3 Release factors and the actin cytoskeleton*

A decrease in the levels of eRF3 in *S.cerevisiae* is known to result in large budded cells with a reduced growth rate and an increase in nonsense codon suppression (Valouev *et al.*, 2002). A mutant expressing only the C-terminal domain of eRF3 (eRF3c) was generated by Valouev at al. The eRF3c mutation conferred an increase in nonsense codon expression but not to the same level as the full length eRF3, suggesting that the N-terminal domain of eRF3 has deleterious effects on the termination function of eRF3. The eRF3c mutant also conferred a severe actin aberration. Cells visualized by fluorescent microscopy were completely devoid of phalloidin staining, indicating the absence of any detectable actin.

In the same paper (Valouev *et al.*, 2002) it was demonstrated the repression of eRF1 causes an accumulation of unbudded cells with 2C and higher genomic content, suggesting an uncoupling of DNA replication and cell budding.

These data suggest a robust link between the actin cytoskeleton and the translational machinery, although there are still significant holes in our knowledge. One further link between these two processes is that of eEF1A and actin. This is undoubtedly the strongest link, and has far reaching implications for many areas of research.

### *1.4.4 eEF1A and the actin cytoskeleton*

As previously described in section 1.2 the canonical role of eEF1A is the delivery of aminoacylated tRNA to the A site of the ribosome during translation elongation. eEF1A is also known to be an actin-binding protein across a range of species from the yeasts *S. cerevisiae*

and *S. pombe*, and the slime mould *Dictyostelium amoebae* to mammals (Yang *et al.*, 1990; Edmonds *et al.*, 1996; Suda *et al.*, 1999; Gross and Kinzy, 2005). It is also known that eEF1A not only binds, but can also cross link F-actin, and in doing so generates actin bundles that possess a unique structure excluding all other actin crosslinkers (Owen *et al.*, 1992). It is estimated more than 70-90% of *D. amoebae* GTP-eEF1A is bound to actin (Edmonds *et al.*, 1998), suggesting a unique actin-eEF1A environment within the cytoplasm that could correlate to changes in cell size or motility, and mRNA translation.

Genetic manipulations of eEF1A have begun to elucidate the mechanism of eEF1A interactions with actin, with studies from the Kinzy lab demonstrating that residues in domains II and III of eEF1A are involved in eEF1As ability to bundle actin (Gross and Kinzy, 2005; Gross and Kinzy, 2007). Their studies revealed two classes of mutations, the first were those which did not affect the rate of protein synthesis, but resulted in a disorganised actin cytoskeleton and reduced actin bundling, although actin binding was unaltered *in vitro* (Gross and Kinzy, 2005). The second class of mutations caused severe actin phenotypes along with slowed growth and decreased levels of translation initiation (Gross and Kinzy, 2007). These data along with that from the Condeelis lab suggests that the binding sites on eEF1A for aa-tRNA and actin overlap (Liu *et al.*, 1996), meaning the functions of actin binding and translation may be mutually exclusive. This indicates there could be two pools of eEF1A in the system; an actin bound, translation incompetent pool, and an actin free pool that is translationally competent. This also means however that at any time there could be a pool of eEF1A, ready for rapid release from the cytoskeleton to increase protein translation.

## 1.5 Research objectives

Due to the highly conserved nature of eEF1A, and of the translational and cytoskeletal machinery, we sought to utilise the budding yeast *S.cerevisiae* to elucidate novel interactive partners of eEF1A. Using this information we aimed to see if these interactions were conserved through to humans by overexpressing the oncogenic human isoform eEF1A2. It was hoped that this study may assist in understanding the differences between the two eEF1A isoforms and their origins, as well as the mechanism of tumourigenesis induced by high levels of eEF1A2.

# Chapter 2: Materials and methods

## 2.1 Media and growth conditions for *Escherichia coli, Saccharomyces cerevisiae* and HEK293 cells

All media, unless specified, was sterilised in a Prestige medical bench-top autoclave at 121 °C, 15 lb/ $in^2$ for 11 minutes. For agar plates 2 % w/v of granulated agar (Difco) was added to broth recipes prior to autoclaving. *Escherichia coli* was grown at 37 °C with liquid cultures grown with rapid aeration at 200 rpm. *Saccharomyces cerevisae* was grown at 30 °C with liquid cultures grown with rapid aeration at 180 rpm. HEK293 cells were grown in a static incubator at 37 °C and 5 % $CO_2$.

### *2.1.1 Yeast media*

#### *2.1.1.1 Yeast extract, peptone, dextrose (YPD) medium*

2 % w/v glucose, 1 % w/v yeast extract (Difco), 2 % w/v bactopeptone (Difco)

#### *2.1.1.2 Synthetic complete (SC) drop-out medium*

2 % glucose, 0.67 % Yeast Nitrogen Base without Amino Acids (Formedium), Yeast Synthetic Complete Drop-out Media Supplement (Formedium) added to manufacturers' guidelines.

#### *2.1.1.3 Media for microscopy*

Because of issues with auto-fluorescence generating background noise during microscopy all strains grown for microscopy were done so in low fluorescence media with sterilisation achieved through filtration rather than autoclaving. The low fluorescence media consisted of 2 % w/v glucose, 0.69 % Yeast Nitrogen Base without Amino Acids and without Folic Acid and Riboflavin - LoFlo (Formedium), Yeast Synthetic Complete Drop-out Media Supplement (Formedium) added to manufacturers' guidelines. This was filtered through a 0.2 µm filter to prevent caramelisation of the glucose.

## *2.1.2 Bacterial media*

### *2.1.2.1 Yeast, Tryptone (YT) medium*

1% yeast extract, 1.6 % tryptone, 0.5% NaCl

## *2.1.3 Cell culture media*

### *2.1.3.1 Media for HEK293 cells prior to Flp-In transfection*

DMEM, High Glucose, GlutaMAX (Invitrogen, 6195-026) with 2 mM glutamine (Invitrogen, 21765-029), 10 % FBS (Invitrogen 16000-044) and 1/1000 Zeocin (Invitrogen)

### *2.1.3.2 Media for HEK293 cells post Flp-In transfection*

DMEM, High Glucose, GlutaMAX (Invitrogen, 6195-026) with 2 mM glutamine (Invitrogen, 21765-029), 10 % FBS (Invitrogen 16000-044) and 100 µg/ml Hygromycin B (Invitrogen, 10687-010)

### *2.1.3.3 HEK293 cell maintainance*

HEK293 cells were grown in DMEM medium as described in 2.1.3.2. Cells were maintained in T25 flasks and upon reaching 75 % confluence they were split 1:10. Cell splitting was carried out by enzymatic trypsinisation of the focal adhesions using Trypsin-EDTA (0.05 % Trypsin, 0.53 mM EDTA.4Na, Invitrogen). The medium that cells were grown in was aspirated off and discarded, 0.75 ml of Trypsin-EDTA was added to the cells and they were incubated at 37 °C for 3 minutes. To detach the cells from the surface of the flask, the flask was hit five to seven times and then 0.75 ml of DMEM was added to neutralise the Trypsin-EDTA. 7 ml of DMEM was put in a new T25 flask and then 150 µl of the cell suspension was added to this. Cells were grown at 37 °C and 5 % $CO_2$.

## 2.2 Strains

### *2.2.1 Yeast strains*

**Table 2.1 – Teast strains used in this study**

| Strain | Genotype | Source/ Reference |
|---|---|---|
| **BY4741** | *MATa his3Δ1 leu2Δ0 met15Δ0 ura3Δ0* | CWG collection |
| **Δabp140** | BY4741 *abp140::KANMX* | Mat a knockout collection |
| **Δacf4** | BY4741 *acf4::KANMX* | Mat a knockout collection |
| **Δaim21** | BY4741 *aim21::KANMX* | Mat a knockout collection |
| **Δaim3** | BY4741 *aim3::KANMX* | Mat a knockout collection |
| **Δaim7** | BY4741 *aim7::KANMX* | Mat a knockout collection |
| **Δaip1** | BY4741 *aip1::KANMX* | Mat a knockout collection |
| **Δadp1** | BY4741 *adp1::KANMX* | Mat a knockout collection |
| **Δarc18** | BY4741 *arc18::KANMX* | Mat a knockout collection |
| **Δark1** | BY4741*ark1::KANMX* | Mat a knockout collection |
| **Δarp1** | BY4741 *arp1::KANMX* | Mat a knockout collection |
| **Δarp5** | BY4741 *arp5::KANMX* | Mat a knockout collection |
| **Δarp6** | BY4741 *arp6::KANMX* | Mat a knockout collection |
| **Δarp8** | BY4741 *arp8::KANMX* | Mat a knockout collection |
| **Δbag7** | BY4741 *bag7::KANMX* | Mat a knockout collection |
| **Δbbc1** | BY4741 *bbc1::KANMX* | Mat a knockout collection |
| **Δbit2** | BY4741 *bit2::KANMX* | Mat a knockout collection |
| **Δbit61** | BY4741 *bit61::KANMX* | Mat a knockout collection |
| **Δbni1** | BY4741 *bni1::KANMX* | Mat a knockout collection |
| **Δbnr1** | BY4741 *bnr1::KANMX* | Mat a knockout collection |
| **Δbsp1** | BY4741 *bsp1::KANMX* | Mat a knockout collection |
| **Δbud6** | BY4741 *bud6::KANMX* | Mat a knockout collection |
| **Δbzz1** | BY4741 *bzz1::KANMX* | Mat a knockout collection |
| **Δcap1** | BY4741 *cap1::KANMX* | Mat a knockout collection |
| **Δcap2** | BY4741 *cap2::KANMX* | Mat a knockout collection |
| **Δcrn1** | BY4741 *crn1::KANMX* | Mat a knockout collection |
| **Δcyk3** | BY4741 *cyk3::KANMX* | Mat a knockout collection |
| **Δend3** | BY4741 *end3::KANMX* | Mat a knockout collection |
| **Δent1** | BY4741 *ent1::KANMX* | Mat a knockout collection |
| **Δent2** | BY4741 *ent2::KANMX* | Mat a knockout collection |
| **Δgea1** | BY4741 *gea1::KANMX* | Mat a knockout collection |
| **Δgip3** | BY4741 *gip3::KANMX* | Mat a knockout collection |
| **Δjnm1** | BY4741 *jnm1::KANMX* | Mat a knockout collection |
| **Δlsb6** | BY4741 *lsb6::KANMX* | Mat a knockout collection |
| **Δmsb3** | BY4741 *msb3::KANMX* | Mat a knockout collection |
| **Δmyo4** | BY4741 *myo4::KANMX* | Mat a knockout collection |

| | | |
|---|---|---|
| **Δplp1** | BY4741 *plp1::KANMX* | Mat a knockout collection |
| **Δrgd1** | BY4741 *rgd1::KANMX* | Mat a knockout collection |
| **Δrvs167** | BY4741 *rvs167::KANMX* | Mat a knockout collection |
| **Δsac6** | BY4741 *sac6::KANMX* | Mat a knockout collection |
| **Δsac7** | BY4741 *sac7::KANMX* | Mat a knockout collection |
| **Δscp1** | BY4741 *scp1::KANMX* | Mat a knockout collection |
| **Δsiw14** | BY4741 *siw14::KANMX* | Mat a knockout collection |
| **Δsla1** | BY4741 *sla1::KANMX* | Mat a knockout collection |
| **Δslo1** | BY4741 *slo1::KANMX* | Mat a knockout collection |
| **Δspa2** | BY4741 *spa2::KANMX* | Mat a knockout collection |
| **Δtpm2** | BY4741 *tpm2::KANMX* | Mat a knockout collection |
| **Δtsc11** | BY4741 *tsc11::KANMX* | Mat a knockout collection |
| **Δtwf1** | BY4741 *twf1::KANMX* | Mat a knockout collection |
| **Δvrp1** | BY4741 *vrp1::KANMX* | Mat a knockout collection |
| **Δyke2** | BY4741 *yke2::KANMX* | Mat a knockout collection |
| **Δysc84** | BY4741 *ysc84::KANMX* | Mat a knockout collection |
| **ARP1-GFP** | BY4741 | Yeast GFP Clone collection |
| **TUB4-GFP** | BY4741 | Yeast GFP Clone collection |
| **TKY881** | *Matα ura3-52, leu2-3, 112 trp1-delta1, lys2-20, met2-1, his4-713, tef1::LEU2, tef2delta, pTEF1-URA3 TRP1* | (Gross and Kinzy, 2007) |
| **TKY882** | *TKY881 pTEF1-URA3 TRP1 N329D Y355C* | (Gross and Kinzy, 2007) |
| **TKY883** | *TKY881 pTEF1-URA3 TRP1 K333E* | (Gross and Kinzy, 2007) |
| **TKY885** | *TKY881 pTEF1-URA3 TRP1 H924A Q296R* | (Gross and Kinzy, 2007) |
| **TKY886** | *TKY881 pTEF1-URA3 TRP1 F308L* | (Gross and Kinzy, 2007) |
| **TKY887** | *TKY881 pTEF1-URA3 TRP1 N305S* | (Gross and Kinzy, 2007) |
| **TKY888** | *TKY881 pTEF1-URA3 TRP1 S405P* | (Gross and Kinzy, 2007) |
| **TKY889** | *TKY881 pTEF1-URA3 TRP1 N329S* | (Gross and Kinzy, 2007) |

The yeast MATa knockout collection was generated by the yeast genome project consortium (http://www-sequence.stanford.edu/group/yeast_deletion_project/consortium.html) and purchased from Open Biosystems (now part of GE Healthcare).

### 2.2.2 Bacterial strains

| | |
|---|---|
| ***DH5α*** | F-*deoR endA1 relA1 gyrA96 hsdT17(rk- mk+) phoA supE44 thi-1 Δ(lacZYA-argF)U169 φ80δlacZΔM15* |

### 2.2.3 Mammalian cell lines

| | |
|---|---|
| **Flp-in HEK293** | Adherent Human embryonic kidney (Graham *et al.*, 1977). pFRT/*lacZeo* |

## 2.3 Plasmids

**Table 2.2 – Plasmids used in this study**

| Name | Description | Source/Reference |
|---|---|---|
| **pCG124** | *pAG425GPD-ccdB, Gateway expression vector, Leu2, 2µ* | Invitrogen |
| **pTHE53** | *pENTR/TEV/D-TOPO TEF1* | TvdH collection |
| **pCG454** | pCG124 containing pTHE53 *Leu2*::TEF1, 2µ | This study |
| **pcDNA5.0/** | *Flp-In control plasmid, hygromycin resistance* | Invitrogen |
| **pcDNA3/1A2** | *Plasmid used for amplification of human eEF1A2* | (Anand *et al.*, 2002) |
| **pcDNA5.0/1A2** | Human eEF1A2 expression vector | This study |

## 2.4 DNA and RNA methods

### *2.4.1 Gateway cloning*

All yeast overexpression vectors were generated using the Gateway PCR Cloning System (Invitrogen). The entry clones were generated in donor vector, pDONR221, with the addition of a gene of interest. The *TEF1* entry vector was generated in our lab by Claudia Solscheid, with all others being generated during this project. Entry clones were created by amplifying a GOI flanked by attB sites using PCR. Recombination of the donor vector and attB-flanked PCR product was catalysed by the addition of BP clonase enzyme mix. The BP clonase reaction results in recombination of the attB-PCR product and the linearised donor vector creating the attL containing entry clone and an attR by product.

Yeast expression clones were generated by recombining the entry clone with a destination vector. Recombination of the attL entry clone and attR-destination vector was catalysed by the addition of LR clonase enzyme mix. The LR clonase reaction results in recombination of

the attL entry clone and the attR destination vector donor vector creating the attB containing expression clone and an attP by product (see figure 2.1)

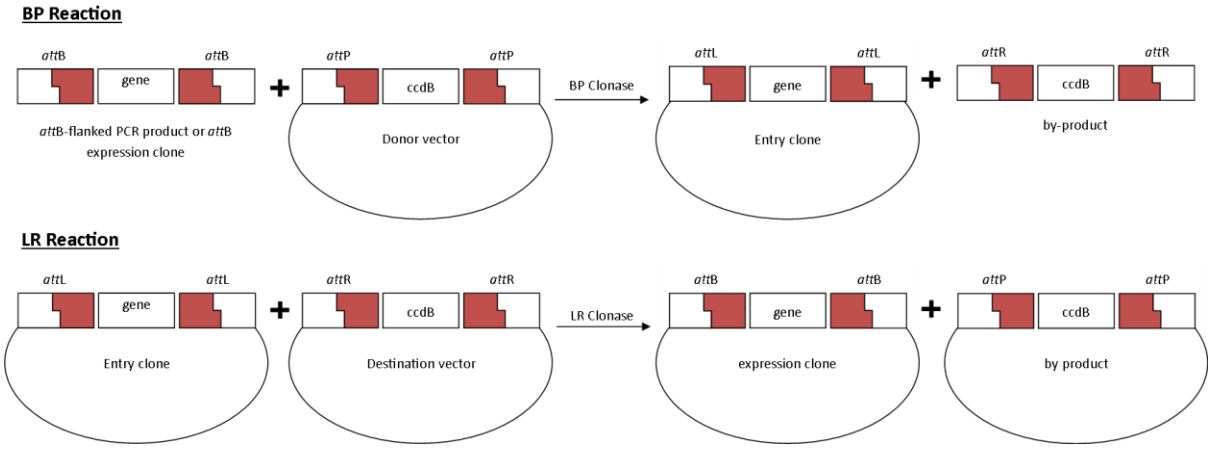


***Figure 2.1, Overview of Gateway BP and LR reactions.*** *The BP reaction catalyses a reaction between attB flanked PCR product and a Donor Vector to generate an Entry Clone. The LR reaction catalyses a reaction between an Entry Clone and a Destination Vector to generate an Expression Clone.*

## *2.4.2 Insertion of DNA into a yeast cell*

### *2.4.2.1 Yeast transformation*

**Table 2.3 - Yeast transformation reagents**

| Reagent | Stock Concentration | Final Concentration |
|---|---|---|
| **TE** | 10 x | 1 x |
| **LiAc** | 1 M | 0.1 M |
| **PEG** | 50 % | 40 % |
| **ssDNA** | 10 mg/ml | 0.1 mg/ml |
| **Plasmid DNA** | 100 – 200 µg/ml | 0.4 – 1 µg/ml |

A freshly streaked yeast colony was picked and inoculated into 5 ml of appropriate media. This was grown overnight at 30 °C with shaking at 180 rpm. 1 ml of overnight culture was collected in a 1.5 ml eppendorf and pelleted using a bench-top centrifuge at 3000 rpm for 4 minutes. The supernatant was discarded and the pellet was resuspended in 500 µl of TE. Cells were pelleted again at 3000 rpm for 4 minutes and the supernatant was discarded. Cells were then resuspended in 500 µl of 0.1 M LiAc in TE and pelleted for a final time at 3000 rpm for 4

minutes, the supernatant was discarded. Cells were resuspended in 100 µl 0.1 M LiAc in TE and then 15 µl of ssDNA and 2 µl of plasmid DNA was added. 700 µl of 40% PEG with 0.1 M LiAc in TE was added and cells were briefly vortexed at full speed. The eppendorfs were placed in a heat block at 42 °C and left to incubate for 15 minutes. Following heat shock cells were pelleted at 3000 rpm for 4 minutes and gently resuspended in 200 µl of selective media before 100 µl of cell suspension was plated on to appropriate plates. Plates were incubated at 30 °C for 3 days and colonies were re-streaked onto appropriate synthetic complete drop-out selection medium.

### *2.4.2.2 Preparation of competent cells*

10 ml of YT was inoculated with DH5-α cells and grown overnight at 37 °C with shaking at 200 rpm. 8 µl of overnight culture was inoculated into 28 ml of YT broth and incubated at 37 °C with shaking at 200 rpm for approximately 4.5 hours. 5 minutes prior to reaching an $OD_{600}$ of 0.5, 3.75 ml of sterile, warm 100% glycerol was slowly added whilst still shaking the flask. The cells were chilled on ice for 10 minutes and then pelleted at 4000 rpm and 4 °C for 10 minutes. The supernatant was discarded and cells were resuspended in an equal volume of ice cold 0.1 M $MgCl_2$ plus glycerol. Cells were pelleted at 3800 rpm and 4 °C for 8 minutes before re-suspending in 6.25 ml of ice cold T-salts. Cells were incubated on ice for 20 minutes with occasional mixing. Cells were pelleted for a final time at 3600 rpm and 4 °C for 6 minutes. Cells were resuspended in 1.25 ml of T-salts and aliquoted into pre-cooled 0.5 ml eppendorfs. The eppendorfs were stored immediately at -80 °C until required.

### *2.4.2.3 Escherichia coli transformation with plasmid DNA*

Competent cells (as previously described) were thawed on ice and gently mixed. 0.2 – 1 µg of DNA was added to 50 µL of competent cells. The transformation was incubated on ice for 30

minutes and then heat shocked at 42 °C for 90 seconds. The cells were pelleted at 4000 rpm for 3 minutes and the supernatant was discarded. Cells were resuspended in 200 µl of YT broth and were allowed to recover at 37 °C with shaking at 200 rpm for 1 hour. 100 µl of cell suspension was plated onto YT plates containing the appropriate antibiotic and plates were incubated at 37 °C overnight.

### *2.4.3 Plasmid amplification and purification*

An *E.coli* colony that contained the plasmid of interest was inoculated into 5 ml of YT broth with the appropriate antibiotic and grown overnight at 37 °C with shaking at 200 rpm. 1 ml of cells was harvested in a 1.5 ml eppendorf by centrifugation at 13,000 rpm for 60 seconds. The plasmid DNA was isolated from the pellet using a Qiagen QIAprep Spin Miniprep Kit as per the manufacturers' instructions.

### *2.4.4 DNA quantification*

A BMG Labtech SPECTROstar Nano was used to measure and calculate DNA concentration. 1 µl of sample was loaded onto the LVis Plate, with upto 15 samples loaded at a time plus an Elution Buffer blank. A reading at $OD_{260}$ was measured allowing measurement of DNA concentration in µg/ml.

### *2.4.5 DNA digestion using restriction enzymes*

Restriction endonucleases for the digestion of DNA plasmids at specific sites were acquired from New England Biolabs, Roche and Promega. Digestions were carried out as per the manufacturers' guidelines but typically consisted of the following reagents per reaction:

**Table 2.4 - Regents for restriction digest**

| Reagent | Amount |
|---|---|
| **10 x Enzyme Buffer** | 2.5 µL |
| **Restriction Enzyme** | 0.5 µL |
| **DNA** | 1 µg |
| **dd$H_2O$** | Up to 25 µL |

All components were added to a 0.5 ml eppendorf and incubated at 37 °C typically for 2 hours but overnight incubation was sometimes required.

## *2.4.6 PCR amplification of DNA fragments*

PCR reactions were required to amplify desired DNA sequences. The PCR utilised the DNA polymerase Taq (Roche), a DNA template, primers and nucleotides. Reactions were performed at optimal conditions dependent upon the length of the fragment to be amplified and the nature of the primers used. A typical PCR reaction consisted of:

**Table 2.5 - Reagents for PCR amplification**

| **Reagent** | **Amount** |
|---|---|
| **10 x Taq Buffer** | 2.5 µL |
| **10 mM dNTPs** | 0.5 µL |
| **10 mM Primers** | 0.5 µL of each |
| **Template DNA** | 1 µg |
| **Taq polymerase** | 0.125 µL |
| **dd$H_2O$** | Up to 25 µL |

A typical program for a 2 kilobase fragment would be:

94 °C for 3 minutes, initial denaturation of temple DNA

94 °C for 30 seconds, short denaturation

54 °C for 1 minute, annealing (varies upon primer length and GC content) } Repeat for

72 °C for 2 minutes, elongation } 30 cycles

72 °C for 10 minutes, final elongation

### *2.4.7 Agarose gel electrophoresis*

Gels were prepared by adding the desired quantity (typically 0.7 g) of molecular biology grade agarose (Melford) to 1 x TAE buffer (40 mM tris, 1 mM EDTA and 20 mM Acetic acid, pH 8.5) and heating until dissolved. 0.5 µl of 10 mg/ml ethidium bromide was added per 30 ml of agarose TAE and then poured into casts with a comb being added following an inspection for bubbles in the molten gel. Once set the comb was removed and the get was transferred to an electrophoresis tank and covered in TAE. A 1 kb ladder was used for sample identification and DNA preps were mixed with 6 x loading buffer prior to loading into the gel. Typical gels were run at 70 V for 45 minutes. Gel analysis was performed using a shortwave transilluminator (312nm) with the image capture by digital camera.

### *2.4.8 DNA gel extraction*

DNA fragments were purified from agarose gels using the Qiagen QIAquick Gel Extraction Kit. Following image capture of the agarose gel it was transferred to a flatbed shortwave transilluminator (312 nm) and the desired bands were excised using a sterile scalpel. DNA was isolated from the gel fragments as per the manufacturers' manual.

### *2.4.9 DNA ligation*

Fragments of DNA were excised from the agarose gel as described in 2.4.8 and the purified DNA was ligated using the Roche Rapid DNA Ligation Kit as per the manufacturers' instructons.

### *2.4.10 Whole cell RNA extraction*

Whole yeast cell RNA extraction for microarray analysis was performed using the Qiagen RNeasy Mini Kit as per the manufacturers' manual.

### *2.4.11 Flp-In recombination*

Stable HEK293 cell lines were generated using the Invitrogen Flp-In Recombination System, as per the manufacturers' guidelines.

## 2.5 Protein methods

### *2.5.1 Whole cell protein extraction*

Whole cell protein extraction was performed as described in (von der Haar, 2007). A cell count was performed on cells in the desired phase of growth and 1 x $10^8$ cells were harvested by centrifugation in a bench-top centrifuge at 13,000 rpm for 1 minute. They were resuspended in 200 µl lysis buffer (0.1 M NaOH, 0.05 M EDTA, 2 % SDS, 2 % β-mercaptoethanol) and incubated at 90 °C for 10 minutes. 5 µl of 4 M acetic acid was added and samples were vortexed for 30 seconds before being incubated for a further 10 minutes at 90 °C. 50 µl of loading buffer (0.25 M Tris-HCl pH 6.8, 50 % glycerol, 0.05 % bromophenol blue) was added to each sample and they were stored at -20 °C until needed.

## *2.5.2 Protein separation by SDS-PAGE*

Proteins were separated by molecular mass using SDS-PAGE. Gels were composed of a resolving layer with acrylamide concentrations of 10 – 12.5 % and a stacking layer of 5 % (see recipes in table 2.3). The gels were prepared by pouring the resolving gel mixture into the ATTO Gel system cast and overlaying with isopropanol. Once the resolving layer had polymerised the isopropanol was discarded and the stacking gel mixture was poured on top followed by insertion of the comb. Once the stacking layer had polymerised the comb was removed and the gasket removed from the cast.

**Table 2.6 - Reagents for acrylamide gels**

| | Acrylamide concentration | | |
|---|---|---|---|
| | **10 %** | **12.5 %** | **5 % (stacking)** |
| **Acrylamide 40 %** | 2 ml | 2.5 ml | 0.375 ml |
| **1.5 M Tris (pH8.8)** | 2 ml | 2 ml | - |
| **0.5 M Tris (pH6.8)** | - | - | 0.75 ml |
| **$H_2O$** | 4 ml | 3.5 ml | 1.875 ml |
| **TEMED** | 5 µl | 5 µl | 3.5 µl |
| **10 % APS** | 35 µl | 35 µl | 35 µl |

The gel was then transferred to the electrophoresis tank and the tank was filled with 1 x TGS running buffer (10x TGS; 250 µM Tris pH8, 1.92 M glycine, 1% SDS, pH8.3). Samples were run at 90 volts until they had passed through the stacking layer, at which point the power was increased to 120 volts and run for a further 2 hours, or until the sample buffer ran off the gel.

## *2.5.3 Protein detection by western blotting and ECL detection*

Following separation by SDS-PAGE proteins were detected by western blot and enhanced chemiluminescence (ECL) detection.

### *2.5.3.1 Semi-dry protein transfer*

The first stage of western blotting was the semi-dry transfer of proteins from the SDS gel to the Polyvinylidene Fluoride (PVDF) membrane. To do this PVDF membrane and 2 sheets of blotting paper were cut to the same dimensions as the SDS gel; the PVDF was soaked in methanol and then placed in transfer buffer together with the blotting paper for 15 minutes. The first piece of the blotting paper was placed on the bottom electrode of a BioRad semi-dry transfer machine and any air bubbles removed. Next the PVDF membrane was placed on top, again removing air bubbles to ensure uniform transfer. The SDS gel was removed from the electrophoresis tank and the cast, and the stacking layer was removed using a scalpel and then discarded. The resolving gel was then gently placed on top of the PVDF membrane ensuring no air bubbles were present. The final piece of blotting paper was placed on top and then the top electrode was locked in place. The power pack was set to 25 V and would be run for 15 minutes per blot. When the transfer was complete the PVDF was removed for use in immunoblotting.

### *2.5.3.2 Immunoblotting*

Immunoblotting was used to detect desired proteins. The PVDF membrane (from the Semi-dry transfer) was placed in blocking buffer (5 % w/v dried milk in PBST [PBS with 0.2% Tween]) and shaken for 45 minutes at room temperature. The membrane was rinsed in PBST and placed in a flat tray containing 20 ml blocking buffer with the appropriate anti-body at the concentration recommended by the manufacturer. This was left shaking at 4 °C overnight. Following the primary anti-body conjugation the membrane was rinsed with PBST and then given one 15 minute, and two 5 minute washes in PBST. The membrane was then placed into a clean flat tray and covered with 20 ml of blocking buffer containing the secondary anti-body at the appropriate concentration. This was left to shake at room temperature for 30 minutes.

Following the secondary anti-body conjugation the membrane was rinsed again in PBST and then given a further 15 minute wash and three 5 minute washes in PBST.

**Table 2.7 - Antibodies used for immunoblotting**

| Name | Raised against | Raised in | Concentration used at |
|---|---|---|---|
| **α-eEF1A1** | Human eEF1A1 | Rabbit | 1/3000 |
| **α-eEF1A2** | Human eEF1A2 | Rabbit | 1/3000 |
| **α-Rabbit HRP** | Rabbit IgG | Goat | 1/5000 |

### *2.5.3.3 ECL detection*

Detection of proteins on the PVDF membrane was performed using ECL detection. The following procedures were carried out in a dark room with red light as the only light source. The two developing solutions (see table 2.4) were mixed at a 1:1 ratio and poured over the PVDF membrane in a clean box, they were left for 1 minute at room temperature and the membrane was then drained and placed between two sheets of plastic wrap inside a developing cassette. A sheet of X-ray film was placed on top of the plastic sheet and the developing cassette was closed for the appropriate amount of time to acquire the desired exposure (approximately 1 minute). The x-ray film was removed and placed into the developing machine (XOgraph Compact X4) completing the detection process.

**Table 2.8 - Reagents for ECL solutions**

| Reagent | Stock concentration | Solution I | Solution II |
|---|---|---|---|
| **Luminol** | 250 mM | 1 ml | - |
| ***p*-coumaric acid** | 90 mM | 0.44 ml | - |
| **TRIS. HCl (pH8.5)** | 1 M | 10 ml | 10 ml |
| **$H_2O_2$** | 30% | - | 64 µl |
| **$H_2O$** | - | Up to 100 ml | Up to 100 ml |

## *2.5.4 Metabolite detection*

To characterise the cellular metabolome in yeast, cells were grown to the desired phase of growth and either had their entire metabolome extracted, or just that of the vacuole. Detection of metabolites was carried out using proton and carbon based NMR.

### *2.5.4.1 Whole cell metabolite extraction*

50 ml cultures were grown to the desired phase of growth and a cell count was performed for quantification purposes. Cells were decanted into 50 ml falcons and cooled on ice before pelleting at 3000 g and 4 °C for 5 minutes. They were then washed twice in 25 ml of ice cold water and the biomass was weighed for quantification purposes. 5ml of boiling 75 % EtOH was added to the pellet together with 2 ml of 0.3 mm glass beads. The samples were vortexed for 30 seconds and then incubated at 80 °C for 3 minutes followed by another 30 second vortex. Samples were decanted into a 15 ml falcon leaving the beads in the 50 ml falcon for a second wash with a further 2 ml of 75 % EtOH that was then combined with the remainder of the sample in the 15 ml falcon. Samples were then aliquoted into 2 ml eppendorfs and centrifuged at 16,000 g for 10 minutes to remove cell debris. Samples were transferred to clean 2 ml eppendorfs and dried overnight in a Rotorvac at 37 °C. Samples were resuspended in 330 µl of $H_2O$ and spun at 5000 rpm for 10 minutes to remove any further debris, before

combining the supernatant into a single 1.5 ml eppendorf. Samples were frozen at -20 °C before being freeze dried overnight. Samples were stored at -20 °C until required.

#### *2.5.4.2 Vacuolar metabolite extraction (adapted from* Destruelle et al., (1995)*)*

100 ml cultures were grown to the desired phase of growth, decanted into 50 ml falcons and cooled on ice. Cells were pelleted at 3000 g and 4 °C for 5 minutes before being washed twice in 25 ml of ice cold water. They were resuspended in 10 ml amino acids buffer (2.5 mM potassium phosphate buffer, pH 6, 0.6 M sorbitol, 10 mM glucose, and 0.2 mM $CuCl_2$), and incubated at 30 °C for 10 minutes. Cell suspensions were harvested by filtration on 0.45 µm membrane filters (Millipore) and washed five times with amino acid buffer lacking 0.2 mM $CuCl_2$. Cells retained on the filter were resuspended in $H_2O$ and boiled for 15 minutes. The cell suspension was then centrifuged at 100,000 g for 1 hour and the supernatant was collected as the vacuolar fraction.

#### *2.5.4.3 Metabolite detection by NMR*

Nuclear Magnetic Resonance (NMR) spectroscopy was used to analyse the metabolite preps. Experiments were performed at 298 K on a Bruker AVANCE 3 600 MHz spectrometer, equipped with a QCI-F cryoprobe. Data sets were acquired with 64k points and a proton window size of 16 ppm. Spectra were referenced against an internal standard of DSS. The excitation sculpting method was used to suppress the water peak using pulsed field gradients.

#### *2.5.4.4 Metabolite analysis*

Analysis of data acquired by NMR spectroscopy was performed using Bruker TopSpin and AMIX data analysis software, as well as CcpNmr Analysis (Vranken *et al.*, 2005). Identification of metabolites was performed by comparison to previously published data on the Madison Metabolomics Consortium Database, peak assignment of 2D spectra, and the generation of a

new metabolite database at the University of Kent that now contains 47 metabolite standards.

#### *2.5.4.5 Metabolite quantification*

Addition of a DSS (4,4-dimethyl-4-silapentane-1-sulfonic acid) standard of known concentration to the sample gave us the ability to quantify the concentration of other metabolites in the NMR spectrum. We utilised Bruker TopSpin to quantify peak intensity, the total area under a peak of interest, for peaks that were known to be unique to assigned metabolites and compared them to the intensity of the DSS standard. Using this method gave us relative values, but for absolute concentrations we needed to know how many protons accounted for each peak. Once we had peak intensities for the DSS standard and the metabolite of interest, and the proton number we were able to use the equation below to calculate the concentration, where X is the peak of interest.

**Concentration (μM) =**

**peak X intensity/((DSS peak intensity/9 protons)*peak X protons)*50**

## 2.6 Phenotypic analyses

### *2.6.1 Fluorescence microscopy*

All fluorescence microscopy was performed on an Olympus IX81 inverted research microscope. Images were captured through a Hamamatsu photonics ORCA AG cooled CCD digital camera, with light excitation from an Olympus MT20 illumination system. Control of the system was through the Olympus Cell^R imaging software. Images were processed using

Huygens deconvolution software from Scientific Volume Imaging. All images were captured using a 60x objective.

#### *2.6.1.1 GFP and RFP tagged proteins*

Observation of proteins in yeast is facilitated by the generation of the GFP library (Huh *et al.*, 2003) that has three quarters of the yeast proteome individually tagged to GFP. This was the primary source for GFP strains, with the remainder of the GFP/RFP strains generated during this project being plasmid based expression systems.

#### *2.6.1.2 Actin visualisation using Rhodamine Phalloidin*

Actin was visualised by staining cells with Rhodamine Phalloidin (Invitrogen). Cells were grown to the desired growth phase and 1 ml of culture was transferred to a 1.5 ml eppendorf. Cells were fixed in 5 % formaldehyde and left at room temperature for 1 hour. Cells were pelleted at 3000 rpm for 4 minutes and then washed twice with PBS + 1 mg/ml BSA + 0.1 % TX-100. The pellet was resuspended in 50 µl of the wash solution + 2 µl of Rhodamine Phalloidin and incubated in the dark for 30 minutes. Following staining, cells were washed in PBS + 1 mg/ml BSA and finally resuspended in an appropriate volume of PBS/BSA ready for visualisation.

#### *2.6.1.3 Immnuofluorescence of yeast cells*

Cells were grown to the desired phase of growth and fixed in 5 % formaldehyde for 1 hour. The cells were pelleted by centrifugation at 3000 rpm for 4 minutes and washed twice in sorbitol buffer (1.2 M sorbitol, 0.1 M potassium phosphate buffer pH7.5), centrifugation during the wash steps was performed at maximum speed in an IEC clinical centrifuge. Cells were resuspended in 0.5 ml sorbitol buffer + 1 µl β-mercaptoethanol + 20 µl 1 mg/ml zymolyase and incubated at 37 °C for 40 minutes. During the incubation, slides were prepared

by loading 15 µl poly-L-lysine (PLL) to the centre and leaving to sit for 2 minutes. Excess PLL was rinsed off with $H_2O$ and the slides were left to air dry. Cells concentration was adjusted to the desired level and 15 µl of cell suspension was added to each slide and allowed to settle for 5 minutes before excess suspension was aspirated off. 10 µl of 0.1 % SDS was added to each slide for 30 seconds and slides were washed ten times with PBS + 1 mg/ml BSA. Slides were handled in a moist environment to prevent dehydration from this point. The primary anti-body was diluted as required in PBS/BSA and 15 µl was added to each slide before being incubated in a damp box overnight at 4 °C. Slides were washed a further ten times with PBS/BSA before adding 15 µl of the secondary anti-body in PBS/BSA and leaving to incubate in the dark at room temperature for 1 hour. Slides were washed ten more times and then a drop of phenylenediamine mounting solution containing DAPI at 1 mg/ml was placed on top of the cells. A cover slip was gently but firmly put in place ensuring the exclusion of all air bubbles and the edges were sealed with nail varnish ready for visualisation.

#### *2.6.1.4 Immunofluorescence of HEK293 cells*

HEK293 cells were grown to 70 % confluence and trypsinised as described in 2.1.3.3. Coverslips placed into 6 well plates, coated with sterile poly-L-lysine 1 mg/ml (Invitrogen-P4707) and left to settle for 15 minutes, the excess PLL was aspirated off, coverslips were washed three times with 2 ml sterile water and left to dry at room temperature. 2 ml of DMEM was added to each well and then 50 µl of cells was added. These were left to grow for 24 hours. Once cells were at 70 % confluence the media was removed, cells were washed with PBS and fixed with 1 ml of 4 % paraformaldehyde in PBS for 15 minutes. Following fixation cells were permeabalised with 0.1 % TX-100 in PBS for 5 minutes and then blocked in 250 µl 3 % BSA/PBS for 15 minutes at room temperature. 25 µl droplets of the primary antibody were applied to a sheet of parafilm and the coverslips were placed cell side down on the drops

and left in a moist environment overnight at 4 °C. Coverslips were then placed on four 100 µl droplets of PBS/0.1 % Tween sequentially and left on each for 5 minutes to wash. During washing the secondary antibody was prepared to the desired concentration and spun down for 10 minutes at 16100 x g to remove any aggregates. 25 µl droplets of the secondary antibody were arranged on a sheet of parafilm in a damp box and the coverslips were placed cell side down and left to incubate at room temperature in the dark for 2 hours. Coverslips were washed a further four times on 100 µl droplets of PBS/ 0.1% Tween as previously described and then placed cell side down onto 25 µl droplets of DAPI for 1 minute followed by two 10 minute washes with PBS. 100 µl 0.1 % *p*-Phenylenediamine anti-fade (Sigma P6001-50G) was mixed with 900 µl 10 % mowiol mounting solution (Sigma 81381-50G), 5 µl droplets of this mounting mix were added to glass slides and the coverslips were placed, cell side down, on top of the droplets, ensuring no air bubbles were present. Prepared slides were left at 4 °C overnight for the mounting solution to set before sealing with nail varnish ready for visualisation.

## *2.6.2 Growth analysis*

### *2.6.2.1 Absorbance assays for growth rate analysis of yeast strains*

A 5 ml overnight culture was grown in the appropriate medium and the cell density of each culture was determined by absorbance at $OD_{600}$ in an Eppendorf BioPhotometer plus. Cells were diluted to a starting $OD_{600}$ of 0.1 in 1 ml of the appropriate media in a greiner bio-one 24 well cell culture plate (Greiner bio-one 662 160) Growth of strains was performed in a BMG LABTECH SPECTROstar$^{Nano}$ plate reader. Protocol settings for growth analysis were are outlined in the table below. All data were exported to excel for further analysis.

Prior to any further analysis all data were blank corrected. Data was then log transformed and the maximal growth rate was calculated over a 3 hour period. This was calculated by subtracting the OD at the earliest point within the three hour window from the final point, and dividing by 3 (the number of hours between points). Conversion of growth rate to doubling time was performed for ease of data presentation and was calculated by dividing 0.693 by the growth rate. Quantification of lag phase was performed by measuring the time it took for cultures to double their initial OD.

**Protocol settings for yeast growth analysis in 24 well plates**

Cycle time (sec): 1800
Flashes per well: 3
Excitiation: 600
Shaking frequency (rpm): 400
Shaking mode: double orbital
Additional shaking time: 30 sec before each cycle
Target temperature (°C): 30
Posistioning delay: 0.5 sec

### *2.6.2.2 Spotting assay for yeast colony size analysis*

A 5 ml overnight culture was grown in the appropriate medium and a cell count was performed. Cells were diluted to 1 x $10^7$ cells/ml and were diluted 1000 fold over three serial dilutions. Cells were then plated onto the appropriate media and allowed to grow at 30 °C for 48-72 hours. Following growth, visual analysis was performed to assess the differences in growth.

### *2.6.2.3 Viability assay for yeast*

A 5 ml overnight culture was grown in the appropriate medium and a cell count (see section 2.6.2.5) was performed. Cells were diluted to 2 x $10^3$ cells/ml and 150 µl (approximately 300 cells) was plated on to the appropriate media. Cells were left to grow at 30°C for 36-72 hours before colony formation was assessed. Colony forming units (CFUs) were counted and the percentage viability was calculated by dividing the number of observed CFUs by the number of expected colonies (300), this was then multiplied by 100.

### *2.6.2.4 Growth analysis of HEK293 cells*

Cells were grown at 37 °C to 70 % confluence in a T75 flask containing the appropriate media. They were trypsinised as described in section 2.1.3.3 a cell count was performed and cells were diluted to 5x$10^4$/ml. 100 µL of media was added to the wells of the Xcelligence plate and allowed to equilibrate at room temperature before a base line cell index (CI) reading was taken. 100 µL of diluted cells was then added to each well resulting in a final concentration of 5x$10^3$ cells per well, these were again allowed to equilibrate at room temperature for 30 minutes before beginning the assay. Cells were placed in the plate reader at 37°C for the duration of the assay, typically 4-5 days. All data were exported to Excel for analysis.

Prior to any further analysis all data were blank corrected. Data was then log transformed and the maximal growth rate was calculated over a 3 hour period. Conversion of growth rate to doubling time was performed for ease of data presentation.

### *2.6.2.5 Yeast cell counting*

Cell counts were performed using a haemocytometer. An overnight culture was diluted 1/25 for ease of counting, log cultures were counted without dilution. 50 µL of culture was loaded onto the haemocytometer and then counted under a light microscope. Cells with buds greater

than one third the size of the mother cell were counted as two cells, otherwise buds were not counted. Only cells contained within, or on the bottom or left hand line of the box were counted. Where possible a minimum of 300 cells were counted.

## 2.7 Health and Safety

All work was carried out following the health and safety guidelines outlined in the relevant material for each procedure, and within the University handbook.

# Chapter 3: Yeast as a model organism to study the effects of eEF1A overexpression

## 3.1 Introduction: Overexpression of eEF1A in yeast results in pleiotropic effects

Previous studies on the function of eEF1A in yeast have suggested that not only does it play a role during protein synthesis, but it also moonlights in a variety of other roles. Studies have characterised eEF1A as an actin binding protein capable of bundling actin into unique structures that exclude all other actin cross linkers (Yang *et al.*, 1990; Owen *et al.*, 1992). It has also been suggested to be involved in protein degradation (Gonen *et al.*, 1994; Hotokezaka *et al.*, 2002), nuclear export (Bohnsack *et al.*, 2002; Calado *et al.*, 2002), viral replication (Mateyak and Kinzy, 2010), aggresome formation (Meriin *et al.*, 2012), possess both pro- and anti-apoptotic properties (Duttaroy *et al.*, 1998; Talapatra *et al.*, 2002) and promote tumour growth (Anand *et al.*, 2002).

The mechanisms of many of these functions are not yet fully understood and this study aimed to elucidate novel interactions between eEF1A and the cellular machinery to assist in the understanding of eEF1A's plethora of functions within the cell.

This chapter presents data suggesting that elevated levels of eEF1A are toxic to the cell and are under strict regulation facilitated by rapid plasmid loss of the overexpression plasmid when selective pressures in favour of keeping the plasmid are lifted.

## 3.2 Growth analysis of yeast cells overexpressing eEF1A isoforms

### *3.2.1 eEF1A levels influence lag and log phase yeast cells*

Previous studies on *TEF1* overexpression have showed that increased levels of eEF1A cause a slow growth phenotype that is not the result of an altered rate of translation (Munshi *et al.*, 2001). It has been proposed that this growth defect may be the result of altered actin

distribution and cell morphology, as elevated levels of eEF1A increases the fraction of un-budded cells, and resulted in larger and rounder cells.

Our studies focussed on the overexpression of one of the two genes encoding eEF1A in yeast, *TEF1*, on a 2μ (high copy) plasmid (pCG454) conferring leucine prototrophy (see figure 3.1). To confirm that overexpression of *TEF1* induced an alteration in growth rate a spotting assay was performed on both, selective minimal media, and non-selective media (see figure 3.2). This revealed that cells overexpressing eEF1A resulted in fewer, slower growing colonies compared to the wild type when grown on -leu. However, growth on non-selective media showed no growth difference between the wild type and *TEF1* overexpression strain suggesting that either, cells overexpressing *TEF1* were defective in leucine synthesis and non-selective media alleviated this defect, or *TEF1* was highly toxic and selected against inducing plasmid loss.

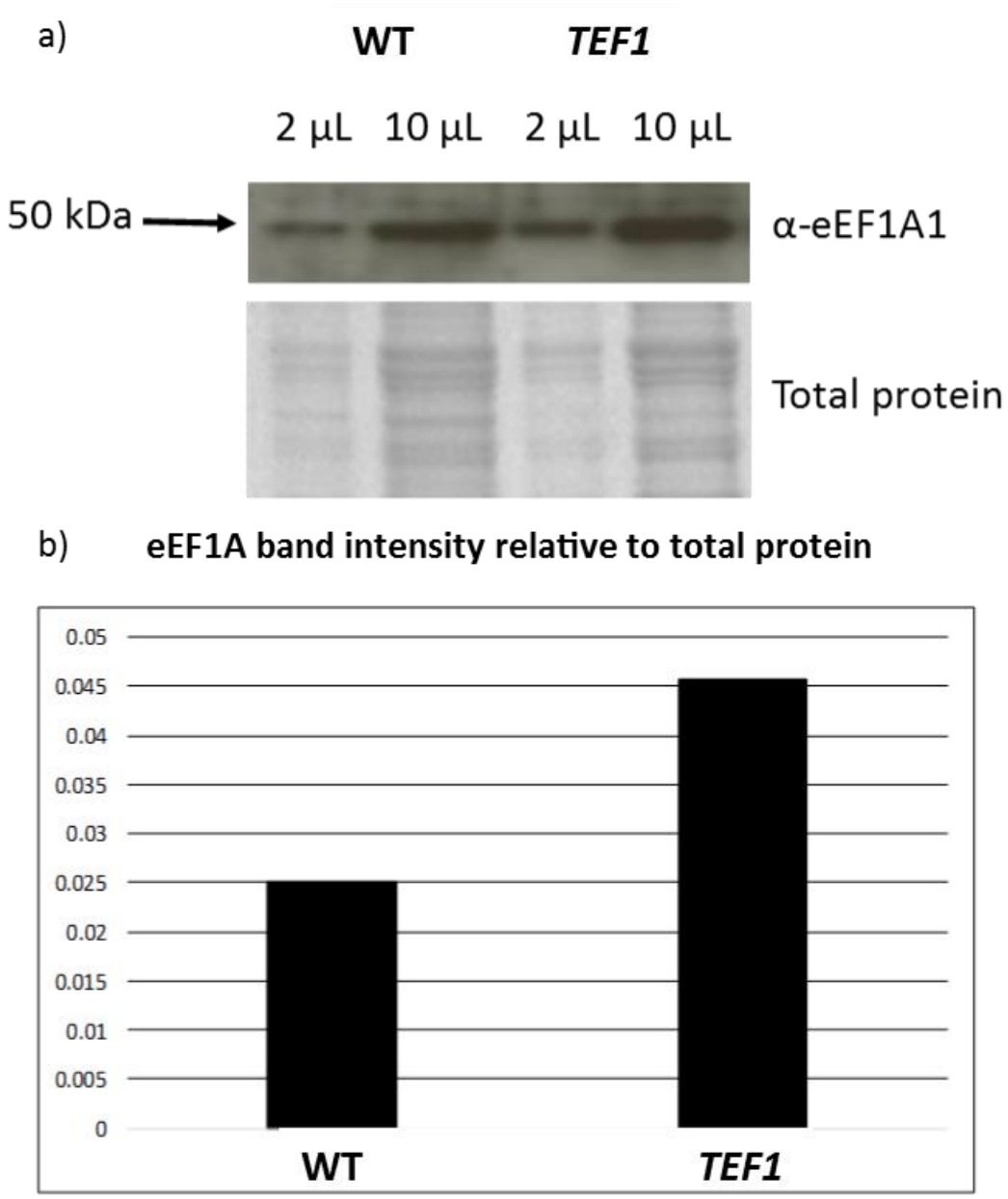


***Figure 3.1. Western blot showing increased levels of eEF1A.*** *a) eEF1A levels in yeast as detected by the anti-human eEF1A1. b) Expression levels are only increased by approximately 80% suggesting that eEF1A levels are under tight regulation by the cell.*

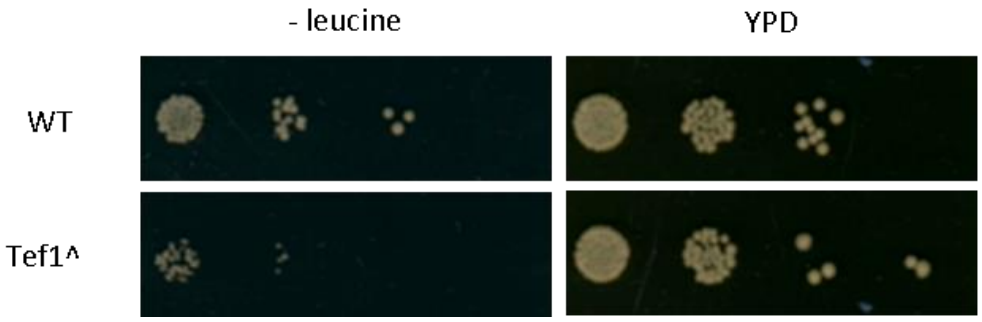


***Figure 3.2.Spotting assay of wild type cells and TEF1 overexpressing cells.*** *Cells were plated onto selective -leu and non-selective YPD media. A growth defect was observed in the TEF1 overexpressing cells when on selective media, When plated onto rich media however, growth was rescued. Cells were serially diluted from 2*10^6/ml to 2*10^3/ml.*

Further, high resolution, growth analysis was performed using a BMG Spectrostar Nano, microplate absorbance reader, as described in Material and Methods (section 2.6.2.1). This method allowed for in depth analysis of various stages of growth, including, lag, log and post diauxic phases (see figure 3.3).

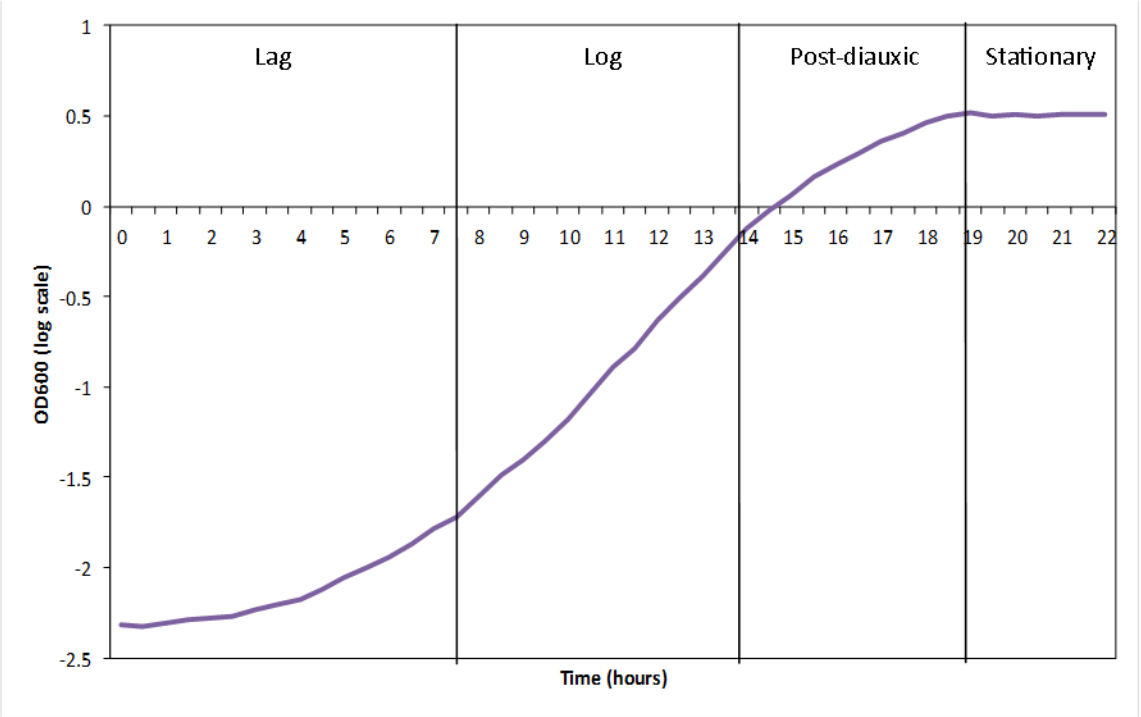


***Figure 3.3 Representation of a logarithmic growth curve.*** *The optical density of cells is measured at $OD_{600}$ and then expressed logarithmically. The initial lag phase of the curve is when the cells are adapting to a new environment. Log phase is when the cells are growing exponentially and are undergoing fermentation, converting sugars within the media to alcohol. Post diauxic is the stage that, when all sugars are depleted, the yeast cells begin to respire in the ethanol rich environment. Eventually all nutrients within the media are depleted and the cell cycle arrests resulting in stationary phase.*

When analysed using this technique it was observed that *TEF1* overexpression induced not only a reduction in the growth rate of cells (see figures 3.4 -a and -b), but also an increase in the lag phase (see figures 3.4 –a and –c). As previously discussed, an increase in doubling time when eEF1A is overexpressed has been well characterised and our observations correlated with this. We observed an increase in doubling time of 17.6% when eEF1A was overexpressed. We also found that the lag phase of these cells was increased by approximately 26%. We hypothesised the increase in lag could have been due to corruption of signalling or biosynthesis pathways, or because of a reduction of cell viability in the presence of elevated levels of eEF1A, therefore fewer viable cells were in the initial inoculum delaying the cultures entry into log phase growth.

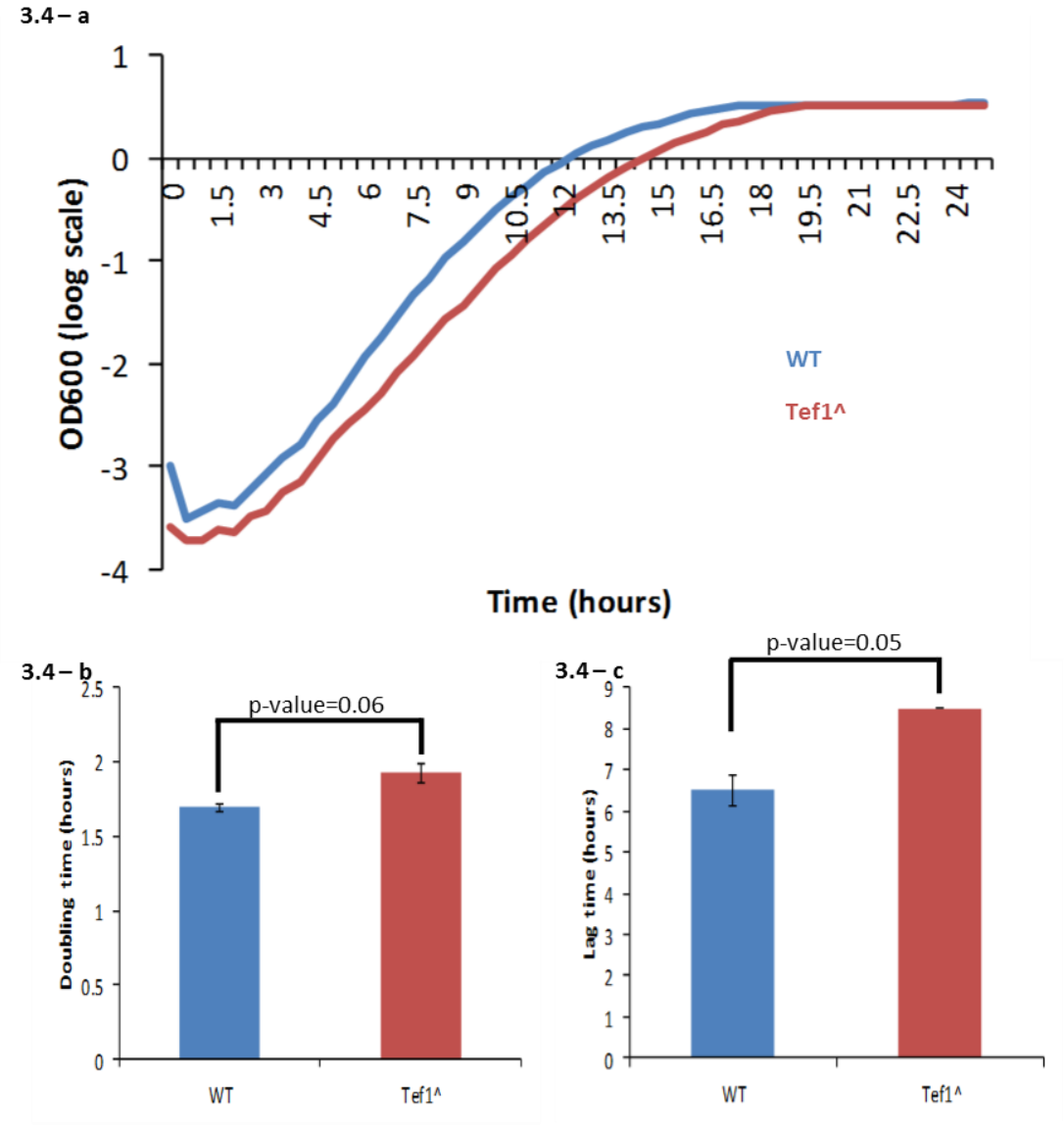


***Figure 3.4 Growth data for wild type and TEF1 overexpressing strains.*** *a) Logarithmic growth curve of wild type cells in blue and TEF1 overexpressing cells in red. b) The doubling time of wild type cells in blue, and TEF1 overexpressing cells in red. TEF1 overexpressing cells exhibit an increase in doubling time of 17.6% compared to wild type cells. c) The lag time of wild type cells in blue, and TEF1 overexpressing cells in red. TEF1 overexpressing cells exhibit an increase in lag time of 26% compared to wild type cells.*

## ***3.2.2 Lag phase of TEF1 overexpressing cells increases in media without leucine following growth in media with leucine***

The observed increase in lag phase led us to hypothesise that the population may be composed of a high proportion of cells that are dead. In response to this we devised an assay to monitor lag phase over a period of time in selective and non-selective media by sub-

culturing cells from -leu to +leu and vice versa over a period of five days (see figure 3.5). An initial overnight plate was grown in liquid media containing wild type and *TEF1* overexpressing cells in biological duplicate and technical triplicate with and without leucine. Cells that were grown in -leu overnight were re-inoculated into a plate with media both with and without leucine, and similarly for cells grown in media with leucine, they were re-inoculated into a separate plate containing media with and without leucine. This process of re-inoculation to and from media with and without leucine was repeated over a 5 day period with continual high resolution growth analysis taking place. This allowed us to monitor the lag phase in cells grown in +leu media while simultaneously monitoring cells maintained in selective -leu media.

This assay was generated to allow us to visualise the viability of cells coming directly from overnight night cultures grown in -leu, compared to those grown in +leu media. We hypothesised that cells grown in media lacking leucine had reduced viability and our aim was to see if addition of leucine to the media rescued either doubling time or the duration of the lag phase. And if there was an observable rescue was this due to an alleviation of the toxic effects of the *TEF1* overexpression plasmid.

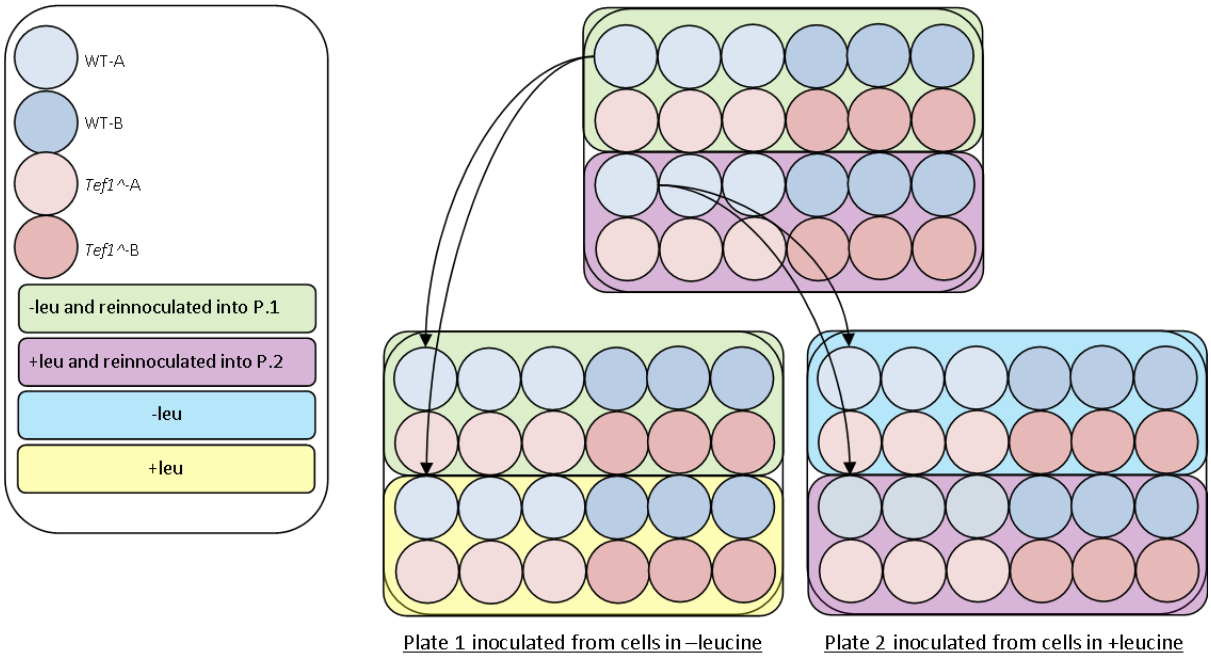


***Figure 3.5 Assay for screening cells growth rate in media with and without leucine.*** *Cells were grown overnight in a 24 well plate, in media with or without leucine. The overnight cultures were then re-inoculated into media with or without leucine and this process was repeated over a 5 day period.*

During the course of this experiment both wild type cells and cells overexpressing *TEF1* that were maintained in selective media without leucine exhibited consistent growth rates, as measured during both lag and log phases (see figures 3.6 a and b respectively). Wild type cells maintained a doubling time of approximately 1.68 hours and had a lag time of 6.7 hours while cells overexpressing *TEF1* maintained a doubling time of approximately 2 hours with a lag time of approximately 8.25 hours throughout the duration of the experiment.

Cells overexpressing *TEF1*, grown in media supplemented with leucine over a period of 1-4 days and then re-inoculated into media lacking leucine exhibited an increasing trend in both their lag and log phase growth rates dependent on the duration of growth in non-selective media with leucine. *TEF1* overexpressing cells re-inoculated from leucine rich media to -leu on day 1 had a doubling time of approximately 2.45 hours. Following sub-culturing into leucine rich media and further re-inoculation into -leu over a period of 4 days, we observed

an increase in doubling time to 2.86 hours. The lag time was affected in a similar, incremental, but more extreme manner. Lag time of *TEF1* overexpressing cells taken from media with leucine and inoculated into -leu media on day 1 was 9.75 hours. After 4 days of sub-culturing into media with leucine and then re-inoculating into -leu, cells over expressing *TEF1* had a doubling time of approximately 20 hours. Wild type cells saw a mild increase in both lag and log growth phase, but these were muted when compared to that of the *TEF1* overexpressing cells. The log phase doubling time for wild type cells increased from approximately 1.88 hours on day 1 to 2.11 hours on day 4. Lag phase increased from 5.75 hours on day 1 to 8 hours on days 3 and 4.

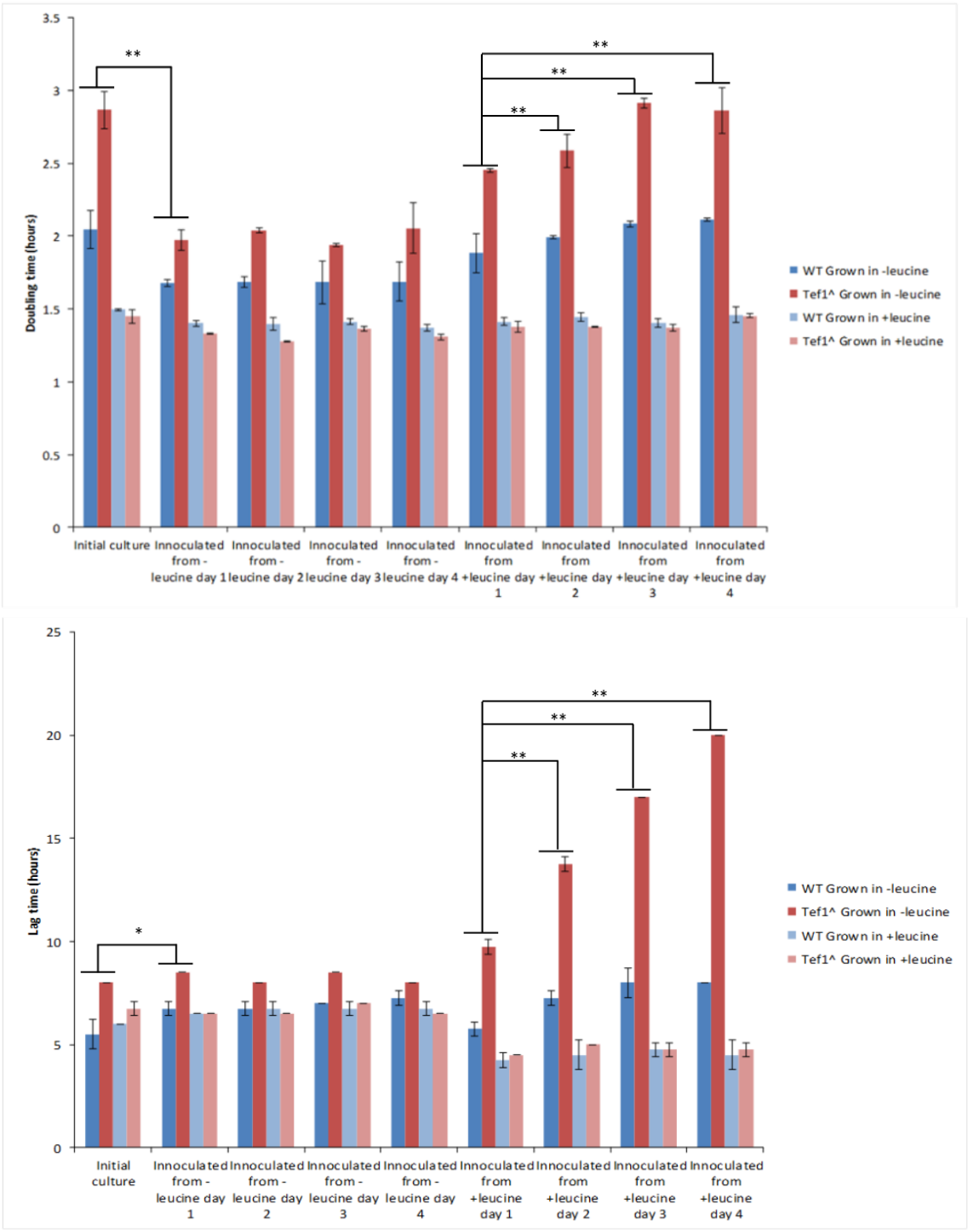


***Figure 3.6 a) & b) Doubling and lag time of cells re-inoculated over a period of 5 days.*** *Cells were grown in media with or without leucine added over a period of 1 to 5 days. Every 24 hours cells were re-inoculated into media with or without leucine and allowed to grow for a further 24 hours. a) shows the doubling time and b) shows the lag time for these cultures over the 5 day period in both media types. Dark blue and light blue show the wild type grown in -leu and +leu media respectively, red and pink show the TEF1 overexpressing strain grown in -leu and +leu media respectively.* p-values are represented by asterisks, *=<0.5, **=<0.05.

These data strongly suggested that when allowed to grow in non-selective media, there was a strong selective pressure against cells with elevated levels of *TEF1*. Although this assay

allowed us to quantify the rate that lag phase increased without any selective pressure it did not elucidate the mechanism that drove this. To further examine this result we checked the viability of cells grown in selective and non-selective media, and quantified plasmid and protein levels during growth in both selective and non-selective media. These assays were chosen because they would allow us to demonstrate if cells grown in -leu have an increased lag phase due to cell death or quiescence, and if this is the result of plasmid loss resulting from eEF1A toxicity.

### *3.2.3 Viability of yeast is unaffected by eEF1A levels*

To confirm the viability of yeast cells overexpressing eEF1A a viability assay was performed. An overnight culture was re-inoculated to 2 x $10^3$ cells/ml and 150 µl (approximately 300 cells) was plated onto selective, -leu, or non-selective, agar plates. These were left to incubate at 30 °C for 36 hours and the colonies were then counted to allow quantification of colony forming units (CFUs). The wild type cells plated onto -leu showed 92% apparent viability compared to just 14% of *TEF1* overexpressing cells, representing a six and a half fold reduction in colony formation in the presence of elevated levels of eEF1A (see figure 3.7). When plated onto +leu plates the wild type and *TEF1* overexpressing cells both had approximately a 106% viability. The ability of *TEF1* overexpressing cells to grow on +leu but not on -leu suggested that eEF1A was not having an effect on cell viability. The *TEF1* overexpressing cells may instead have a defect in a signalling or biosynthesis pathway, or the plasmid could be highly toxic and rapidly selected against when the requirement for the leucine marker is removed. It is possible cells with fewer copies of the plasmid were able to out compete their higher copy number counterparts, or simply that the higher copy cells are non-dividing.

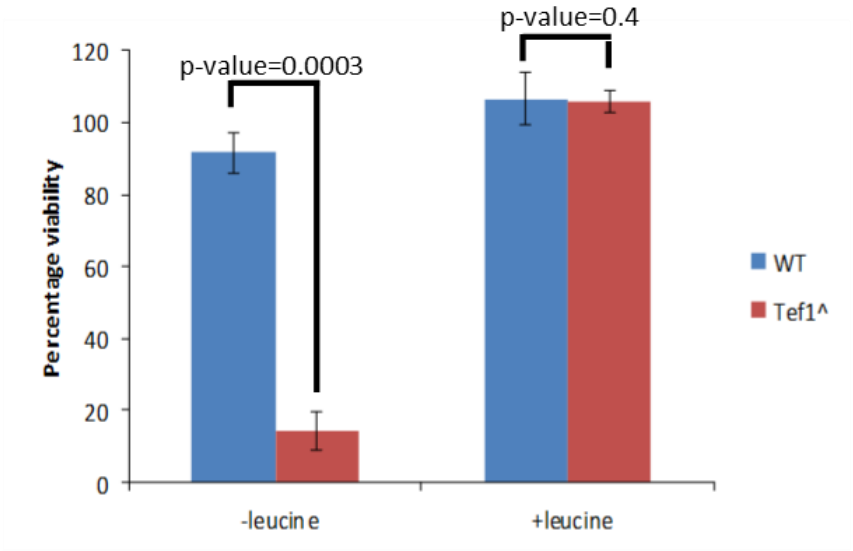


***Figure 3.7 Percentage of cells forming colonies from wild type and TEF1 overexpressing strains plated on selective and non-selective media.*** *Overexpression of TEF1 resulted in a decrease in colony forming units when plated onto -leu media. TEF1 overexpression had no effect on colony forming units when plated onto +leu media meaning that the cells are still viable and are simply quiescent.*

## 3.2.4 TEF1 overexpression induces increased whole cell respiration

Because cells with elevated levels of eEF1A exhibited slower growth and a decreased capacity to form colonies on selective media, we checked cellular respiration to to ask whether cells were still respiring. Cells were grown overnight in -leu and counted before 1 x $10^8$ cells were loaded into the respirometer. The respirometer allowed detection of intact cell respiration by placing the cells into a sealed compartment and measuring oxygen levels in the media over a time course.

Compared to the wild type cells, cells with increased levels of eEF1A exhibited approximately a 25% increase in cell respiration (see figure 3.8). This observable difference in respiration, in addition to the rescue of colony forming units when grown on non-selective media, suggests that when grown in -leu, cells are not dying, but are metabolically active whilst not actually growing, indicating they are entering a quiescent state.

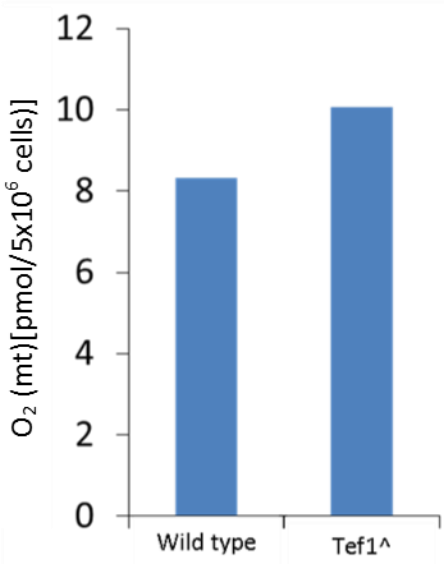


***Figure 3.8, Whole cell respiration of wild type and TEF1 overexpression cells.*** *Whole cell respiration was measured as outlined in the materials and methods. Upon overexpression of TEF1 cells exhibited an increase in respiration approximately 25% greater than the wild type cells.*

## 3.3 Non-selective media has different effects on eEF1A protein levels and *TEF1* gene copy nuber

Because overexpression of *TEF1* resulted in cell growth defects that were rescued upon addition of leucine we checked whether levels of *TEF1* and eEF1A were constant throughout growth, both with and without leucine in the media. It was expected that the rescue observed in the growth rate of *TEF1* overexpressing cells could be attributed to a reduction in protein levels and that when grown in non-selective media the selective pressure against cells with higher levels of eEF1A would result in rapid suppression of protein levels.

### *3.3.1 eEF1A levels appear to remain constant throughout early log when grown in both selective and non-selective media*

eEF1A levels were detected by western blot. Cells were grown overnight in -leu and re-inoculated to an $OD_{600}$ of 0.2 in media with and without leucine. Cultures were grown at 30 °C and 5 $OD_{600}$ units were harvested at an $OD_{600}$ of approximately 0.3, 0.7 and 1.2. Separation

and detection of eEF1A was achieved by SDS-PAGE gel, western blotting and ECL detection as outlined in the materials and methods.

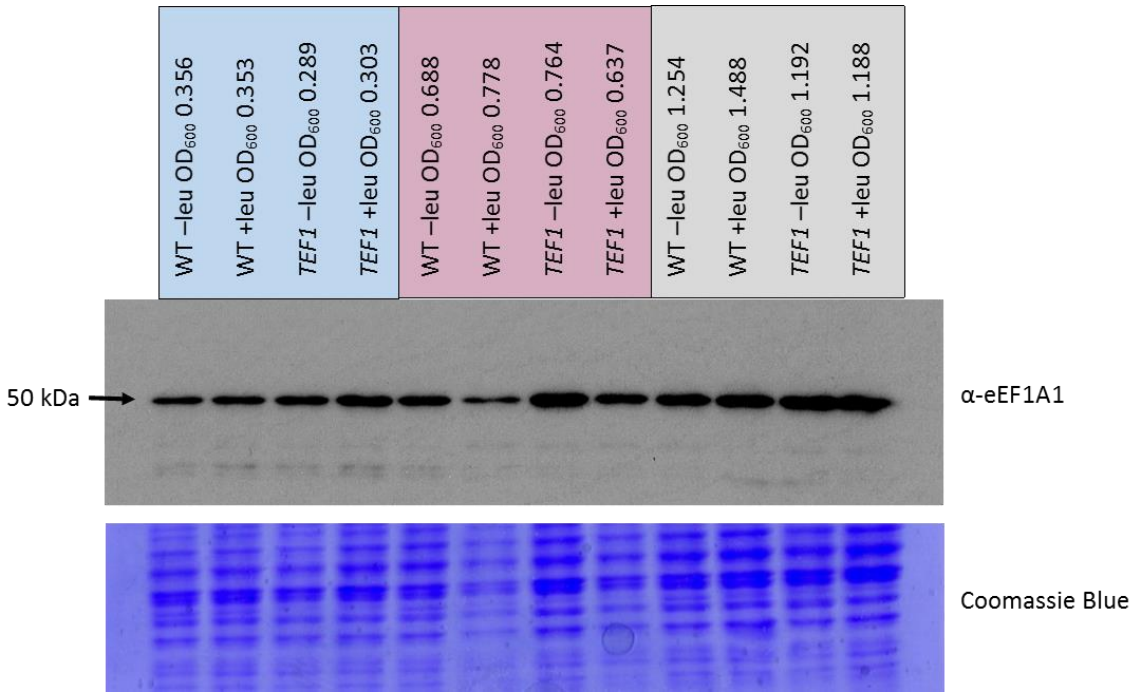


***Figure 3.9 Detection of eEF1A levels during logarithmic growth.*** *eEF1A levels were detected using α-human eEF1A1. Samples were grown overnight in -leu and inoculated to an $OD_{600}$ of 0.2 in media with (+) and without (-) leucine. Protein samples were harvested from 5 OD units at optical densities of approximately 0.3 (blue) 0.7 (red) and 1.2 (yellow)*

The samples taken at $OD_{600}$ 0.3 grown in both media, with or without leucine, showed that the *TEF1* overexpressing cells expressed eEF1A at a levels higher than wild type cells. As the cells passed through exponential growth, those grown in -leu maintained the elevated levels of eEF1A in the *TEF1* overexpressing strain. The cells that were grown in media supplemented with leucine showed a gradual decline in eEF1A levels in the *TEF1* overexpressing strain, but levels were still higher than the wild type cells. This suggests that although there is a selective pressure against cells with elevated levels of eEF1A the decline observed during growth in media with leucine was probably not rapid enough to induce the rescue in lag phase growth upon the addition of leucine to the media.

### *3.3.2 TEF1 overexpression is suppressed upon addition of leucine to the growth media*

As little change in the levels of eEF1A was observed upon addition of leucine to the media we hypothesised that TEF1 may possess toxic properties and so the cell may be selecting against the plasmid itself. To check plasmid levels qPCR was performed with plasmid levels being monitored relative to a genomic standard during early log growth in media both with and without leucine. Cells were grown overnight in -leu and re-inoculated to an $OD_{600}$ of 0.2, they were grown in media both with and without leucine at 30°C and 2OD units were harvested at $OD_{600}$ of approximately 0.4, 0.8 and 1.6. Plasmid levels were assessed using a pair of *LEU2* primers to quantify plasmid copy number and the genomic control was measured using *LEU3* primers allowing quantification of a chromosomal reference gene.

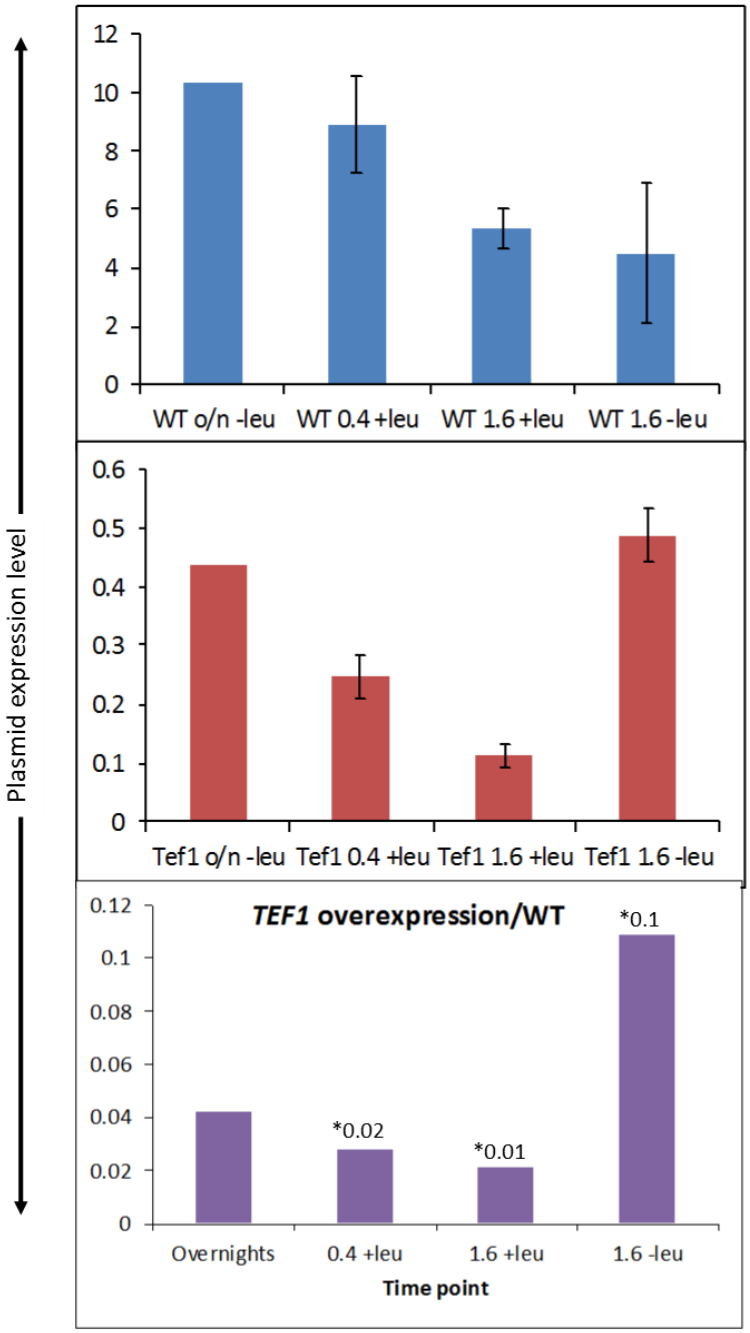


***Figure 3.10, Normalised expression levels of LEU2 in the wild type and TEF1 overexpression strains.*** *LEU2 plasmid levels relative to genomic LEU3 levels at different stages of growth in selective and non-selective media in (a) Wild type (b) TEF1 overexpression and (c) TEF1 relative to wild type. Values highlighted by an asterisk denote the p-value when comparing the WT and TEF1 overexpression data at the relevant optical densities.*

Genomic and plasmid signals were quantified using the genomic based *LEU3* and the plasmid based *LEU2*. The signal for the *LEU2* gene was then normalised to the chromosomal *LEU3* gene (see figures 3.10 a and b). When grown in +leu media, wild type cells exhibited a gradual

reduction to plasmid number with cells at the final time point possessing plasmid levels approximately 55% that of the starting cells. When grown in selective media without leucine wild type cells showed a similar rate of plasmid loss but they had significant variation in plasmid levels suggesting that this loss was entirely random. *TEF1* overexpressing cells exhibited a greater rate of plasmid loss when there was no selective pressure to keep the plasmid with plasmid number approximately 25% that of the starting overnight culture at the final time point. When grown in selective media, cells overexpressing *TEF1* maintained a constant, low, plasmid level with no detectable decrease in levels throughout growth. Interestingly, plasmid levels in the wild type and the *TEF1* overexpression strain were significantly different, with *TEF1* overexpression appearing to have such a strong suppressive effect on plasmid levels that they were only about 5% that of the wild type levels throughout the assay. When expressed relative to the wild type plasmid number (see figure 3.10 c), *TEF1* overexpression still resulted in plasmid levels dropping by 50% throughout growth in non-selective media suggesting that the cells were selecting against the plasmid due to the toxic effects it conferred.

## 3.4 Discussion of results

It is known that eEF1A plays a wide variety of roles in the cell, and that many of these roles are crucial to cell survival. It appears counterintuitive therefore that elevated levels of eEF1A should be viewed as toxic to the cell, but the data presented in this chapter suggests just that.

Increased levels of eEF1A are known to result in a decrease in growth rate of yeast cells (Munshi *et al.*, 2001), and we have demonstrated that only a modest increase in the levels of eEF1A induces an almost 20% increase in doubling time. Removal of the selective pressure for the plasmid, by growing in media with leucine, results in recovery of the growth rate which

appears, in part, to be due to the loss of the *TEF1* plasmid. How elevated *TEF1* levels caused the growth defect is not fully understood, but it is clear that eEF1A had a strong influence over cell cycle dynamics and cell metabolism.

The viability assay outlined, demonstrated that in addition to rescuing growth rate, supplementing the media with leucine also rescues a previously uncharacterised quiescent state that is induced upon overexpression of *TEF1*. The cells lack of ability to grow on media without leucine was demonstrated to not simply be caused by cell death as they were observed to still be respiring, and at an increased level to wild type cells, suggesting that there may be a nutrient signalling defect, leading the cells to assume they are starving.

The qPCR result, together with the long-term growth assay, indicate that in the absence of the selective pressure of media lacking leucine, a culture of *TEF1* overexpressing cells preferentially select for cells with the lowest levels of eEF1A. These two experiments demonstrate that when grown in non-selective media, *TEF1* overexpressing cells see plasmid loss rates of about 25% per population doubling, which in turn, causes the increase in lag phase observed when cells are re-inoculated into selective -leu. When quantified using qPCR the plasmid number in the *TEF1* overexpression strain were approximately 20 times lower than in the wild type. This is due to the stochastic distribution of a 2µ plasmid during cell division and plasmids conferring toxic effects do so in a dose dependent manner. This results in the average plasmid level decreasing over time as cells with lower copy numbers have a growth advantage over those with a higher copy number (Moriya *et al.*, 2006). The discrepancy observed in these levels is further evidence to suggest that *TEF1* overexpression is strongly selected against, and it seems that the population overexpressing *TEF1* maintains the plasmid at the minimum level required to grow on -leu. Together with the data from the

long term growth assay it is clear that growth in media with leucine results in loss of the *TEF1* plasmid to levels so low that the population is unable to rapidly respond when leucine is removed from the growth media, resulting in significantly increased lag phases.

Although not detectable, it is possible that eEF1A levels are also affected by the addition of leucine to the media, but at such low levels that using a non-quantitative method we are unable to detect it. Another possibility is that eEF1A turnover is so low that a drop in plasmid levels may take several generations to manifest itself at the protein level across the population.

Data presented in this chapter suggest that elevated *TEF1*/eEF1A levels have an inhibitory effect on a cells ability to proliferate, but removal of the selective pressure for keeping the *TEF1* plasmid results in an instant rescue of all detectable defects. This rescue mainly appears to be due to rapid plasmid loss resulting in a minor decrease of the level of eEF1A. eEF1A appears to have a strong influence on cell cycle dynamics and cell metabolism in response to leucine levels suggesting a novel role for eEF1A in nutrient sensing.

# Chapter 4: eEF1A is involved in cell cycle regulation via dynactin-mediated interactions

## 4.1 Introduction: The dynactin complex

Because eEF1A has a well characterised interaction with actin we utilised the yeast knockout collection in an attempt to elucidate any proteins associated with actin that could play a role in facilitating eEF1A's interaction with actin. We overexpressed *TEF1* in an array of strains deleted for genes that are known to interact with, or control the function of actin. Mutants that exhibited synthetic interactions, as assessed by growth, were candidates for further investigation. Many of the hits from this screening process were found to be components of the dynactin complex, an essential multi-subunit protein found in eukaryotes. It has an essential dynein-activating activity, facilitating bidirectional intracellular transport of cargoes and there are few, if any, processes that utilise dynein that do not also require dynactin.

### *4.1.1 Dynactin structure*

Dynactin (figure 4.1) is an asymmetric molecule that consists of a 10 x 40 nm Arp1 rod and a 50 nm p150$^{glued}$ side arm (Schafer *et al.*, 1994), along with a 7 other polypeptide subunits.

Resembling a short actin filament, the Arp1 rod is an octameric polymer of the actin-related protein Arp1. The rod binds to cellular cargo via its association with spectrin family proteins, such as βIII spectrin, a specialised isoform found on Golgi membranes (Holleran *et al.*, 1996; Holleran *et al.*, 2001). The rod terminates at its "barbed" end with the actin capping protein CapZ (Schafer *et al.*, 1994). The opposite end consists of a further actin-related protein Arp11 (Eckley *et al.*, 1999) and the dynactin subunit p62, bound to the two smallest subunits p25 and p27.

Projecting from the Arp1 rod is the flexible and extendable side arm that is made up of the remaining three subunits, p150$^{glued}$, dynamitin, and p24/22. The elongated structure of the side arm of the dynactin complex means it has a large surface area relative to its mass.

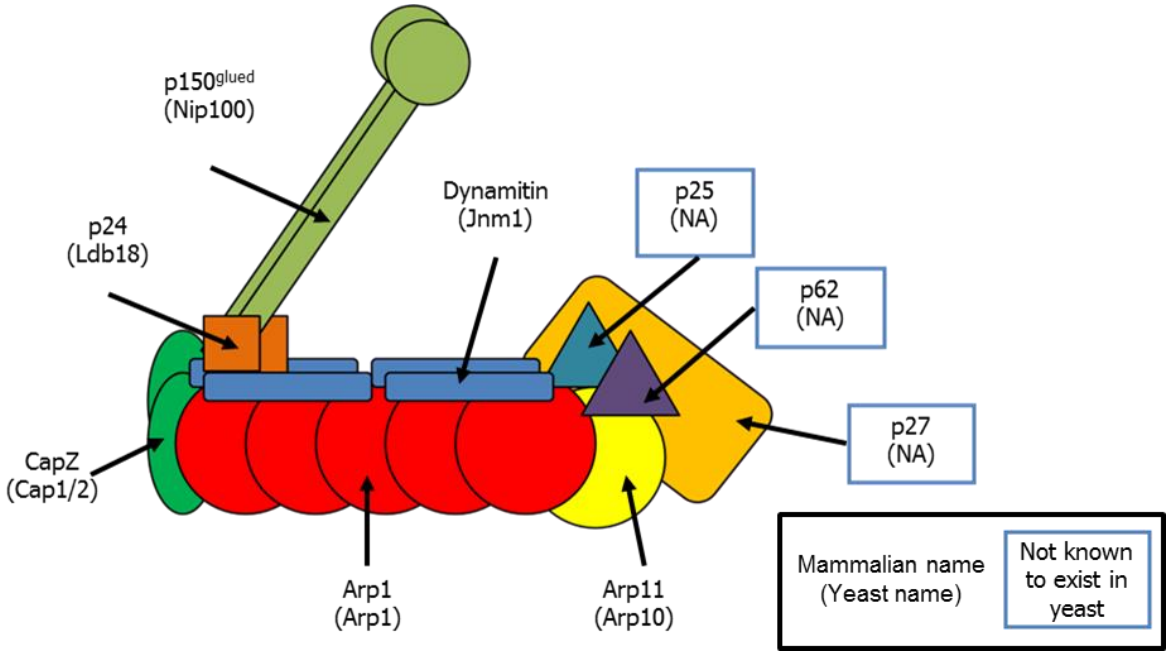


***Figure 4.1 Diagram of the dynactin complex.*** *Human and yeast protein names (yeast names in brackets) are given for each subunit. The three subunits in blue, p25, p27 and p62, are not known to exist in yeast.*

## *4.1.2 Binding partners of the dynactin subunits*

p150$^{glued}$ is the largest of all the dynactin subunits and is predicted to adopt an α-helical structure and self-associate via coiled coils. It is predicted to form an elongated dimer made from two central coils with a region of undefined structure in between. Within the globular heads at the tip of the arm are conserved CAP-Gly (cytoskeleton-associated protein, glycine rich) motifs (Riehemann and Sorg, 1993). This CAP-Gly motif is contained in the N terminus (aa1-110) and is involved in the binding of dynactin to microtubules, as has been shown both *in vitro* and *in vivo* (Waterman-Storer *et al.*, 1995; Vaughan *et al.*, 2002). Further binding partners of the p150$^{glued}$ CAP-Gly domain include the microtubule-binding proteins EB1 and CLIP-170, although it is unknown if it can bind these proteins and microtubules simultaneously, or if they are mutually exclusive functions. It is a possibility that dynactin activity is regulated by the binding of other proteins and protein kinases to the CAP-Gly

domain as phosphorylation at S19 reduces p150$^{glued}$s affinity for microtubules (Vaughan *et al.*, 2002).

Binding interactions with microtubule-based motors, such as dynein, are supported by the middle portion of p150$^{glued}$. Various studies have revealed different sites of potential dynein interaction (Vaughan and Vauee, 1995; Waterman-Storer *et al.*, 1995; Vaughan *et al.*, 2002; King *et al.*, 2003) suggesting that there could be several regions, possibly in multiple dynactin subunits, that allow for dynein-dynactin interactions.

The dynamitin subunit links dynactins two major components, the Arp1 rod, and the p150$^{glued}$ side arm. It exists as an assembly of four subunits that associate with each other, p150$^{glued}$ and p24/22 through three coiled-coil motifs (McMillan and Tatchell, 1994; Echeverri *et al.*, 1996). Overexpression of dynamitin results in collapse of the dynactin complex through disassociation of the Arp1 rod and the p150$^{glued}$ side arm, although the exact mechanism of disruption is, as yet, unknown. Overexpression of the N-terminal fragment (aa1-87) inhibits organelle movement via dynein without disrupting the structure of dynactin (Valetti *et al.*, 1999) suggesting the N terminus of dynamitin may act as an inhibitor of dynein-dynactin interactions. Other components reported to bind to the N-terminal region of dynamitin include, calmodulin together with MacMARKS (Jin *et al.*, 2001), the kinetochore protein Zw10 (Starr *et al.*, 1998), and the Golgi-associated protein, BICD (Hoogenraad *et al.*, 2001). These interactions suggest that the N terminus of dynactin is likely to be exposed on dynactins surface.

P24/22 binds directly to dynamitin at a 1:2 ratio. It is speculated that p24/22 may also interact with p150$^{glued}$ as both of these proteins are liberated from the dynactin complex upon addition of excess dynamitin (Karki *et al.*, 1998; Eckley *et al.*, 1999).

### *4.1.3 Functions of dynactin*

The array of functions that dynactin is involved in means that is has been found in a variety of subcellular localisations, from the centrosomes (spindle pole bodies in yeast), to a variety of endomembranes (Gill *et al.*, 1991; Paschal *et al.*, 1993; Habermann *et al.*, 2001). At the centrosome, dynactin is reported to have involvement in microtubule anchoring (Quintyne *et al.*, 1999). Endomembrane localisation includes membranes in the Golgi region and endocytic organelles (Habermann *et al.*, 2001). Localisation to the nuclear membrane has been reported to be cell cycle dependant (Salina *et al.*, 2002). Dynactin is able to control microtubule dynamics and recruit proteins to the plus ends of microtubules (Quintyne *et al.*, 1999). Localisation to the cell cortex allows for dynactin to influence rotational movement of the mitotic spindle and direct movement of motile cells (Skop and White, 1998; Gönczy *et al.*, 1999; Dujardin *et al.*, 2003).

Although the data given (Gill *et al.*, 1991; Paschal *et al.*, 1993; Skop and White, 1998; Gönczy *et al.*, 1999; Quintyne *et al.*, 1999; Habermann *et al.*, 2001; Salina *et al.*, 2002; Dujardin *et al.*, 2003) suggests highly unique and specific roles for dynactin, in all examples highlighted dynactin is implicated in the regulation of dynein targeting and/or recruitment. However, given dynein is able to bind cellular cargo without dynactin (Tai *et al.*, 1999), and that intact dynactin is essential for metazoan viability (Mcgrail *et al.*, 1995), it would seem that dynactin does far more than bind dynein and facilitate motor processivity.

## 4.2 eEF1A interacts with the dynactin complex in yeast

### *4.2.1 eEF1A levels affect the growth dynamics of dynactin complex mutants*

As discussed eEF1A has a well characterised interaction with actin, because of this we overexpressed *TEF1* in an array of strains deleted for genes that are known to interact with,

or control the function of actin. Synthetic interactions between eEF1A and deleted gene products were initially assessed using the Singer Rotor high throughput screening robot. Cells were grown overnight in biological triplicate at 30 °C in 384 well plates. They were then plated at the same density onto agar plates and growth was assessed after 36 hours at 30 °C. Cells were plated as biological triplicates in rows, with the *TEF1* overexpressing strains plated in the row below (for table see App.1)

*TEF1* overexpression resulted in varied effects across the array of strains with some colonies showing a dramatic reduction in growth and others showing no difference between the deletion strain and the strain overexpressing *TEF1*. It was observed that many of the deletions that resulted in significant differences in growth came from the essential activator of dynein, the dynactin complex (see figure 4.2) (for the full array see App.2).

In the *Δarp1* and *Δcap1* strains *TEF1* overexpression had no significant effect on colony formation compared to the deletion strains suggesting these were potential interactive partners of eEF1A. However, in the *Δcap2* and *Δjnm1* strains the inhibitory effect of *TEF1* overexpression was greater than in the wild type further implicating eEF1A as an inhibitory interactive partner of one of the other components of the dynactin complex.

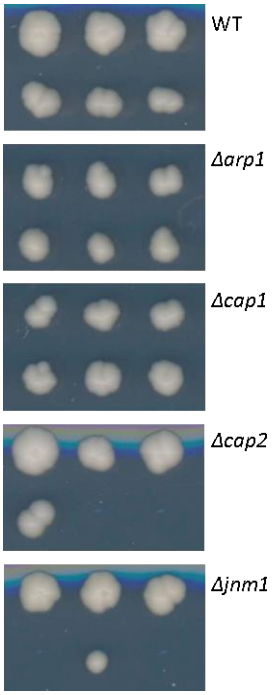


***Figure 4.2 Array of viable actin mutant strains with TEF1 overexpressed.*** *Strains that had been deleted for genes known to interact with, or control the function of actin were assayed for synthetic interactions with eEF1A. Strains were arranged horizontally in biological triplicate. Cells containing the control plasmid were in the upper row, with the TEF1 overexpression vector in the row below. Shown are the "hits" from this screen that are components of the dynactin complex.*

As a there were a number of interactions between eEF1A and different components of the dynactin complex, this was selected as the primary target for the experiments reported in the remainder of this chapter. Further interrogation of the dynactin complex was performed, with the addition of further deletion strains that were not present in the viable actin mutant screen; *Δnip100* ($p150^{glued}$) the largest of the dynactin subunits, and the major component of the extending arm, and *Δldb18* (p24) the smallest of all the dynactin subunits, and a component of the hinge joint between the arp1 rod and the nip100 arm.

In total there were six viable deletion strains that were characterised using high resolution growth analysis (as previously described) *Δarp1, Δcap1, Δcap2, Δjnm1, Δldb18* and *Δnip100 (see figure 4.3)*. When *TEF1* was overexpressed in the wild type strain an increase of

approximately 17% was observed in the doubling time. Deletion of *ARP1*, the major component of the dynactin backbone, resulted in a decrease in doubling time to 92% that of the wild type, but overexpression of *TEF1* in the *Δarp1* mutant resulted in a rescue of the doubling time similar to that observed in the wild type with *TEF1* overexpression. Deletion of both *CAP1* and *CAP2* genes which encode orthologues of the mammalian capZ actin capping protein, resulted in an increase in doubling time to 124% and 113% respectively. *TEF1* overexpression in both of these strains resulted in a further increase in doubling time to 153% that of the wild type. Deletion of *Jnm1*, orthologue of dynamitin, caused an increase in doubling time of 114% relative to the wild type, with *TEF1* overexpression resulting in a minor rescue to 110% of the wild type level. Deletion of *Ldb18* had the most severe growth defect with an increase in doubling time of 139% relative to wild type, with *TEF1* overexpression causing a further increase to 172% relative to the wild type. The final gene deletion, *NIP100*, orthologue of $p150^{glued}$, resulted in no significant growth defect with an increase in doubling time to 104% of the wild type, overexpression of *TEF1* in the *Δnip100* mutant only had a minor effect on growth increasing it to 109% that of the wild type (see figures 4.3 -a and -c).

Upon comparison of the lag time of these strains, a similar varied effect was observed, to that seen when the doubling time was quantified (see figures 3.8 -b and -c). *TEF1* overexpression in the wild type resulted in a similar increase in the lag time to 117% that of the wild type, suggesting that *TEF1* has a similar influence over both phases of growth. Unlike the effect of *TEF1* in wild type cells, no correlation between lag phase and doubling time was observed in the dynactin mutants. With the exception of the *Δcap1* mutant, *TEF1* overexpression resulted in a decrease in lag phase in all the dynactin mutants. Lag phase in the *Δarp1* mutant was reduced to 78% of the wild type time, with *TEF1* overexpression further decreasing the lag

time to almost 50% the wild type duration. Interestingly, although the *Δcap1* and *Δcap2* mutants caused a similar reduction in lag time to 69% and 63% of the wild type respectively, *TEF1* overexpression in these mutants had dramatically different effects on lag time. Overexpression of *TEF1* in the *Δcap1* mutant resulted in an increase in lag phase similar to the observed change in doubling time, increasing lag time to 160% that of the wild type. In the *Δcap2* mutant the opposite effect was observed, with the lag time of *Δcap2* cells with *TEF1* overexpressed exhibiting a reduction of lag time to 67% that of the wild type. Deletion of *Jnm1* resulted in a reduction of the lag time to 65% that observed in the wild type with *TEF1* overexpression inducing a recovery of this to 89%. The *Δldb18* mutant had a lag phase similar to the wild type with *TEF1* overexpression causing a reduction to 74% that of the wild type. The final mutant *Δnip100* resulted in a reduction of the lag phase to 67% that of the wild type with *TEF1* overexpression inducing a minor recovery up to 78% of the wild type rate.

The variation observed upon comparing the growth dynamics of the dynactin mutants in the presence of endogenous and elevated levels of eEF1A indicate a high degree of interaction between these highly conserved proteins. eEF1A is a well characterised multifunctional protein that appears to play roles in many essential cellular functions and interaction between eEF1A and the dynactin complex, another highly conserved and interactive complex, makes logical sense allowing these two promiscuous components to allow further cross talk and interplay throughout a dynamic range of cellular functions and processes, offering eEF1A influence over a large array of regulatory mechanisms.

To characterise the far reaching effects of eEF1A on several cellular components further analysis was performed utilising a varied array of techniques.

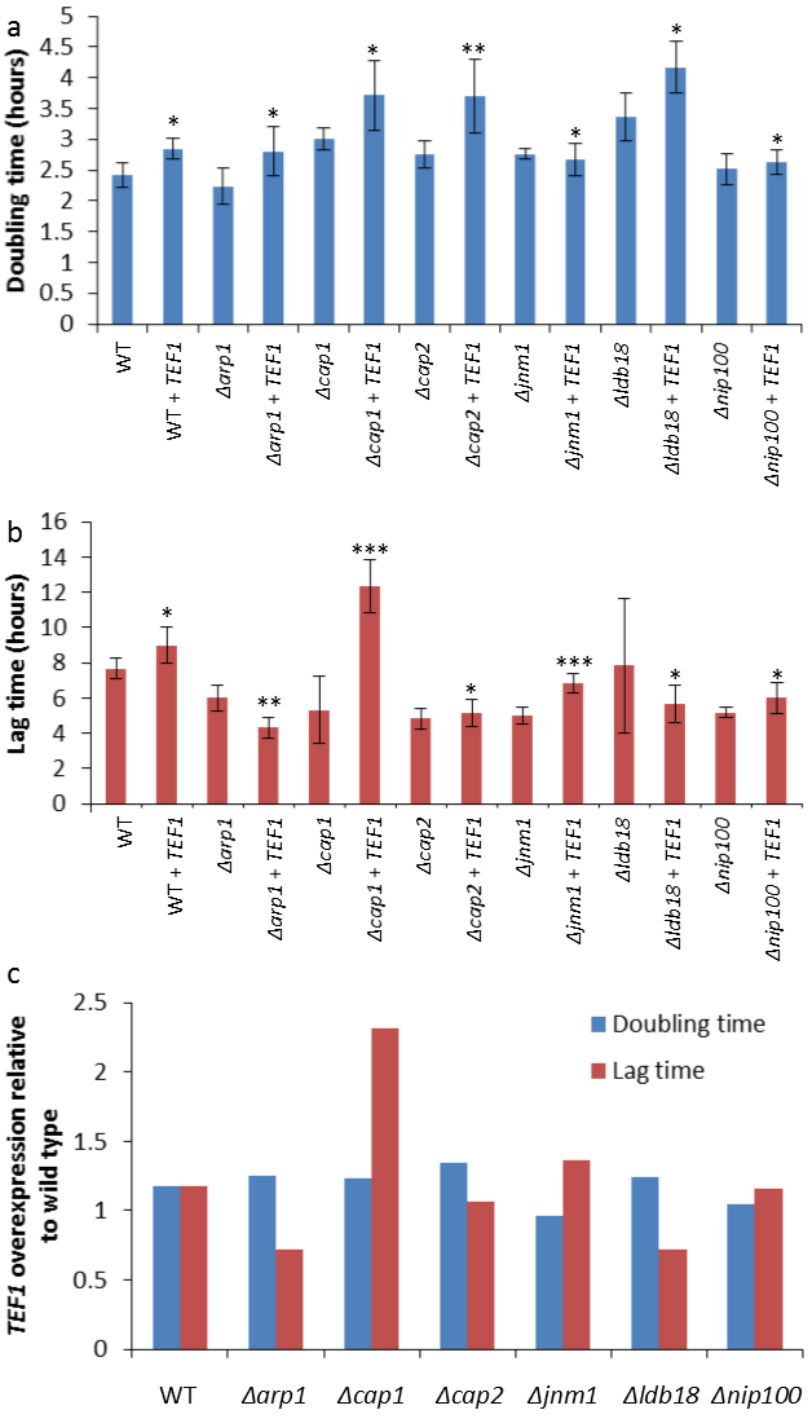


***Figures 4.3 –a-c. Growth analysis of dynactin mutants with TEF1 overexpression.*** *–a shows the doubling time of the dynactin with and without TEF1 overexpression. –b shows the lag time of the dynactin mutants with and without TEF1 overexpression. –c is a compilation of the lag time and the doubling time of the dynactin mutants with the TEF1 overexpression values over the control plasmid values. p-values are represented by asterisks, *=<0.5, **=<0.05, ***=<0.005*

### *4.2.2 eEF1A levels effect chromosome segregation in dynactin complex mutants*

Dynactin is known to participate in chromosome alignment and nuclear positioning and it has been previously shown that deletion of dynactin subunits results in aberrant spindle pole body positioning and chromosome segregation (Maruyama *et al.*, 2002; Yeh *et al.*, 2012). To check for ploidy aberrations resulting from improper chromosome segregation cells were analysed using FACS to check intercalation of propidium iodide (PI), allowing for quantification of genomic content within individual cells.

Cells were grown overnight and re-inoculated in selective -leu to an $OD_{600}$ of 0.2. They were then grown at 30 °C until they reached an $OD_{600}$ of 0.7. 1 x $10^7$ cells were harvested and fixed by addition of 1 ml of 70% EtOH at -20 °C whilst vortexing. Cells were rehydrated and PI was added to a final concentration of 6 μg/ml. Analysis was performed using a FACSCalibur flow cytometer and fluorescence microscopy, as described in the Materials and methods (Section 2.6.3)

Using FACS analysis of PI stained cells we were able to show that *TEF1* overexpression in wild type yeast cells resulted in no significant alteration to the distribution of cells during the cell cycle. It was observed however, that all peaks in the FACS spectrum shifted significantly to the right indicating increased levels of genomic content (see figure 3.9 –a-f). Observation of these cells by fluorescence microscopy confirmed that cells in the presence of elevated levels of *TEF1* exhibited larger and brighter nuclei, but had normal nuclear distribution (see figure 3.10 a).

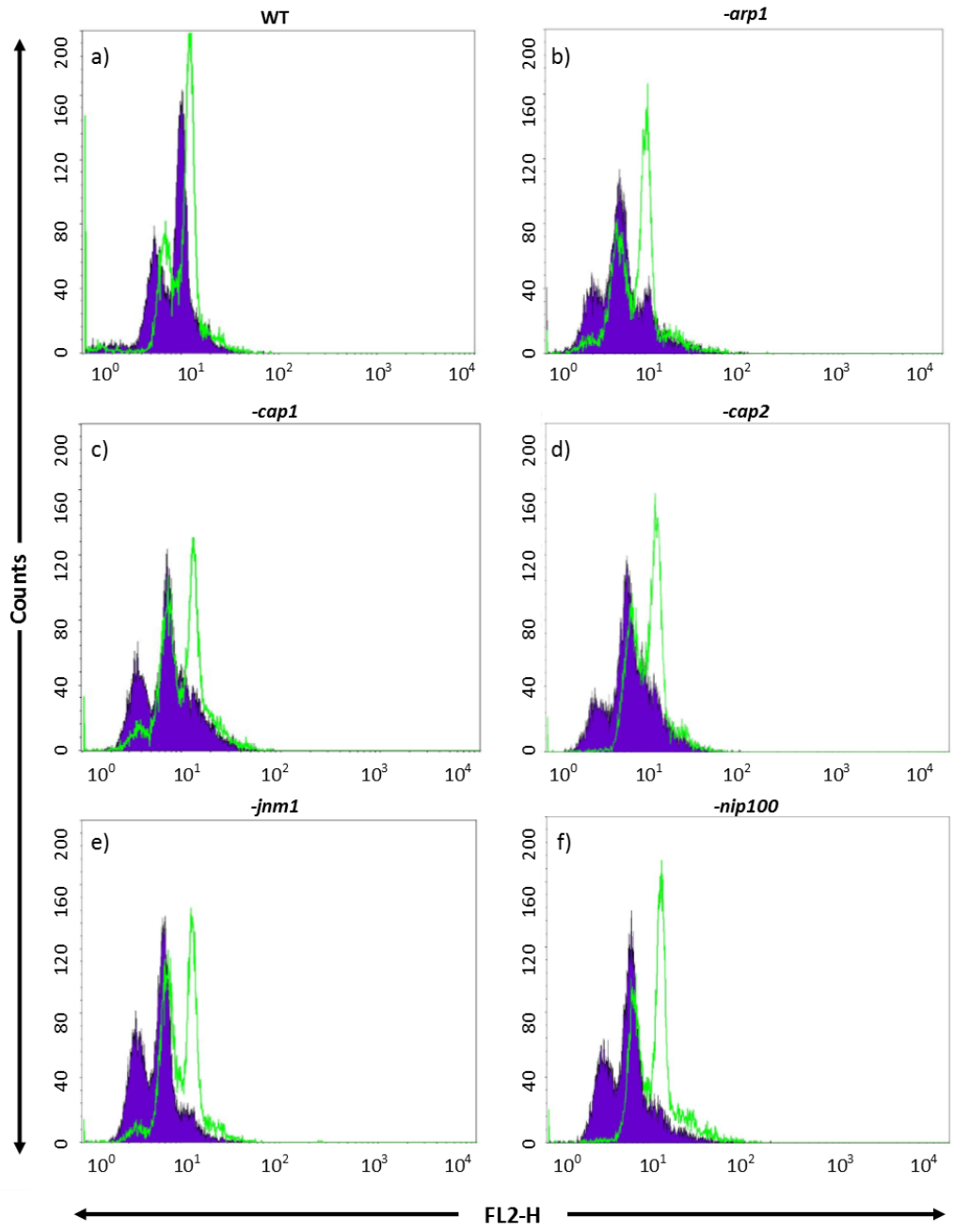


***Figure 4.4 –a-f, FACS analysis of cells stained with propidium iodide.*** *Data was captured using the BD FACSCalibur flow cytometer and analysed using BD FACSStation data management system. Further quantitative analysis was performed and is shown in figure 4.5. Data in purple represents parent strains, with TEF1 overexpressing strains in green.*

Analysis of the dynactin mutants revealed, that as previously discussed (section 4.2.2), deletion of some of the dynactin components results in aneuploidy, and we were able to observe a significant increase in multinucleate cells by fluorescence microscopy (see table

4.2). Overexpression of *TEF1* resulted in a similar observable shift in all peaks across the dynactin mutants (see figure 4.4), indicating that this aberration occurs independently of any phenotypes influenced by the interactions between eEF1A and the dynactin complex. When *ARP1* was deleted, an extra peak to the right of the two main peaks was observed (see figure 4.4 –b), and when this was visualised by fluorescence microscopy it correlated to a population of multinucleate cells that was not seen in the wild type cells (see figure 4.5 –c). Overexpression of *TEF1* in the *Δarp1* mutant resulted in the disappearance of the extra peak when analysed by FACS (see figure 4.4 –b), however, this did not correlate with the fluorescence microscopy images as an increase in the occurrence of multinucleate cells was observed (see figure 4.5 –d). Deletion of *CAP1* and *CAP2* resulted in a decrease in the quantity of cells in the haploid population compared to the wild type cells and there was also a noticeable shoulder to the right of this population indicating significant genomic heterogeneity within the sample (see figures 4.4 c and d). Overexpression of *TEF1* in both these strains induced a rescue of both the unbalanced haploid-diploid populations and the heterogeneity observed in the mutants (see figures 4.4 c and d). Microscope analysis of these strains showed further similarity to the wild type strain with a very low occurrence of multinucleate cells and larger and brighter nuclei in the presence of elevated levels of eEF1A (see figures 4.5 e-h). The *Δjnm1* and *Δnip100* mutants exhibited similar genomic distribution to that of the wild type cells with the addition of a slight peak to the right of the diploid population (see figures 4.4 e and f). Overexpression of *TEF1* in both these deletion strains resulted in an almost complete ablation of the third peak, with more cells present in the haploid population (see figures 4.4 e and f). Microscopy analysis of these strains differed however. In the *Δjnm1* mutant nuclei appeared to be smaller and dimmer than in the wild type strain and in any of the other dynactin mutants. *TEF1* overexpression in the *Δjnm1*

mutant resulted in larger, brighter nuclei, similar to those observed in the other strains with elevated levels of eEF1A (see figures 4.5 i and j). The *Δnip100* mutant exhibited the highest proportion of multinucleate cells in the presence of endogenous levels of eEF1A, and *TEF1* overexpression had no significant effect on this (see figures 4.5 k and l).

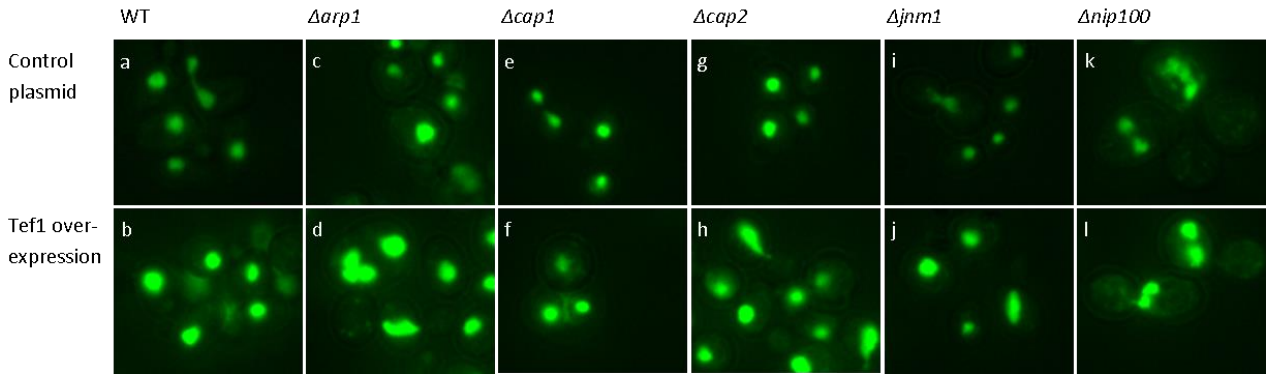


***Figure 4.5 a-l, Microscopy of PI stained cells.*** *Cells were stained with propidium iodide and visualised by fluorescence microscopy. The top row shows cells containing the control plasmid, with the bottom row corresponding to cells with TEF1 overexpression. Cells with elevated levels of eEF1A appeared to have larger, brighter nuclei than cells with endogenous levels.*

**Table 4.2 - Proportion of cells quantified using FACS and microscopy**

| | FACS analysis* | | | | Microscopy |
|---|---|---|---|---|---|
| | **Peak 1** | **Peak 2** | **Peak 3** | **Peak 4** | **% of cells that appear multinucleate** |
| WT | 32.69 | 54.19 | 7.05 | | 0.46 |
| WT+*TEF1^* | 29.65 | 59.89 | 6.03 | | 0.43 |
| *Δarp1* | 22.04 | 53.90 | 15.10 | 5.04 | 20.83 |
| *Δarp1+TEF1^* | 3.68 | 37.93 | 49.29 | 7.34 | 30.52 |
| *Δcap1* | 22.53 | 46.75 | 17.73 | 9.86 | 3.66 |
| *Δcap1+TEF1^* | 7.88 | 44.27 | 39.87 | 6.32 | 4 |
| *Δcap2* | 16.81 | 60.81 | 18.56 | | 3.62 |
| *Δcap2+TEF1^* | 41.74 | 54.62 | 2.12 | | 4.18 |
| *Δjnm1* | 32.94 | 56.65 | 7.86 | | 4.52 |
| *Δjnm1+TEF1^* | 4.51 | 48.78 | 40.10 | 5.10 | 3.55 |
| *Δnip100* | 29.01 | 55.75 | 11.38 | 3.04 | 22.91 |
| *Δnip100+TEF1^* | 36.43 | 42.16 | 7.94 | | 23.88 |

*FACS analysis shows cells that were either haploid, diploid or possessed a different quantity of propidium iodide to either of those populations. Microscopic analysis shows the percentage of cells from 300 that possessed more than one nucleus at the incorrect point in its cell cycle. *These peaks may not correspond to each other due the shift observed upon TEF1 overexpression.*

## *4.2.3 eEF1A levels affect spindle organisation in Δarp1 mutants*

Dynactin plays a role in chromosome alignment and spindle organisation during mitosis, as well as driving spindle checkpoint inactivation (Echeverri *et al.*, 1996; Howell *et al.*, 2001). As the spindle check point is known to prevent aberrant chromosome segregation, and therefore aneuploidy we checked for aberrant spindle organisation in the presence of elevated levels of eEF1A as this would be indicative of eEF1A having a direct influence on cell ploidy.

Spindle organisation was assessed using immunofluorescence with cells grown to mid log growth and then samples prepared as described in the Material and methods (section 2.6.1.3). Tubulin was detected with a primary murine antibody raised against beta-tubulin. Beta-tubulin is encoded by the *TUB2* gene and forms a dimer with alpha-tubulin that polymerises to form microtubules. The secondary antibody was an anti-mouse-TxRED conjugate allowing ease of distinction from the DNA dye, DAPI.

When visualised using fluorescence microscopy wild type cells possessed normal spindle morphology with intact spindles originating from the spindle pole body and spanning the length of the cell from one tip in the mother cell, to the polar opposite tip in the daughter (see figure 4.6 a). *TEF1* overexpression in wild type cells appeared to have no significant effect on spindle formation, and the majority of cells observed had normal spindles although the intensity was diminished in approximately 30% of the population (see figure 4.6 b). In both these strains spindle pole bodies also appeared to localise to the poles of the nucleus and migrated to the poles of the mother and daughter cells correctly. The *Δarp1* mutant exhibited the most severe phenotype observed in the dynactin mutants with the majority of cells not possessing obvious spindle pole bodies. They also exhibited an apparent uncontrolled growth of spindles that frequently continued to grow upon reaching the cell pole. This caused spindles to wrap around the cell cortex and cells appeared to contain many overgrown spindles. These cells also had severe ploidy defects possessing multiple nuclei (see figure 4.6 c). Interestingly *TEF1* overexpression in the *Δarp1* mutant appeared to induce a significant rescue of both the spindle pole body defect and the uncontrolled growth of spindles (see figure 4.6 d).

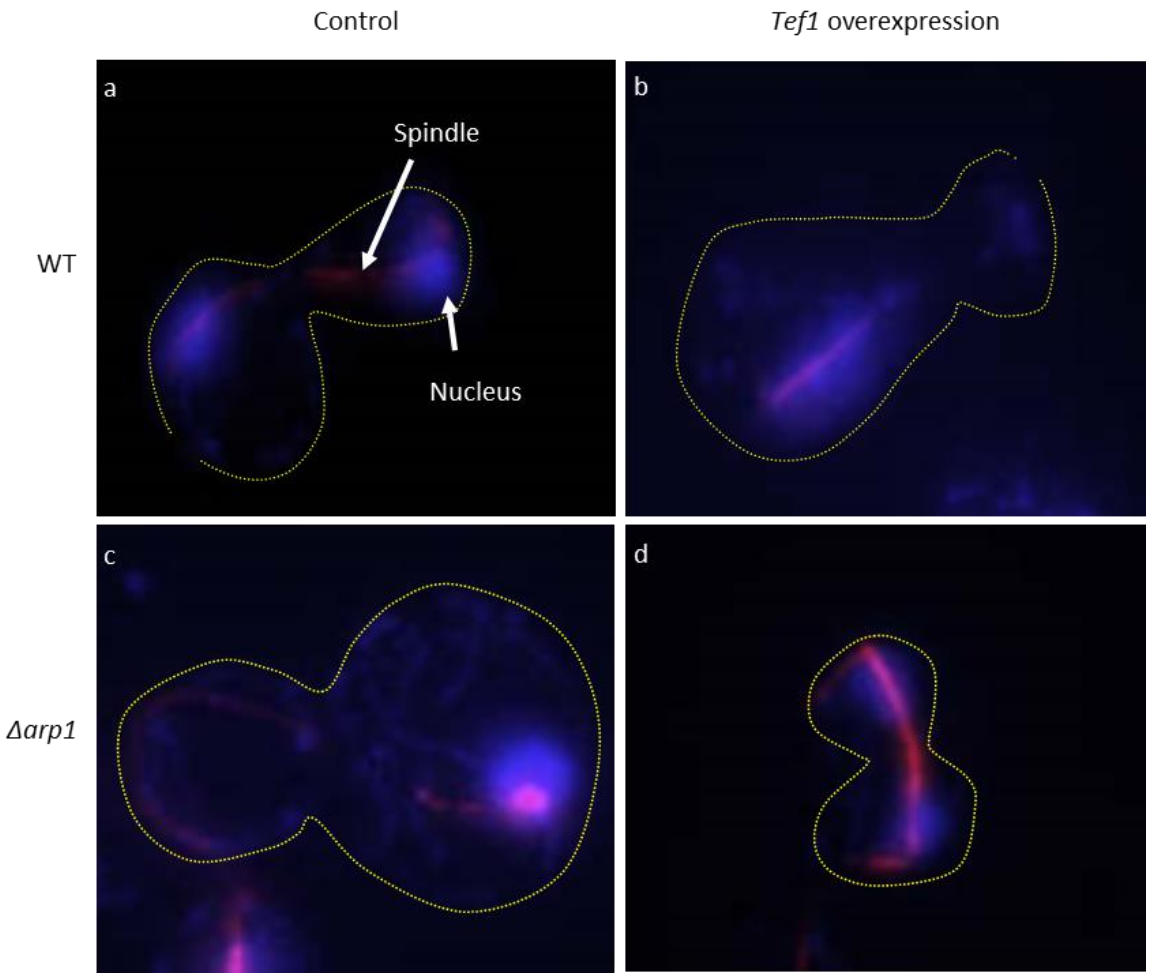


***Figure 4.6 a-d, immunofluorescence of wild type and Δarp1 strains with endogenous and elevated levels of eEF1A.*** *Genomic content can be observed as blue, stained by DAPI, the spindles appear red as they were probed using a TxRed secondary conjugate.*

How elevated levels of eEF1A induce such a dramatic rescue in the *Δarp1* mutant is, as yet, unknown. Deletion of *ARP1* results in the collapse of the dynactin complex, which in turn results in the aberrant spindles observed in the *Δarp1* mutant (figure 3.11 c). Arp1 forms short stable octameric polymers similar in structure to those formed by actin. As eEF1A is known to stabilise actin it is a possibility that actin could replace Arp1 in the Arp1 rod of the dynactin complex resulting in the restoration of the complex. Arp1 and Act1p share 47.1% identity at the polypeptide level and Arp1 and Arp11p are known to co-cycle with actin filaments (Eckley and Schroer, 2003). Furthermore, actin binds the dynactin components Arp1, Arp11p and p62

*in vitro* (Garces *et al.*, 1999) reinforcing its potential as a viable substitute for Arp1 in the dynactin complex. Whether it is the stabilisation of actin by eEF1A, or another, as yet, unknown mechanism that results in the potential ability of actin to replace Arp1 in the dynactin complex is unknown.

Further analysis of the effect of eEF1A on the spindle pole bodies in wild type cells was conducted by utilising the yeast GFP collection, a collection that covers three-quarters of the *S.cerevisiae* proteome (Huh *et al.*, 2003). The collection contains genes tagged at the carboxy terminal end of open reading frames with the coding sequence of *Aequorea victoria* GFP. These were tagged chromosomally using oligonucleotide-directed homologous recombination simultaneously introducing the c-terminal GFP tag and a selectable *HIS3* tag. We used the *TUB4*-GFP strain to allow visualisation of the spindle pole bodies. *TUB4* encodes gamma-tubulin, a conserved component of microtubule organising centres in eukaryotes and is involved in nucleating microtubules from the nuclear and cytoplasmic faces of the spindle pole body. The *TUB4*-GFP expressing strain was transformed with the control plasmid (pCG124) and the *TEF1* overexpression plasmid (pCG454) and colonies were selected and grown to mid-log phase. Cells were visualised live by fluorescence microscopy as detailed in the Material and methods (section 2.6.1.3).

Visualisation of γ tubulin-GFP with both endogenous and elevated levels of eEF1A showed normal spindle pole body distribution throughout the cell cycle in concurrence with the observation made by immunofluorescence. *TEF1* overexpression resulted in brighter spindle pole bodies and a greater cytoplasmic intensity suggesting an increase in the levels of γ tubulin. The increase observed in γ tubulin levels could be explained by higher levels of eEF1A

exerting stress on DNA replication. *TUB4* levels have previously been observed to increase in abundance in response to various stresses exerted on DNA replication (Tkach *et al.*, 2012).

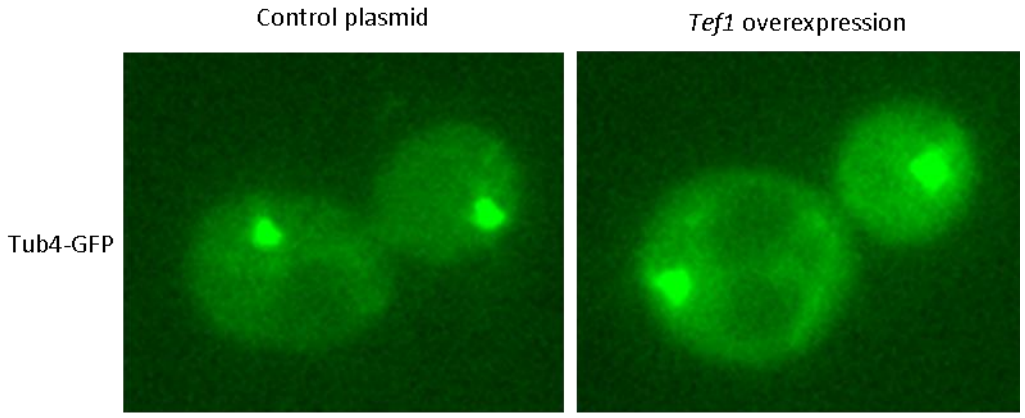


***Figure 4.7 a and b, Fluorescence microscopy of Tub4GFP strains.***

## *4.2.4 Increased levels of eEF1A induce Arp1 translocation*

We have observed that upon deletion of *ARP1* cells develop a severe aneuploidy phenotype with approximately 20% of cells appearing multinucleate when visualised by fluorescence microscopy (see table 4.2). Immunofluorescence results indicated that upon deletion of *ARP1* cells also develop severe microtubule defects (see figure 4.6 c), and it is reasonable to assume that this is what leads to the aneuploidy phenotype previously mentioned. Upon overexpression of eEF1A we observed a rescue of the spindle defect in the *Δarp1* mutant (see figure 4.6 d) but a worsening of the aneuploidy with approximately 30% of cells appearing multinucleate (see table 4.2). This indicates that the defects in spindle formation and ploidy upon deletion of *Arp1* are separable and interestingly although eEF1A overexpression can alleviate one it results in worsening of the other.

To observe the direct effect of *TEF1* overexpression on Arp1 we utilised the yeast GFP collection to visualise Arp1 in the presence of endogenous and elevated levels of eEF1A.

When visualised by fluorescence microscopy Arp1-GFP was primarily cytoplasmic with several clearly defined features that were localised to the spindle pole bodies and microtubules as well as decorating what were actin filaments (see figure 4.7 a). Considering the canonical roles of dynactin in microtubule anchoring at the spindle pole body and regulation of microtubule dynamics (Quintyne *et al.*, 1999), and that Arp1 is known to co-cycle with actin (Melki *et al.*, 1993), this localisation was to be expected. Overexpression of *TEF1* induced a dramatic translocation of Arp1 to the nucleus but the mechanism that caused this is currently not understood (see figure 4.7 b). As previously discussed eEF1A has been reported to play a role in nuclear export but under normal conditions it has not been shown to enter the nucleus (Calado *et al.*, 2002) and no known role for eEF1A in nuclear import exists.

Analysis of the eEF1A and Arp1 sequences using nuclear localisation sequence (NLS) prediction software (Kosugi *et al.*, 2009) indicated that Arp1 has no predicted NLSs, and eEF1A only has a single low scoring (5.2 out of 10) NLS. Analysis of the GFP-His3 C-terminally tagged Arp1 also revealed no NLS ruling out simple shuttling into the nucleus via traditional transport mechanisms.

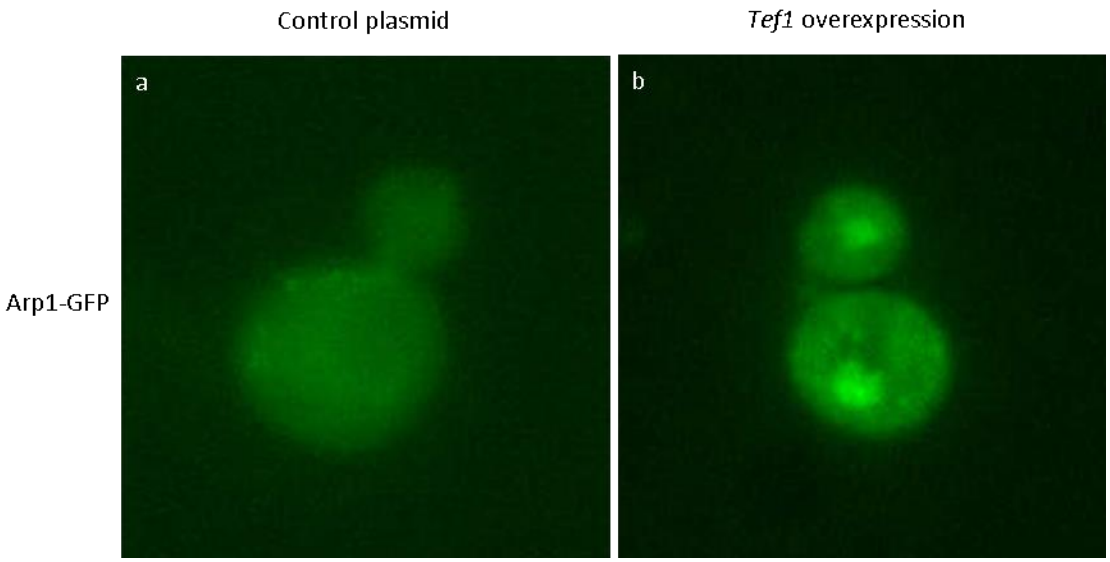


***Figure 4.8 a and b, Fluorescence microscopy of Arp1-GFP strains.*** *a shows Arp1 decorating microtubules and actin filaments. b shows translocation of Arp1 to the nucleus in the presence of elevated levels of eEF1A.*

Further characterisation of the other dynactin components was attempted using other GFP strains but they all lacked a strong enough signal to be detected by fluorescence microscopy.

## 4.3 Mutations in eEF1A cause spindle pole body defects and effect Arp1 localisation

Previous studies on eEF1A have primarily focussed on its canonical role during protein synthesis and its non-canonical role as an actin-binding protein. Work from the Kinzy lab focussed on introducing point mutations in eEF1A to elucidate residues that effect actin-binding and rates of translation. As previously discussed they revealed two classes of mutations that rescued the growth defect observed upon eEF1A overexpression. The first were those which did not affect the rate of protein synthesis, but resulted in a disorganised actin cytoskeleton and reduced actin bundling, although actin binding was unaltered *in vitro* (Gross and Kinzy, 2005). The second class of mutations caused severe actin phenotypes along with slowed growth and decreased levels of translation initiation (Gross and Kinzy, 2007). We acquired the strains characterised in these studies, isolated the overexpression plasmids and

using marker swapped GFP tagged strains were able to analyse the effects of the point mutations on γ tubulin and Arp1p localisation.

### *4.3.1 Point mutations in eEF1A effect Arp1 localisation*

To see if the actin binding ability of eEF1A affected its influence on Arp1 location the Arp1-GFP expressing strain was transformed with an array of eEF1A overexpression plasmids with point mutations introduced known to affect actin binding. These plasmids were a *TEF1-URA3* fusion to prevent degradation of eEF1A (Gross and Kinzy, 2005).

Overexpression of the wild type eEF1A-Ura3p fused protein resulted in a similar translocation of Arp1 to the nucleus as was observed when eEF1A was overexpressed as an unfused product (see figure 4.9 a). The translocation was not as severe as with the unfused protein, but this was likely due to a lower level of eEF1A overexpression, even though the fusion was intended to drive higher levels of eEF1A. Four of the eEF1A mutations, N329D Y355C, F308L, N305S and S405P, resulted in a rescue of Arp1 localisation similar to the wild type, although some showed potential localisation to the mitochondria, which was not observed in the wild type cells (see figures 4.9 b,c,d and e). Dynactin is known to be involved in the regulation of subcellular mitochondrial location (Varadi *et al.*, 2004) and it appears that eEF1A promotes the interaction between Arp1 and the mitochondria. The two other mutations K333E and N329S resulted in an almost complete loss of Arp1-GFP signal. Only very faint localisation to the actin filaments was visible (see figures 4.9 c and d) strongly indicating a requirement for eEF1A in Arp1 fulfilling its role as a member of the dynactin complex. These data suggest that the residues of eEF1A that affect its ability to bind actin also influence its ability to induce translocation of Arp1 to the nucleus, and, furthermore residues N329 and K333 are essential for normal Arp1 distribution. As can be seen in figure 4.10 N329 and K333 are in close

proximity to each other close to the boundary between domains II and III suggesting this region is likely to be involved in the interaction between Arp1 and eEF1A.

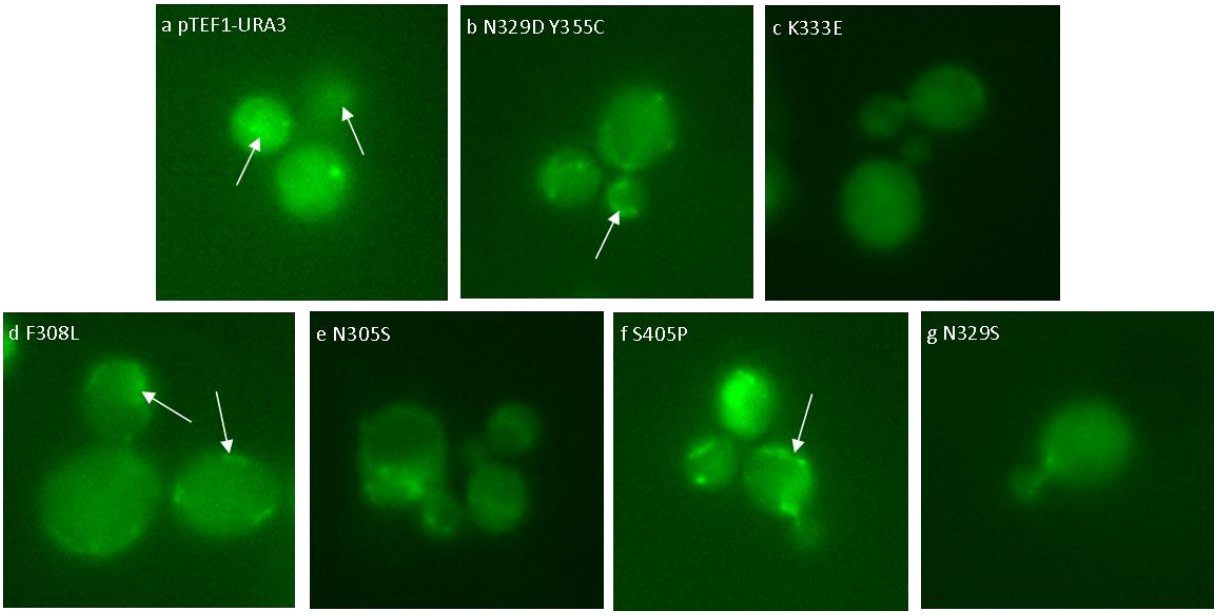


***Figure 4.9 a-g, Arp1-GFP with eEF1A overexpressed with various point mutations.*** *eEF1A fused to URA3 was overexpressed in Arp1-GFP. Point mutations that are known to effect actin binding and translational fidelity were introduced to observe their effect on Arp1 localisation. All of the mutations resulted in a rescue of Arp1 translocation to the nucleus that was observed upon overexpression of both eEF1A and eEF1A fused to URA3.*

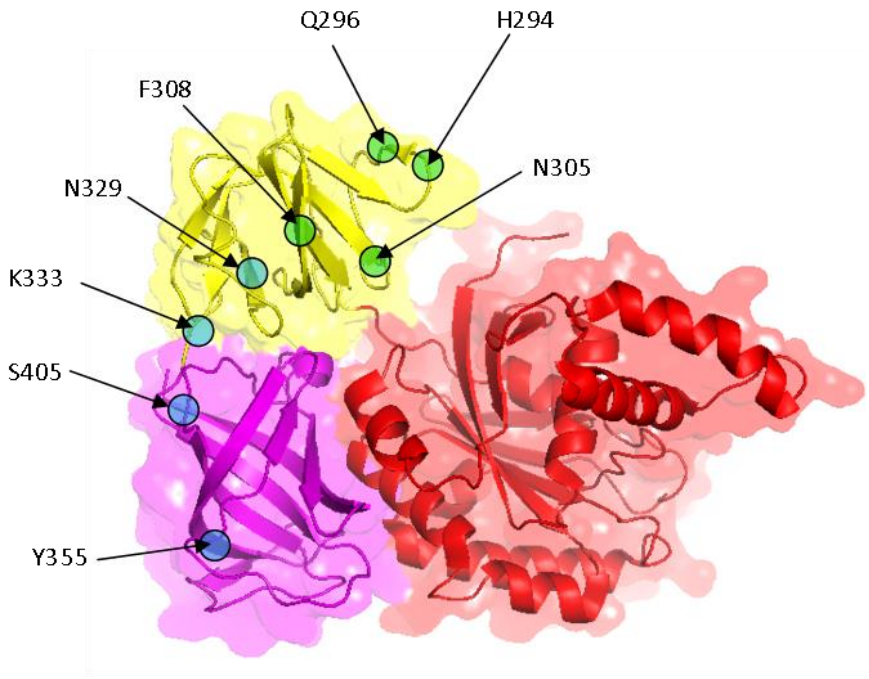


***Figure 4.10 Model of yeast eEF1A showing mutations known to rescue the growth defect observed when TEF1 is overexpressed.***

## *4.3.2 Point mutations in eEF1A have no significant effect on spindle pole bodies*

Further characterisation of the eEF1A mutants was carried out by expressing them in the Tub4-GFP expressing strain. Although no difference in spindle pole body localisation was observed when *TEF1* was overexpressed (see figure 4.7), deletion of *ARP1* resulted in spindle defects (see figure 4.6). Our aim was to utilise the eEF1A point mutations to see if altering the interaction between eEF1A and Arp1 had any observable effect on spindle pole bodies.

When we overexpressed wild type eEF1A fused to *URA3* a similar increase in Tub4-GFP fluorescence intensity was observed as in the unfused overexpression system, but there was no observable difference in Tub4 localisation. None of the point mutations appeared to have an observable effect on Tub4 localisation throughout the cell cycle. Similar to both the *URA3* fused and unfused overexpression strains, all the mutants resulted in an increase in

fluorescence intensity relative to the wild type with exception of the F308L mutant that exhibited similar fluorescence intensity to the wild type.

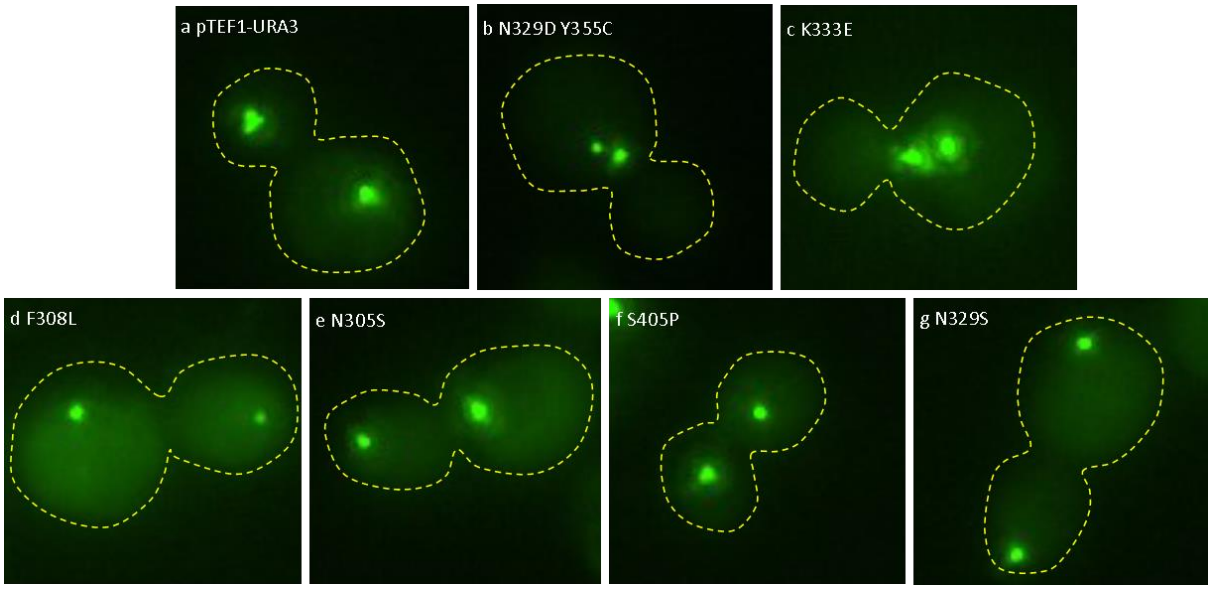


*Figure 4.11 a-g* ***Tub4-GFP with eEF1A overexpressed with various point mutations.*** *eEF1A fused to URA3 was overexpressed in Tub4-GFP. Point mutations that are known to effect actin binding and translational fidelity were introduced to observe their effect on Tub4p localisation. None of the mutations resulted in altered Tub4 location, but all but the F308L mutant caused an increase in Tub4 fluorescence.*

## 4.4 Discussion

In this chapter we utilise results derived from a high throughput screening method to elucidate a novel, putative interactive partner of eEF1A. Through overexpression of *TEF1* in an array of strains deleted for genes that are known to interact with or control the function of actin, we were able to identify a cluster of proteins that delivered a synthetic interaction with eEF1A that belonged to the dynactin complex. Further investigation into the interaction between eEF1A and other components of the dynactin complex yielded significant data that indicated an interaction between eEF1A and at least one component of the dynactin complex.

### *4.4.1 eEF1A overexpression rescues dynactin dependant aberrations*

FACS and microscopy analysis of dynactin mutants with endogenous and elevated levels of eEF1A showed that deletion of components of the dynactin complex resulted in significant genomic heterogeneity, with *TEF1* overexpression reducing the observable heterogeneity in all the dynactin mutants suggesting a role for eEF1A in regulating the cell cycle in response to genomic integrity. *TEF1* overexpression also resulted in the ablation of the third peak observed in the *Δarp1* mutant although when observed by microscopy *TEF1* overexpression induced an increase in observable multinucleate cells. Because of the significant homology between Arp1 and Act1, and because of the strong functional and physical interactions between eEF1A and Arp1 we had observed up to this point, the remainder of our efforts were focussed on elucidating the mechanism that eEF1A utilised to interact with Arp1 and the dynactin complex. We observed that the *Δarp1* mutant exhibited severe spindle aberrations, with most cells possessing seemingly uncontrolled spindle growth resulting in spindles positioned along the cell cortex, but also forming aberrant patterns throughout the cytoplasm. Overexpression of *TEF1* in the *Δarp1* mutant resulted in the rescue of the spindle aberrations, but not the aneuploidy as observed by microscopy. This demonstrated that overexpression of eEF1A was able to rescue the spindle defects, but not the aneuploidy induced upon deletion of *Arp1*. It is possible that eEF1A is able to stabilise actin in short filaments that are then able to substitute for Arp1 in the dynactin complex. This could result in the restoration of the complex that is then able to either fully or partially complete its roles. How eEF1A overexpression is able to rescue the spindle defect whilst causing a more severe aneuploidy defect is unclear. One possibility is that levels of eEF1A are involved in the regulation of cell cycle check points and elevated levels of eEF1A result in the bypass of these essential steps of cell growth, we do not however see a marked increase in aneuploidy in the

wild type cells with elevated levels of eEF1A indicating that this may not be the case. It could also be true that Arp1 is involved in the regulation of cell cycle check points and deletion of *Arp1* results in dis-regulation of controlled growth. Furthermore it may not be that be that Arp1 alone is involved in cell cycle regulation, but the entire dynactin complex. If *TEF1* overexpression is able to restore the dynactin complex it is possible that it does so in an inadequate manner in which it is unable to fulfil all of its roles. It may be able to restore correct positioning of the cytoplasmic spindles, but it is possible that due to the absence of actin fibres in the nucleus that actin is unable to substitute for Arp1 in the dynactin complex within the nucleus. This would result in correct positioning of the cytoplasmic spindles but aberrant nuclear spindles, potentially inducing aneuploidy.

### *4.4.2 Domains II and III of eEF1A mediate Arp1 translocation to the nucleus*

It is well known that residues in domains II and III of eEF1A are essential for its ability to bundle actin (Gross and Kinzy, 2005). We have found that overexpression of eEF1A results in significant translocation of Arp1 to the nucleus via a mechanism that is yet to be defined. We have clearly demonstrated that the residues in domains II and III of eEF1A known to be involved in eEF1A binding to actin are also involved in its ability to mediate Arp1 translocation to the nucleus. Mutation of any of these residues resulted in eEF1A overexpression no longer causing Arp1 translocation to the nucleus. Upon overexpression of four of the six eEF1A mutants, N329D Y355C, F308L, N305S and S405P, Arp1 appeared to localise to actin, microtubules and spindle pole bodies, as observed in the wild type cells, as well as apparent localisation to the mitochondria although this was not confirmed using co-localisation microscopy. Two of the mutants, K333E and N329S resulted in the loss of defined Arp1-GFP fluorescence indicating an inability of Arp1 to bind to other cellular components suggesting

that interactions between Arp1 and its interactive partners are facilitated by eEF1A in its native form.

These data suggest that eEF1A plays a significant role in cell cycle dynamics via mediation of Arp1 interactions with the dynactin complex and other interactive partners. It is also possible that eEF1A is able to stabilise actin in a form that can substitute for Arp1 in the dynactin complex in the *Δarp1* mutant.

# Chapter 5 Conservation of eEF1A interactions in humans

## 5.1 Introduction: eEF1A2 is an oncogenic isoform of the eukaryotic elongation factor 1A

As previously discussed, eEF1A is a highly conserved protein that is required during the elongation step of protein synthesis. Throughout eukaryotic species eEF1A has been characterised to fulfil the same canonical role, as well as other moonlighting functions. The different isoforms of eEF1A can be expressed at different stages of development or differentially expressed in various tissues. Although highly conserved, sharing 92% amino acid identity amongst isoforms in humans, these proteins display distinct expression patterns, and unique interaction profiles (see figures 5.1 a and b). The interaction profiles shown in figure 5.1 suggest that eEF1A1 plays a greater role in translation, as can be seen by the cluster of ribosomal proteins (Rps8,Rpl3, etc), eEF1A2 appears to have a strong interactions with the nucleoporins (Ranbp1, Rangap1, etc) and also several proteins involved in responses to JAK-STAT signalling (Ptpn1, Socs1, etc).

Elevated levels of eEF1A2 have been found in many tumours, and expression of eEF1A2 in non-native tissues is known to induce tumourigenesis (Anand *et al.*, 2002). Following on from our studies in yeast we aimed to characterise overexpression of the oncogenic *eEF1A2* in human cells, and to ask whether eEF1A overexpression-related phenotypes are conserved in higher eukaryotes. To do this we utilised the Invitrogen Flp-in system, allowing us to rapidly generate stable cell lines overexpressing eEF1A2 maintained in the presence of the antibiotic Hygromycin. We used human embryonic kidney cells (HEK293) for several reasons; the first is that kidney cells do not normally express eEF1A2 and so overexpression should mirror expression of eEF1A2 in normal tissue during the onset of tumourigenesis. The second reason for using HEK293 cells is that they are a rapidly growing adherent cell line, facilitating

observation of the cytoskeleton. Finally HEK293 cells were chosen over NIH3T3s (mouse fibroblasts) despite being transformed, because it has been reported that the CMV (cytomegalosvirus) promoter utilised in the Flp-In system is down-regulated over time in murine and rodent cells due to histone deacetylation, although the mechanism that mediates this is unknown.

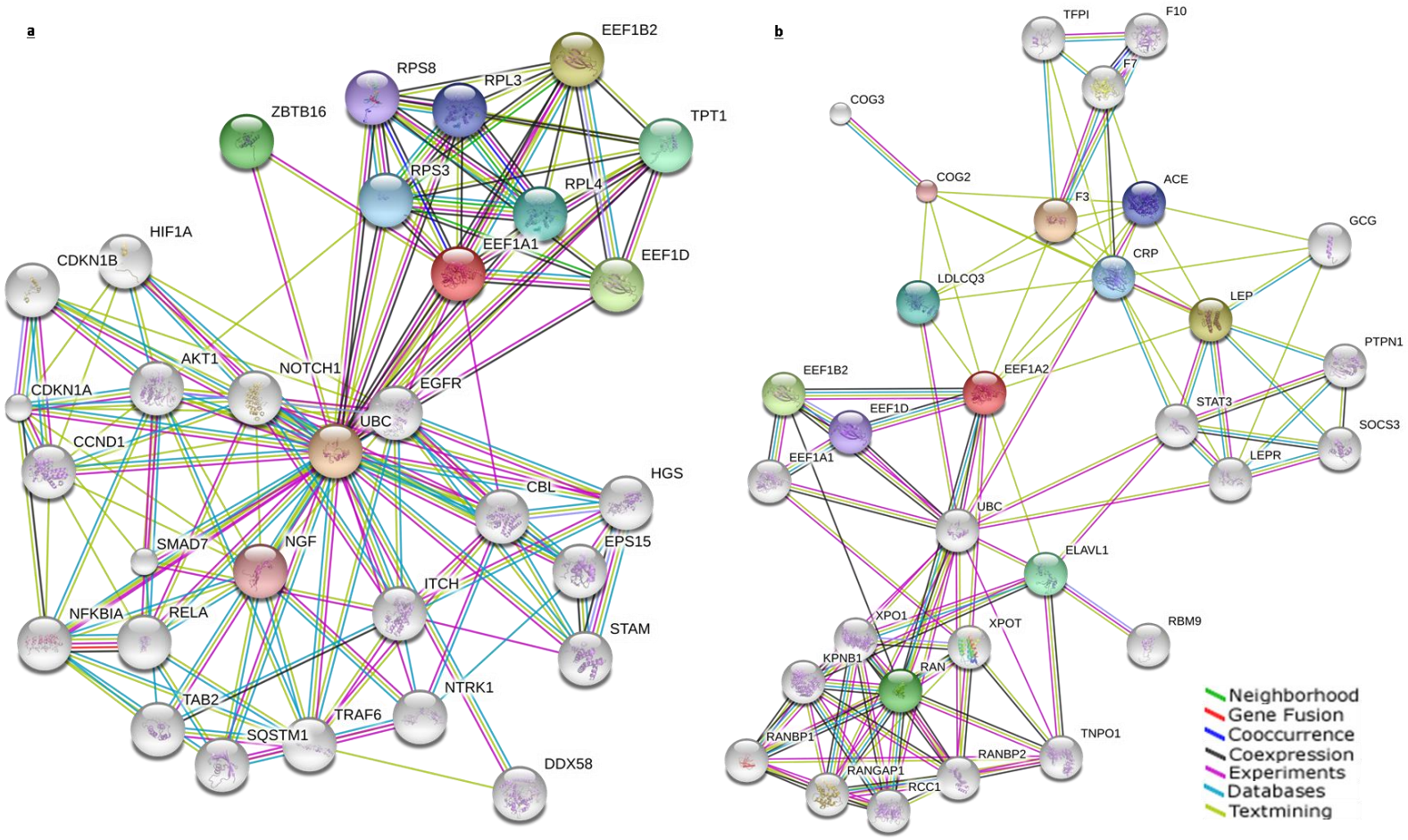


***Figure 5.1 a and b, Known and predicted protein interactions with eEF1A1 and eEF1A2.*** *Both a and b show the primary protein in red, with known and predicted protein interactions indicated by the connections. Generated using string.db.org* (Franceschini *et al.*, 2013).

## 5.2 Generation of eEF1A2 overexpression HEK293 cells

### *5.2.1 Cloning eEF1A2 into the pcDNA5/FRT expression vector*

To study the effects of eEF1A2 overexpression in human cells we generated a Flp-in expression vector that induced overexpression of eEF1A2 isolated from a human breast tumour (Anand *et al.*, 2002).

A pcDNA3.0 overexpression plasmid containing eEF1A2 was kindly provided by Jonathan Lee (University of Ottawa, Canada), using this and the pcDNA5/FRT expression vector we performed double digests with *HindIII* and *XhoI*, resulting in excision of eEF1A2 from the pcDNA3.0 vector, and a linearised fragment of pcDNA5/FRT that we ligated together (see figure 5.2 a and b) using the method described in section 2.4.9

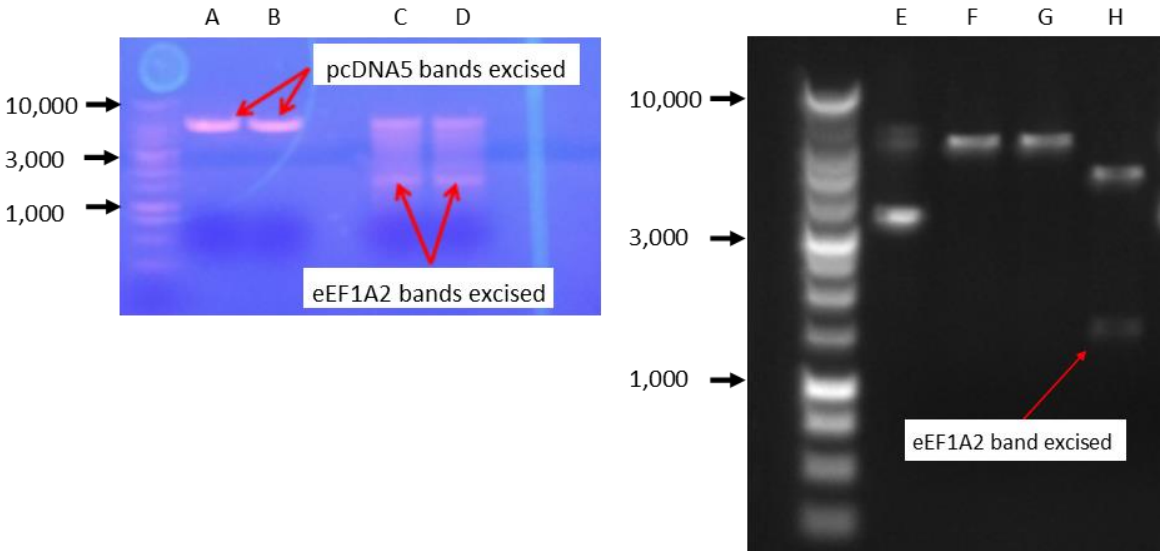


***Figure 5.2,*** *a) Digest of pcDNA5/FRT and pcDNA3.0 containing eEF1A2 and, b) digestion of ligated products. a) shows a double digest of pcDNA5/FRT and of pcDNA3.0 containing eEF1A2, these were digested with HindIII and XhoI, A and B are duplicates of the pcDNA5 digest, and C and D are duplicates of the pcDNA3 containing eEF1A2 digest, bands highlighted were excised and ligated together as described in the materials and methods. b) shows the ligated product (E), it also shows single cuts using HindIII (F) and XhoI (G), and it shows the double digest using both HindIII and XhoI (H), the highlighted band shows eEF1A2.*

## *5.2.2 Transfection of the pcDNA5/FRT-eEF1A2 overexpression vector into HEK293 Flp-in cells.*

HEK293 Flp-in cells were transfected as described in Chapter 2 (section 2.4.11). Cells containing the control vector (pcDNA5.0) or the eEF1A2 overexpression vector (pcDNA5.0/1A2) were confirmed by their ability to grow in media containing Hygromycin, and a sensitivity to Zeocin. eEF1A2 overexpression was confirmed by western blotting and probing for eEF1A2 using a rabbit polyclonal to eEF1A2 (abcam, ab82912), see figure 5.3.

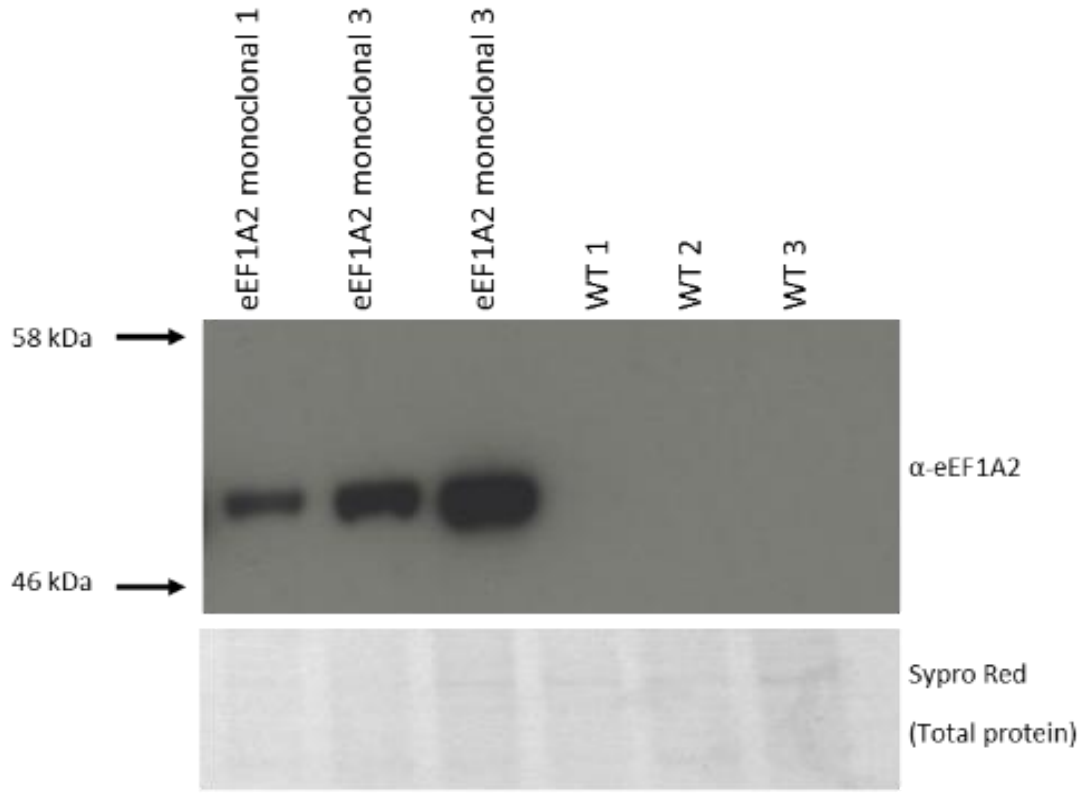


***Figure 5.3, Western blot showing eEF1A2 overexpression in HEK293 cells.*** *Western blots were probed with an antibody specific to eEF1A2. Total protein was detected using fluorescent sypro red. Three monoclonals were isolated for the eEF1A2 overexpressing cell line and for the wild type. All experiments were carried out with eEF1A2 monoclonal 3 as this had the highest levels of expression.*

## 5.3 Overexpression of eEF1A2 results in an increased growth rate in HEK293s

Because we had observed alterations in growth rate, cytoskeletal defects and genomic aberrations in yeast cells, these were the primary targets for characterisation in the HEK293 cells. We began by assessing growth using the ACEA Biosciences Xcelligence RTCA DP Analyser. This is an automated system that allows growth analysis of adherent cell lines by continuous measurement of the impedance of an electric current across a gold plated well (see figure 5.4) . As cells grow over the electrode at the bottom of the well the impedance increases and the system converts the impedance to an arbitrary value called Cell Index (CI). CI is also affected by the strength of a cell's adhesion to the surface and cells with more focal adhesions will result in a higher CI.

Growth analysis on HEK293 cells was performed as described in the Chapter 2 (section 2.6.2.4).

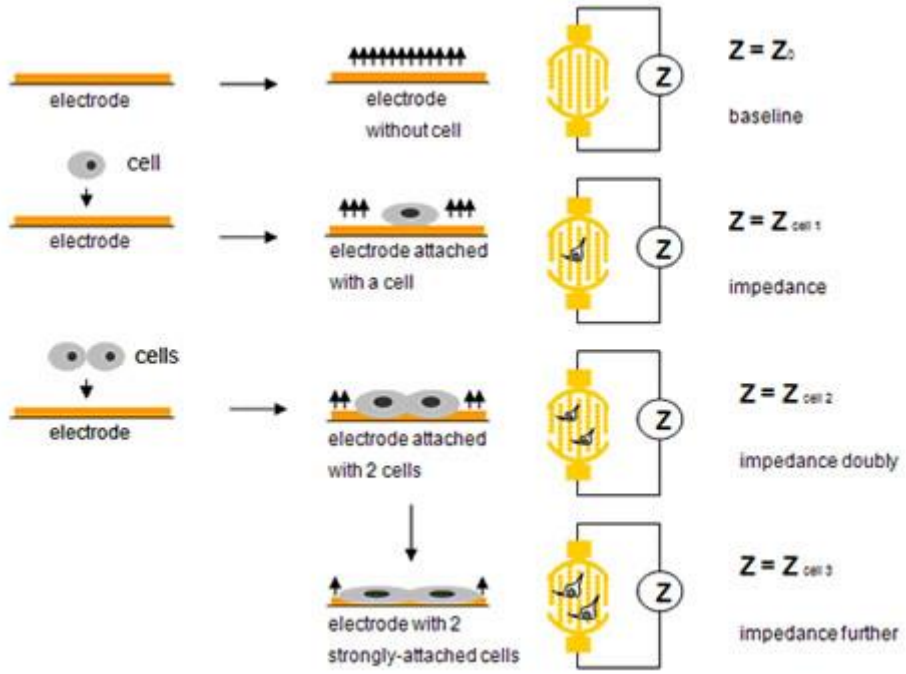


***Figure 5.4, Schematic view of the Xcelligence electrode with proliferating cells.*** *Each plate for the Xcelligence system contains 16 wells with each well containing a gold electrode in the bottom as shown in this figure. The electrode is an incomplete gold mesh that when covered with growth media generates a baseline signal. Addition of cells to the well affects the ionic environment causing an increase in electrode impedance. The addition of more cells (proliferation) or the number of focal adhesions will increase the impedance. This value of impedance is converted to an arbitrary value known as the cell index (CI). Image taken from http://www.aceabio.com.*

Analysis of the wild type and *eEF1A2* overexpressing cells revealed that in HEK293 cells elevated levels of eEF1A2 induced a reduction in doubling time, as previously reported to occur in NIH3T3 cells (Anand *et al.*, 2002). HEK293 cells with endogenous levels of eEF1A2 had a doubling time of approximately 26 hours, with an increase in eEF1A2 levels inducing a reduction of 23% to approximately 20 hours (see figure 5.5-b). Cells overexpressing eEF1A2 also adhered to the surface more rapidly (see figure 5.5-c). This rapid adherence may be due to the effect of the interaction of eEF1A2 with actin, promoting actin remodelling and a greater number of focal adhesions, however further experimentation would be required to test this possibility. Further evidence that eEF1A2 promotes stronger adhesion to the substrate can be observed at the peak of the growth curve (see figure 5.5-a) where it is clear that the eEF1A2 overexpression lines reach a higher CI than the wild type cells. There are two

possible reasons for the higher CI observed at around 100 hours into the assay, the first, as discussed, is that eEF1A2 promoted stronger focal adhesions to the surface. The second is that eEF1A2 inhibited apoptosis and the cells were growing on top of each other resulting in multiple layers of cells for the current to pass through. However, either reason, indicates that HEK293 cells responded in an aberrant manner to elevated levels of eEF1A2.

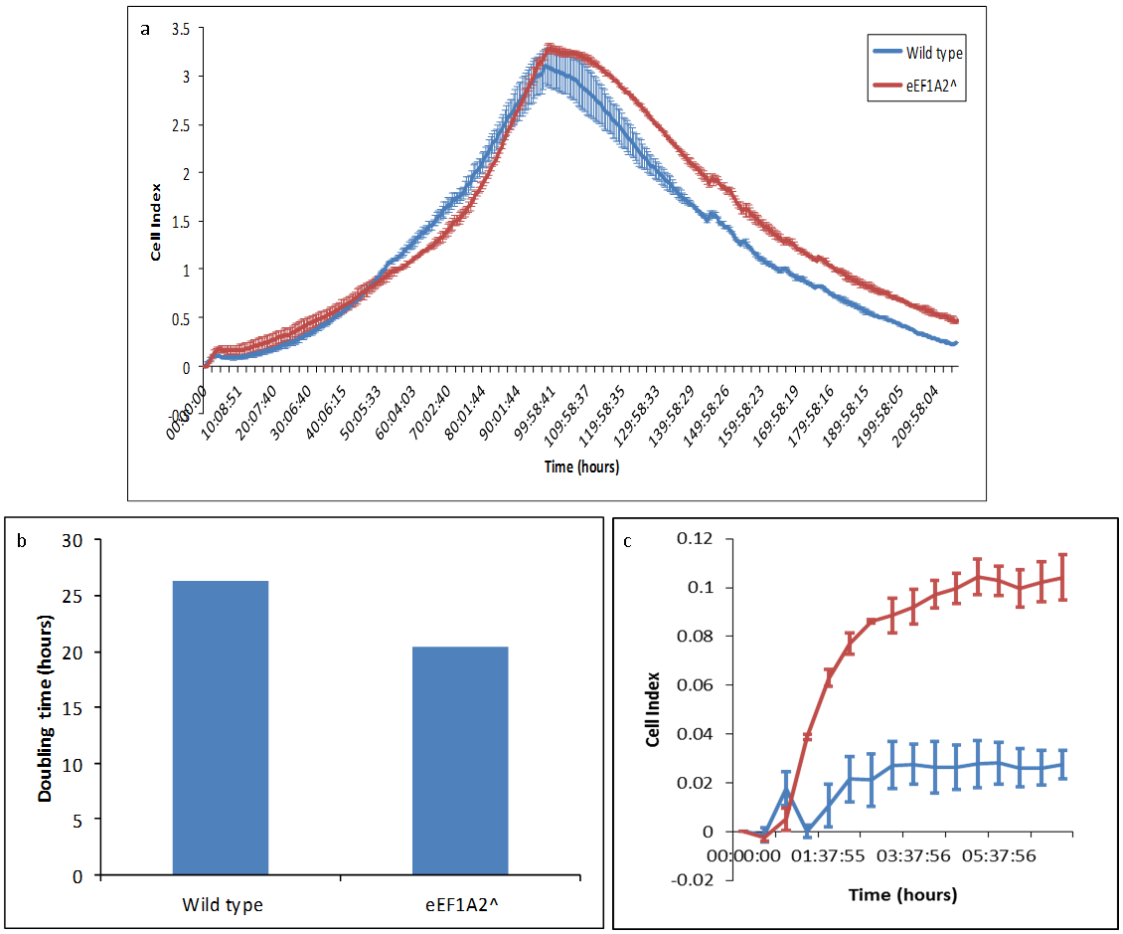


***Figure 5.5 a-c Growth curve and doubling time of wild type and eEF1A2 overexpressing HEK293 cells.*** *Growth analysis was performed using the Xcelligence plate reader, figure 5.5-a shows the entire growth curve over the period of almost 10 days, this allowed us to not only capture the growth of the cells, but also the death kinetics. Figure 5.5-b shows the doubling time of the wild type and eEF1A2 overexpressing cells taken during the maximal log phase of growth. Figure 5.5-c shows the first seven hours of the assay highlighting the rapid adherence by the cells overexpressing eEF1A2.*

### *5.3.1 HEK293 cells with increased levels of eEF1A2 respond to drugs*

To further understand the effect of increased levels of eEF1A2 on HEK293 cells growth analysis was performed in the presence of various inhibitory drugs. It was hoped that eEF1A2 might confer sensitivity to some of the drugs and resistance to others, thereby elucidating a possible mechanism it utilises to effect cell growth.

The drugs chosen were Nocodazole and Rapamycin. Nocodazole was chosen for its known effects on microtubule polymerization as we had observed effects on the spindles by *TEF1* overexpression in yeast (see section 4.2.3). Rapamycin was chosen for its inhibitory effect on the TOR (target of rapamycin) pathway. Components of the TOR pathway were elucidated as potential interactive partners of eEF1A during this study (not discussed in this thesis), TOR is also known to play a significant role in the development of cancer (For a review see Beauchamp & Platanias, 2013).

When grown in the presence of Rapamycin wild type cells exhibited a moderate increase in doubling time of approximately 14% to 30 hours whether grown in 10 or 20 µM (see figures 5.6 a and b). Wild type cells also showed an increase in lag phase of almost 50 hours suggesting a dramatic effect on the TOR pathway and an inability of the cells to respond to its nutritional environment. Treatment of the eEF1A2 overexpressing cells with 10 µM Rapamycin resulted in a similar increase in doubling time observed in the wild type cells to approximately 30 hours. However, upon addition of 20 µM of Rapamycin to cells overexpressing eEF1A2 an increase in doubling time of 42% was observed, resulting in a doubling time of almost 38 hours. The lag phase of eEF1A2 overexpressing cells was affected similarly to the wild type cells with an increase in lag phase growth of almost 50 hours.

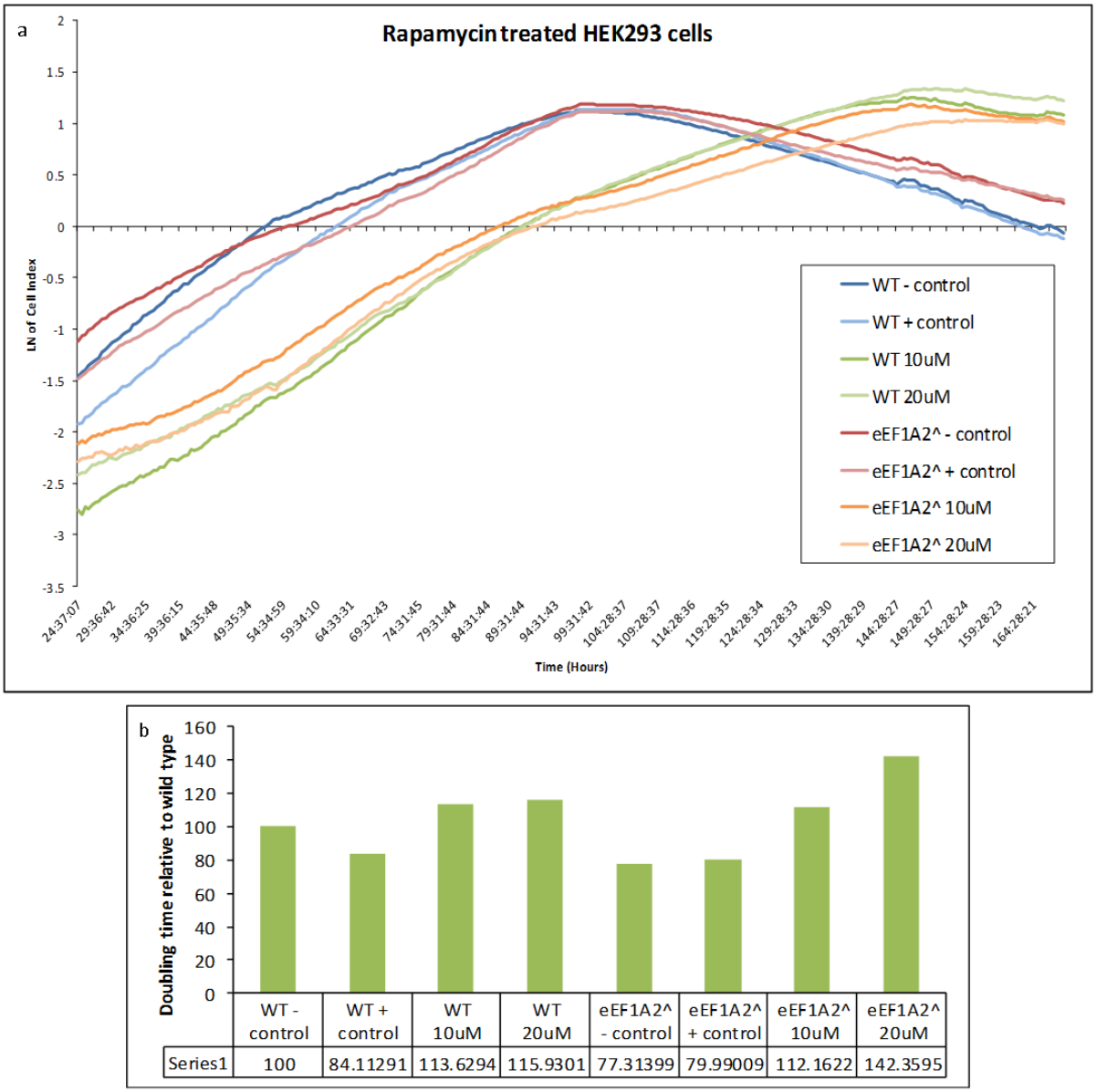


***Figure 5.6 a and b, growth analysis of HEK293 cells with endogenous and elevated levels of eEF1A2 treated with Rapamycin.*** *Treatment of HEK293 cells with Rapamycin caused a similar increase in lag and log phase growth rates. However treatment of the eEF1A2 overexpressing strain with 20 µM resulted in an observable sensitivity in this cell line.*

Addition of 2 mM Nocodazole to the growth media resulted in no effect on the maximal rate growth of wild type cells with a doubling time of approximately 26 hours (see figure 5.7 b). Upon addition of Nocodazole to wild type cells their growth dynamics mimicked that of the eEF1A2 overexpressing line with a more rapid adhesion to the substrate and an increase in the final peak intensity prior to cell death (see figure 5.7 a). However, it is not known if this is

due to an increase in the rate of growth or simply due to an increase in focal adhesions made by the cell. eEF1A2 overexpressing cells exhibited sensitivity to Nocodazole with a decrease in both the rate lag time and log phases of growth, with an increase of a doubling time of 5% relative to the untreated eEF1A2 overexpressing cells taking the doubling time to approximately 23 hours. The initial adhesion phase of the eEF1A2 overexpressing cells was also affected with cells appearing to settle on, and attach to the substrate far slower and similar to that observed for wild type cells.

eEF1A2 overexpression conferred sensitivity to both drugs suggesting that cells with elevated levels of eEF1A2 are unable to tolerate additional stress imparted by drug treatments. It is possible that eEF1A2 overexpression has deleterious effects on both pathways affected by the separate drug treatments. As discussed in chapter 3 (section 3.4) eEF1A may play a role in nutrient sensing, which in part, is mediated by TOR signalling, and in chapter 4 (section 4.2) it was documented that eEF1A also plays a significant role in facilitating the functions of dynactin, the activating complex of dynein, which in turn plays a role in spindle formation. It is therefore probable that in the presence of elevated levels of eEF1A2 cells, are already burdened and the extra stress from treatment with any drug is enough to further impede growth.

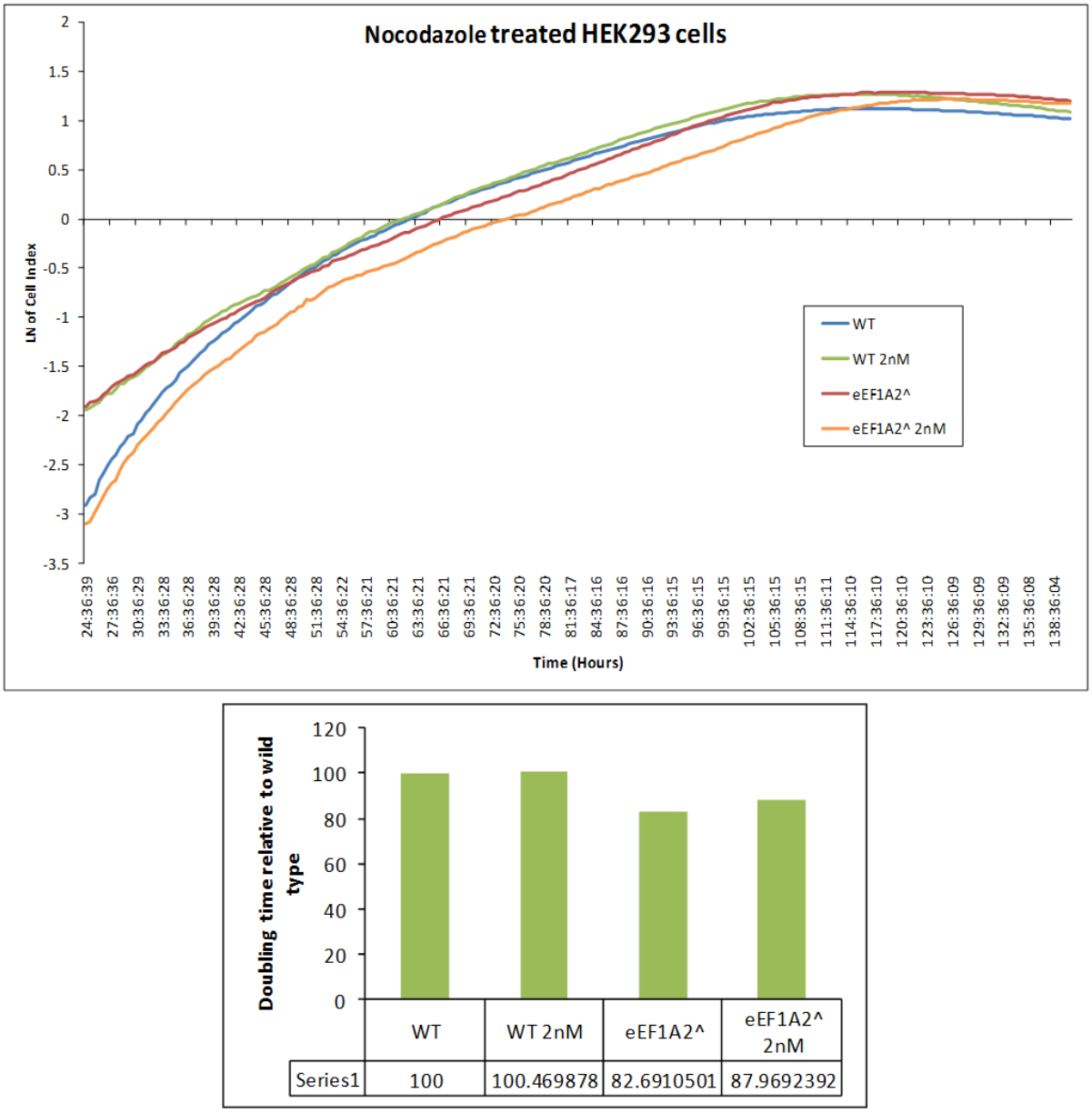


***Figure 5.7 a and b, growth analysis of HEK293 cells with endogenous and elevated levels of eEF1A2 treated with Nocodazole.*** *Treatment of HEK293 cells with Nocodazole, treatment appeared to have no significant effect on the growth of wild type cells but resulted in a decrease of both lag and log phase growth rates in eEF1A2 overexpressing cells.*

## 5.4 eEF1A2 overexpression results in similar genomic aberrations as observed in yeast.

As discussed in the introduction (section 1.2.1) eEF1A2 expression is limited to certain tissue types in higher eukaryotes with expression in abnormal tissues promoting tumour development. Tumour development is known to occur because of aberrations in genomic content resulting in altered metabolism and constitutive growth signals resulting in uncontrolled proliferation. We observed in our yeast system that when analysed by FACS, overexpression of eEF1A resulted in a significant shift of DNA peaks to the right, when analysed by FACS (see figure 4.4) and bigger, brighter nuclei when visualised by microscopy (see figure 4.5), suggesting that cells contained increased levels of DNA, or that overexpression of *TEF1* resulted in incomplete chromosome condensation and increased uptake of DNA staining dyes. To answer the question "Is this phenotype is conserved through to higher eukaryotes?" we performed the same assay on HEK293 cells.

Cells were grown in a T75 flask to 70% confluence and trypsinized, counted and $1x10^7$ cells were pelleted and fixed in 1 mL of -20°C 70% EtOH whilst vortexing. The cells were then rehydrated and PI was added to a final concentration of 6 µg/mL. As with the yeast samples all analysis was performed using the FACSCalibur flow cytometer.

Analysis of the wild type cells by FACS revealed two peaks representing two complete haploid sets (2C) and cells that have undergone genome duplication (4C) in preparation for mitosis, (see figure 5.8 a). Analysis of these cells by fluorescence microscopy revealed most cells contained a single, spherical nucleus that filled approximately 60-70% of the total cell volume (see figure 5.8 b). Overexpression of *eEF1A2* in the HEK293 cells resulted in a similar shift to the right in the FACS spectrum, as was observed in yeast upon overexpression of *TEF1* (see

figure 5.8 a). How eEF1A in yeast and eEF1A2 in HEK293 cells cause this change is not understood, but it appears to correlate with cells that possess larger nuclei when observed by microscopy (see figure 5.8 c) suggesting an inability of cells to correctly segregate chromosomes. Overexpression of *eEF1A2* resulted in the majority of cells containing abnormal, elongated nuclei (see figure 5.8-c), and a small proportion that were multinucleate.

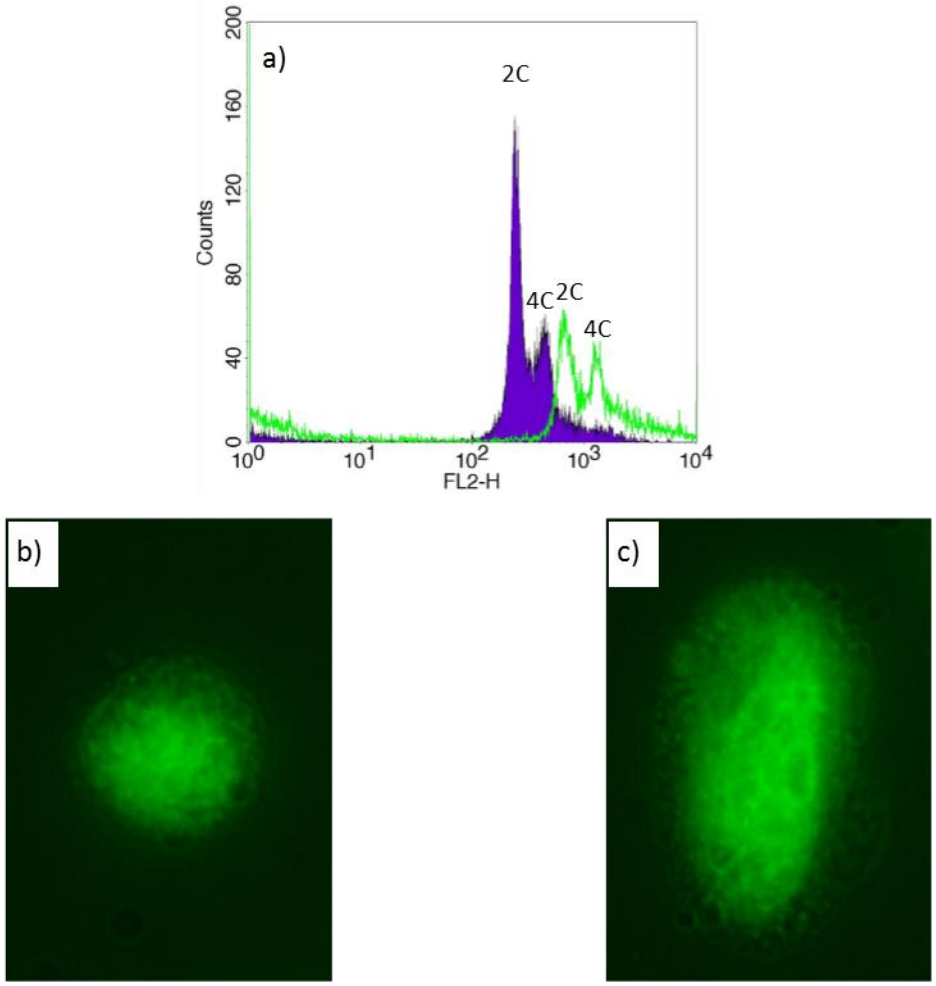


***Figures 5.8 a-c, HEK293 cells stained with PI and analysed by FACS and fluorescence microscopy.*** *HEK293 cells expressing endogenous and elevated levels of eEF1A2 were stained with PI and then analysed using FACS (a) shows the peaks shift to the right in the cells containing elevated levels of eEF1A2. Fluorescence microscopy (b and c) shows a HEK293 cell with endogenous levels of eEF1A2, and HEK293 cell with elevated levels of eEF1A2 containing an elongated nucleus. Images were acquired using a 60x objective. Purple line represents the parental cell line, and the green line is the eEF1A2 overexpressing cell line.*

## 5.5 eEF1A2 overexpression induces microtubule aberrations in HEK293 cells

As we had previously observed an interaction between yeast eEF1A and components of the dynactin complex resulting in microtubule defects, and the effects of eEF1A overexpression on genomic content appeared to be conserved from yeast to humans, we next asked the question "Is there was any observable interaction between eEF1A2 and microtubules in HEK293 cells?"

To assess microtubule integrity in HEK293 cells the cells had to be grown on coverslips coated with poly-lysine to facilitate adherence as they are only semi-adherent and do not stick to the glass coverslips. Cells were grown to 70% confluence and then immunofluorescence was performed as described in chapter 2 (section 2.6.1.4). Although repeated on several occasions this procedure yielded poor success rates, with very few cells adhering to the surface, and fewer of those acquiring the fluorescent signal. This meant there were not enough observable cells to generate any statistically significant conclusions (between 60-80 per sample). However, there were consistent differences observed between the samples as discussed below.

Wild type cells exhibited a slightly more elongated, slender morphology compared to the eEF1A2 overexpressing cells that appeared larger, rounder and squatter. The wild type cells had longer, more defined microtubules that exhibited an ordered arrangement emanating from the cell poles in an astral array (see figure 5.9 a). The microtubules in the eEF1A2 overexpressing cells lacked the organisation exhibited by the wild type cells with microtubules growing in aberrant patterns with no obvious point of origin (see figure 5.9 b). DAPI staining of the nucleus allowed the observation of the nuclei that were larger in the eEF1A2

overexpressing cell line than in the wild type. This observation was in concurrence with the microscopy acquired from the PI staining (section 5.4).

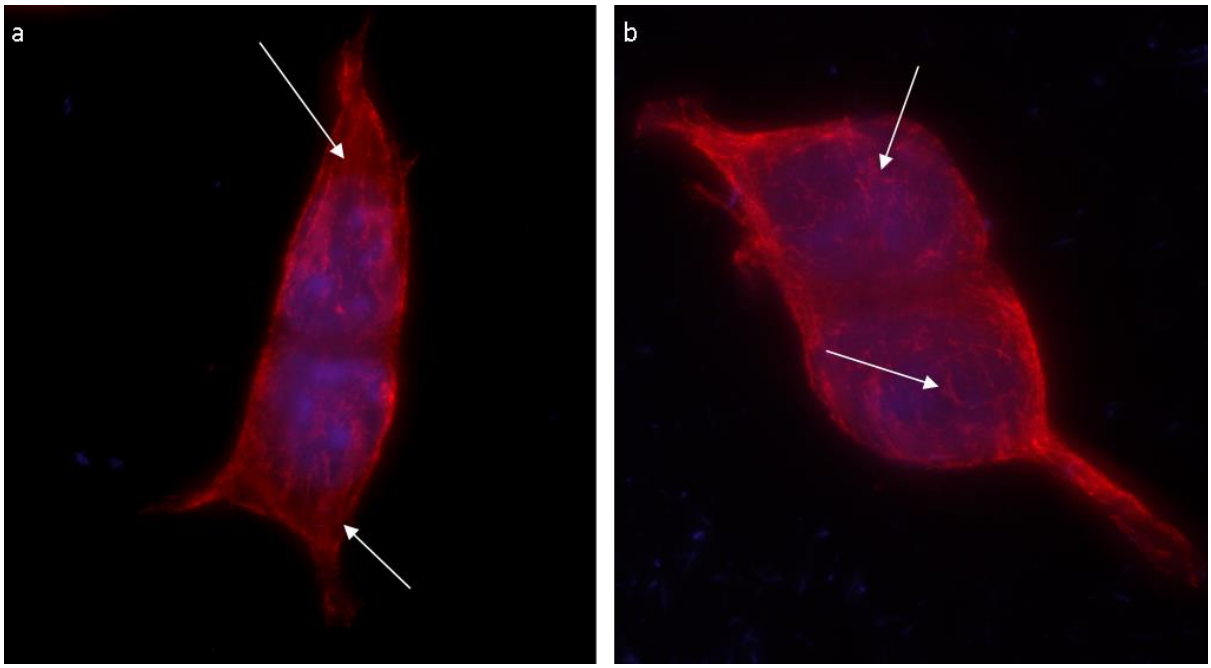


***Figures 5.9 a and b, Immunofluorescence of HEK293 cells allowing visualisation of the microtubules and the nuclei.*** *HEK293 cells were probed using an anti-tubulin primary anti-body with a TexRed secondary anti-body (red), they also stained with DAPI (blue). Arrows on 5.9-a show the origin point of many of the microtubules that can be seen to project along the length of the cell. Arrows on 5.9-b show highlight some of the microtubules that appear to be growing in a disordered manner.*

## 5.6 Human eEF1A isoforms expressed in yeast do not function to replace yeast eEF1A

As we had seen conservation of eEF1A interactions from yeast to human cells we asked whether they were functionally redundant. To do this we utilised a yeast strain generated in John McCarthy's lab (University of Warwick) (Firczuk et al., 2013) that had *TEF2* deleted and where *TEF1* was placed under control of a TetO7 promoter, allowing almost complete ablation of native eEF1A expression through addition of doxycycline to the growth medium. We transformed this strain with a plasmid expressing either yeast *TEF1*, or human *eEF1A1* or *eEF1A2* all under control of the strong constitutive *TDH3* promoter (plasmids were provided

by Chris Grant, University of Manchester). When grown in the presence of 10 µg/mL Doxycycline, enough to suppress expression of native *TEF1,* the only source of eEF1A came from the plasmid based expression allowing us to observe the ability of human eEF1A isoforms to fulfil the role of yeast eEF1A. All analysis was performed by assessing growth rate as a measure of cell fitness.

Knockdown of native *TEF1* in the wild type strain resulted in very poor growth and cells that had a maximal doubling time of almost 8 hours, 3.5 times longer than the wild type (see figure 5.10 a pale blue trace and 5.10 b). Because eEF1A was expressed at low levels we had hypothesised that cells would struggle to grow. Expression of *TEF1* resulted in a slight increase in doubling time relative to the wild type, probably due to the toxicity associated with elevated levels of eEF1A as previously discussed (section 3.2). Knockdown of native eEF1A in the *TEF1* overexpression strain had no effect on growth rate as the plasmid-based *TEF1* was able to fully compensate for the loss of chromosomal expression (see figures 5.10 a red and pink lines and 5.10 b). Expression of eEF1A1 in the presence of native *TEF1* levels resulted in an increase in doubling time of 53% suggesting that eEF1A1 induced increased levels of toxicity relative to yeast eEF1A. Suppression of *TEF1* expression induced by Doxycycline resulted in severe growth retardation when eEF1A1 was the only form of eEF1A available to the cells, with an observed increase in doubling time of almost 4 times the wild type suggesting that eEF1A1 is unable to fulfil the essential roles required by the yeast cells (see figures 5.10 a dark and light green lines and 5.10 b). Expression of eEF1A2 in the presence of native eEF1A resulted in an increase of 40% in doubling time relative to the wild type suggesting, similar to eEF1A1 expression, that eEF1A2 is confers significant toxicity to yeast cells. Knock down of eEF1A leaving eEF1A2 as the only eEF1A isoform resulted in a greater

increase in doubling time than with eEF1A1, resulting in an increase in doubling time to more than 4 times the wild type, and barely growing better than cells containing the control plasmid (see figures 5.10 a dark and light purple lines and 5.10 b). This suggests that eEF1A1 and eEF1A2 are able to carry out different roles in yeast cells, with eEF1A1 facilitating yeast proliferation better than eEF1A2.

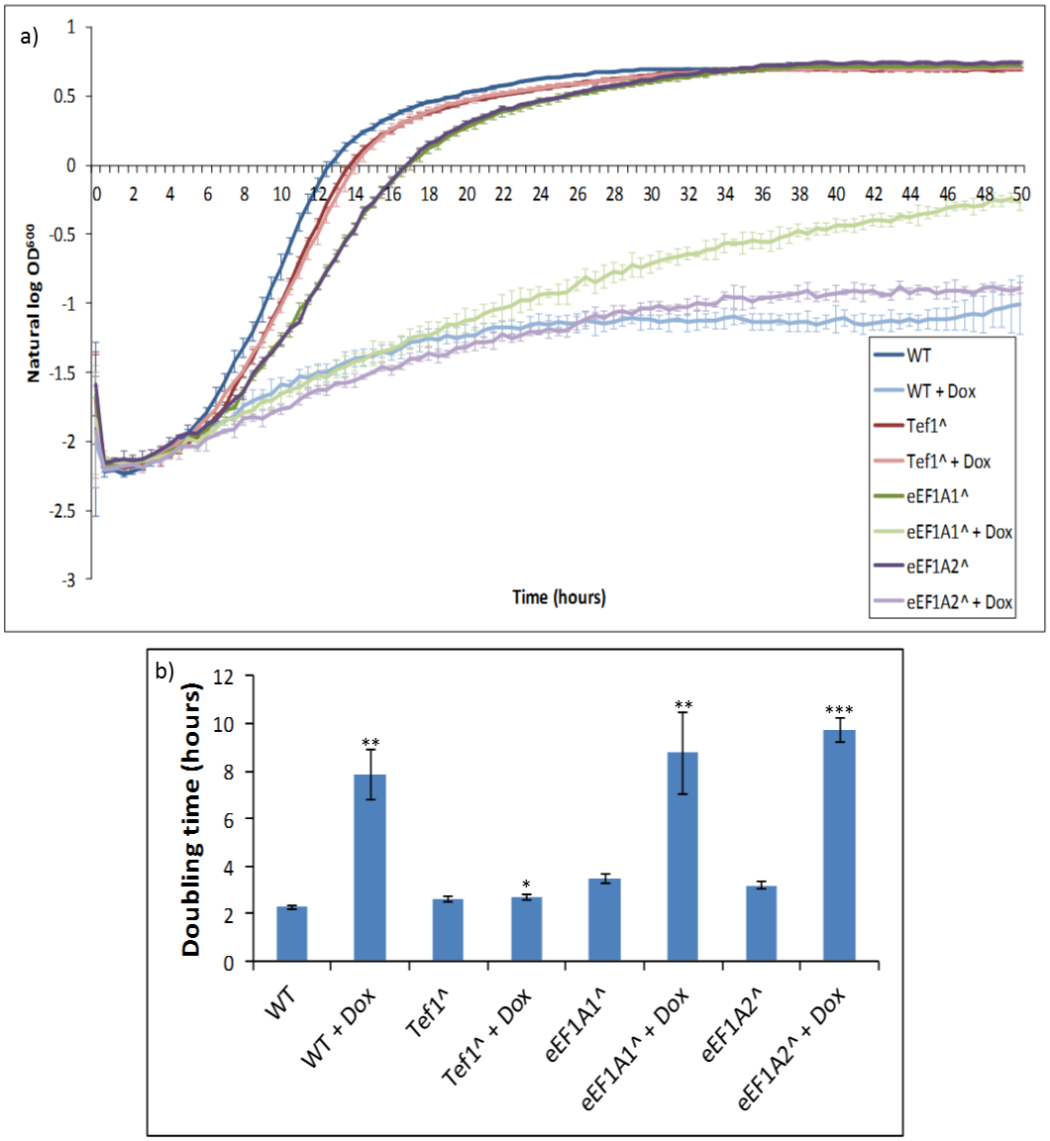


***Figures 5.10 a and b, Growth analysis of yeast cells expressing different eEF1A isoforms.*** *a- Cells containing either yeast eEF1A or human eEF1A1 or eEF1A2 were grown in the presence of Doxycycline which suppressed levels of native eEF1A allowing us to monitor the effect of different eEF1A isoforms on yeasts ability to proliferate. b- Doubling times for each of the strains analysed, it is clear to see that eEF1A1 and eEF1A2 are unable to fulfil the role of yeast eEF1A. . p-values are represented by asterisks, *=<0.5, **=<0.05, ***=<0.005.*

## 5.7 Discussion of results

Because of the high degree of conservation between *TEF1* and *eEF1A2* we were able to perform rapid, inexpensive analysis of eEF1A overexpression in yeast to facilitate identification of interactive partners in higher eukaryotes. Here we have identified several effects of eEF1A overexpression in yeast that are conserved through to humans.

We have demonstrated that similar to previously published data in NIH3T3 cells, eEF1A2 overexpression induces an increase in growth rate in cells from higher eukaryotes. Furthermore we have demonstrated that overexpression of eEF1A2 in HEK293 cells results in similar effects as seen with eEF1A overexpression in yeast.

We have confirmed that a shift to higher genomic content in FACS analysis of PI stained cells, as observed in yeast cells with elevated levels of eEF1A, is conserved through to HEK293 with elevated levels of eEF1A2. Although the reason for the shift is not understood, and likewise, the mechanism that mediates it, eEF1A2 overexpression also results in aberrations in microtubule arrangement, suggesting a conserved mechanism for eEF1A to modulate cell cycle dynamics although this clearly needs further investigation to confirm this hypothesis.

Although we have demonstrated that several phenotypes induced by eEF1A overexpression are conserved through to human cells, we also demonstrated that yeast and human eEF1A isoforms appear to have unique functional profiles and that human isoforms are unable to substitute for yeast eEF1A in *S.cerevisiae*. By deleting *TEF2* and knocking down *TEF1* we were able to ensure that eEF1A expressed from a plasmid was the sole source of eEF1A in the cell. This gave us the ability to identify if eEF1A1 or eEF1A2 were able to substitute for eEF1A in yeast cells. eEF1A1 expression resulted in better growth of yeast cells than eEF1A2 suggesting that it is able to carry out at least some of the functions of eEF1A. eEF1A2 expression however,

resulted in the complete retardation of growth suggesting that it is completely unable to fulfil any of the roles required of it by the yeast cell. This is a very strong indication that eEF1A1 and eEF1A2 have different functional profiles, which would explain why they are differentially expressed during development and in different tissue types. Furthermore the inability of eEF1A2 to function in yeast could be due to its decreased affinity for both GTP and its GEF eEF1B, reinforcing that eEF1A2 may have evolved to favour one of its extra functions over its canonical role during translation elongation.

# Chapter 6: Transcriptome analysis of *TEF1* overexpressing cells

## 6.1 Introduction

We have observed that eEF1A overexpression in both yeast and HEK293 cells can induce growth defects, and genomic and cytoskeletal aberrations. We have also observed that in yeast, *TEF1* overexpression has a plethora of other effects on a wide array of cellular components and pathways. To assess the global effects of *TEF1* overexpression on cells we carried out a transcriptome analysis using microarrays. We chose to use this method as it would provide us with a large data set that could elucidate the transcriptional alterations associated with elevated levels of *TEF1.*

### *6.1.1 The affymetrix Yeast 2.0 GeneChip*

It is well known that cellular functions can be controlled through the regulated expression of genes in response to a variety of signalling pathways. Microarray is a common method for observing gene expression profiles on a global scale. This method allowed us to visualise the effects of *TEF1* overexpression upon mRNA levels relative to wild type. In order to generate these data total RNA was isolated from yeast cells during log phase growth. The RNA samples were sent to Source Biosciences for them to perform the remaining steps of the microarray process. Following reverse transcription reactions the cDNA template was hybridised to an Affymetrix Yeast 2.0 GeneChip array. The raw data obtained from analyses carried out by Source Biosciences were then processed using the Bioconductor plugin, affylmgui (Wettenhall *et al.*, 2006) following the worked example found at http://bioinf.wehi.edu.au/affylmGUI/Doc/estrogen.html and Affymetrix Expression Console Software found at http://www.affymetrix.com/estore/browse/level_seven_software_products_only.jsp?productId=131414#1_3. A cut off point was established for genes that were designated to have

significantly altered expression; this was denoted as those genes with a B-statistic greater than 1.5. This analysis resulted in a total of 319 significantly up-regulated genes and 61 significantly down-regulated genes in the presence of *TEF1* overexpression.

## 6.2 Pre-processing of data

Prior to any analysis or quality assessment of microarray data, the raw unprocessed data must be pre-processed to ensure that it is of the highest possible quality and free from variation due to background noise and variation introduced by technical replicates.

### *6.2.1 Background correction*

As with most fluorescence-based assays, background fluorescence is a problem for microarrays. It is likely to occur even if slides are only treated with labelled sterile water which is then hybridised to the array causing a low level of fluorescence to still be detected by the scanner. Other sources of background fluorescence are non-specific binding of the labelled sample, noise from the scanner or deposits left behind after washing. To reduce background noise we used the Robust Multi-Array Average (RMA) algorithm (Bolstad *et al.*, 2003). This algorithm corrects the raw intensity values by log2 transformation and quantile normalisation. It then fits a linear model to the normalised data in order to obtain an expression measure for each probe set on each array.

### *6.2.2 Normalisation*

Normalisation is used to adjust the data for technical variation, rather than for biological differences between the samples. Due to the nature of the assay the hybridisation process will always result in variations leading to scaling differences between the fluorescence intensity levels across arrays. The normalisation process corrects for these differences in fluorescence intensity by comparing like for like.

## 6.3 Quality assessment of the microarray data set

Prior to any biological interpretation of the microarray data set there were a variety of methods employed to ensure that the data was robust. The first step was to perform background correction and normalisation of the raw data as described in section 6.2 above. This was because the raw unprocessed data was likely to contain variation due to the variable nature of technical replication. Normalisation of the raw data removed a large amount of the variation in order to guarantee that all interpretation was performed on data that was robust. Following normalisation, an array of quality assessment steps was performed to ensure that the data were of the highest possible quality. We employed several statistical methods to check the integrity of the raw and normalised data, and visual analysis of artificially generated images of the residuals was performed to check for any defects present on the chip surface. We also checked RNA degradation to check the quality of the mRNA that was used for the hybridisation.

### *6.3.1 Visualising residual images*

Prior to any further analysis synthetic images were generated using the affylmgui package and the "Image quality plot" command. These allowed us to visualise the gene chips to check for any physical damage that may result in aberrant readings. Damage may have occurred through handling or during manufacture. Common abnormalities that cause aberrant readings are scratches or fingerprints on the coverslip, bubbles under the coverslip, or diffuse artefacts arsing from irregularities in washing.

Inspection of our residual images (see figure 6.1 a-e) revealed that all of our gene chips appeared to be well prepared with the exception of 6.1-d which appeared to have an abnormality caused by either irregular washing or a bubble trapped under the coverslip.

Other artefacts such as empty patches and striations were observed but they are common across all affymetrix gene chips.

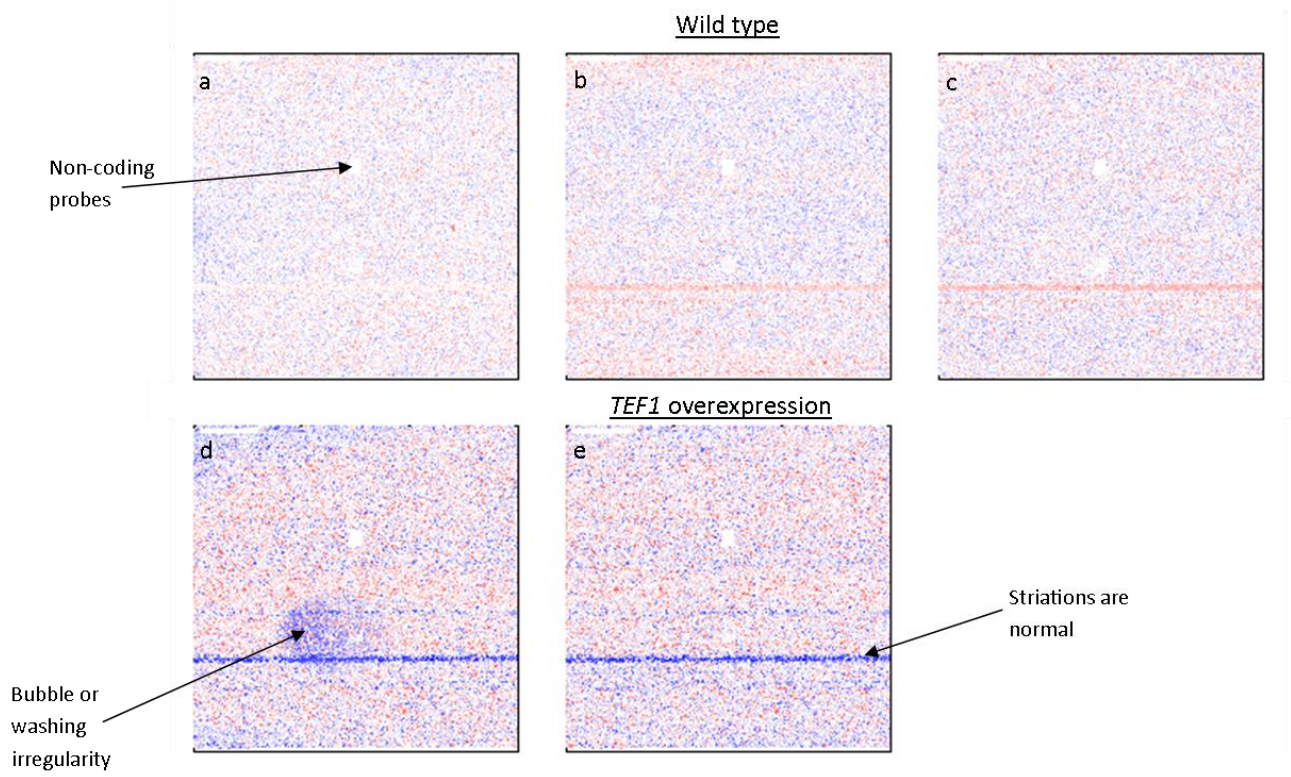


***Figure 6.1, Synthetic images of residuals.*** *Images show negative residuals as blue and positive as red. These images allowed us to visualise the gene chips and inspect them for any aberrations that may result in abnormal values.*

## *6.3.2 RNA degradation plot*

The next quality assessment step was to ensure that the mRNA used for the array was of sufficient quality. RNA degradation can occur during preparation resulting in a poor measure of gene expression. Degradation begins at the 5' end and progresses towards the 3' end, this allowed us to easily measure degradation using oligonucleotide arrays. Sequential numbering of perfect match (PM) probes from the 5' end of the targeted mRNA transcript to the 3' end allowed a graphical representation of mRNA degradation (see figure 6.2). RNA degradation is

represented by elevated values at the 3' end compared to the 5' end. Higher quality RNA typically exhibits a slope between 0.5 and 1.7, and slopes that are greater than twice this value are considered to be due to excessive degradation of mRNA resulting in poor quality results.

Figure 6.2 shows that the RNA used for this array was not excessively degraded, meaning that all samples were of good quality. The RNA also exhibited similar degradation slopes across the five samples (three wild type and two *TEF1* overexpression) showing that there was agreement between the gene chips, and because all the arrays are similar then comparisons within genes across the arrays are still likely to be valid even if RNA degradation had occurred.

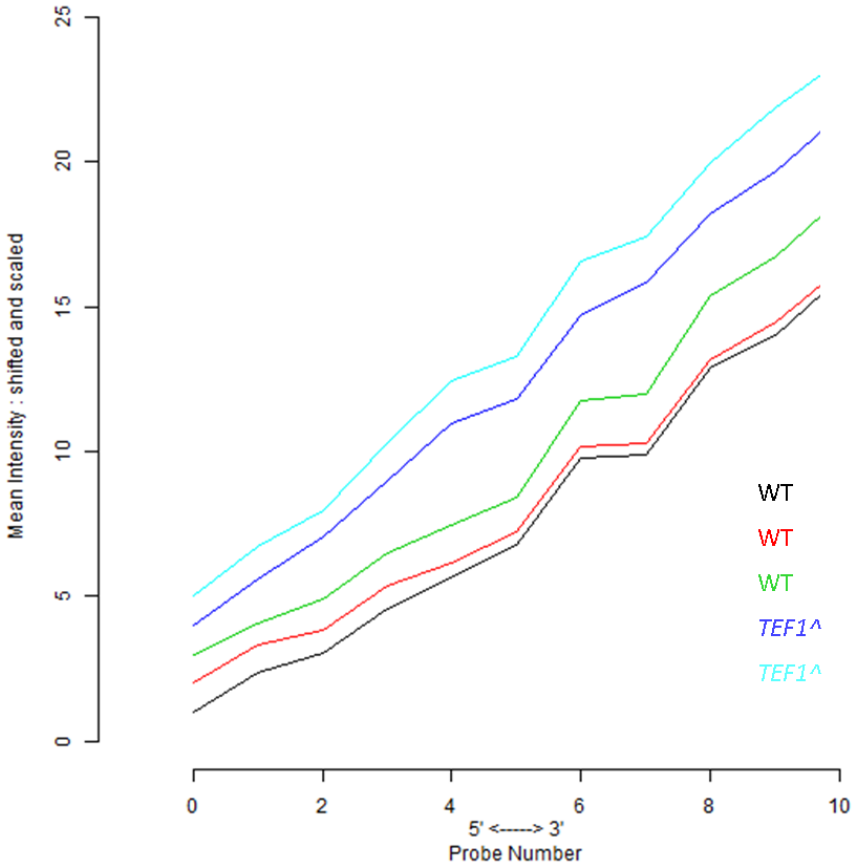


***Figure 6.2, RNA degradation plot.*** *A plot of the five RNA samples analysed using microarray. All samples exhibited a similar slope suggesting degradation at a similar rate.*

## *6.3.3 Statistical analysis of microarray data*

The strength in microarray analysis is that it allows us to monitor the expression of almost the entire yeast genome simultaneously (5,841 of the 6,334 genes). However, because of the enormous quantity of data generated from such a small number of replicates it is vital to interrogate the robustness of the data acquired. To achieve this we had put our data through a variety of statistical analyses that are presented here.

### *6.3.3.1 Box plots generated using affylmGUI on R*

Visualising the data in a box plot is a quick method to compare the probe intensity levels between arrays. When using box plots it is vital to understand what each point on the plot means; each end of the box represents the upper and lower quartiles (the median of the upper and lower half of the data sets). The line across the middle of the box is the median of the data set for that array. The horizontal lines that are connected to the box by the "whiskers" represent the largest and the smallest data points that are not considered to be outliers. With outliers (not shown) defined as values that are 1.5 times the interquartile range from the first of the third quartile (these are the edges of the box).

Using this method it was easy to check that all data, following normalisation, had similar intensity levels, and that there was no variation to cause a problem when processing the data further (see figures 6.3 a and b).

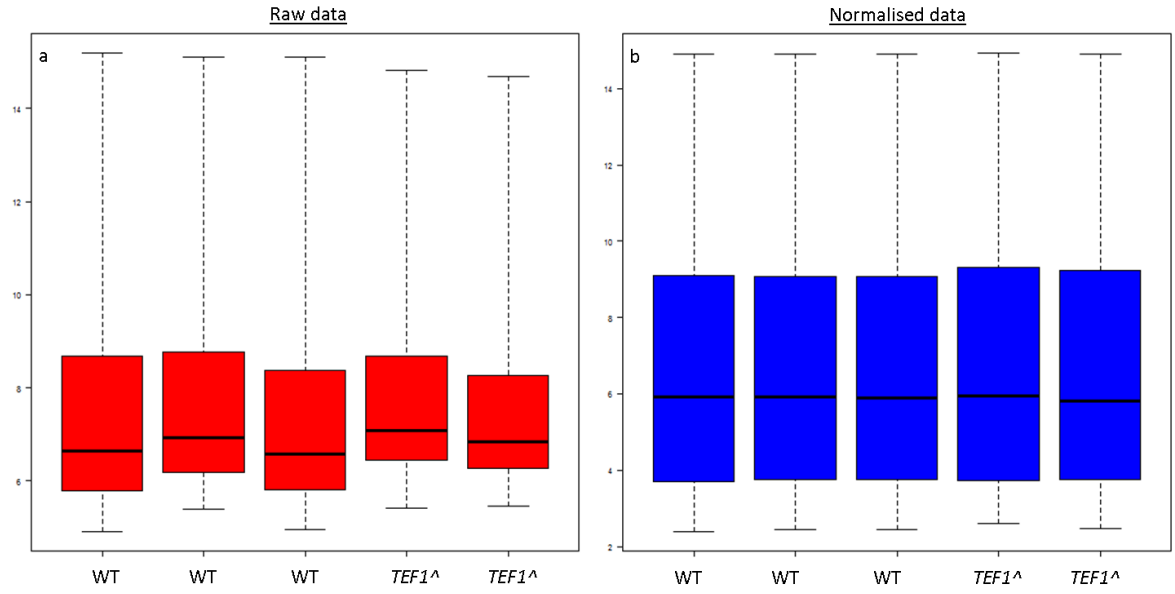


***Figure 6.3, Box plots of raw and normalised data.*** *a- A box plot of the raw data indicating that there was little variation across the assays prior to normalisation. b- A box plot of the RMA processed data showing that following normalisation all arrays had similar probe intensity.*

Using box plots also allowed us to visualise probe level analysis. For this we performed Relative Log Expression (RLE) (see figure 6.4 a) that shows the deviation of gene expression level for each array, from the median gene expression level for that gene across all arrays. If an array has a quality problem then it will exhibit different values from the other arrays in the assay. We also calculated the Normalised Unscaled Standard Error (NUSE) (Wilson *et al.*, 2004) (see figure 6.4 b) . This shows the chip-wise distribution of standard error estimates that are obtained for each gene on each array. Both of these checks confirmed that although there is variation between the wild type and *TEF1* overexpression strains, all data fell within acceptable error ranges.

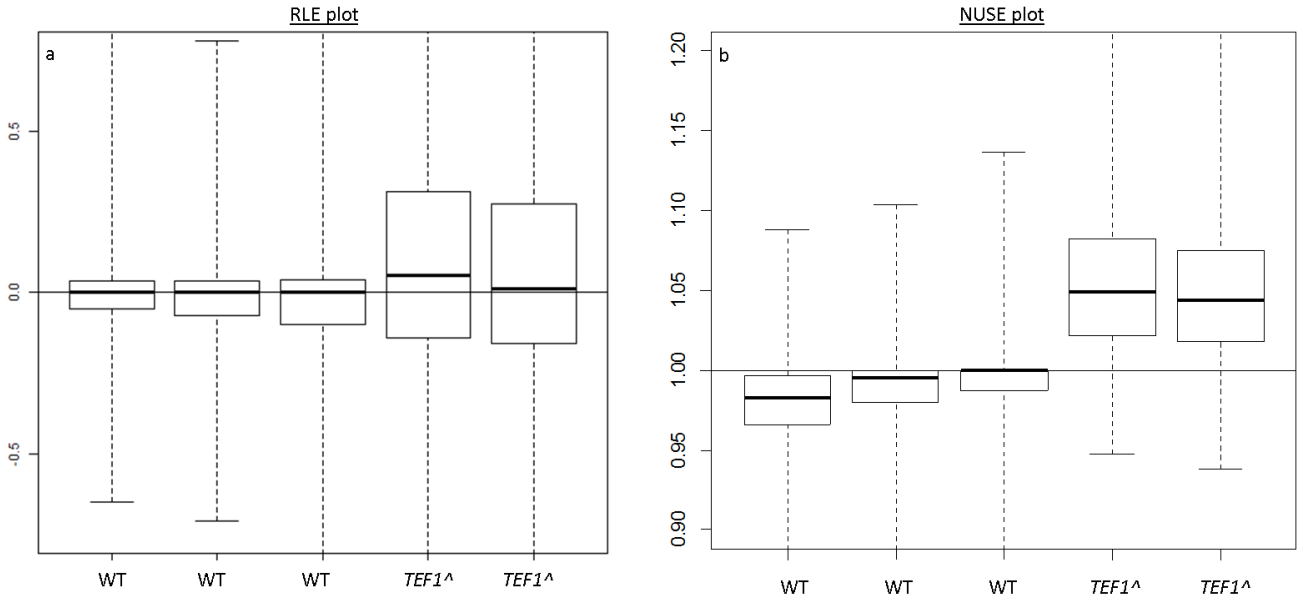


***Figure 6.4, Box plots of RLS and NUSE data.*** *a- A box plot of the RLE data indicating that one of the TEF1^ expression samples showed slightly altered gene expression levels. b- A box plot of the NUSE data suggesting that the TEF1^ strains contained more standard errors than the wild type strains.*

## 6.4 Interpretation of microarray data

Following the rigorous checks to ensure that our microarray data were robust we then sorted the significant data (genes up or down-regulated with a B-stat greater than 1.5) into groups for processing using Gene Ontology (GO) Slim Mapper. This method allows understanding of a collection of genes by grouping them according to one of three biological criteria. Sets of genes were uploaded to the website (http://www.yeastgenome.org/cgi-bin/GO/goSlimMapper.pl) and then sorted by; cellular component (e.g. nucleus, mitochondria, etc), molecular function (e.g. signal transducer activity, enzyme binding, etc) or biological process (e.g. protein folding, rRNA processing, etc). Clustering of genes into these groups allowed us to check for enrichment of specific terms relating to sub-groups. Once it had assigned terms to the groups of genes the Slim Mapper also showed us which GO terms were significantly enriched based on the frequency of gene clustering. This was assessed by

comparing gene cluster frequency to whole genome frequency. From this a ratio was generated of cluster frequency to genome frequency, with anything greater than 1.5 being enriched in the cluster. Here we present only the data that we have defined as enriched (a complete list of both up and down-regulated genes can be found in the appendix (see appendix- App.3)

### *6.4.1 GO Slim Mapper analysis of significantly up-regulated genes*

A total of 319 genes were found to be significantly up-regulated as defined by the restrictions previously discussed. This group of genes were uploaded to the GO Slim Mapper and then processed as described in section 6.4. The first term that the genes were clustered in were biological processes (see table 6.2). This showed enrichment for 19 biological processes. The most enriched process from the up-regulated gene cluster was carbohydrate transport and 4 of the 6 genes group (*HXT1, HXT6, HXT7* and *HXT9*) in this process belong to the *HXT* family of genes involved in hexose uptake. A reassuring observation with these data was that the majority of the processes concur with previous observations made during this research. For example there are several processes that are linked to metabolic processes and the cells response to apparent starvation for example generation of precursor metabolites and energy, cellular amino acid metabolic process, carbohydrate metabolic process and response to starvation. The highest enrichment was observed in carbohydrate transport with 6 of the 319 genes in the up-regulated dataset present, four times more enrichment than observed in the genome.

**Table 6.2 - Go-Slim mapped biological processes generated by the up-regulated microarray data set**

| GO Process | Frequency (of 319 genes) | Genome Frequency (of 6,344 genes) | Freq/Gen Freq | Gene(s) Up regulated |
|---|---|---|---|---|
| **carbohydrate transport** | 6 - 1.9% | 33 - 0.5% | 3.8 | *GLK1,HXT7,HXT6,HXT1,HXT9,GAL2* |
| **oligosaccharide metabolic process** | 6 - 1.9% | 37 - 0.6% | 3.17 | *TPS1,NTH1,TPS2,HSP104,TSL1,SNF2* |
| **lipid transport** | 9 - 2.8% | 55 - 0.9% | 3.11 | *DRS2,SWH1,OSH2,DNF2,DNF1,SUT1,PRY3,UPS1,FAA1* |
| **cytokinesis** | 13 - 4.1% | 95 - 1.5% | 2.73 | *CDC15,BOI1,SDS24,BOI2,DSE2,SWE1,MYO3,CHS5,VRP1,MYO5,ZDS1,BNI1,THP1* |
| **response to osmotic stress** | 12 - 3.8% | 88 - 1.4% | 2.71 | *CYC8,GPD1,NRG1,GPP2,GRE3,SLN1,MYO3,SSK1,MYO5,TCO89,HSP82,OPY2* |
| **endocytosis** | 12 - 3.8% | 96 - 1.5% | 2.53 | *DRS2,SWH1,ECM21,SDS24,OSH2,DNF2,DNF1,MYO3,ENT2,VRP1,MYO5,SCD5* |
| **amino acid transport** | 5 - 1.6% | 47 - 0.7% | 2.29 | *BAP2,RTC2,AVT6,AUA1,MUP3* |
| **cellular amino acid metabolic process** | 27 - 8.5% | 241 - 3.8% | 2.24 | *ADH5,HIS7,ILV6,HIS4,CIT2,LYS14,HOM2,UME6,TRP4,HOM3,TRP2,UGA1,ARG4,THR1,CPA2,MAE1,OXP1,SRY1,DPS1,MET17,LEU3,ARG7,IDH1,MET4,IDH2,CDC60,ASN1* |
| **cell budding** | 6 - 1.9% | 58 - 0.9% | 2.11 | *BOI1,BOI2,KIC1,MYO3,VRP1,MYO5* |
| **carbohydrate metabolic process** | 27 - 8.5% | 269 - 4.2% | 2.02 | *UBP14,TPS1,ADH5,GLK1,CIT2,NTH1,TPS2,UME6,GLC3,GPP2,SAK1,IGD1,PYC1,SOL4,GRE3,TDH1,GLG1,HSP104,GAL2,GSY2,CHS5,YLR345W,TSL1,PFK2,GLO4,SNF2,TCO89* |
| **protein folding** | 9 - 2.8% | 90 - 1.4% | 2 | *CNE1,SSE2,AHA1,EUG1,HSP104,SSE1,FLC1,HSP82,CIN2* |
| **response to starvation** | 9 - 2.8% | 96 - 1.5% | 1.87 | *SUT1,SIP2,CLG1,PCL5,TAX4,ATG2,SNF2,OPY2,ATG13* |
| **protein maturation** | 4 - 1.3% | 46 - 0.7% | 1.86 | *MAP2,DAP2,RAM2,ATG19* |
| **generation of precursor metabolites and energy** | 14 - 4.4% | 160 - 2.5% | 1.76 | *ADH5,GLK1,GLC3,RGI1,IGD1,SHY1,TDH1,GLG1,GSY2,YLR345W,ISF1,PFK2,IDH1,IDH2* |
| **ion transport** | 20 - 6.3% | 229 - 3.6% | 1.75 | *DRS2,BAP2,RTC2,DNF2,PIC2,AVT6,DNF1,AUA1,FET5,TPO2,YHL008C,MUP3,YKE4,COX19,UPS1,PFK2,ATO2,COT1,FAA1,FLC1* |
| **response to heat** | 6 - 1.9% | 69 - 1.1% | 1.73 | *TPS1,TPS2,AHA1,HSF1,HSP104,SIN3* |
| **exocytosis** | 4 - 1.3% | 48 - 0.8% | 1.63 | *SWH1,OSH2,MYO3,MYO5* |
| **cell wall organization or biogenesis** | 15 - 4.7% | 199 - 3.1% | 1.52 | *ROT2,YPS7,KIC1,MHP1,TAX4,GON7,MYO3,YPS3,CHS5,MYO5,KRE1,HRD1,HPF1,TCO89,FLC1* |

| | | | | |
|---|---|---|---|---|
| **cell morphogenesis** | 2 - 0.6% | 28 - 0.4% | 1.5 | *DOT6,KIC1* |
| **biological process unknown** | 62 - 19.4% | 1139 - 18% | 1.08 | *FUN19,BDH2,MOH1,YBL113W-A,PAR32,YDR545C-A,GTT3,YEL043W,YEL077W-A,YER053C-A,YER079W,YER134C,YER152C,YER190C-B,YFL042C,YFL067W,YFL068W,YFR018C,YFR035C,YGL117W,YGR127W,YGR237C,YGR296C-B,AIM17,YHL050W-A,YHR219C-A,YIL060W,YIL092W,ASG1,OM45,YIL177W-A,REE1,YJL225W-A,YKL023W,SEG2,PMU1,YLL066W-A,YLL067W-A,SKG3,YLR278C,YLR326W,YLR466C-A,YLR467C-A,NAB6,YML133W-B,YMR105W-A,YMR160W,ICY1,YMR196W,YNL034W,TOS6,YNL339W-B,YNR014W,YNR034W-A,YOL029C,YOL131W,YOL159C,YOR012W,YOR396C-A,YPL109C,YPL283W-B,YPR204C-A* |

*319 genes that had a B-Stat greater than 1.5 were analysed and processes that were enriched 1.5 times higher in the cluster than is found in the genome, are displayed here. Data is presented in enrichment order. Also includes gene cluster of unknown process.*

The second term that the up-regulated genes were clustered by was molecular function (see table 6.3). Clustering by function resulted in 12 functions that were enriched in our up-regulated gene set. The most significantly enriched function was hydrolase activity, acting on glycosyl bonds, which was increased three-fold compared to genomic levels. Several of the functions within table 6.3 suggested that *TEF1* overexpressing cells had to respond to nutrient deprivation, as suggested by the data in table 6.1. Many of the functions listed are related to recycling cellular nutrients for use elsewhere, there are genes that are involved in carbohydrate storage in the form of trehalose such as *TSL1* and *TPS1*, and genes that are involved in the degradation of trehalose such as *NTH1*, which is required for thermotolerance and mediation of resistance to other cellular stresses (Zähringer *et al.*, 1997).

**Table 6.3 - Go-Slim mapped molecular functions generated by the up-regulated microarray data set**

| GO Function | Frequency (of 319 genes) | Genome Frequency (of 6,344 genes) | Freq/Gen Freq | Gene(s) Up regulated |
|---|---|---|---|---|
| **hydrolase activity, acting on glycosyl bonds** | 7 - 2.2% | 45 - 0.7% | 3.14 | *YPC1,ROT2,NTH1,DSE2,PNP1,HPF1,YDC1* |
| **transferase activity, transferring alkyl or aryl (other than methyl) groups** | 5 - 1.6% | 39 - 0.6% | 2.67 | *ARO3,ARO1,RAM2,MET17,MRS6* |
| **enzyme binding** | 7 - 2.2% | 55 - 0.9% | 2.44 | *ECM21,CYC8,DST1,SSK1,SCD5,MRS6,GIP3* |
| **hydrolase activity, acting on carbon-nitrogen (but not peptide) bonds** | 7 - 2.2% | 63 - 1% | 2.2 | *RIB1,YPC1,HIS7,HIS4,PNC1,OXP1,YDC1* |
| **lyase activity** | 9 - 2.8% | 86 - 1.4% | 2 | *ARO1,TRP2,TCD1,ARG4,YHR112C,APN1,YKL151C,SRY1,MET17* |
| **unfolded protein binding** | 6 - 1.9% | 67 - 1.1% | 1.73 | *CNE1,HSP42,EUG1,SHY1,HSP104,HSP82* |
| **protein binding transcription factor activity** | 11 - 3.4% | 128 - 2.0% | 1.7 | *CYC8,NRG1,UME6,SSN2,DST1,BAS1,IFH1,MET4,SIN3,TFC7,NDD1* |
| **transferase activity, transferring glycosyl groups** | 8 - 2.5% | 96 - 1.5% | 1.67 | *TPS1,HIS7,TRP4,GLC3,GLG1,PNP1,GSY2,TSL1* |
| **nucleic acid binding transcription factor activity** | 13 - 4.1% | 159 - 2.5% | 1.64 | *LYS14,NRG1,UME6,ACA1,HSF1,MGA1,STP2,RSF2,BAS1,LEU3,TAF8,TFC7,RLM1* |
| **kinase activity** | 15 - 4.7% | 198 - 3.1% | 1.50 | *CDC15,GLK1,ARO1,MSS4,HOM3,SAK1,SIP2,THR1,KIC1,PKP1,SLN1,TPK1,SWE1,YLR345W,PFK2* |
| **signal transducer activity** | 3 - 0.9% | 39 - 0.6% | 1.5 | *GPR1,SLN1,SSK1* |
| **oxidoreductase activity** | 21 - 6.6% | 280 - 4.4% | 1.5 | *BDH1,BDH2,ADH5,HIS4,MXR2,GPD1,YDL124W,ARO1,HOM2,EUG1,FRD1,FET5,GRE3,AYR1,TDH1,AAD10,MAE1,HMG2,IDH1,GOR1,IDH2* |

*319 genes that had a B-Stat greater than 1.5 were analysed and processes that were enriched 1.5 times higher in the cluster than is found in the genome, are displayed here. Data is presented in enrichment order.*

The final term that the up-regulated genes were clustered by was cellular component (see table 6.4). Clustering by component resulted in 6 components that were enriched in our up-regulated gene set. The most enriched component was the peroxisome with enrichment increased two-fold compared to genomic levels. *GPD1* is an NAD-dependent glycerol-3-phosphate dehydrogenase that plays a major role in lipid biosynthesis via the reduction of

dihydroxyacetone phosphate to glycerol-3-phosphate, simultaneously oxidising NADH to NAD+ (see figure 6.5). *PNC1* is known to play a role in the NAD+ salvage pathway converting nicotinamide to nicotinic acid (Ghislain *et al.*, 2002). PEX21, PEX14 and PEX30 are all peroxisome related proteins. *GPD1*, *PNC1* and *PEX21* are all known to increase in expression in response to DNA replication stress (Tkach *et al.*, 2012). *CIT2* is a peroxisomal isozyme involved in the glyoxylate cycle catalysing the condensation of acetyl coenzyme A and oxaloacetate to form citrate (Kim *et al.*, 1986; Lewin *et al.*, 1990) and *LPX1* is a peroxisomal matrix-localised lipase that is required for normal peroxisome morphology.

**Table 6.4 - Go-Slim mapped cellular components generated by the up-regulated microarray data set**

| GO Component | Frequency (of 319 genes) | Genome Frequency (of 6,344 genes) | Freq/Gen Freq | Gene(s) Up regulated |
|---|---|---|---|---|
| **peroxisome** | 7 - 2.2% | 69 - 1.1% | 2 | *CIT2,GPD1,PNC1,PEX14,PEX21,PEX30,LPX1* |
| **plasma membrane** | 33 - 10.4% | 376 - 5.9% | 1.76 | *BOI1,BAP2,STP22,GLK1,OSH2,GPR1,YDL124W,DNF2,HOM2,MSS4,HXT7,HXT6,FRD1,DNF1,PTR3,SIP2,TPO2,HXT1,CAP2,SLN1,TDH1,HXT9,GAL2,YPS3,MET17,PLB1,BNI1,ATO2,FAA1,PDR12,TCO89,OPY2,OPT2* |
| **cell cortex** | 11 - 3.5% | 138 - 2.2% | 1.59 | *ABP1,OSH2,CAP2,BBC1,MYO3,ENT2,VRP1,MYO5,BNI1,SCD5,PIN3* |
| **site of polarized growth** | 18 - 5.7% | 237 - 3.7% | 1.54 | *CDC15,BOI1,ABP1,OSH2,SEC31,BOI2,KIC1,CAP2,SWE1,SKG3,ENT2,CHS5,VRP1,MYO5,ZDS1,BNI1,YPT11,FLC1* |
| **vacuole** | 20 - 6.3% | 259 - 4.1% | 1.54 | *RTC2,MCH1,VMA1,PIB1,AVT6,FET5,TPO2,YHL008C,VMR1,DAP2,ECM14,APE1,VPS38,YMR160W,ICY1,COT1,YDC1,TCO89,FLC1,OPY2* |
| **extracellular region** | 2 - 0.6% | 27 - 0.4% | 1.5 | *DSE2,HPF1* |
| **cellular component unknown** | 45 - 14.2% | 720 - 11.4% | 1.25 | *FUN19,MOH1,YBL113W-A,YDR545C-A,GTT3,YEL077W-A,YER190C-B,AUA1,YFL042C,YFL067W,YFL068W,YFR018C,YFR035C,YGL117W,PDE1,YGR127W,YGR296C-B,YHL050W-A,THR1,YHR219C-A,YIL060W,YIL177W-A,YJL225W-A,AAD10,SEG2,SRY1,GLG1,YLL066W-A,YLL067W-A,YLR326W,YLR466C-A,YLR467C-A,YML133W-B,ISF1,YMR105W-A,YNL034W,YNL339W-B,YOL029C,YOL131W,YOL159C,YOR012W,YOR396C-A,CIN2,YPL283W-B,YPR204C-A* |

*319 genes that had a B-Stat greater than 1.5 were analysed and processes that were enriched 1.5 times higher in the cluster than is found in the genome, are displayed here. Data is presented in enrichment order. Also includes gene cluster of unknown component.*

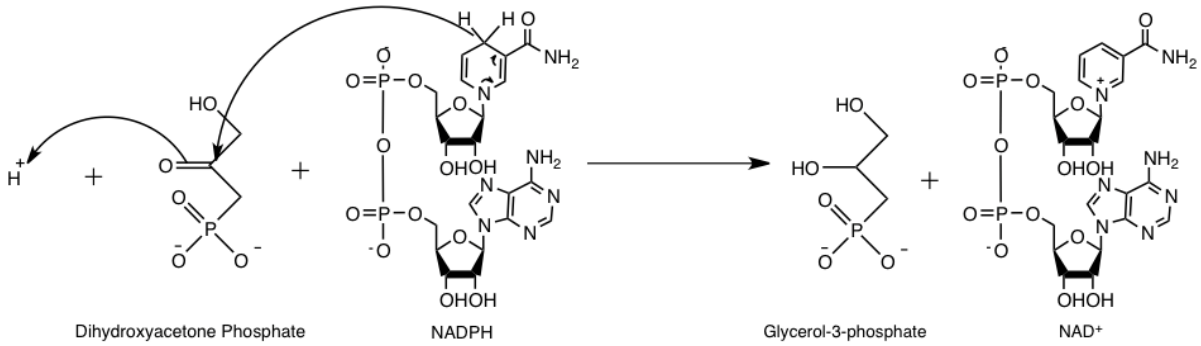


***Figure 6.5, Glycerol-3-phosphate dehydrogenase reaction mechanism.*** *This reaction shows how Gpd1 reduces dihydroyacetone to glycerol-3-phosphate, whilst simultaneously oxidising NADH to NAD+.*

## *6.4.2 GO Slim Mapper analysis of significantly down-regulated genes*

A total of 61 genes were found to be significantly down-regulated as defined by the restrictions previously discussed. This group of genes were uploaded to the GO Slim Mapper and then processed as described in section 6.4. The first term that the genes were clustered in were biological processes (see table 6.5). This table shows enrichment for 17 biological processes and a large group of 17 genes that belong to unknown processes. A large proportion of the biological processes found to be down-regulated in the *TEF1* overexpression strain were involved in RNA processing including transcription from RNA polymerase I and III promoters, and several translational processes including biogenesis of the small and large ribosomal subunits.

**Table 6.5 - Go-Slim mapped biological processes generated by the down-regulated microarray data set**

| GO Process | Frequency (of 61 genes) | Genome Frequency (of 6,344 genes) | Freq/Gen Freq | Gene(s) Down regulated |
|---|---|---|---|---|
| **mitochondrial translation** | 5 - 8.2% | 137 - 2.2% | 3.73 | *PET122,RRF1,PTH1,MRPL38, MRPL33* |
| **transcription from RNA polymerase I promoter** | 2 - 3.3% | 64 - 1.0% | 3.3 | *RRN3,RPB10* |
| **carbohydrate transport** | 1 - 1.6% | 33 - 0.5% | 3.2 | *HXT17* |
| **pseudohyphal growth** | 2 - 3.3% | 69 - 1.1% | 3 | *PGU1,HMS1* |
| **transcription from RNA polymerase III promoter** | 1 - 1.6% | 39 - 0.6% | 2.67 | *RPB10* |
| **snoRNA processing** | 1 - 1.6% | 40 - 0.6% | 2.67 | *RRP45* |
| **ribosomal small subunit biogenesis** | 3 - 4.9% | 129 - 2.0% | 2.45 | *LOC1,FCF2,FYV7* |
| **rRNA processing** | 7 - 11.5% | 297 - 4.7% | 2.45 | *RRP45,NUG1,LOC1,FCF2,FYV 7,RMP1,PUS7* |
| **protein folding** | 2 - 3.3% | 90 - 1.4% | 2.36 | *EMC5,CUR1* |
| **ribosomal large subunit biogenesis** | 2 - 3.3% | 88 - 1.4% | 2.36 | *NOP16,LOC1* |
| **ribosomal subunit export from nucleus** | 1 - 1.6% | 45 - 0.7% | 2.29 | *NUG1* |
| **tRNA processing** | 2 - 3.3% | 105 - 1.7% | 1.94 | *FMT1,PUS7* |
| **mitochondrion organization** | 6 - 9.8% | 342 - 5.4% | 1.81 | *PET122,RRF1,PTH1,MRPL38, COX17,MRPL33* |
| **translational initiation** | 1 - 1.6% | 60 - 0.9% | 1.78 | *DED1* |
| **lipid transport** | 1 - 1.6% | 55 - 0.9% | 1.78 | *RFT1* |
| **DNA-dependent transcription, initiation** | 1 - 1.6% | 66 - 1.0% | 1.6 | *RRN3* |
| **sporulation** | 2 - 3.3% | 132 - 2.1% | 1.57 | *SPO73,RIM9* |
| **biological process unknown** | 17 - 27.9% | 1139 - 18% | 1.55 | *YAR023C,YBR298C-A,YCR024C-B,YCR100C,BSC1,NKP1,YGR174W-A,MTC6,RRT14,YLR363W-A,YLR412C-A,AIM34,YMR030W-A,YMR230W-A,KSH1,YNL162W-A,YPR153W* |

*61 genes that had a B-Stat greater than 1.5 were analysed and processes that were enriched 1.5 times higher in the cluster than is found in the genome, are displayed here. Data is presented in enrichment order.*

The second term that the down-regulated genes were clustered by was molecular function (see table 6.6). Clustering by function resulted in 10 functions that were enriched in our down-regulated gene set with a group of 30 genes of unknown function. Most of the functions in table 6.6 consisted of only a single gene, with only "translation factor activity, nucleic acid binding" and "protein binding transcription factor activity" consisting of two genes. Two of the genes *PET122* and *RRF1* encode mitochondrial proteins, Pet122 is a mitochondrial translational activator that is specific for the *COX3* mRNA (Naithani *et al.*, 2003). Rrf1 is essential for mitochondrial translation and respiratory function as it is a mitochondrial ribosome recycling factor (Kanai *et al.*, 1998; Teyssier *et al.*, 2003). Rrn3 is required for transcription of rDNA by RNA polymerase I. Whi5 binds SCB (Swi4/6-dependent cell cycle box) binding factor at SCB target promoters in early G1 to repress G1 transcription, this repression can be relieved by phosphorylation of Whi5 by Cdc28 (Spellman *et al.*, 1998; Costanzo *et al.*, 2004).

**Table 6.6 - Go-Slim mapped molecular function generated by the down-regulated microarray data set**

| GO Function | Frequency (of 61 genes) | Genome Frequency (of 6,344 genes) | Freq/Gen Freq | Gene(s) Down regulated |
|---|---|---|---|---|
| **translation factor activity, nucleic acid binding** | 2 - 3.3% | 44 - 0.7% | 4.71 | *PET122,RRF1* |
| **protein transporter activity** | 2 - 3.3% | 53 - 0.8% | 4.13 | *SSS1,SBH1* |
| **signal transducer activity** | 1 - 1.6% | 39 - 0.6% | 2.67 | *IZH4* |
| **hydrolase activity, acting on glycosyl bonds** | 1 - 1.6% | 45 - 0.7% | 2.29 | *PGU1* |
| **protein binding, bridging** | 1 - 1.6% | 49 - 0.8% | 2 | *ERG28* |
| **enzyme binding** | 1 - 1.6% | 55 - 0.9% | 1.78 | *RRN3* |
| **isomerase activity** | 1 - 1.6% | 58 - 0.9% | 1.78 | *PUS7* |
| **GTPase activity** | 1 - 1.6% | 59 - 0.9% | 1.78 | *NUG1* |
| **protein binding transcription factor activity** | 2 - 3.3% | 128 - 2.0% | 1.65 | *RRN3,WHI5* |
| **molecular function unknown** | 30 - 49.2% | 1937 - 30.6% | 1.61 | *YAR023C,RFT1,YBR298C-A,YCR024C-B,YCR100C,BSC1,RRP45,NKP1,NOP16,SPO73,BRR6,VMA21,YGR174W-A,MTC6,EMC5,DPH1,RRT14,FCF2,FYV7,LCL2,YLR363W-A,YLR412C-A,AIM34,YMR030W-A,RIM9,YMR230W-A,KSH1,YNL162W-A,COS10,YPR153W* |

*61 genes that had a B-Stat greater than 1.5 were analysed and processes that were enriched, that is present at a higher frequency in the cluster than is found in the genome, are displayed here. Data is presented in enrichment order.*

The final term that the down-regulated genes were clustered by was cellular component (see table 6.7). Clustering by component resulted in four components that were enriched in our down-regulated gene set and a large group of 13 genes from unknown cellular components. Excluding the extracellular region which comprises of a single gene *PGU1*, the most enriched cellular component was the nucleolus. Similar to biological processes of the down-regulated genes (table 6.5) the majority of the genes that are categorised as nucleolar are related to

ribosomal biogenesis and rRNA processing; *RRP45, NOP16, NUG1, LOC1, RRT14, FCF2, FYV4, RMP1* and *RPB10*.

**Table 6.7 - Go-Slim mapped cellular component generated by the down-regulated microarray data set**

| GO Component | Frequency (of 61 genes) | Genome Frequency (of 6,344 genes) | Freq/Gen Freq | Gene(s) Down regulated |
|---|---|---|---|---|
| **extracellular region** | 1 - 1.6% | 27 - 0.4% | 4 | *PGU1* |
| **nucleolus** | 10 - 16.4% | 328 - 5.2% | 3.15 | *RRP45,NOP16,NUG1,LOC1,RRT14,RRN3,FCF2,FYV7,RMP1,RPB10* |
| **endomembrane system** | 8 - 13.1% | 371 - 5.9% | 2.22 | *RFT1,SSS1,ERG28,SBH1,BRR6,VMA21,EMC5,COS10* |
| **cellular component unknown** | 13 - 21.3% | 720 - 11.4% | 1.87 | *YAR023C,YBR298C-A,YCR024C-B,BSC1,YGR174W-A,MTC6,LCL2,YLR412C-A,YMR030W-A,YMR230W-A,KSH1,HMS1,YPL113C* |
| **endoplasmic reticulum** | 7 - 11.5% | 405 - 6.4% | 1.8 | *RFT1,SSS1,ERG28,SBH1,VMA21,EMC5,COS10* |

*61 genes that had a B-Stat greater than 1.5 were analysed and processes that were enriched, that is present at a higher frequency in the cluster than is found in the genome, are displayed here. Data is presented in enrichment order.*

## *6.4.3 Transcription factor analysis using Yeastract*

Following interrogation of the microarray dataset using GO we then asked the question, was there a set of transcription factors up or down-regulated in the significantly altered genes that could induce the majority of the observed differences through transcriptional regulation. To perform this analysis we utilised an online tool called Yeastract (**YEA**st **S**earch for **T**ranscriptional **R**egulators **A**nd **C**onsensus **T**racking) (Teixeira *et al.*, 2014). This is a curated database of more than 206,000 regulatory associations between transcription factors and target genes in *S.cerevisiae*.

Data acquired from the GO analysis was utilised to elucidate transcription factors that regulated processes in the up and down-regulated data sets by inputting clusters from certain

processes into the Yeastract site along with the up and down-regulated transcription factors from the microarray data set in the potential transcription factor field. We were then able to visualise the interaction network between transcription factors and regulated genes using the visualise network command on the Yeastract website.

### *6.4.4.1 Regulatory transcription factors of carbohydrate processing*

As one of the largest clusters from the GO analysis, the 27 genes found to be up-regulated and involved in carbohydrate processing were analysed using Yeastract. This allowed us to visualise the interactions between specific transcription factors and the up-regulated genes that are involved in carbohydrate processing. First we compared the inhibitory transcription factors to the carbohydrate processing cluster. We took the top four inhibitory TFs and mapped a network with the cluster of genes from carbohydrate processing (see figures 6.6 a and b). Figure 6.6 a shows the inhibitory effect of Rpn4 (Regulatory Particle Non-ATPase) on the up-regulated genes involved in carbohydrate processing. *RPN4* itself is found at slightly lower levels (approximately 4%) in the *TEF1* overexpression strain, reinforcing its position as an inhibitory TF of these up-regulated genes. Rpn4 is known to stimulate expression of proteasome genes, and it in turn is regulated by the 26S proteasome by a negative feedback mechanism. Rpn4 levels are known to increase and it is known to translocate to the nucleus upon DNA replication stress (Xie and Varshavsky, 2001; Tkach *et al.*, 2012). The second inhibitory TF that is shown (see figure 6.6 b) is Zap1 (Zinc-responsive Activator Protein 1). Zap1 is a TF that binds to zinc-responsive promoters to induce transcription of genes in the presence of zinc (such as *ADH5*). Zap1 is also known to repress other genes in low zinc. Zap1 was found at similar levels in the *TEF1* overexpression strain.

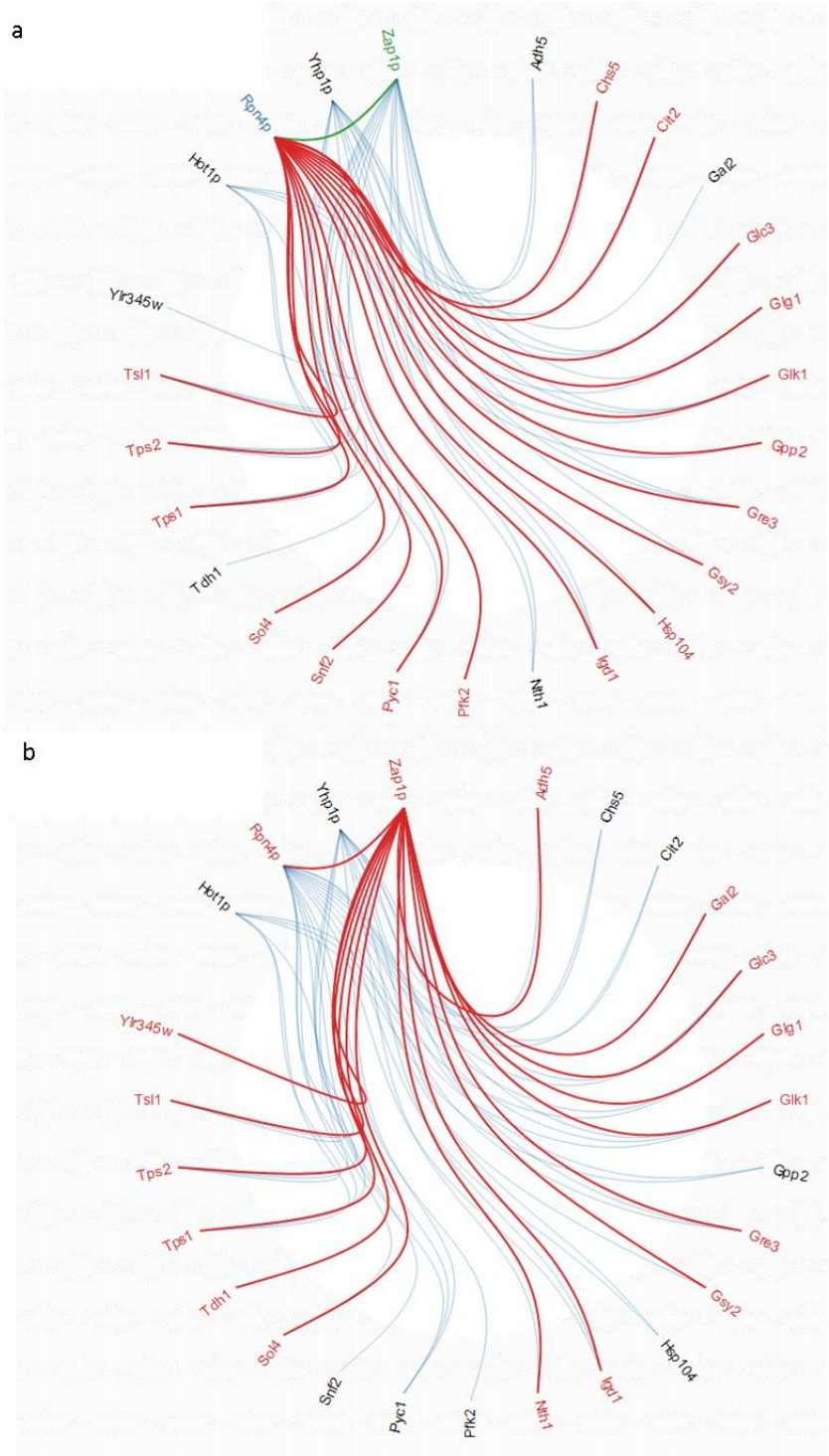


***Figures 6.6, Network of inhibitory transcription factors and up-regulated genes involved in carbohydrate processing.*** *Red lines and red nodes indicate what genes are regulated by the selected transcription factor, green lines and green nodes indicate if any other the other transcription factors in the network regulate the selected transcription factor. 6.6-a shows the regulatory network of Rpn4. 6.6-b shows the regulatory network of Zap1.*

Following analysis of the inhibitory TFs we analysed the activating TFs. We found that there were 18 enriched TFs that activated the up-regulated genes involved in carbohydrate processing (see figure 6.7). Of the eighteen TFs, seventeen were found to be transcribed at elevated levels in the *TEF1* overexpression strain, with only *WTM2* detected at lower levels in the microarray data set. The most prolific TF was Cbf1 this was found to activate 16 of the 23 genes involved in carbohydrate processing as well as 4 of the other TFs in the network. Cbf1 is required for chromosome segregation and is associated with kinetochore proteins (Cai and Davis, 1990). Cbf1 levels are known to increase in response to DNA replication stress (Tkach *et al.*, 2012).

Due to the quantity of significant, activating TFs a table containing a summary of their functions is presented below (see table 6.8). Upon analysis of the functions of all 18 TFs there is no single function that appears to be more prevalent than any other suggesting that up-regulation of carbohydrate processing in *TEF1* overexpressing cells is due to an array of cellular processes.

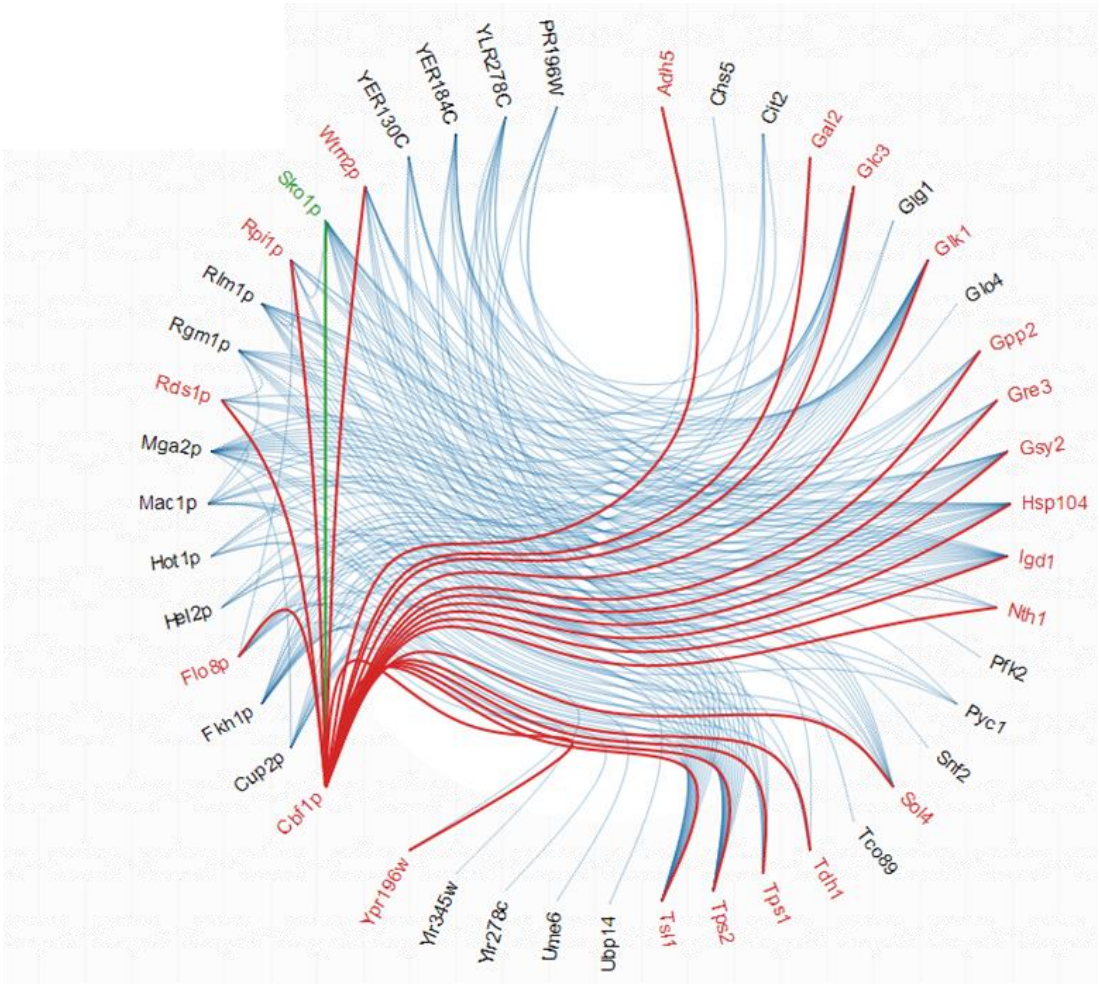


***Figure 6.7, Network of activating transcription factors and up-regulated genes in carbohydrate processing.*** *Red lines and red nodes indicate what genes are regulated by the selected transcription factor, green lines and green nodes indicate if any other the other transcription factors in the network regulate the selected transcription factor. This figure shows the regulatory network of Cbf1.*

**Table 6.8 - Transcription factors that are involved in activating the carbohydrate processing cluster of genes**

| Gene Name | % increase of RNA levels in *TEF1^* cells | Description |
|---|---|---|
| ***CBF1*** | 7 | Helix-loop-helix protein that binds the motif CACRTG, which is present at several sites including MET gene promoters and centromere DNA element I (CDEI); required for nucleosome positioning at this motif; targets Isw1p to DNA |
| ***CUP2*** | 8 | Copper-binding transcription factor; activates transcription of the metallothionein genes CUP1-1 and CUP1-2 in response to elevated copper concentrations |

| | | |
|---|---|---|
| ***FKH1*** | 4.9 | Forkhead family transcription factor with a minor role in the expression of G2/M phase genes; negatively regulates transcriptional elongation; positive role in chromatin silencing at HML and HMR; regulates donor preference during switching |
| ***FLO8*** | 2.8 | Transcription factor required for flocculation, diploid filamentous growth, and haploid invasive growth; genome reference strain S288C and most laboratory strains have a mutation in this gene |
| ***HEL2*** | 7.1 | Protein of unknown function that may interact with ribosomes, based on co-purification experiments;green fluorescent protein (GFP)-fusion protein localizes to the cytoplasm; contains a RING finger domain |
| ***HOT1*** | 3.2 | Transcription factor required for the transient induction of glycerol biosynthetic genes GPD1 and GPP2 in response to high osmolarity; targets Hog1p to osmostress responsive promoters; has similarity to Msn1p and Gcr1p |
| ***MAC1*** | 1 | Copper-sensing transcription factor involved in regulation of genes required for high affinity copper transport |
| ***MGA2*** | 5.5 | ER membrane protein involved in regulation of OLE1 transcription, acts with homolog Spt23p; inactive ER form dimerizes and one subunit is then activated by ubiquitin/proteasome-dependent processing followed by nuclear targeting |
| ***RDS1*** | 4.5 | Zinc cluster protein involved in conferring resistance to cycloheximide |
| ***RGM1*** | 8.3 | Putative transcriptional repressor with proline-rich zinc fingers; overproduction impairs cell growth |
| ***RLM1*** | 16.1 | MADS-box transcription factor, component of the protein kinase C-mediated MAP kinase pathway involved in the maintenance of cell integrity; phosphorylated and activated by the MAP-kinase Slt2p |
| ***RPI1*** | 5.3 | Putative transcriptional regulator; overexpression suppresses the heat shock sensitivity of wild-type RAS2 overexpression and also suppresses the cell lysis defect of an mpk1 mutation |
| ***SKO1*** | 6 | Basic leucine zipper (bZIP) transcription factor of the ATF/CREB family, forms a complex with Tup1p and Ssn6p to both activate and repress transcription; cytosolic and nuclear protein involved in osmotic and oxidative stress responses |
| ***WTM2**** | <2.5 | Transcriptional repressor involved in regulation of meiosis and silencing; contains WD repeats |
| ***YER130C*** | 15.4 | Hypothetical protein |

| | | |
|---|---|---|
| ***YER184C*** | 0.8 | Putative zinc cluster protein; deletion confers sensitivity to Calcufluor white, and prevents growth on glycerol or lactate as sole carbon source |
| ***YLR278C*** | 9 | an essential gene |
| ***YPR196W*** | 2 | Putative maltose activator |

*Genes are sorted by alphabetic order, alongside the change in expression level from wild type to TEF1 overexpressing cells, and the protein description.*

### *6.4.4.2 Regulatory transcription factors of amino acid metabolism*

GO analysis revealed the amino acid metabolism process contained a cluster of 27 genes similar to that of carbohydrate processing. We processed these using Yeastract as described in section 6.4, allowing us to visualise the interactions between specific transcription factors and the up-regulated genes that are involved in amino acid metabolism. First we compared the inhibitory transcription factors to the amino acid metabolism cluster. This analysis revealed only two enriched inhibitory TFs, Leu3 and Met32, that are known to have an effect on the genes in the amino acid metabolism cluster (see figure 6.8). Leu3 is a zinc-knuckle, repressing and activating transcription factor. It is known to regulate genes involved in ammonia assimilation but also is a primary regulator of branched chain amino acid (BCAA) synthesis. In the presence of high levels of leucine it represses BCAA synthesis, with an accumulation of the leucine intermediary, alpha-isopropylmalic acid, causing Leu3 to act as an activator of BCAA synthesis (Baichwal *et al.*, 1983; Friden and Schimmel, 1988; Sze *et al.*, 1992). *LEU3* RNA levels were 10% higher in *TEF1* overexpressing cells than wild type. Met32 is a zinc-finger DNA-binding transcription factor that is involved in the transcriptional regulation of methionine biosynthetic genes (Blaiseau *et al.*, 1997). *MET32* RNA levels were at levels 4.5% higher in *TEF1* overexpressing cells than wild type.

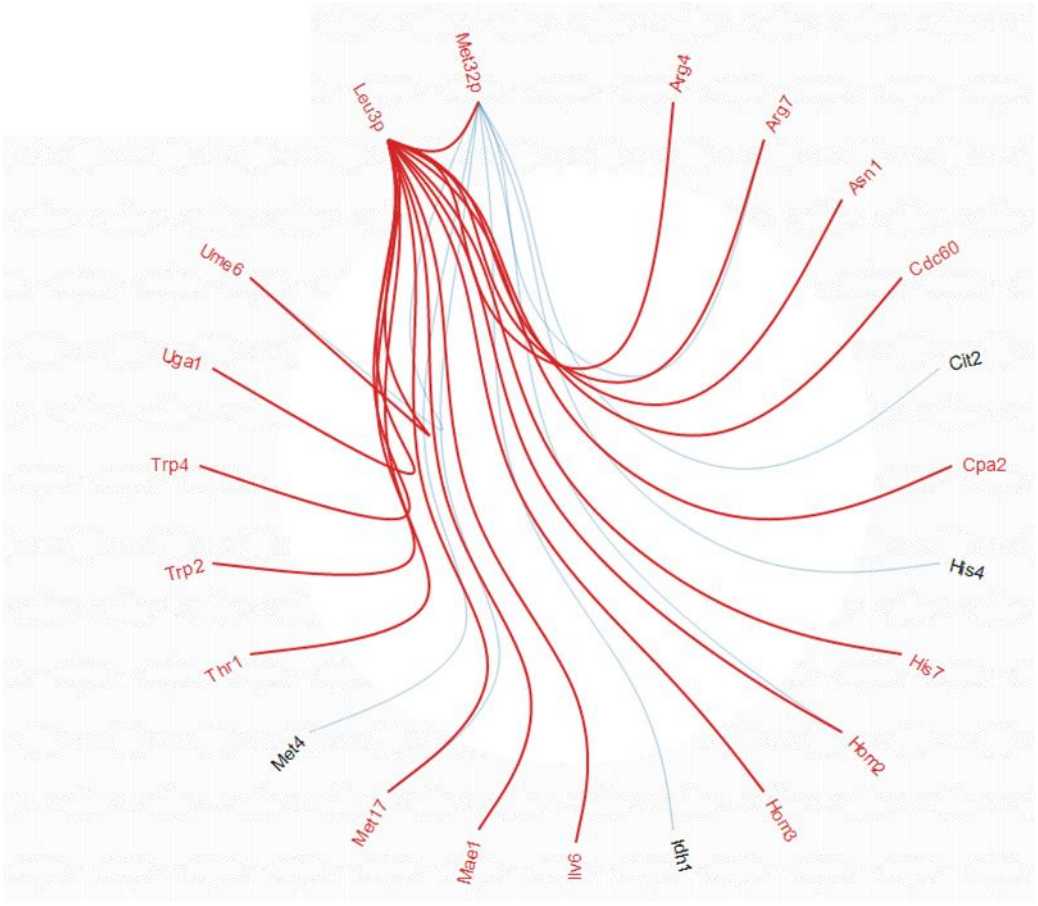


***Figure 6.8 Network of inhibitory transcription factors and up-regulated genes in amino acid metabolism.*** *Red lines and red nodes indicate what genes are regulated by the selected transcription factor, green lines and green nodes indicate if any other the other transcription factors in the network regulate the selected transcription factor. This figure shows the regulatory network of Leu3.*

Following analysis of the TF that inhibited the transcription of the genes involved in amino acid metabolism, we next analysed the activating TFs. We found that there were three enriched TFs that regulated genes from the amino acid metabolism cluster, but, that they were only involved in the activation of 6 of the 27 genes from the cluster (see figure 6.9). The three TFs were Rgt2, Ssn3 and Sua7. Rgt2 is a plasma membrane, high glucose sensor involved

in the induction of hexose transporters (Ozcan *et al.*, 1996; Ozcan *et al.*, 1998). Rgt2 RNA levels were 3.2% higher in the *TEF1* overexpressing strain compared to the wild type. Ssn3 is involved in glucose repression, it is also a cyclin-dependent protein kinase involved in the phosphorylation of the RNA polymerase II C-terminal domain (Liao *et al.*, 1995; Balciunas and Ronne, 1995). Ssn3 RNA levels were 3.7% lower in the *TEF1* overexpressing strain compared to the wild type. Sua7 is an essential, general transcription factor that is required for transcription initiation and start site selection by RNA polymerase II (Pinto *et al.*, 1992; Pinto *et al.*, 1994). Sua7 RNA levels were 0.8% higher in the *TEF1* overexpressing strain compared to the wild type. The six genes regulated by Rgt2, Ssn3 and Sua7 are *MET17, HOM3, HIS4, CIT2, ARG4* and *ARG7*. Arg4 and Arg7 catalyse steps of the arginine biosynthesis pathway. Met17 is required for methionine and cysteine biosynthesis and His4 is catalyses steps 2, 3, 9 and 10 of histidine biosynthesis. Hom3 is an aspartokinase that is known to catalyse the first step in the common biosynthesis pathway of threonine and methionine. Cit2 catalyses the condensation of acetyl coenzyme A and oxaloacetate to form citrate. Citrate is known to be the precursor to glutamine, glutamate, arginine, proline, and lysine.

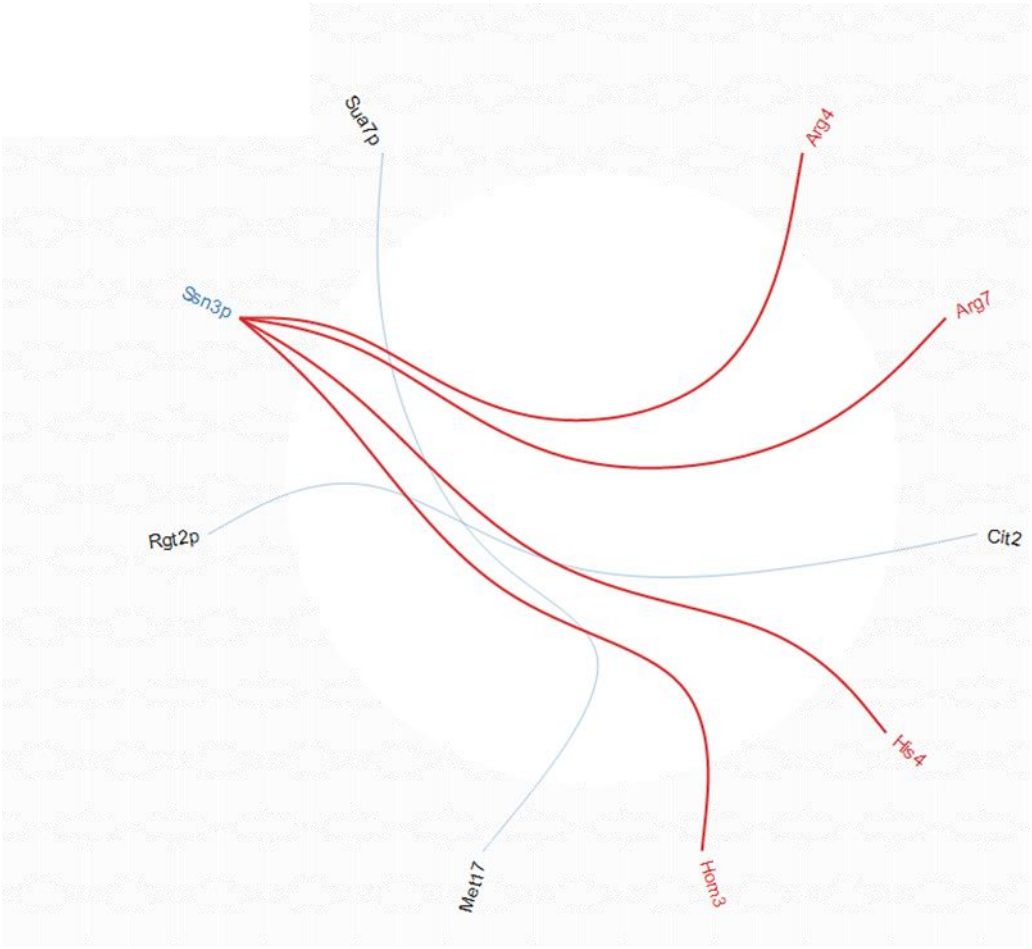


***Figure 6.9, Network of inhibitory transcription factors and up-regulated genes in amino acid metabolism.*** *Red lines and red nodes indicate what genes are regulated by the selected transcription factor, green lines and green nodes indicate if any other the other transcription factors in the network regulate the selected transcription factor. This figure shows the regulatory network of Ssn3*

.

### *6.4.4.3 Regulatory transcription factors of ribosomal biosynthesis*

GO analysis revealed a cluster of 12 down-regulated genes involved in ribosomal biosynthesis. Using Yeastract we found that there are seven activating TFs that regulate this cluster at enriched levels in comparison to their genomic regulatory levels (see figure 6.10). The seven activating TFs were Aro80, Cup9, Esc2, Gal11, Sds3, Taf14 and Thi2 (see table 6.9). There were no inhibitory TFs that were enriched for the gene cluster from ribosomal biosynthesis.

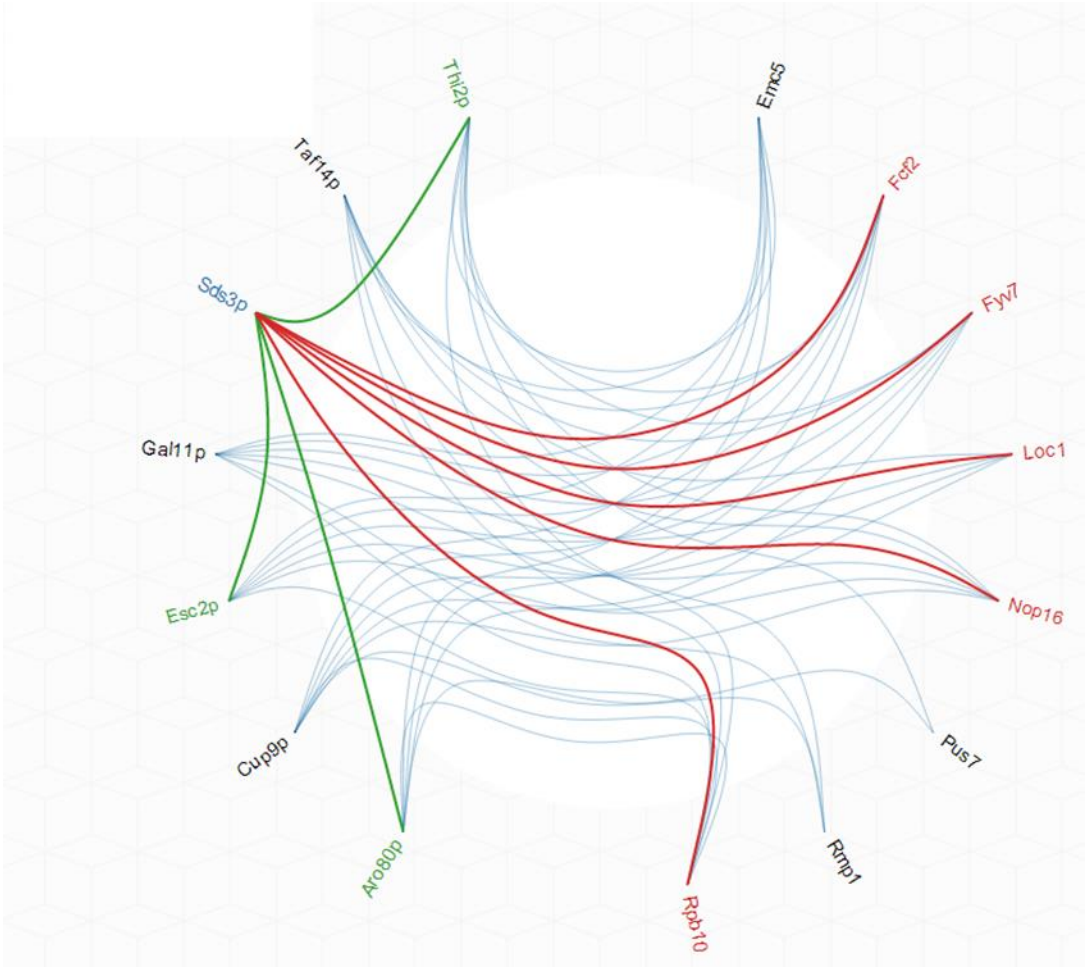


***Figure 6.10, Network of inhibitory transcription factors and up-regulated genes in amino acid metabolism.*** *Red lines and red nodes indicate what genes are regulated by the selected transcription factor, green lines and green nodes indicate if any other the other transcription factors in the network regulate the selected transcription factor. This figure shows the regulatory network of Sds3.*

**Table 6.9 - Activating transcription factors which regulate the down-regulated genes of ribosomal biosynthesis.**

| Gene name | % increase in *TEF1^* cells | Description |
|---|---|---|
| ***ARO80*** | 4.1 | Zinc finger transcriptional activator of the Zn2Cys6 family; activates transcription of aromatic amino acid catabolic genes in the presence of aromatic amino acids |
| ***CUP9*** | 8.4 | Homeodomain-containing transcriptional repressor of PTR2, which encodes a major peptide transporter; imported peptides activate ubiquitin-dependent |
| ***ESC2*** | 1.9 | Protein involved in mating-type locus silencing, interacts with Sir2p; probably functions to recruit or stabilize Sir proteins |
| ***GAL11*** | 8.3 | Component of the Mediator complex; interacts with RNA polymerase II and the general transcription factors to form the RNA polymerase II holoenzyme; affects transcription by acting as target of activators and repressors |
| ***SDS3*** | <3.3 | Component of the Rpd3p/Sin3p deacetylase complex required for its structural integrity and catalytic activity, involved in transcriptional silencing and required for sporulation; cells defective in SDS3 display pleiotropic phenotypes |
| ***TAF14*** | 0.7 | Subunit of TFIID, TFIIF, INO80, SWI/SNF, and NuA3 complexes, involved in RNA polymerase II transcription initiation and in chromatin modification; contains a YEATS domain |
| ***THI2*** | <0.1 | Zinc finger protein of the Zn(II)2Cys6 type, probable transcriptional activator of thiamine biosynthetic genes |

## 6.5 Analysis of microarray data suggests that aneuploidy is not due to a chromosomal duplication

Data presented in previous chapters suggest that overexpression of eEF1A induces aneuploidy phenotypes. We have utilised our microarray data, together with data previously published by Torres et al. (2007) to reveal that eEF1A overexpression does not result in a single chromosomal duplication event.

As we have previously shown by FACS analysis and microscopy (section 4.2.2), overexpression of eEF1A results in cells with large, bright nuclei, and an increase in genomic content. We have hypothesised that this may be due to a relaxation of chromosomal condensation resulting in an increase in the uptake of PI and DAPI.

However, analysis of our microarray data indicated that cells expressing elevated levels of eEF1A contained a disproportionate level of significantly up-regulated genes (319) to down-regulated genes (61). Upon comparison of the entire microarray data set (see figure 6.11-b) it is clear that a large proportion of the genome is up-regulated in *TEF1* overexpressing cells relative to wild type. Interestingly we do not see single chromosomal amplification as can be seen in figure 6.11-a, which was generated using data known to originate from a strain containing a duplication of chromosome IV (Torres *et al.*, 2007).

This demonstrates that almost the entire genome is amplified in the presence of elevated levels of eEF1A, which is likely to result in the previous aneuploidy phenotypes we had observed.

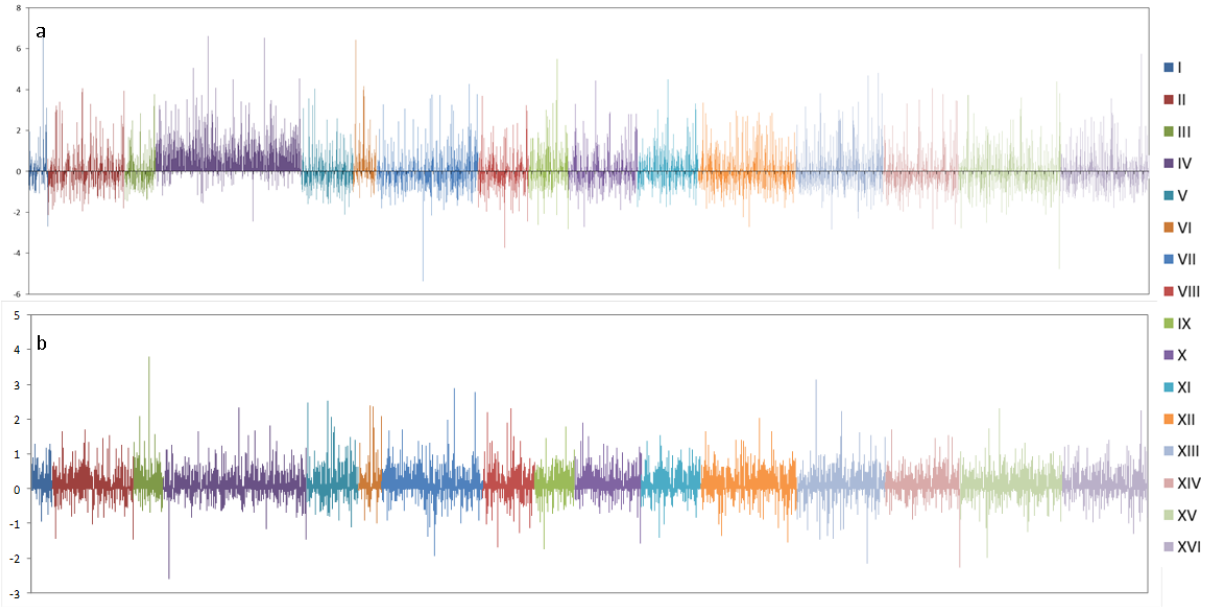


***Figure 6.11, Mapping of gene expression levels relative to wild type cells.*** *–a shows amplification of chromosome IV generated from data from a study on aneuploidy yeast. b- shows levels of gene expression in TEF1 overexpressing cells, this shows that eEF1A levels do not result in entire chromosomal amplification, but that in fact, almost, the entire genome appears to be amplified.*

## 6.6 Discussion

Using microarray analysis we have assessed whole cell transcription to verify the up or down-regulation of entire cellular processes. We performed stringent statistical analysis to ensure that all the data pursued for interpretation were robust and as free from background noise as possible. Subsequent data interrogation was only performed on data that were statistically significant and that was enriched by at least 1.5 fold relative to its control.

Data were initially ranked by the degree of change in expression level. This low level interrogation of the data revealed that cells overexpressing *TEF1* up-regulated transcription of genes related to carbohydrate processing, and down-regulated genes involved in transcription and translation. The results of this preliminary analysis concurs with our earlier hypothesis (see section 3.4) that cells overexpressing *TEF1* sense they are in a nutrient deprived environment and are starving. This response to starvation may trigger the cells to

produce storage carbohydrates such as trehalose whilst simultaneously decreasing the rate of cell growth to conserve resources.

GO analysis of the microarray data confirmed conclusions from the preliminary analysis that carbohydrate processing was increased, and transcription and translation were down-regulated. The most enriched process from the up-regulated data set was carbohydrate transport, and carbohydrate processing was the largest process cluster containing 27 genes. Most of the up-regulated processes all appeared to be in relation to cells responding to a perceived decrease in available nutrients. Cells overexpressing *TEF1* were observed to up-regulate a range of processes involved in carbohydrate and amino acid biosynthesis and transport, and several processes that were responses to various stresses including heat stress and starvation. In contrast down-regulated processes that were elucidated by GO analysis included an array of processes essential for cell growth. The majority of the down-regulated processes were involved in transcription and translation suggesting cells sensed they lacked the available nutrients necessary for sustained growth. Comparison of the up and down-regulated processes presents compelling evidence that the cells are either unable to utilise nutrients available to them, or that they are unable to sense that they are available to them.

Analysis of the TFs involved in the regulation of the processes discussed revealed that cells were making a concerted effort to achieve the alterations observed. Most of the processes had several TFs with significantly altered transcription levels that resulted in large clusters of genes with increased or decreased transcription. Many of the transcription factors that had elevated transcription as measured by the microarray are known to increase in level in response to DNA replication stress. This response has been highlighted throughout this study and will be further discussed in Chapter 8. Regulation of amino acid biosynthesis by Leu3 was

assigned by Yeastract as a repressive interaction. However, as discussed (see section 6.4.4.2), it is only in the presence of high levels of leucine that Leu3 acts as a repressor of branched chain amino acid synthesis. Interestingly, when in the presence of high levels of the leucine intermediate, alpha-isopropylmalic acid, Leu3 acts as an activator of BCAA synthesis, suggesting that Leu3 may not be having a repressive effect on the transcription of all the genes highlighted in figure 6.8.

# Chapter 7: Metabolome analysis of *TEF1* overexpressing cells

## 7.1 Introduction

Data from the previous chapters suggest that *TEF1* overexpression in yeast results in alterations to cell growth due to a variety of effects of eEF1A overexpression. We have shown that elevated levels of eEF1A result in aberrant organisation of both the actin and tubulin cytoskeletons. Our data also illustrated that larger and brighter nuclei were observed upon eEF1A overexpression when visualised using propidium iodide suggesting that eEF1A overexpression leads to chromosomal abnormalities. We also observed that increased cellular respiration and decreased cell viability resulted from eEF1A overexpression. When grown in selective media cells suppress plasmid copy number and display reduced growth rate. However, upon addition of leucine to the media we observed rapid plasmid loss, suggesting that high levels of eEF1A are toxic to the cell.

Analysis of the microarray data suggested that cells overexpressing *TEF1* react as if they are starving. This may result from a lack of available nutrition or from defective signalling within the cell as a result of eEF1A overexpression.

To further explore the "apparent starving" phenotype we asked if cells actually had depleted levels of essential metabolites. To answer this we performed global metabolome analysis using NMR, which allowed us to visualise individual and global metabolite levels in both wild type and *TEF1* overexpressing cells. Because the yeast vacuole is a major reservoir for nutrients, we also visualised the vacuole by fluorescence microscopy to check for vacuolar aberrations in the *TEF1* overexpressing cells, which could result in the cells inability to access any nutrients that are stored inside.

Metabolite profiling was performed using proton ($^1$H) NMR spectroscopy and chemical shifts ranging from +14 to -4 ppm were assigned to produce a spectrum for each sample. A

reference peak at 0 ppm was added to each sample by the addition of 20 µM DSS (4,4-dimethyl-silapentane-1-sulfonic acid) after sample preparation, but before running through the NMR. Metabolite samples were dissolved in $D_2O$ allowing deuterium to exchange with the protons present in the OH peaks ensuring exchangeable hydrogens were removed from the spectra. All proton spectra presented were processed using excitation sculpting (Hwang and Shaka, 1995) in order to suppress the water peak at 4.3 ppm. Two dimensional (2D) proton and carbon NMR spectroscopy was performed on, one of each of the wild type and *TEF1* overexpression samples (see figure 7.1-a and b). These allowed us to identify compounds using the methods described in section 7.3.2.1. One-dimensional (1D) proton NMR spectroscopy was then performed on all twelve samples allowing us to compare peak intensity across samples, and quantify metabolite levels (see figure 7.2)

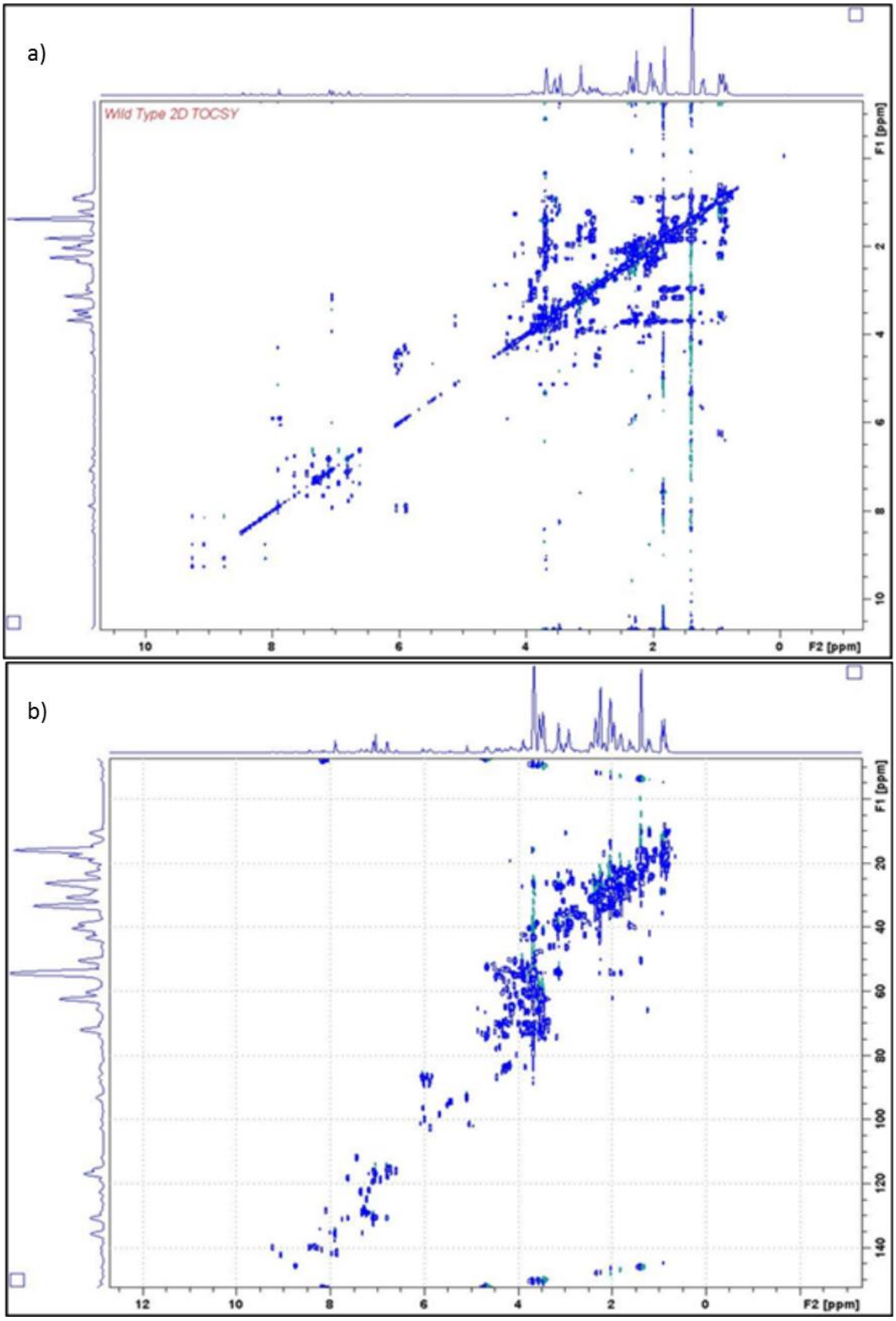


***Figure 7.1, 2D 1H and 13C spectra for wild type cells.*** *7.2-a is the 2D proton spectrum and 7.2-b is the 2D carbon spectrum. These were overlaid with the TEF1 spectra to show differences in peak position, but also for identification purposes as described in section 7.3.2.1. The blue and green peaks represent positive (blue) and negative (green) intensity.*

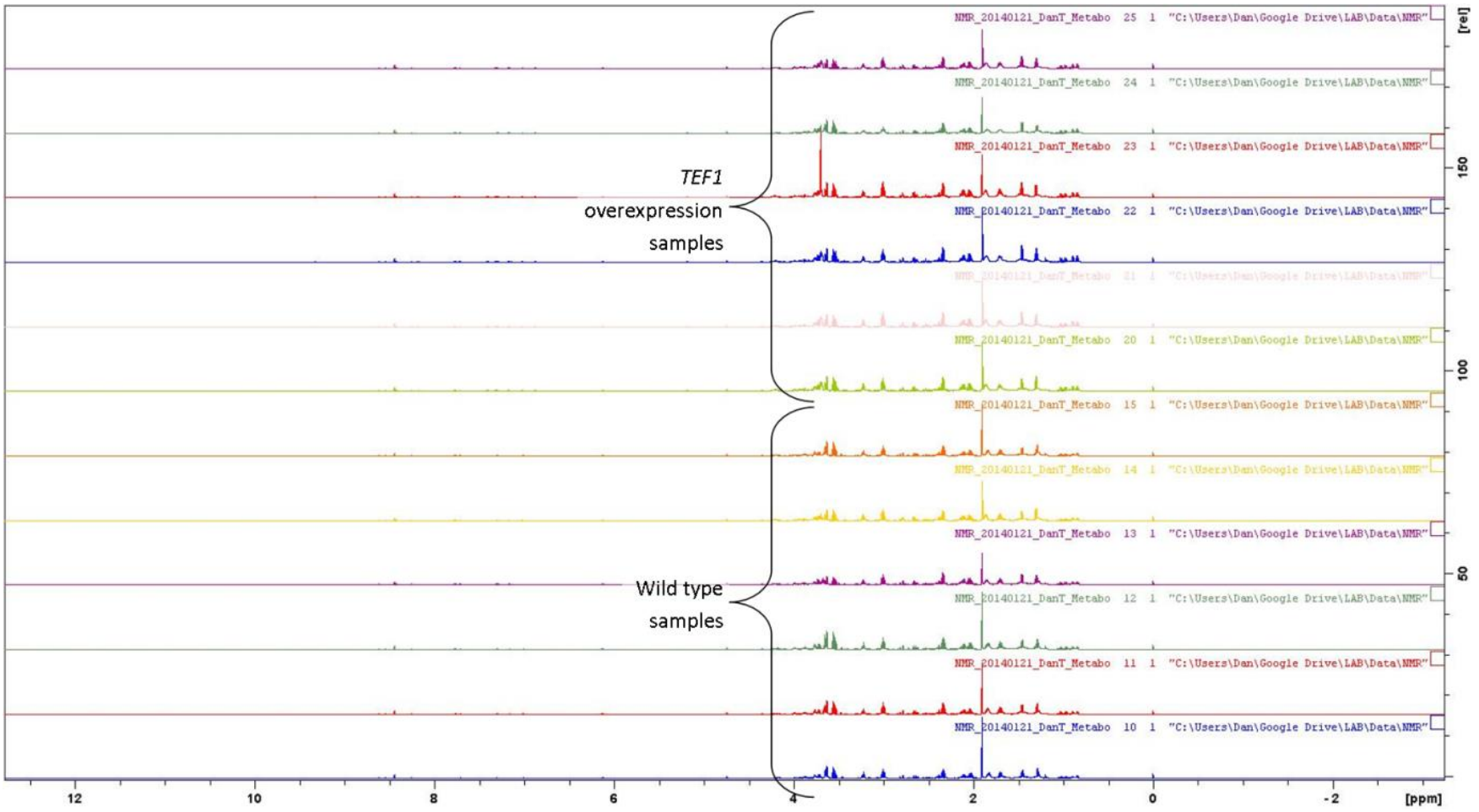


***Figure 7.2, Alignment of 1D proton spectra for the wild type and TEF1 overexpression cells.*** *There were six wild type samples (bottom) and six TEF1 overexpressing samples (top). The samples were processed so that the DSS peak at 0 ppm was aligned.*

## 7.2 Identification and assignment of metabolite peaks

The 1D proton spectra were overlaid to check for differences in peak intensity, and the appearance or disappearance of peaks from the wild type to the *TEF1* overexpression strain (see figure 7.3). Using figure 7.3 as an example we can see three different effects of *TEF1* overexpression on metabolite levels. To the left of the spectra there is a group of peaks that has shifted towards the higher end of the spectrum, overexpression of *TEF1*resulted in shifts to both the higher and the lower ends of the spectrum. The quintet in the centre of the spectrum shows a metabolite that has decreased in level in the *TEF1* overexpression strain. Overall, *TEF1* overexpression induced both increases and decreases in metabolite levels. The final example on the right of the spectrum shows a doublet present in the wild type sample, which disappears in the *TEF1* overexpression strain. *TEF1* overexpression also induced the appearance and disappearance of several peaks throughout the spectrum.

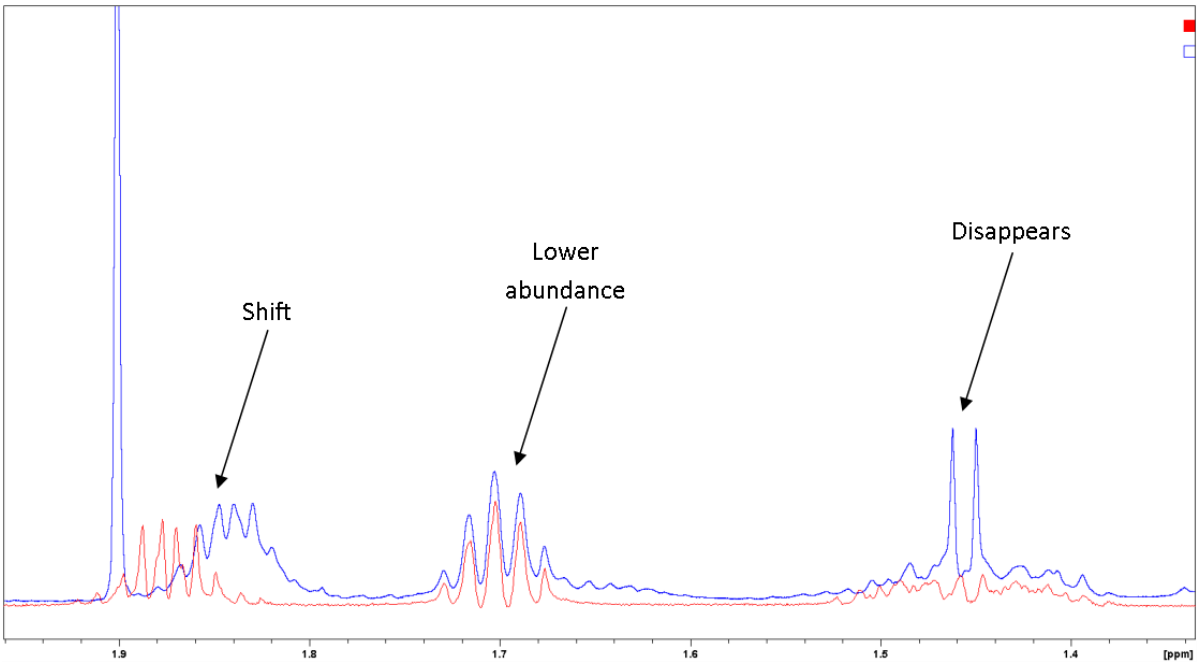


***Figure 7.3, wild type and TEF1 overexpression spectra overlaid.*** *A single wild type (blue) and TEF1 overexpression strain (red) have been overlaid. This figure only shows peaks from 1.3-2 ppm. The three points highlighted on the spectrum shows a group of peaks shift, a doublet that disappears in the TEF1 overexpression strain, and a quintet that is at lower abundance in the TEF1 overexpression strain than the wild type. The large blue peak at 1.9 ppm is from acetic acid, in the TEF1 overexpression strain this has shifted to the left just out of the image.*

## *7.2.1 Identification of altered peaks using AMIX*

The entire spectrum was processed using AMIX software which automatically detected differences in peak intensity between wild type and *TEF1* overexpression cells across the entire data set, although it was unable to account for peaks that had shifted. The output from AMIX was a graphical output that showed increases or decreases in peak intensity in the *TEF1* overexpression strain relative to wild type cells. This output was manually compared to the wild type and *TEF1* overexpression spectra to assess if peaks had altered in intensity or had shifted, it was then annotated accordingly (see figure 7.4, for entire loading comparison see appendix App.5a-e).

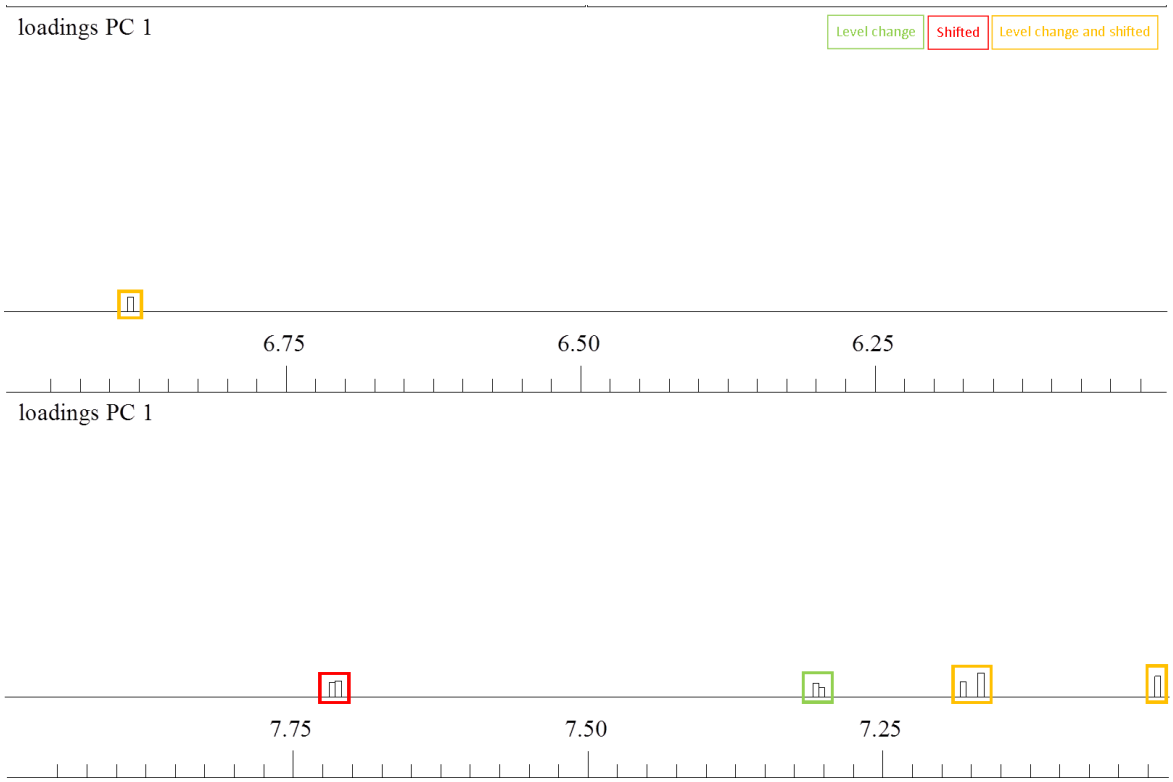


***Figure 7.4, Differences in peak intensity as detected by AMIX.*** *The output from AMIX was compared to the spectra of wild type and TEF1 overexpression cells to assess whether intensity differences were due to altered metabolite levels or to peak shifts. These were annotated using coloured boxes, green boxes indicate peaks that are of a different intensity, red boxes indicate peaks that have shifted from wild type to TEF1 overexpression cells, and orange boxes indicate peaks that have both shifted and altered in intensity.*

## *7.2.2 Assignment of metabolites*

Following identification of peaks that were altered from the wild type to the *TEF1* overexpression samples we had to assign peaks to metabolites. As this is a fledgling technique online repositories were sparsely populated with standard metabolites, and the majority of assignments were made by utilising a variety of sources.

### *7.2.2.1 Tools for metabolite assignment*

The primary tools for metabolite assignment were online databases consisting of previously analysed metabolites. These were useful in identifying potential metabolites of interest, but analysis using such databases appeared to be prone to error and misidentification. The first database was the Madison Metabolomics Consortium Database (MMCD) (http://mmcd.nmrfam.wisc.edu/). Using this website we were able to search by compound name, if we had a tentative idea of the metabolite, or we could search by peak shift (ppm) and the database would generate a list of potential metabolites based on their proximity to the peak shifts we had submitted. The second database that we utilised was the Yeast Metabolome Database (YMDB) (www.ymdb.ca). This database was not as comprehensive as the MMCD, but it had several metabolites that we were unable to find using MMCD. The final database utilised was the mining tool, Metabominer (http://wishart.biology.ualberta.ca/metabominer/). This was an executable package rather than accessed online and allowed interrogation of all of the peaks within a single spectrum. The peak list was input into the software and it attempted to find peaks in patterns that were comparable to metabolites contained in its database. It then generated a list of potential candidates allowing us to highlight peaks of interest (see figure 7.5).

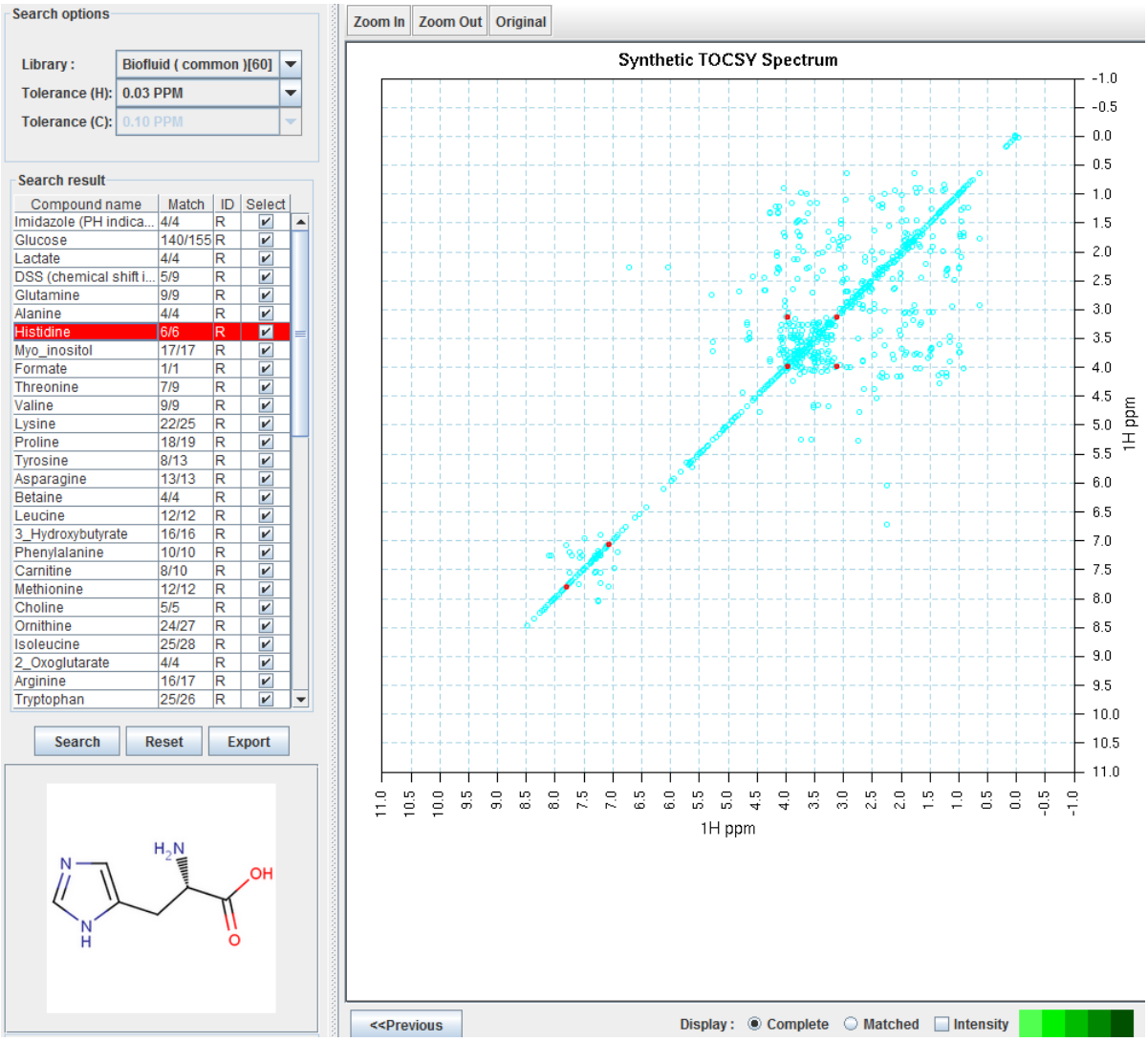


***Figure 7.5, An overview of metabominer.*** *This shows the 2D proton spectrum of the wild type sample (blue dots). The list to the right is of potential metabolites present in the sample. Highlighted in red are the peaks that the software has predicted correlate to histidine.*

We also utilised the NMR prediction software ACD Predictor (http://www.acdlabs.com/products/adh/nmr/nmr_pred/). This allowed us to draw chemical structures of metabolites that we thought we may have discovered in a spectrum. The software then generated a predicted peak shift list as well as drawing the predicted spectrum (see figure 7.6). Although a powerful tool its major drawback was that this was all based on prediction, rather than acquired data, and it occasionally made errors.

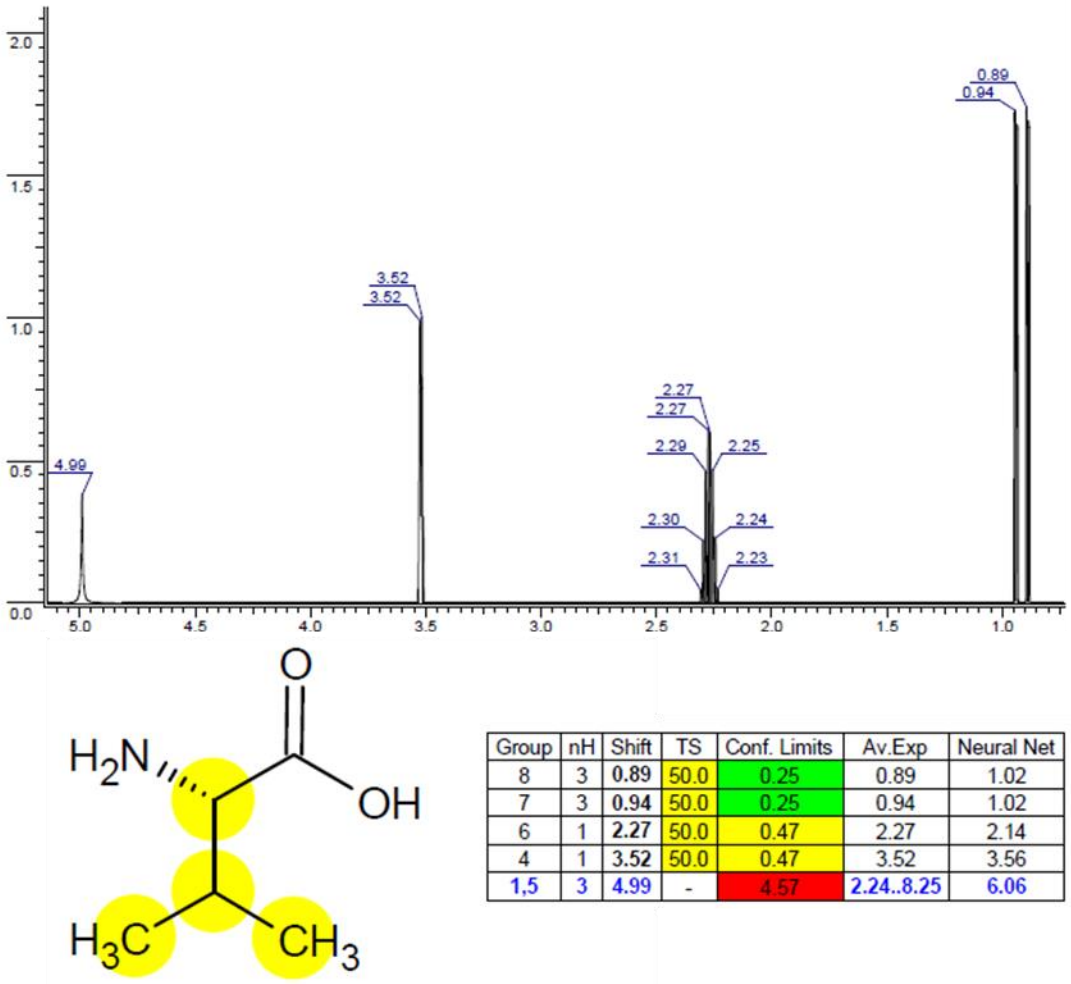


| Group | nH | Shift | TS | Conf. Limits | Av.Exp | Neural Net |
|---|---|---|---|---|---|---|
| 8 | 3 | 0.89 | 50.0 | 0.25 | 0.89 | 1.02 |
| 7 | 3 | 0.94 | 50.0 | 0.25 | 0.94 | 1.02 |
| 6 | 1 | 2.27 | 50.0 | 0.47 | 2.27 | 2.14 |
| 4 | 1 | 3.52 | 50.0 | 0.47 | 3.52 | 3.56 |
| 1,5 | 3 | 4.99 | - | 4.57 | 2.24..8.25 | 6.06 |

***Figure 7.6, Output from ACD NMR predictor.*** *This shows the predicated peak shifts for valine along with the origin of each peak on the chemical structure. The table to the lower right lists the shifts along with the confidence limts.*

The next tool used for peak assignment was CcpNmr Analysis (http://www.ccpn.ac.uk/software/analysis). CcpNmr is a graphics-based program which allows NMR spectrum visualisation, resonance assignment and data analysis. This software was utilised to visualise both the 1D and 2D spectra simultaneously. This allowed us to pick peaks from the 1D spectrum that had been highlighted by the AMIX analysis and find them in the 2D spectrum. The 2D spectrum was generated using Total Correlation Spectroscopy (TOCSY) which is a method for, in theory, correlating all of the spins in a set of mutually coupled spins, allowing identification of an entire set of resonances from a single metabolite.

Once a peak from the 1D spectrum had been identified in the 2D spectrum we could then identify other peaks coupled to this peak allowing us to decipher the structure of the unknown metabolite (see figure 7.7). Coupling of peaks using the 2D spectrum was performed by tracing a vertical, or horizontal line from the initially identified peak (number 1 in figure 7.7), once another peak is encountered (peak 2) a horizontal line was traced back to the diagonal revealing the peak at 1.39 ppm (peak 3) is coupled to the peak at 4.35 ppm (peak 1). The process is repeated until no more peaks can be coupled together. In this example only the peak at 8.25 ppm (peak 5) can be coupled via peak 4. It is possible that a peak may also exist between peaks 2 and 4 (shown in red) although depending on the abundance of the metabolite and the sensitivity of the machine this may not be present.

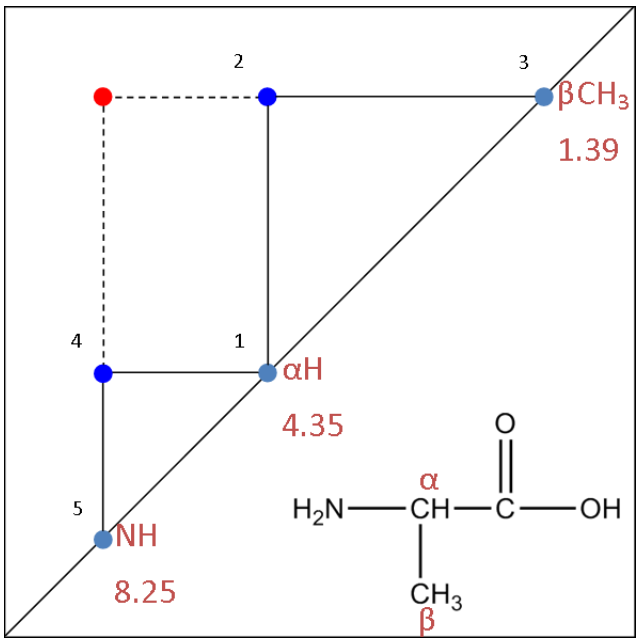


***Figure 7.7, Demonstration of coupled peak shifts using alanine.*** *How peak assignment is performed using the 2D spectra. This shows the proton peak shifts of the α and β carbons together with the protons of the amine group. In order to identify these as peaks from a single compound we had to use the CCPNMR software to draw horizontal and vertical lines from each peak allowing us to visualise proton coupling.*

## 7.3 Metabolite identification and quantification

Following identification of peaks that were different between the wild type and *TEF1* overexpression strain, and by utilising all the tools at our disposal to reliably identify as many metabolites as possible, we had confidently assigned 19 metabolites (see table 7.1 and figure 7.8), and made a further 15 tentative assignments (see appendix App.6). Confident assignments were those that showed consensus across multiple tools used for assignment, tentative assignments were those that displayed conflict using multiple tools. The majority of metabolites identified were amino acids, with several other metabolites identified.

**Table 7.1 - Metabolite assignments**

| Metabolite | Peaks Identified (ppm in wild type) |
|---|---|
| 3-hydroxycinnamic acid | 6.86, 7.16, 7.3 |
| Acetic acid | 1.9 |
| Alanine | 3.75 |
| AMP/ATP | 6.12 |
| Arginine | 1.83, 3.22 |
| Aspartate | 2.64, 2.79, 3.87 |
| Glutamate | 3.71 |
| Isoleucine | 0.92, 0.99, 1.29, 1.43 |
| Isopropylmalic acid | 0.84, 0.89 |
| Leucine | 0.94, 0.95, 1.69 |
| Lysine | 1.45, 3.01 |
| NADH | 2.9 |
| NAD/NADP | 6.03, 6.07, 8.18, 8.54, 8.83, 9.15, 9.32 |
| Threonine | 1.3 |
| Trehalose | 5.18 |
| Tryptophan | 3.54, 3.64 |
| Valine | 0.97, 1.02, 2.33 |

*A list of the 19 confident metabolite assignments made from the NMR spectra.*

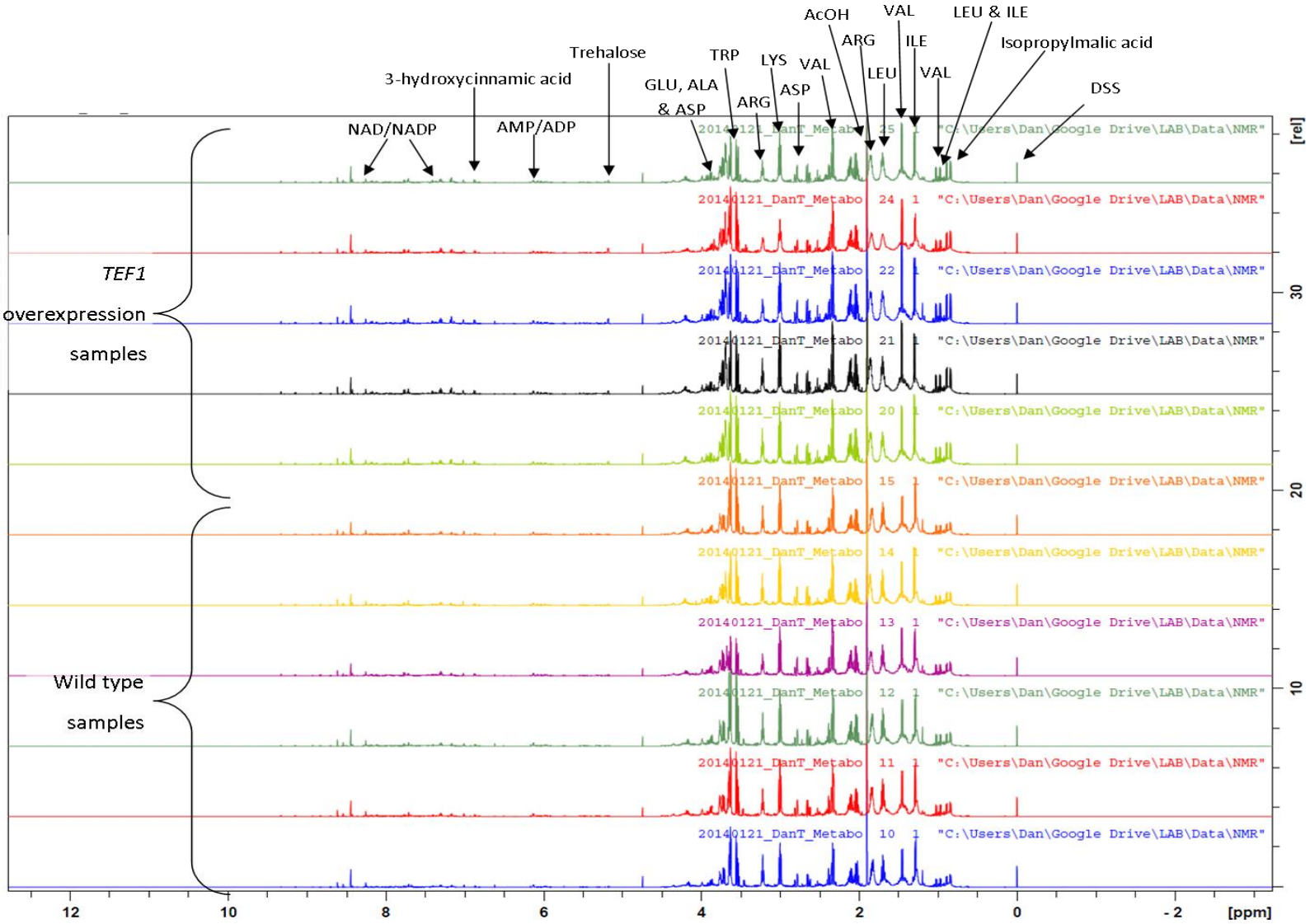


***Figure 7.8, Aligned spectra with metabolite annotations.*** *The total spectra for wild type and TEF1 overexpressing cells with annotations for known metabolites.*

### *7.3.1 Metabolite quantification and generation of a small compound library*

Following assignment of metabolites that we were confident with, we then aimed to quantify them. This required that we identified unique peaks for each metabolite, and that we know how many protons were represented by each peak. We used Bruker TopSpin data analysis software for each sample. This software allowed the interrogation of data at high resolution facilitating the identification of peaks from one metabolite that may be overlaid with peaks from another metabolite.

With the ability to visualise spectra at high resolution there were still problems identifying peaks in crowded regions. One region of particular interest, 0.9-1.0 ppm, contained peaks corresponding to the δ and γ carbons of the branched chain amino acids leucine, isoleucine and valine. As previously discussed the addition of leucine to media rescued the viability and growth defects observed in yeast when *TEF1* was overexpressed. Also, Leu3 was discussed as a regulatory transcription factor of the up-regulated genes involved in BCAA biosynthesis. Leu3 is known to act as a repressor in leucine rich environments and an activator in high levels of the leucine biosynthesis intermediate isopropylmalic acid (also assigned in the NMR spectra). This led us to ask the following three questions. If levels of isopropylmalic acid or levels of leucine were affecting Leu3, was it acting as an activator or a repressor? Also if we were able to identify altered levels of leucine in the *TEF1* overexpressing cells, was it higher? And if leucine was higher, how did leucine supplementation rescue the phenotypes previously mentioned?

To assist in finding peaks unique to leucine we began to generate a metabolite database. We prepared samples of leucine, isoleucine and valine to analyse using NMR (see figure 7.9). This gave us standards that allowed us to compare to our spectra simply by overlaying the

spectrum of the known amino acid with the spectrum containing the unknown peaks. This method proved to be very efficient and so we expanded the metabolite database to include all amino acids as well as some other metabolic compounds of interest (see figure 7.10 for an example of an overlay using this method). A list of metabolite standards generated for use in this study can be found in the Appendix 7). Utilising the metabolite database we were able to identify unique peaks for 12 of the 19 certain assignments we had made (see table 7.2).

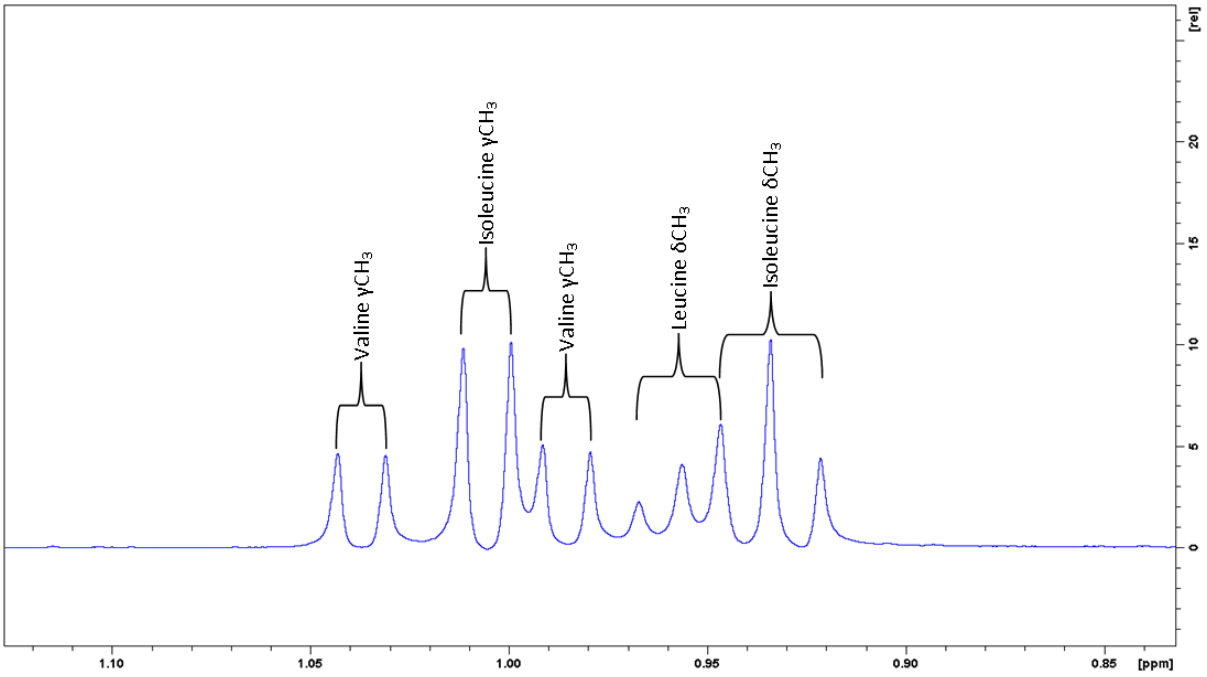


***Figure 7.9, Isoleucine, leucine and valine standards****. Isoleucine, leucine and valine samples were prepared and mixed at 80 µM, 20 µM and 40 µM respectively. This facilitated identification of unique peaks. The peaks corresponding to leucine and the isoleucine δCH3 are overlaid making them unusable for quantification purposes. The leucine peaks are two sets of doublets overlaid in a triplet arrangement, and the left peak of the isoleucine δCH3 over lays with the right peak from the leucine triplet.*

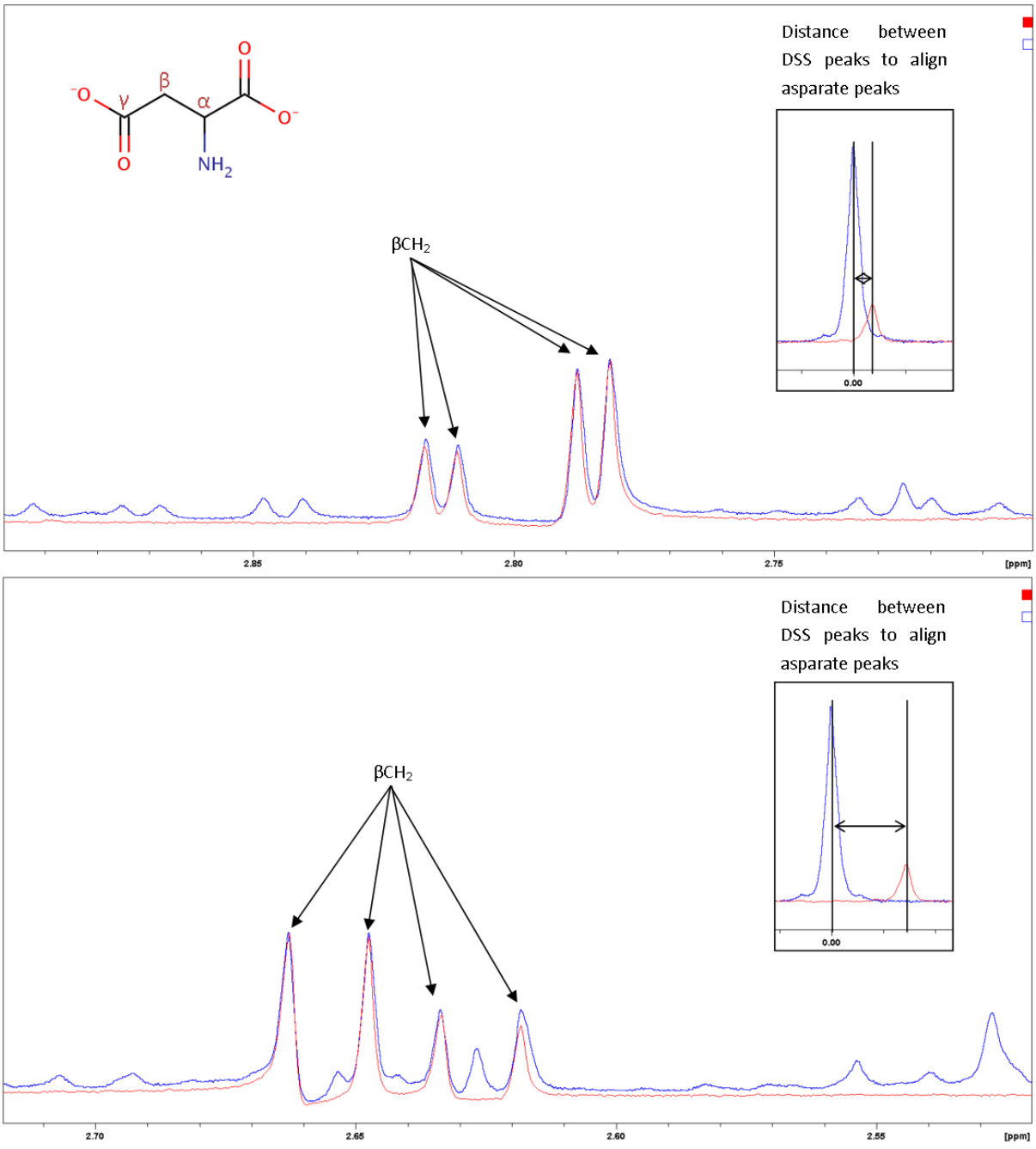


***Figure 7.10, Aspartate standard laid over a wild type spectrum.*** *The wild type spectrum is shown in blue, with the aspartate standard overlaid (the red spectrum). The boxed window shows the DSS zero for each sample, these are not overlaid as the environment of the sample preparations differed resulting in a shift of the peaks from aspartate.*

**Table 7.2 - Unique peaks that allowed metabolite quantification**

| Metabolite | Peak Shift | Number of peaks used for quantification |
|---|---|---|
| **Isopropylmalic acid** | 0.842 | 2 |
| **Isoleucine** | 0.925 | 3 |
| **Leucine** | 0.946 | 1 |
| **Valine** | 0.974 | 2 |
| **Threonine** | 1.302 | 2 |
| **Alanine** | 1.459 | 2 |
| **Acetic acid** | 1.9 | 1 |
| **Glutamate** | 2.33 | 6 |
| **Aspartate** | 2.797 | 4 |
| **NADH** | 2.906 | 3 |
| **Lysine** | 3.006 | 3 |
| **Trehalose** | 5.183 | 2 |

To calculate metabolite concentration we used the DSS peak at 0 ppm which provided us with a peak of known concentration (20 µM). We compared the DSS peak intensity to the intensity of the unique peaks of the other metabolites and using the equation described in the Materials and methods (section 2.5.4.5) we were able to express metabolite levels as a molar concentration(see figure 7.11). Reassuringly there were some metabolites that were up-regulated and some that were down-regulated in the *TEF1* overexpression strain indicating that the extraction process was effective in both strains and we hadn't liberated a disproportionate level of metabolites from one strain relative to the other. Metabolites we found at significantly increased levels in the *TEF1* overexpression strain were alanine, valine, the leucine biosynthesis intermediary isopropylmalic acid, and trehalose. NADH was the only metabolite identified that had significantly decreased levels in the *TEF1* overexpression strain.

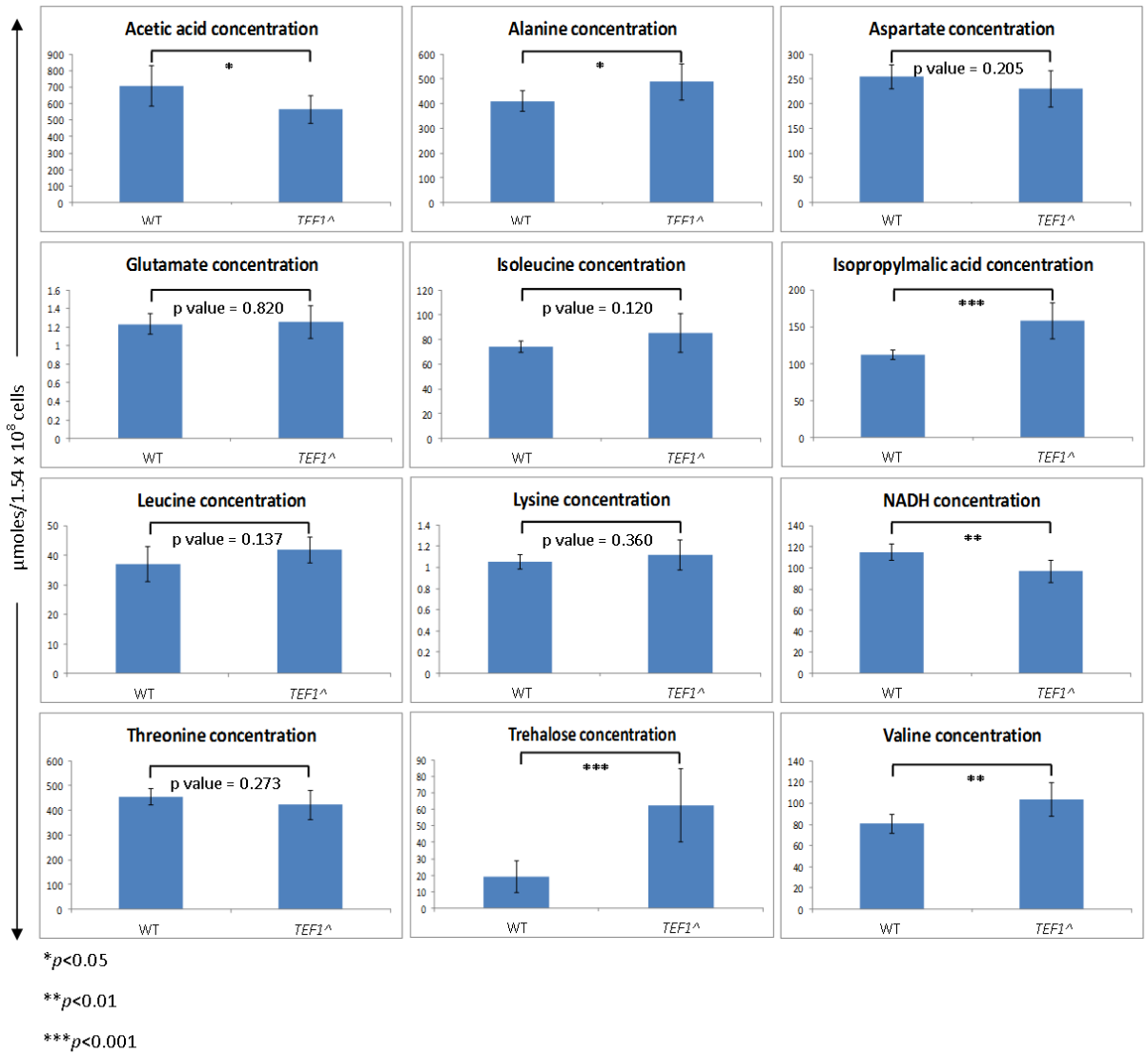


***Figure 7.11, Metabolite concentrations in wild type and TEF1 overexpression strains.*** *Metabolite concentration was calculated per sample, with each sample containing approximately 1.54 x $10^8$ cells.*=p<0.05, **=p<0.01,***=p<0.001.*

### *7.3.1.1 eEF1A levels affect levels of amino acids*

All branched chain amino acids exhibited a large increase in their levels in the *TEF1* overexpression cells. Leucine showed a 35.2% increase, valine showed a 55.3% increase, isoleucine showed a 38.6% increase, and the leucine intermediate isopropylmalic acid showed a 55% increase. As well as these increases, an increase was also detected in alanine of 19.2%. It is known that leucine, isoleucine, valine and alanine are all derived from pyruvate (see figure

7.12). Unfortunately we were unable to confidently identify pyruvate using NMR and so are unable to provide an estimate of pyruvate levels in the cell. We were able to identify and quantify threonine, a precursor to isoleucine found at 38.6% higher in *TEF1* overexpressing cells, which was found to be present at levels 7% lower in *TEF1* overexpressing cells than wild type suggesting that accumulation of the BCAAs is not due to a reduced need for them, but rather a concerted global effort to increase levels. When taken together with the microarray data analysis that ranked amino acid biosynthesis as one of the most increased processes in cells overexpressing *TEF1* (see sections 6.9 and 6.10), this strengthens the argument for *TEF1* levels affecting cellular metabolism.

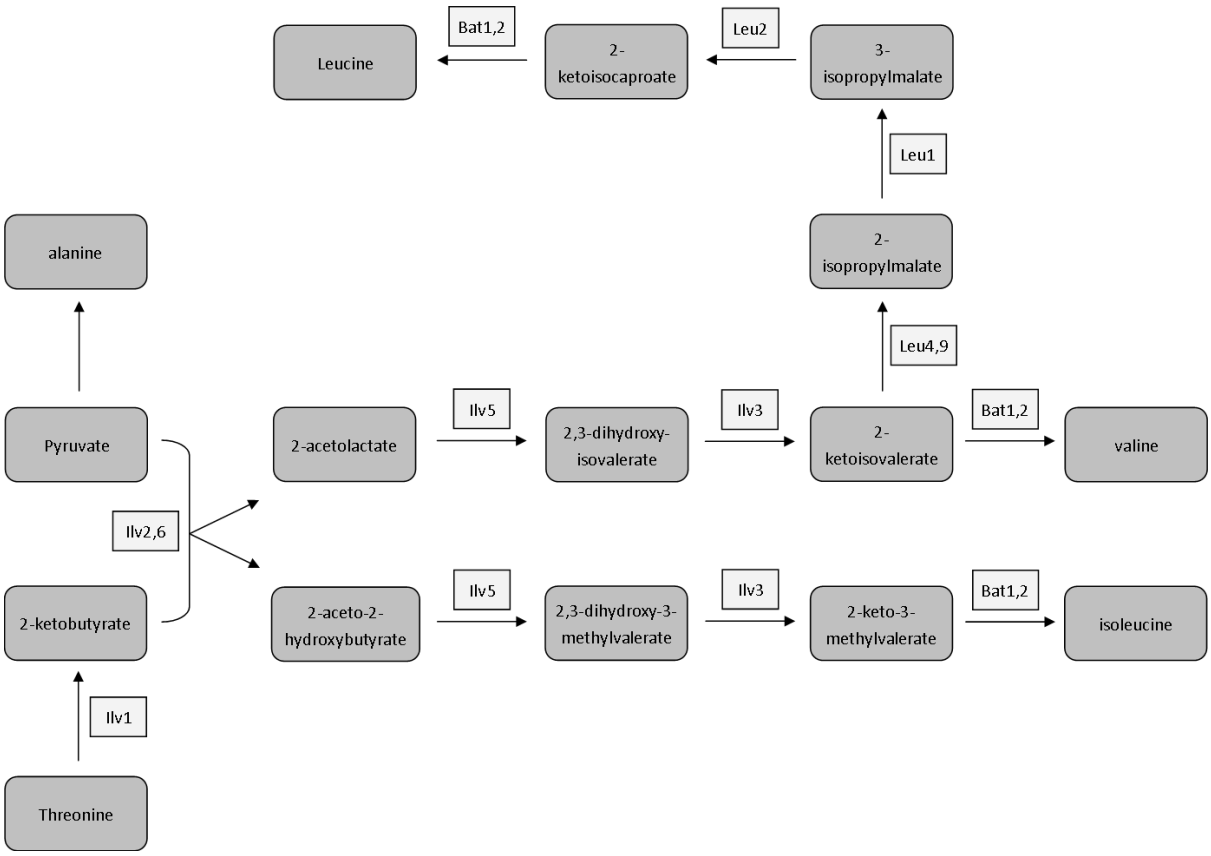


***Figure 7.12, Pyruvate family.*** *Biosynthesis pathway for pyruvate derivatives alanine, and the branched chain amino acids leucine, isoleucine and valine.*

Furthermore increased levels of isopropylmalic acid (the leucine biosynthesis intermediate) suggest that Leu3 (discussed in 6.4.2.2) may not be acting as an inhibitor BCAA biosynthesis as discussed, but in fact be acting as an activator. Leu3 is known to act as a regulator of genes involved in BCAA biosynthesis (Friden and Schimmel, 1988). It acts as a repressor in leucine rich environments and an activator in isopropylmalic acid rich environments (Sze *et al.*, 1992). As both leucine and isopropylmalic acid are increased it is unclear how Leu3 is acting in *TEF1* overexpressing cells, but as all BCAAs are increased it is logical to assume that Leu3 is likely to be acting as an activator of BCAA biosynthesis.

#### *7.3.1.2 eEF1A levels affect levels of the storage carbohydrate trehalose*

Trehalose is found in *TEF1* overexpressing cells at levels almost three-fold higher than in wild type (Fig 7.11). As previously discussed (see section 3.4), *TEF1* overexpressing cells exhibited a starvation phenotype with up-regulation of several processes involved in metabolite biosynthesis. The disaccharide trehalose is canonically described as a storage carbohydrate, readily available when cells require a carbohydrate source upon recommencing growth. It is also known as a protectant against desiccation and heat shock in yeast (Singer and Lindquist, 1998). How trehalose protects against these stresses is not fully understood, but it is thought that it protects cells by stabilising proteins in their native state, preventing denaturation. It is also thought to suppress aggregation of denatured proteins in a similar manner (Singer and Lindquist, 1998).

Trehalose accumulation has also been recorded in cells with retarded growth, and it is thought that duration of the G1 phase may influence the rate of trehalose accumulation (Paalman *et al.*, 2003). We have observed a reduction in growth rate of approximately 20% in cells overexpressing *TEF1* (see fig. 3.4), and an increase in cell volume of a similar quantity.

Although cell cycle analysis was not performed during this study, the increased cell size observed upon the overexpression of *TEF1* suggests that cells with elevated levels of eEF1A may possess a cell cycle with an extended G1 phase. However, given the data presented in this thesis suggesting that cells overexpressing *TEF1* are responding to starvation, the likely explanation for trehalose accumulation is that cells are simply responding to a lack of accessible nutrients.

Due to the observable in increase in the level of BCAAs, including leucine, upon overexpression of *TEF1*, the question arose of how leucine supplementation alleviates phenotypes that are induced in the presence of elevated levels of eEF1A (see section 3.2). If cells overexpressing *TEF1* already have increased levels of leucine compared to wild type, how can adding leucine rescue these phenotypes? Were cells sequestering leucine in defective vacuoles rendering it inaccessible, or was leucine present in the cytoplasm and cells were unable to detect it.

## 7.4 The effects of *TEF1* overexpression on vacuoles

To answer the question of whether cells contained inaccessible leucine within defective vacuoles we performed fluorescence microscopy, and took a preliminary look at metabolite levels from isolated vacuoles.

### *7.4.1 TEF1 overexpression causes vacuolar aberrations*

Observation of wild type and *TEF1* overexpressing cells by fluorescence microscopy using the fluorescent vacuolar dye Blue CMAC (7-amino-4-chloromethylcoumarin) and the vacuole localised Gtr2-GFP revealed that *TEF1* overexpression resulted in severe vacuolar aberrations (see figure 7.13). Wild type Gtr2-GFP cells presented a homogenous distribution of both GFP and DAPI signals throughout the vacuole, containing one to two large spherical vacuoles per

cell. Upon overexpression of *TEF1* we observed fragmentation of vacuoles, with translocation of Gtr2 to the vacuolar membrane, blue CMAC also appeared limited in its ability to enter the cells. This suggested that elevated eEF1A levels were having a negative effect on vacuoles resulting in the inability of small compounds to enter and exit.

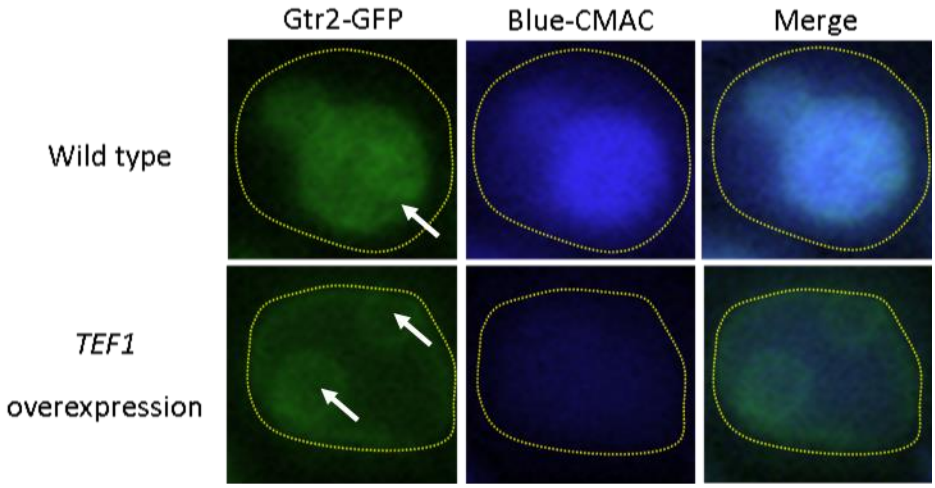


***Figure 7.13, Fluorescence microscopy of Gtr2-GFP and TEF1 overexpression stained with Blue CMAC.*** *Upon TEF1 overexpression the vacuoles fragment, Gtr2 migrates to the vacuolar membrane and Blue CMAC appears unable to enter the vacuole. Cell boundary is in yellow and vacuoles are highlighted by arrows.*

## ***7.4.2. TEF1 overexpression results in high quantities of metabolites accumulating in the vacuole***

Analysis of the vacuole by fluorescence microscopy demonstrated that overexpression of *TEF1* resulted in aberrant vacuoles that were unable to take up the dye Blue CMAC (Fig 7.13). This led us to ask if the increased levels of detectable metabolites in *TEF1* overexpressing cells was due to an accumulation of inaccessible metabolites in defective vacuoles. To answer this we performed vacuole isolations followed by metabolite extractions on the vacuolar fraction (see Materials and methods 2.5.4.2).

Due to the fact that we were only analysing metabolite levels isolated from the vacuoles, we harvested six times more cells for the vacuolar metabolite samples to facilitate ease of detection using NMR. As this was a preliminary experiment to check the efficacy of the protocol there were only single samples run for both the wild type and the *TEF1* overexpression strains.

A comparison of the spectra from the vacuolar metabolite preparations and the whole cell extract showed that were significant differences in the observable peaks (see figure 7.14) (For the entire vacuolar spectra and comparison to the whole cell extraction see appendix App.8a-e). The peaks that we had assigned to isopropylmalic acid were no longer detectable in the wild type sample, and were very low in the *TEF1* overexpression sample. There were other differences across the spectra in both assigned and unassigned metabolites. We were still able to detect trehalose in both of the vacuolar extractions (see figure 7.15) suggesting that the cells were attempting to suppress its levels by degradation using the vacuolar trehalase Ath1. It was anticipated that trehalose would be present at lower levels in the vacuole as the glycoside hydrolase enzyme, trehalase localises to the vacuole (Keller *et al.*, 1982) and can catalyse the conversion of trehalose to glucose.

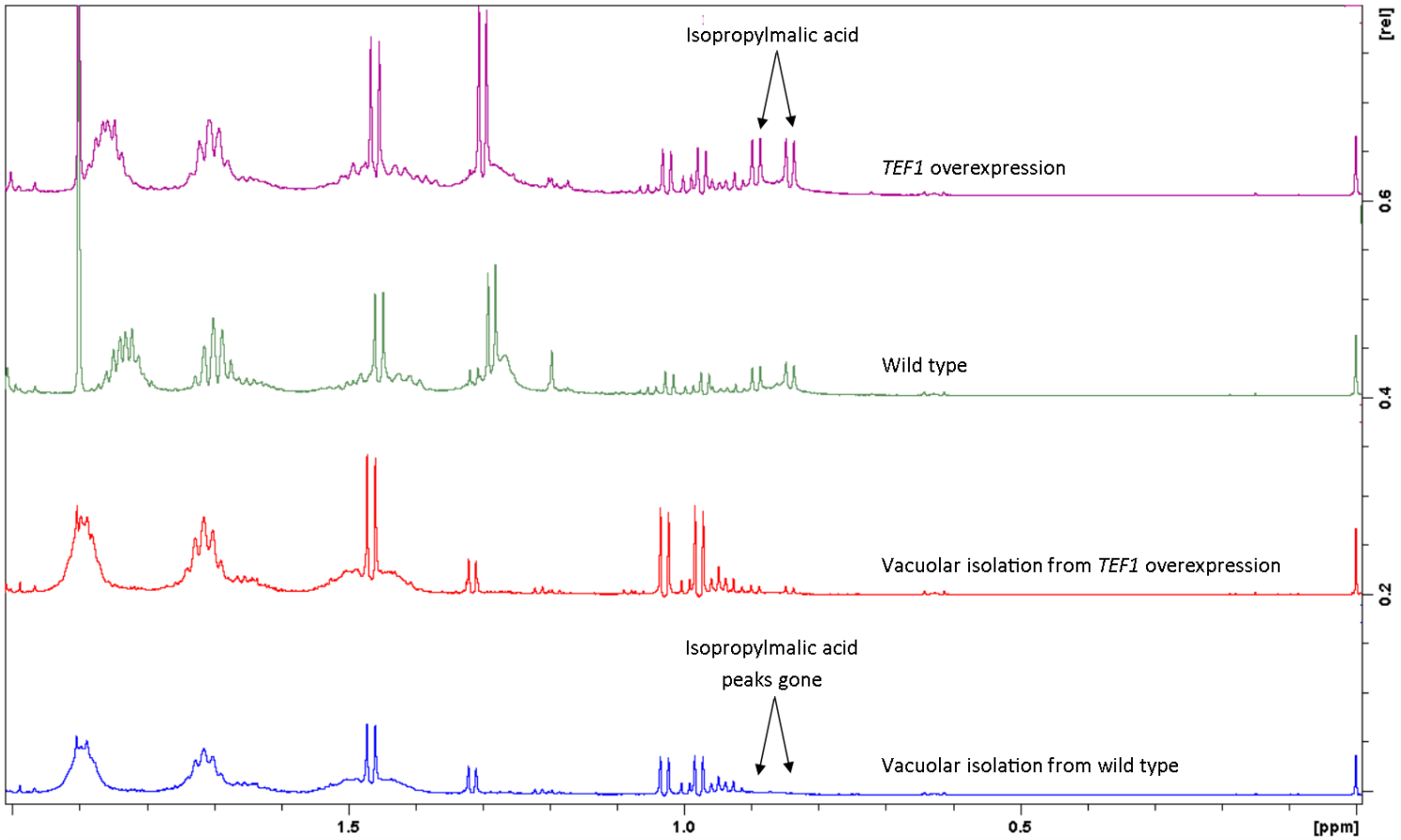


***Figure 7.14, Alignment of wild type and TEF1 overexpression whole cell and vacuolar metabolite preparations***. *Samples have been aligned at 0 ppm and spectra are displayed showing 0-2 ppm. Highlighted is the difference in isopropylmalic acid levels between the whole cell and the vacuolar metabolite preparations.*

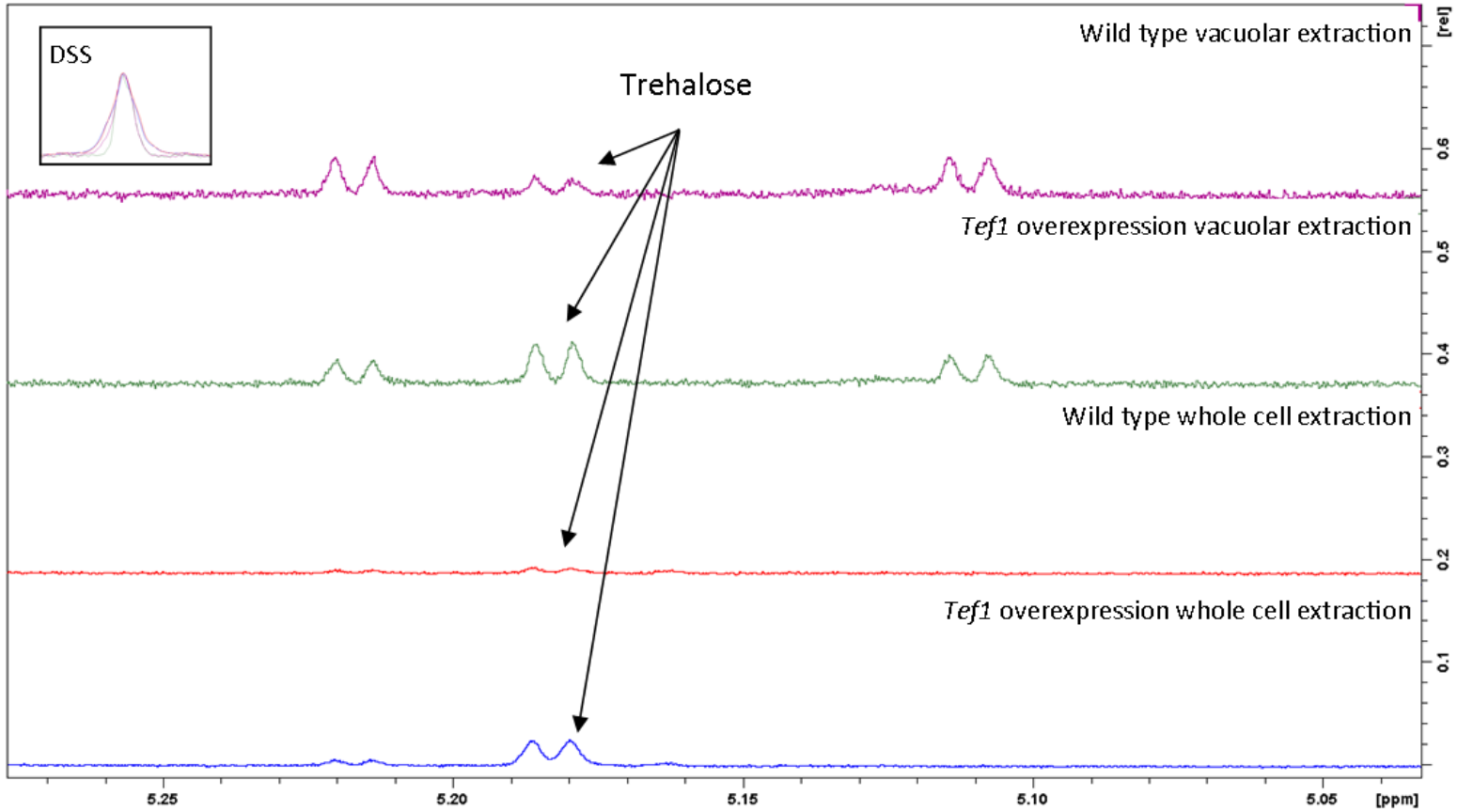


***Figure 7.15, Alignment of wild type and TEF1 overexpression whole cell and vacuolar metabolite preparations.*** *Samples have been aligned at 0 ppm (inset) and spectra are displayed showing 5.05-5.25 ppm. Trehalose has been highlighted to show that it was still detectable in the vacuolar metabolite preparation. Although trehalose peaks from the vacuolar extract appear greater in intensity than the whole cell extract this is due to metabolites being extracted from six times more cells. When quantified this is corrected for.*

Similar to the whole cell metabolite extracts we performed quantification on the vacuolar metabolites that we had identified unique peaks for, but as these were only performed as single experiments no statistical analyses could be performed to ensure the significance of the data (see figure 7.16).

Analysis of the branched chain amino acids showed that in the vacuole, leucine, isoleucine and isopropylmalic acid were present at lower levels in the *TEF1* overexpression strain relative to the wild type. Leucine levels decreased by 9.1%, isoleucine levels dropped by 32.5%, and isopropylmalic acid was undetectable in wild type vacuoles, but still present at 18.96 µmoles/9.24 x $10^8$ cells in *TEF1* overexpression cells. Valine levels increased in the *TEF1* overexpression strain by 25.1%. Threonine showed a 23.2% decrease in levels in the *TEF1* overexpression strain. Alanine, glutamate and lysine showed no difference in levels between wild type and *TEF1* overexpression cells. Similar to the global metabolome analysis, trehalose showed the largest difference with a 246% increase in *TEF1* overexpression cells.

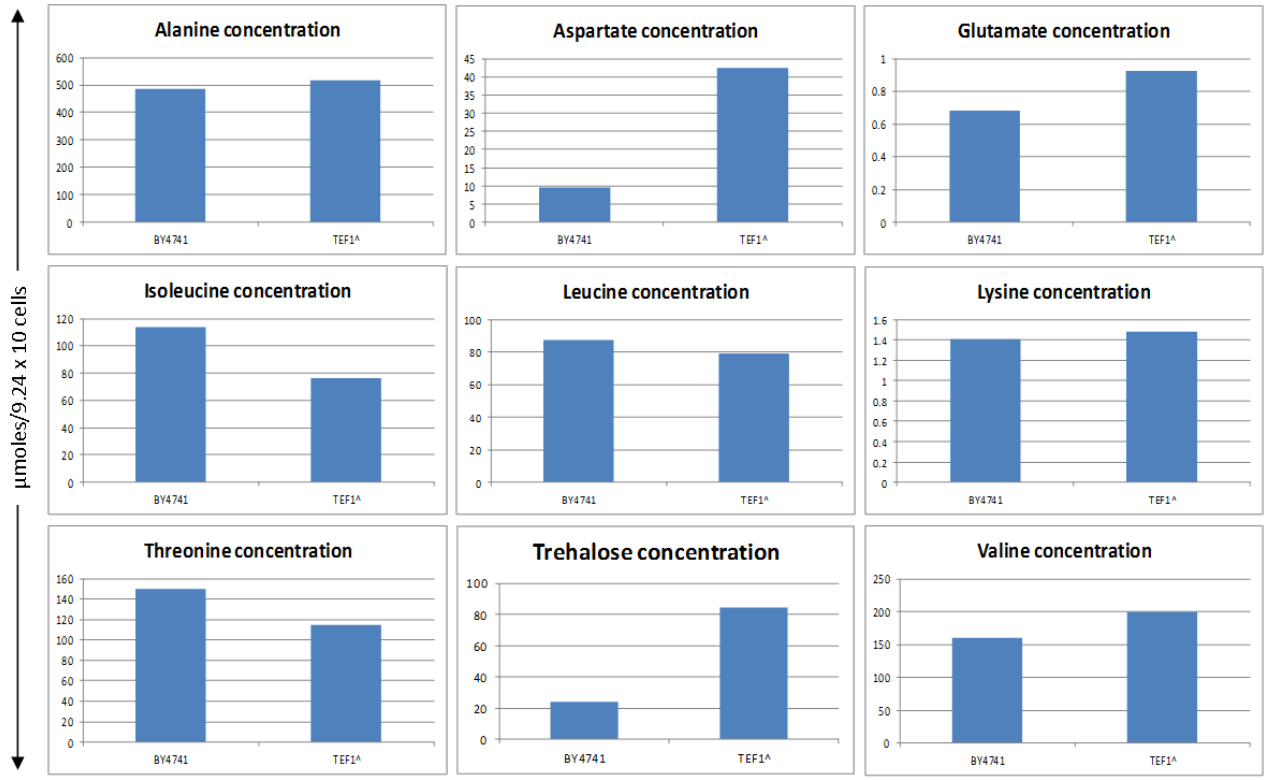


***Figure 7.16, Vacuolar metabolite concentrations in wild type and TEF1 overexpression strains.*** *Metabolite concentration was calculated per sample, with each sample containing approximately 9.24 x $10^8$ cells.*

## 7.6 Discussion

Following indications that elevated levels of *TEF1* affect cell metabolism we utilised NMR spectroscopy to analyse metabolite levels in wild type and *TEF1* overexpression cells. Although still in the development stages this method showed promise in its ability to provide us with high resolution details about the metabolic flux of the cell in the presence of endogenous and elevated levels of eEF1A. Together with the transcriptome data from chapter 6, this method had the potential to provide data for entire pathways allowing us to visualise the precise points in biosynthetic pathways that are influenced by elevated levels of eEF1A.

Whole cell metabolite concentrations concurred with transcriptome data and indicated that cells overexpressing *TEF1* are up-regulating metabolite biosynthesis in response to perceived

starvation (merging of these data will be discussed further in the final chapter). The majority of the quantified metabolites were present at elevated concentrations in the *TEF1* overexpression strain relative to the wild type, with only acetic acid and NADH showing a decrease in levels.

The presence of leucine at elevated levels posed the question. "How could leucine supplementation rescue phenotypes caused by *TEF1* overexpression if leucine is already available in abundance relative to the wild type?" We hypothesised that *TEF1* overexpression resulted in leucine accumulation in the vacuole and that, for an as yet unexplained reason, the cell was unable to access it. Using fluorescence microscopy we revealed that *TEF1* overexpression results in vacuole fragmentation and membrane aberrations that prevent the vacuolar dye Blue-CMAC entering (Fig 7.13). It seems that these vacuolar defects also prevented the cells from accessing any of the metabolites that were sequestered within the vacuole as our preliminary analysis of metabolite levels within the vacuole revealed that most metabolites were present at elevated levels in cells overexpressing *TEF1* (Fig 7.16).

Further evidence that cells with elevated levels of eEF1A were responding to starvation came from the significant increase in trehalose and isopropylmalic acid levels. In both the whole cell extractions and the vacuolar extraction, cells overexpressing *TEF1* resulted in levels of trehalose more than 250% higher than wild type. As discussed trehalose is known to perform a variety of roles in the cell (see section 7.3.1.2), but its primary role is a storage carbohydrate that is produced upon depletion of glucose in the environment. This suggests that cells are unable to sense or utilise the glucose available to them and so are implementing measures to commence growth when more favourable conditions are encountered. Furthermore, elevated levels of isopropylmalic acid correlated with the transcriptome analysis suggesting

cells were increasing the rate of BCAA synthesis. An increase in the rate of BCAA synthesis again correlates with the cells inability sense or access nutrients that are readily available to them.

We have presented data that implicates elevated levels of eEF1A in the generation of defective vacuoles. These defective vacuoles appear to contain levels of many amino acids at higher levels than wild type vacuoles, yet cells with increased *TEF1* expression are unable to utilise them. We propose that metabolites that are contained within these defective vacuoles are completely inaccessible to the cell, as demonstrated by the inability of Blue-CMAC to enter the vacuole. Because of this metabolite deprivation, cells respond by attempting to increase amino acid and carbohydrate production. However, these attempts at recovering metabolite levels appear to be in vain as only upon the supplementation of leucine to the media did we observe a detectable rescue in growth rate (see section 3.2.2).

# Chapter 8: Final Discussion

Although its canonical role in translation elongation is well characterised, the moonlighting functions of eEF1A are yet to be fully understood. As one of the most abundant proteins in the cell, accounting for between 3 and 10 % of all soluble proteins, understanding the additional roles that eEF1A performs in the cell is essential. It is known that overexpression of the human isoform, eEF1A2, induces tumour growth making understanding the interactions of this highly conserved protein necessary.

During this study we sought to utilise the highly amenable budding yeast *S. cerevisiae,* to elucidate novel interactions and pathways that eEF1A may be involved in. We have used both classical phenotypic analysis, and modern, global, transcriptome and metabolome analysis to describe putative interactions between eEF1A and other essential cellular components, as well as characterising alterations in metabolic pathways in response to elevated levels of eEF1A. Furthermore we characterised eEF1A2 overexpression in HEK293 cells to observe if any interactions observed in yeast were conserved through to humans. The results of these experiments are discussed below.

## 8.1 eEF1A overexpression causes spindle defects resulting in DNA replication stress

Previous studies on *TEF1* overexpression in yeast revealed that elevated levels of eEF1A resulted in cytoskeletal aberrations and slowed growth (Munshi *et al.*, 2001). It was demonstrated that eEF1A was able to bundle actin and that point mutations in eEF1A could inhibit its ability to do this, in some cases simultaneously rescuing any growth defects observed (Gross and Kinzy, 2005).

To further investigate the interaction between eEF1A and actin we utilised an array of strains deleted for genes known to interact with or control the function of actin. Overexpression of

*TEF1* in these deletion strains was assessed by its effect on growth rate and it was recognised that components of the dynactin complex demonstrated enriched synthetic interaction with eEF1A when assessed using this method (see figure 4.3 a-c). Further investigation into the interactions between the dynactin complex and eEF1A revealed that upon deletion of *ARP1*, the backbone of the dynactin complex, we saw a rescue of the spindle defect observed in *TEF1* overexpression strains (see figure 4.6 a-d). However, although the *Δarp1* strain rescued the spindle defect, we still observed chromosomal instability as highlighted by the peak shifts in the FACS analysis of DNA content (see figure 4.4 a-l).

We also observed that, when visualised by fluorescence microscopy, the TUB4-GFP strain exhibited brighter spindle pole bodies in the *TEF1* overexpression strain relative the wild type. Tub4 protein abundance is known to increase in response to DNA replication stress (Tkach *et al.*, 2012). It is possible that the effects of eEF1A overexpression on spindle organisation, and chromosomal segregation has the potential to activate stress response pathways in an attempt to recover from this defect.

Further evidence that cells were responding to DNA replication stress exerted by elevated levels of *TEF1* came from the transcription factor analysis of the microarray data (see section 6.4.3). We found that the transcription factor Cbf1, known to activate carbohydrate processing, including trehalose storage, was present at elevated levels in our microarray data. Cbf1 is also known to be required for proper chromosome segregation (Cai and Davis, 1990). As *TEF1* overexpressing cells contain elevated levels of Cbf1 this suggests that cells are indeed responding to DNA replication stress.

## 8.2 eEF1A toxicity causes suppression of plasmid copy number resulting in cell starvation

The chromosomal abnormalities, together with cells entering quiescence appear to result in a toxic effect on cells overexpressing *TEF1*. We have found that cells with elevated levels of eEF1A have a reduced viability, and that they express high levels of plasmid loss usually associated with plasmid toxicity.

As previously described (see section 3.4) we suggest that the *TEF1* overexpression was toxic to yeast cells. In agreement with this hypothesis our studies revealed that when grown in selective, -leu media, cells containing a constitutively expressed, 2µ, *LEU2*::*TEF1* plasmid stably over-expressed, low levels of eEF1A and the *LEU2* plasmid throughout growth, from lag, to log, and finally stationary phase, as detected by western blotting and qPCR. However, in non-selective, leucine rich media, the absence of any selective pressure in favour of the *LEU2* plasmid resulted in rapid selection against the *TEF1* overexpression plasmid with levels decreasing to one fifth of those grown in selective media. These data suggest that in the absence of leucine, cells containing the *TEF1* overexpression plasmid are required to precisely balance a need for the *LEU2* gene on the plasmid with the toxicity conferred by the elevated levels of *TEF1* also encoded for on the plasmid. Furthermore accumulation of the leucine biosynthesis intermediate, isopropylmalic acid, suggests that cells are not producing sufficient 3-isopropylmalate dehydrogenase (*LEU2*) resulting in a bottle neck in the synthesis pathway.

Our data suggest that *TEF1* toxicity is strong enough to induce selective plasmid loss in cells grown in media containing leucine, and that cells grown in media without leucine appear to suppress plasmid copy number as low as possible to reduce the toxic effects of increased levels of eEF1A. We also observed the control plasmid present at significantly higher levels,

suggesting that the copy number of the *TEF1* overexpression plasmid may not be maintained at levels high enough to synthesise levels of leucine sufficient for normal cell growth (see figure 8.1). In section 8.3 we will discuss the data we have presented that suggest that cells overexpressing *TEF1* sense they are starving and, in response, activate amino acid biosynthesis.

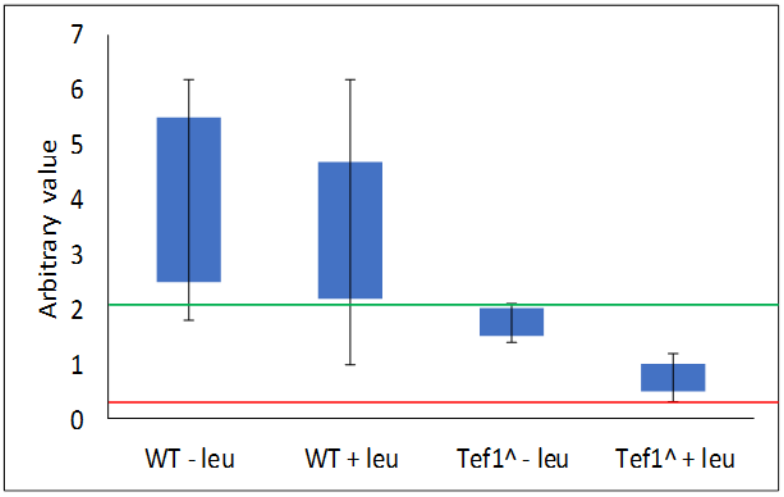


***Figure 8.1, Demonstration of plasmid copy number levels with TEF1 acting as an active suppressor of plasmid copy number.*** *This is to demonstrate the suppressive effect of TEF1 overexpression on plasmid copy number. Wild type cells containing the control plasmid are subject to random plasmid segregation, because there is no selective pressure against the plasmid, plasmid copy number varies greatly because plasmid loss is random. Because elevated levels of TEF1 are toxic to the cell there is a strong selective pressure against it. In cells that are grown in media lacking leucine they must balance the toxic effects of TEF1 with the minimal level of the plasmid required to encode LEU2 (represented by the green line). In TEF1 overexpressing cells grown in media containing leucine, the LEU2 gene on the plasmid is no longer required for leucine synthesis and so the only selective pressure on the plasmid is the negative pressure of TEF1 overexpression. The green line represents the minimum plasmid copy number that cells need to maintain in order to grow in a leucine deplete environment. The red line represents the suppressive effect the elevated levels of TEF1 has on the cell, and the high levels of plasmid loss that are associated with the toxicity. Values are arbitrary and not representative of actual plasmid copy number.*

Further evidence of amino acid deprivation is the accumulation of trehalose observed in the *TEF1* overexpression strains. Trehalose is a disaccharide storage carbohydrate that is readily broken down upon encountering favourable growth conditions allowing cells to rapidly re-commence growth. We have shown that trehalose levels in cells overexpressing *TEF1* are almost three-fold higher than in wild type, and that transcriptome levels of the trehalose synthase complex are also higher in these cells (see figure 8.2).

Interestingly, interrogation of the microarray data also revealed that both *NTH1* and *ATH1* transcripts were present at elevated levels, 13 % and 11 % compared to the wild type respectively, in *TEF1* overexpressing cells. Both Nth1 and Ath1 are known to degrade trehalose. Nth1 (neutral trehalase) degrades cytoplasmic trehalose at a pH optimum of around 7.0, whilst Ath1 (acid trehalase) is required for degradation of vacuolar trehalose with a pH optimum around 4.5 (Destruelle *et al.*, 1995; Zähringer *et al.*, 1997).

It is possible that, because we see an increase in trehalose degradation, as well as trehalose accumulation in *TEF1* overexpressing cells, trehalose synthesis is a by-product of up-regulation of Cbf1. Cbf1 is the transcription factor known to up-regulate trehalose biosynthesis that is also known to increase in abundance due to DNA replication stress (Tkach *et al.*, 2012). However, together with other metabolite and transcriptome data discussed here, we suggest that the accumulation is likely to be the result of both direct effects of eEF1A on DNA replication, and of the toxic effects of this stress resulting in low *LEU2* plasmid copy number.

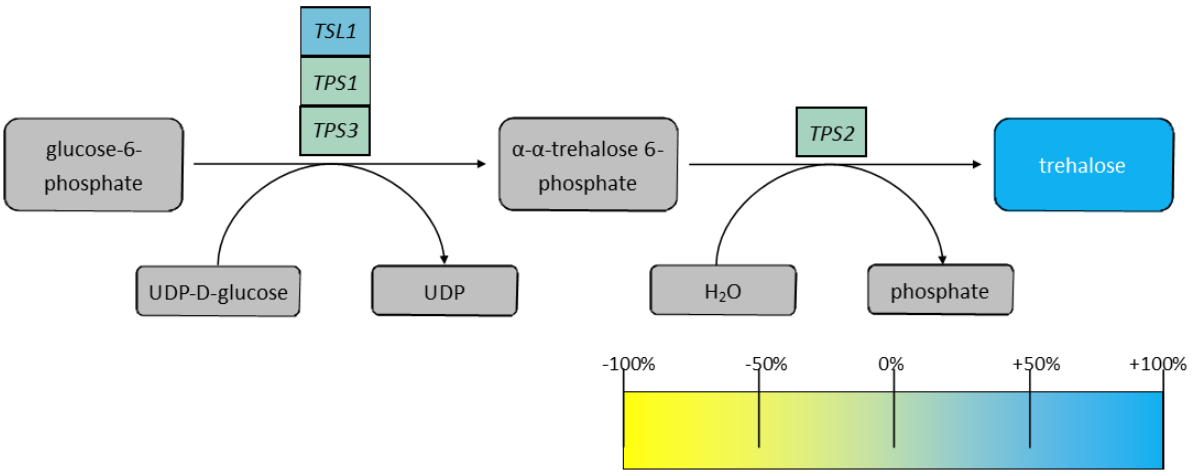


***Figure 8.2, Trehalose biosynthesis pathway.*** *This shows the biosynthesis pathway of trehalose with alterations in metabolite and transcript level as detected by analysis of the microarray and NMR spectroscopy. Boxes in grey represent metabolites of unknown concentration. *Trehalose was actually detected at 295% higher in TEF1 overexpressing cells.*

## 8.3 eEF1A overexpressing cells respond to starvation through increasing amino acid biosynthesis.

As discussed (see section 3.4) *TEF1* overexpression induces toxic effects on cells, such as, chromosomal instability and DNA replication stress, exerted by eEF1A's interactions with the dynactin complex. We have already discussed (see section 3.3.2) that toxicity resulting from the *TEF1* overexpression plasmid appears to suppress plasmid copy numbers to levels so low that the leucine protrophy also encoded for by the plasmid may not be able to supply leucine at levels sufficient to support healthy cell growth. Here we discuss the evidence that cells overexpressing *TEF1* sense this as leucine starvation and increase branched amino acid biosynthesis to compensate.

Microarray and NMR data from chapters 6 and 7, suggest that cells overexpressing *TEF1* are up-regulating an array of biosynthesis pathways to facilitate normal growth, in the presence of elevated levels of eEF1A. One pathway of particular interest was the biosynthesis of branched chain amino acids (BCAA). During the transcriptome and metabolome analysis of cells overexpressing *TEF1,* we found that all genes involved in BCAA biosynthesis were up-regulated as well as all down-stream metabolites, with the only metabolite in BCAA biosynthesis detected at lower levels being threonine. Threonine yields the isoleucine precursor 2-ketobutyrate through deamination, so lower levels correlate with increased synthesis of isoleucine (see figure 8.3).

We also saw higher levels of the regulator of BCAA biosynthesis *LEU3* and, as discussed (see section 7.3), the leucine biosynthesis intermediate isopropylmalic acid. Accumulation of isopropylmalic acid is probably due to decreased levels of *LEU2* in the *TEF1* overexpression strain. *LEU2* encodes 3-isopropylmalate dehydrogenase that is required for catalysing the

conversion of isopropylmalic acid to 2-ketoisocaproate. We hypothesise therefore, that the decrease in plasmid copy number in the *TEF1* overexpression strain results in a positive feedback loop of continuous promotion of BCAA biosynthesis and isopropylmalic acid accumulation.

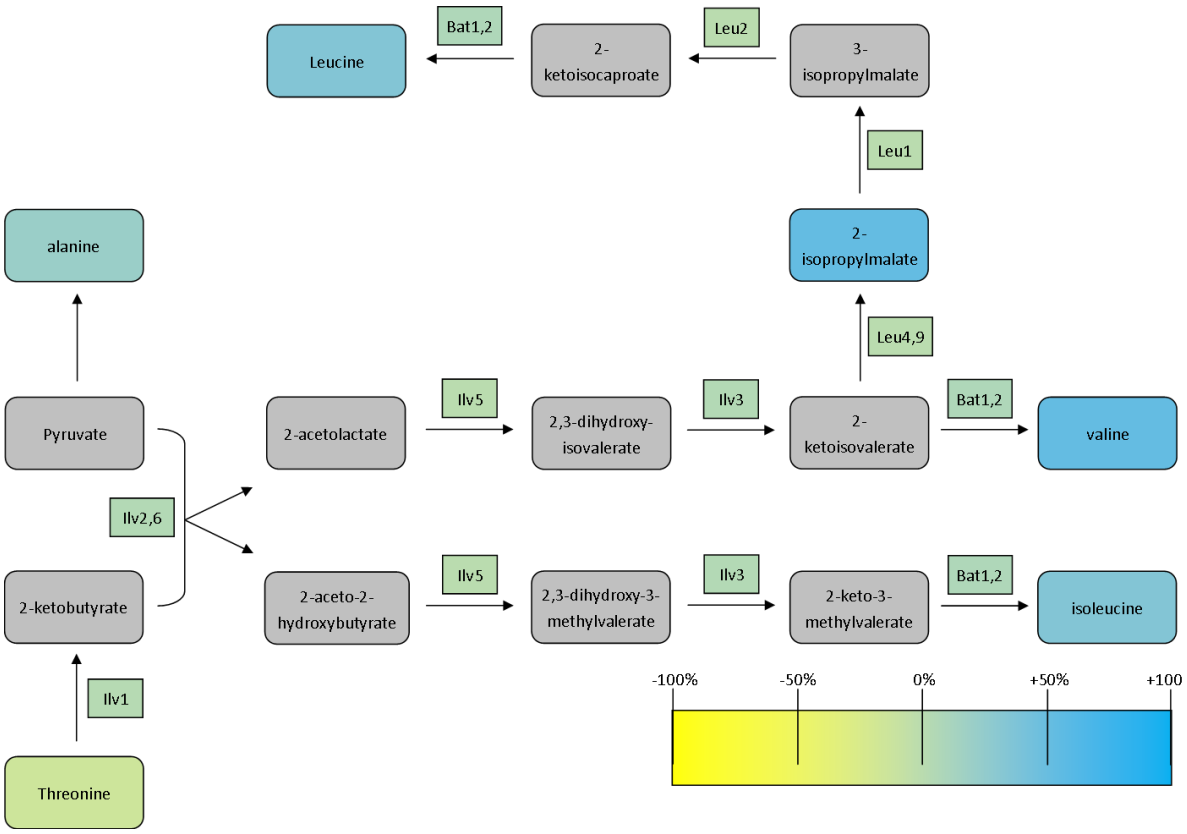


***Figure 8.3, Schematic of branched chain amino acid biosynthesis.*** *This shows the biosynthesis pathway of the branched chain amino acids with alterations in metabolite and transcript level as detected by analysis of the microarray and NMR spectroscopy. Boxes in grey represent metabolites of unknown concentration.*

## 8.4 eEF1A overexpression restores dynactin function in *Δarp1* mutants

We have discussed the possible interactions between eEF1A and components of the dynactin complex. However, a further conclusion from this study is that eEF1A overexpression was able to rescue the severe spindle defect, and the aneuploidy observed in the *Δarp1* mutant (see

figures 4.4 and 4.6). Here we will discuss the possible mechanism by which eEF1A is able to achieve this.

Within the dynactin complex Arp1 forms a short, stable octameric polymer. This is similar in structure to an actin filament and is capped at its barbed end with the actin capping protein Cap1 (Schafer *et al.*, 1994). Act1 and Arp1 share 47.1 % identity at the polypeptide level (Eckley and Schroer, 2003). Furthermore, interrogation of highly purified dynactin revealed a single β-actin monomer present in each dynactin molecule (Schafer *et al.*, 1994; Eckley *et al.*, 1999). These data suggest that Act1 and Arp1 may share enough sequence similarity that, in the presence of eEF1A, they are able to substitute for the other during some canonical or non-canonical functions.

eEF1A is known to stabilise actin filaments resulting in bundles of actin filaments (Edmonds *et al.*, 1998). We have observed that in the presence of elevated levels of eEF1A, dynactin function restored. We see that the aberrant spindles observed in the absence of Arp1 are restored to wild type spindles, and that genomic content, as assessed by FACS analysis, resulted in a loss of a population containing greater than 4n genomic content. We propose that in the absence of Arp1, short actin filaments, stabilised in the presence of elevated levels of eEF1A, are able to substitute for Arp1 in the dynactin complex allowing it to perform its function in spindle alignment.

## 8.5 Human eEF1A isoforms are unable to perform translational functions in yeast

As previously discussed, eEF1A is encoded by highly conserved genes from prokaryotes to eukaryotes. Following characterisation of eEF1A overexpression in yeast, we were interested

in the effect of eEF1A2 overexpression in human cells (HEK293 cells) to see if phenotypes observed in yeast were conserved through to humans.

Although, as discussed (see section 5.3), we saw an effect on the growth of HEK293 cells we were unable to confirm that any of the cytoskeletal aberrations caused by elevated levels of eEF1A in yeast were conserved through to humans. Interestingly however, we did see that upon overexpression of eEF1A2 in HEK293 cells, the chromosomal aberration observed in yeast, a shift in the peaks of the FACS analysis, and larger and brighter nuclei when observed by microscopy, was also present. This suggests that yeast and human isoforms do have similar interaction profiles, raising the question could human isoforms function in yeast and vice versa.

To answer this question we utilised a yeast strain that had *TEF2* deleted and where *TEF1* was placed under control of a TetO7 promoter, allowing almost complete ablation of native eEF1A expression through addition of doxycycline to the growth medium. This was transformed with a plasmid expressing either yeast *TEF1*, or human *eEF1A1* or *eEF1A2* all under control of the strong constitutive TDH3 promoter. This allowed us to observe the effect of having the plasmid as the only source of eEF1A.

Using this system revealed that, when assessed by growth, human eEF1A isoforms are unable to function correctly in yeast. It was observed that eEF1A1 was able to recover growth slightly better than eEF1A2, but neither resulted in a full recovery. This suggests that both eEF1A1 and eEF1A2 are unable to function to their full capacity in yeast, and we propose that both isoforms are actually unable to fulfil one of their many crucial roles in the cell.

Considering the polypeptide homology between yeast and human eEF1A isoforms (approximately 80 %) it is remarkable that human isoforms are unable to function in yeast. Whether it is a loss of translational function, of actin binding, or one of the other functions that eEF1A is involved in has yet to be elucidated. However, given the dramatic reduction in growth rate observed, it seems plausible that human isoforms are unable to function within translation in yeast.

## 8.6 Conclusions and future work

Given the abundance of eEF1A and its known involvement in a variety of cancers, understanding the interactions of this highly conserved translation elongation factor are essential. Overexpression of eEF1A2 can result in tumour growth, but the mechanism by which this occurs is not understood.

Using an array of techniques we have revealed that in yeast eEF1A overexpression results in spindle defects that cause chromosome abnormalities, with these abnormalities appearing to lead to DNA replication stress. It seems that the stress induced by these chromosomal abnormalities is severe enough to induce toxic effects in cells that contain only a few copies of the plasmid encoding *TEF1*. Naturally cells containing high levels of eEF1A that are toxic to the cell are selected against resulting in a population of cells containing very low plasmid copy number. The resulting decrease in *LEU2* expression, due to the lower plasmid copy number, appears to cause a bottle neck in the leucine biosynthesis pathway indicated by the increase in the leucine biosynthesis intermediate isopropylmalic acid. Isopropylmalic acid promotes *LEU3* activation of branched chain amino acid biosynthesis, resulting in a positive feedback loop of isopropylmalic acid accumulation and promotion of BCAA biosynthesis. We hypothesise that the observed effects of eEF1A toxicity, have a synthetic effect together with

the effects caused by the suppression of plasmid copy number, resulting in the observed growth rescue upon leucine supplementation to the media.

Furthermore, we have observed that *TEF1* overexpression results in an array of other metabolic alterations. We hypothesise that whilst some of these alterations are likely to be related to low levels of *LEU2*, it is probable that others are the result of the direct effects of *TEF1* overexpression on translation, the cytoskeleton and DNA replication. We suggest that the observable increase in trehalose levels is probably due to a combination of cells responding to starvation induced by low plasmid copy number and a direct effect of DNA replication stress exerted by elevated levels of eEF1A disrupting spindle organisation.

Finally, we have demonstrated that although highly conserved, human and yeast eEF1A isoforms appear to be diverse enough that human isoforms are unable to function in yeast cells. This raises the question of whether there are further residues that have yet to be classified that play an essential role in translation, or if one of the moonlighting roles of eEF1A is more essential for cell viability than previously assumed.

Below are some of the questions that need answering following this research, and how answering them would further our knowledge of eEF1A interactions and functions within the cell.

- How does *ARP1* deletion rescue the growth defect observed upon *TEF1* overexpression?

  The synthetic interaction we observed between eEF1A and Arp1 suggests that there is a strong functional link between these two proteins. However, to conclusively answer the question, regarding the nature of this interaction, it is required that an

assay that allows us to observe direct interactions between these two proteins is performed, such as a Co-Immunoprecipitation (Co-IP). If we were to perform Co-IP in wild type cells and *Δarp1* cells overexpressing *TEF1* we could assess if the dynactin complex is still intact and if it was, analysis of the bands corresponding to dynactin by mass spectrometry would allow us to identify the components.

- Are trehalose levels reduced by the addition of leucine or the deletion of *CBF1*?

  We observed that the addition of leucine to the media resulted in a rescue to the growth rate of *TEF1* overexpressing cells, and that the translation factor Cbf1, that promotes trehalose biosynthesis, was also elevated in these cells. It would be useful to determine whether trehalose levels return to wild type levels following leucine addition or *CBF1* deletion as this would tell us if trehalose accumulation is the result of cells responding to low plasmid levels, or DNA replication stress caused by elevated levels of eEF1A.

- Is the extra eEF1A in the system contributing to translation, or is it being utilised elsewhere?

  We observed that eEF1A overexpression had a dramatic effect on a wide array of cellular processes. By performing ribosomal profiling we could observe a global profile of ribosomes in the cell allowing us to identify if they are being utilised for translation. In cells overexpressing *TEF1* we would anticipate that there should be an increase in 80S ribosomes, and polysomes if the extra eEF1A in the system is contributing to translation.

- Is yeast eEF1A able to function in human cells?

  We have demonstrated that human eEF1A isoforms are unable to function in yeast suggesting a difference in the functionality of eEF1A between these two species. It

would be interesting to see if yeast eEF1A is able to replace human isoforms as this may elucidate functions of either isoform that is essential in one species but not the other.

- How does *TEF1* overexpression rescue the *Δarp1* growth defect?

  We observed that deletion of *ARP1* resulted in severe spindle aberrations and aneuploidy, with *TEF1* overexpression rescuing both these defects. We hypothesised that elevated levels of eEF1A may achieve this through stabilisation of actin into short octamers, that were able to substitute for Arp1 as the backbone of the dynactin complex, resulting in restoration of dynactin function. Further analysis of this is required to ascertain if actin does indeed replace Arp1 in dynactin, and if it does, does this have any other effects on the dynactin complex.

- What is the chromosomal abnormality that is causing the nuclei to appear larger when observed down the microscope, and causes a shift of the peaks in the FACS analysis?

  We observed a conserved aneuploidy phenotype from yeast to human cells. However, although we have speculated that this may be due to either a global up-regulation of a large proportion of genes, or an increase in dye uptake due to relaxed chromosomal packaging, he were unable to definitively answer this question. How we would be able to assess this is uncertain as most assays to quantify genomic content rely on uptake of a dye. However, as this is likely to be the driving force behind the toxicity associated with elevated levels of *TEF1,* it is crucial that we answer this question.

# References

References

Anand, N., Murthy, S., Amann, G., Wernick, M., Porter, L. a, Cukier, I.H., *et al.* (2002) Protein elongation factor EEF1A2 is a putative oncogene in ovarian cancer. *Nat Genet* **31**: 301–5

Baichwal, V.R., Cunningham, T.S., Gatzek, P.R., and Kohlhaw, G.B. (1983) Leucine biosynthesis in yeast : Identification of two genes (LEU4, LEU5) that affect α-Isopropylmalate synthase activity and evidence that LEU1 and LEU2 gene expression is controlled by α-Isopropylmalate and the product of a regulatory gene. *Curr Genet* **7**: 369–77

Balciunas, D., and Ronne, H. (1995) Three subunits of the RNA polymerase II mediator complex are involved in glucose repression. *Nucleic Acids Res* **23**: 4421–5

Beauchamp, E.M., and Platanias, L.C. (2013) The evolution of the TOR pathway and its role in cancer. *Oncogene* **32**: 3923–32

Blaiseau, P.L., Isnard, A.D., Surdin-Kerjan, Y., and Thomas, D. (1997) Met31p and Met32p, two related zinc finger proteins, are involved in transcriptional regulation of yeast sulfur amino acid metabolism. *Mol Cell Biol* **17**: 3640–8

Bohnsack, M.T., Regener, K., Schwappach, B., Saffrich, R., Paraskeva, E., Hartmann, E., and Görlich, D. (2002) Exp5 exports eEF1A via tRNA from nuclei and synergizes with other transport pathways to confine translation to the cytoplasm. *EMBO J* **21**: 6205–15

Bolstad, B.M., Irizarry, R.., Astrand, M., and Speed, T.P. (2003) A comparison of normalization methods for high density oligonucleotide array data based on variance and bias. *Bioinformatics* **19**: 185–93

Cai, M., and Davis, R.W. (1990) Yeast centromere binding protein CBF1, of the helix-loop-helix protein family, is required for chromosome stability and methionine prototrophy. *Cell* **61**: 437–46

Calado, A., Treichel, N., Müller, E.-C., Otto, A., and Kutay, U. (2002) Exportin-5-mediated nuclear export of eukaryotic elongation factor 1A and tRNA. *EMBO J* **21**: 6216–24

Cao, H., Zhu, Q., Huang, J., Li, B., Zhang, S., Yao, W., and Zhang, Y. (2009) Regulation and functional role of eEF1A2 in pancreatic carcinoma. *Biochem Biophys Res Commun* **380**: 11–6

References

Chambers, D.M., Peters, J., and Abbott, C.M. (1998) The lethal mutation of the mouse wasted (wst) is a deletion that abolishes expression of a tissue-specific isoform of translation elongation factor 1alpha, encoded by the Eef1a2 gene. *Proc Natl Acad Sci U S A* **95**: 4463–8

Chuang, S., and Chen, L. (2005) Proteasome-mediated degradation of cotranslationally damaged proteins involves translation elongation factor 1A. *… Cell Biol* **25**: 403–13

Costanzo, M., Nishikawa, J.L., Tang, X., Millman, J.S., Schub, O., Breitkreuz, K., *et al.* (2004) CDK activity antagonizes Whi5, an inhibitor of G1/S transcription in yeast. *Cell* **117**: 899–913

Courjal, F., Cuny, M., Rodriguez, C., Louason, G., Speiser, P., Katsaros, D., *et al.* (1996) DNA amplifications at 20q13 and MDM2 define distinct subsets of evolved breast and ovarian tumours. *Br J Cancer* **74**: 1984–9

Destruelle, M., Holzer, H., and Klionsky, D.J. (1995) Isolation and characterization of a novel yeast gene, ATH1, that is required for vacuolar acid trehalase activity. *Yeast* **11**: 1015–25

Drugeon, G., Jean-Jean, O., Frolova, L., Goff, X. Le, Philippe, M., Kisselev, L., and Haenni, a L. (1997) Eukaryotic release factor 1 (eRF1) abolishes readthrough and competes with suppressor tRNAs at all three termination codons in messenger RNA. *Nucleic Acids Res* **25**: 2254–8

Dujardin, D.L., Barnhart, L.E., Stehman, S. a, Gomes, E.R., Gundersen, G.G., and Vallee, R.B. (2003) A role for cytoplasmic dynein and LIS1 in directed cell movement. *J Cell Biol* **163**: 1205–11

Duttaroy, a, Bourbeau, D., Wang, X.L., and Wang, E. (1998) Apoptosis rate can be accelerated or decelerated by overexpression or reduction of the level of elongation factor-1 alpha. *Exp Cell Res* **238**: 168–76

Echeverri, C.J., Paschal, B.M., Vaughan, K.T., and Vallee, R.B. (1996) Molecular characterization of the 50-kD subunit of dynactin reveals function for the complex in chromosome alignment and spindle organization during mitosis. *J Cell Biol* **132**: 617–33

References

Eckley, D.M., Gill, S.R., Melkonian, K. a, Bingham, J.B., Goodson, H. V, Heuser, J.E., and Schroer, T.A. (1999) Analysis of dynactin subcomplexes reveals a novel actin-related protein associated with the arp1 minifilament pointed end. *J Cell Biol* **147**: 307–20

Eckley, D.M., and Schroer, T.A. (2003) Interactions between the evolutionarily conserved , actin-related protein , Arp11 , Actin , and Arp1. **14**: 2645–54.

Edmonds, B.T., Belle, A., Wyckoff, J., Condeelis, J., and Leyh, T.S. (1998) The effect of F-actin on the binding and hydrolysis of guanine nucleotide by Dictyostelium elongation factor 1A. *J Biol Chem* **273**: 10288–95

Edmonds, B.T., Wyckoff, J., Yeung, Y.G., Wang, Y., Stanley, E.R., Jones, J., *et al.* (1996) Elongation factor-1 alpha is an overexpressed actin binding protein in metastatic rat mammary adenocarcinoma. *J Cell Sci* **109**: 2705–14

Franceschini, A., Szklarczyk, D., Frankild, S., Kuhn, M., Simonovic, M., Roth, A., *et al.* (2013) STRING v9.1: protein-protein interaction networks, with increased coverage and integration. *Nucleic Acids Res* **41**: 808–15

Friden, P., and Schimmel, P. (1988) LEU3 of Saccharomyces cerevisiae activates multiple genes for branched-chain amino acid biosynthesis by binding to a common decanucleotide core sequence. *Mol Cell Biol* **8**: 2690–7

Garces, J. a, Clark, I.B., Meyer, D.I., and Vallee, R.B. (1999) Interaction of the p62 subunit of dynactin with Arp1 and the cortical actin cytoskeleton. *Curr Biol* **9**: 1497–500

Ghislain, M., Talla, E., and François, J.M. (2002) Identification and functional analysis of the Saccharomyces cerevisiae nicotinamidase gene, PNC1. *Yeast* **19**: 215–24

Gill, S.R., Schroer, T.A., Szilak, I., Steuer, E.R., Sheetz, M.P., and Cleveland, D.W. (1991) Dynactin, a conserved, ubiquitously expressed component of an activator of vesicle motility mediated by cytoplasmic dynein. *J Cell Biol* **115**: 1639–50

Ginestier, C., Cervera, N., Finetti, P., Esteyries, S., Esterni, B., Adélaïde, J., *et al.* (2006) Prognosis and gene expression profiling of 20q13-amplified breast cancers. *Clin Cancer Res* **12**: 4533–44

Gonçalves, J., and Malta-Vacas, J. (2005) Modulation of translation factor's gene expression by histone deacetylase inhibitors in breast cancer cells. *Clin Chem Lab Med **43:** 151-156*

Gönczy, P., Pichler, S., Kirkham, M., and Hyman, a a (1999) Cytoplasmic dynein is required for distinct aspects of MTOC positioning, including centrosome separation, in the one cell stage Caenorhabditis elegans embryo. *J Cell Biol* **147**: 135–50

Gonen, H., Smith, C.E., Siegel, N.R., Kahana, C., Merrick, W.C., Chakraburtty, K., *et al.* (1994) Protein synthesis elongation factor EF-1 alpha is essential for ubiquitin-dependent degradation of certain N alpha-acetylated proteins and may be substituted for by the bacterial elongation factor EF-Tu. *Proc Natl Acad Sci U S A* **91**: 7648–52

Graham, F.L., Smiley, J., Russell, W.C., and Nairn, R. (1977) Characteristics of a human cell line transformed by DNA from human adenovirus type 5. *J Gen Virol* **36**: 59–74

Grassi, G., Scaggiante, B., Farra, R., Dapas, B., Agostini, F., Baiz, D., *et al.* (2007) The expression levels of the translational factors eEF1A 1/2 correlate with cell growth but not apoptosis in hepatocellular carcinoma cell lines with different differentiation grade. *Biochimie* **89**: 1544–52

Green, R., and Noller, H.F. (1997) Ribosomes and translation. *Annu Rev Biochem* **66**: 679–716

Gross, S.R., and Kinzy, T.G. (2005) Translation elongation factor 1A is essential for regulation of the actin cytoskeleton and cell morphology. *Nat Struct Mol Biol* **12**: 772–8

Gross, S.R., and Kinzy, T.G. (2007) Improper organization of the actin cytoskeleton affects protein synthesis at initiation. *Mol Cell Biol* **27**: 1974–89

Grosshans, H., Hurt, E., and Simos, G. (2000) An aminoacylation-dependent nuclear tRNA export pathway in yeast. *Genes Dev* **14**: 830–40

References

Firczuk, H., Kannambath, S., Pahle, J., Claydon, A., Beynon, R., Duncan, J., *et al.* (2013) An in vivo control map for the eukaryotic mRNA translation machinery. *Mol Syst Biol* 635

Haar, T. von der (2007) Optimized protein extraction for quantitative proteomics of yeasts. *PLoS One* **2**: e1078

Habermann, a, Schroer, T.A., Griffiths, G., and Burkhardt, J.K. (2001) Immunolocalization of cytoplasmic dynein and dynactin subunits in cultured macrophages: enrichment on early endocytic organelles. *J Cell Sci* **114**: 229–40.

Hashemzadeh-Bonehi, L., Curtis, P.S., Morley, S.J., Thorpe, J.R., and Pain, V.M. (2003) Overproduction of a conserved domain of fission yeast and mammalian translation initiation factor eIF4G causes aberrant cell morphology and results in disruption of the localization of F-actin and the organization of microtubules. *Genes Cells* **8**: 163–78

Hodgson, J.G., Chin, K., Collins, C., and Gray, J.W. (2003) Genome amplification of chromosome 20 in breast cancer. *Breast Cancer Res Treat* **78**: 337–45

Holleran, E. a, Ligon, L. a, Tokito, M., Stankewich, M.C., Morrow, J.S., and Holzbaur, E.L. (2001) beta III spectrin binds to the Arp1 subunit of dynactin. *J Biol Chem* **276**: 36598–605

Holleran, E. a, Tokito, M.K., Karki, S., and Holzbaur, E.L. (1996) Centractin (ARP1) associates with spectrin revealing a potential mechanism to link dynactin to intracellular organelles. *J Cell Biol* **135**: 1815–29

Hoogenraad, C.C., Akhmanova, a, Howell, S. a, Dortland, B.R., Zeeuw, C.I. De, Willemsen, R., *et al.* (2001) Mammalian Golgi-associated Bicaudal-D2 functions in the dynein-dynactin pathway by interacting with these complexes. *EMBO J* **20**: 4041–54

Hotokezaka, Y., Tobben, U., Hotokezaka, H., Leyen, K. Van, Beatrix, B., Smith, D.H., *et al.* (2002) Interaction of the eukaryotic elongation factor 1A with newly synthesized polypeptides. *J Biol Chem* **277**: 18545–51

Howell, B.J., McEwen, B.F., Canman, J.C., Hoffman, D.B., Farrar, E.M., Rieder, C.L., and Salmon, E.D. (2001) Cytoplasmic dynein/dynactin drives kinetochore protein transport to the spindle poles and has a role in mitotic spindle checkpoint inactivation. *J Cell Biol* **155**: 1159–72

Huh, W.-K., Falvo, J. V, Gerke, L.C., Carroll, A.S., Howson, R.W., Weissman, J.S., and O'Shea, E.K. (2003) Global analysis of protein localization in budding yeast. *Nature* **425**: 686–91

Hwang, T., and Shaka, A. (1995) Water suppression that works. Excitation sculpting using arbitrary wave-forms and pulsed-field gradients. *J Magn Reson Ser A* **112:** 275-9

Jaskunas, S.R., Lindahl, L., Nomura, M., and Burgess, R.R. (1975) Identification of two copies of the gene for the elongation factor EF–Tu in E. Coli. *Nature* **257**: 458–462

Jin, T., Yue, L., and Li, J. (2001) In vivo interaction between dynamitin and MacMARCKS detected by the fluorescent resonance energy transfer method. *J Biol Chem* **276**: 12879–84

Johnsson, a, Zeelenberg, I., Min, Y., Hilinski, J., Berry, C., Howell, S.B., and Los, G. (2000) Identification of genes differentially expressed in association with acquired cisplatin resistance. *Br J Cancer* **83**: 1047–54

Kabsch, W., Mannherz, H., Suck, D., Pai, E., and Holmes, K. (1990) Atomic structure of the actin: DNase I complex. *Nature* **347:** 37-44

Kahns, S., Lund, a, Kristensen, P., Knudsen, C.R., Clark, B.F., Cavallius, J., and Merrick, W.C. (1998) The elongation factor 1 A-2 isoform from rabbit: cloning of the cDNA and characterization of the protein. *Nucleic Acids Res* **26**: 1884–90

Kallioniemi, a, Kallioniemi, O.P., Piper, J., Tanner, M.M., Stokke, T., Chen, L., *et al.* (1994) Detection and mapping of amplified DNA sequences in breast cancer by comparative genomic hybridization. *Proc Natl Acad Sci U S A* **91**: 2156–60

Kanai, T., Takeshita, S., Atomi, H., Umemura, K., Ueda, M., and Tanaka, A. (1998) A regulatory factor, Fil1p, involved in derepression of the isocitrate lyase gene in Saccharomyces cerevisiae--a possible mitochondrial protein necessary for protein synthesis in mitochondria. *Eur J Biochem* **256**: 212–20

Karki, S., Lamonte, B., and Holzbaur, E.L.F. (1998) Characterization of the p22 subunit of dynactin reveals the localization of cytoplasmic dynein and dynactin tot the midbody of dividing cells. *J Cell Biol*. **142**: 1023–1034.

Keller, F., Schellenberg, M., and Wiemken, A. (1982) Localization of trehalase in vacuoles and of trehalose in the cytosol of yeast (Saccharomyces cerevisiae). *Arch Microbiol* **131**: 298–301

Khacho, M., Mekhail, K., Pilon-larose, K., Pause, A., and Lee, S. (2008) eEF1A Is a novel component of the mammalian nuclear protein export machinery. *Mol Cell Biol* **19**: 5296–5308.

Khalyfa, a, Bourbeau, D., Chen, E., Petroulakis, E., Pan, J., Xu, S., and Wang, E. (2001) Characterization of elongation factor-1A (eEF1A-1) and eEF1A-2/S1 protein expression in normal and wasted mice. *J Biol Chem* **276**: 22915–22

Kim, K.S., Rosenkrantz, M.S., and Guarente, L. (1986) Saccharomyces cerevisiae contains two functional citrate synthase genes. *Mol Cell Biol* **6**: 1936–42

King, S.J., Brown, C.L., Maier, K.C., Quintyne, N.J., and Schroer, T.A. (2003) Analysis of the Dynein – Dynactin Interaction In Vitro and In Vivo. *Mol Cell Biol* **14**: 5089–5097.

Kobayashi, M., Ishida, H., Shindo, T., Niwa, S.-I., Kino, M., Kawamura, K., *et al.* (2008) Molecular analysis of multifocal prostate cancer by comparative genomic hybridization. *Prostate* **68**: 1715–24

Komar, A. a, Gross, S.R., Barth-Baus, D., Strachan, R., Hensold, J.O., Goss Kinzy, T., and Merrick, W.C. (2005) Novel characteristics of the biological properties of the yeast Saccharomyces cerevisiae eukaryotic initiation factor 2A. *J Biol Chem* **280**: 15601–11

Kosugi, S., Hasebe, M., Tomita, M., and Yanagawa, H. (2009) Systematic identification of cell cycle-dependent yeast nucleocytoplasmic shuttling proteins by prediction of composite motifs. *Proc Natl Acad Sci U S A* **106**: 10171–6

Kudryashov, D.S., Grintsevich, E.E., Rubenstein, P. a, and Reisler, E. (2010) A nucleotide state-sensing region on actin. *J Biol Chem* **285**: 25591–601

Kulkarni, G., Turbin, D. a, Amiri, A., Jeganathan, S., Andrade-Navarro, M. a, Wu, T.D., *et al.* (2007) Expression of protein elongation factor eEF1A2 predicts favorable outcome in breast cancer. *Breast Cancer Res Treat* **102**: 31–41

Lam, D.C.L., Girard, L., Suen, W.-S., Chung, L., Tin, V.P.C., Lam, W., *et al.* (2006) Establishment and expression profiling of new lung cancer cell lines from Chinese smokers and lifetime never-smokers. *J Thorac Oncol* **1**: 932–42

Lee, S., Ann, D.K., and Wang, E. (1994) Cloning of human brain and mouse brain cDNAs coding for S1, the second member of the mammalian Elongation factor-1 alpha gene family: Analysis of a possible evolutionary pathway. *Biochem Biophys Res Commun* **203**: 1371–1377.

Lee, S., Francoeur, a M., Liu, S., and Wang, E. (1992) Tissue-specific expression in mammalian brain, heart, and muscle of S1, a member of the elongation factor-1 alpha gene family. *J Biol Chem* **267**: 24064–8

Lewin, A.S., Hines, V., and Small, G.M. (1990) Citrate synthase encoded by the CIT2 gene of Saccharomyces cerevisiae is peroxisomal. *Mol Cell Biol* **10**: 1399–405

Li, D., Wei, T., Abbott, C.M., and Harrich, D. (2013) The unexpected roles of eukaryotic translation elongation factors in RNA virus replication and pathogenesis. *Microbiol Mol Biol Rev* **77**: 253–66

Li, R., Wang, H., Bekele, B.N., Yin, Z., Caraway, N.P., Katz, R.L., *et al.* (2006) Identification of putative oncogenes in lung adenocarcinoma by a comprehensive functional genomic approach. *Oncogene* **25**: 2628–35

Liao, S.M., Zhang, J., Jeffery, D.A., Koleske, A.J., Thompson, C.M., Chao, D.M., *et al.* (1995) A kinase-cyclin pair in the RNA polymerase II holoenzyme. *Nature* **374**: 193–6

Ligt, J. de, Willemsen, M.H., Bon, B.W.M. van, Kleefstra, T., Yntema, H.G., Kroes, T., *et al.* (2012) Diagnostic exome sequencing in persons with severe intellectual disability. *N Engl J Med* **367**: 1921–9

Liu, G., Tang, J., Edmonds, B.T., Murray, J., Levin, S., and Condeelis, J. (1996) F-actin sequesters elongation factor 1alpha from interaction with aminoacyl-tRNA in a pH-dependent reaction. *J Cell Biol* **135**: 953–63

Lund, E., Güttinger, S., Calado, A., Dahlberg, J.E., and Kutay, U. (2004) Nuclear export of microRNA precursors. *Science* **303**: 95–8

Lutsep, H.L., Rodriguez, M., and Moses, M.D. (1989) Ultrastructural, morphometric, and immunocytochemical study of anterior horn cells in mice with “wasted” mutation. *J Neuropathol Exp Neurol* **48**: 519–533

Mansilla, F., Friis, I., Jadidi, M., and Nielsen, K. (2002) Mapping the human translation elongation factor eEF1H complex using the yeast two-hybrid system. *Biochem J* **676**: 669–676

Maruyama, J., Nakajima, H., and Kitamoto, K. (2002) Observation of EGFP-visualized nuclei and distribution of vacuoles in Aspergillus oryzae arpA null mutant. *FEMS Microbiol Lett* **206**: 57–61

Mateyak, M.K., and Kinzy, T.G. (2010) eEF1A: thinking outside the ribosome. *J Biol Chem* **285**: 21209–13

Mcgrail, M., Gepner, J., Silvanovich, A., Ludmann, S., Serr, M., and Hays, T.S. (1995) Regulation of cytoplasmic dynein function in vivo by the. **131**: 411–425.

McMillan, J., and Tatchell, K. (1994) The JNM1 gene in the yeast Saccharomyces cerevisiae is required for nuclear migration and spindle orientation during the mitotic cell cycle. *J Cell Biol* **125**: 143–158

Melki, R., Vainberg, I.E., Chow, R.L., and Cowan, N.J. (1993) Chaperonin-mediated folding of vertebrate actin-related protein and gamma-tubulin. *J Cell Biol* **122**: 1301–10

Meriin, A.B., Zaarur, N., and Sherman, M.Y. (2012) Association of translation factor eEF1A with defective ribosomal products generates a signal for aggresome formation. *J Cell Sci* **125**: 2665–74

Merrick, W. (1992) Mechanism and regulation of eukaryotic protein synthesis. *Microbiol Rev* 291–315

Mita, K., Morimyo, M., Ito, K., Sugaya, K., Ebihara, K., Hongo, E., *et al.* (1997) Comprehensive cloning of Schizosaccharomyces pombe genes encoding translation elongation factors. *Gene* **187**: 259–266

Mohler, J.L., Morris, T.L., Ford, O.H., Alvey, R.F., Sakamoto, C., and Gregory, C.W. (2002) Identification of differentially expressed genes associated with androgen-independent growth of prostate cancer. *Prostate* **51**: 247–55

Moore, P., and Steitz, T. (2003) After the ribosome structures: How does peptidyl transferase work? *RNA* 155–159

Moriya, H., Shimizu-Yoshida, Y., and Kitano, H. (2006) In vivo robustness analysis of cell division cycle genes in Saccharomyces cerevisiae. *PLoS Genet* **2**: e111

Moseley, J.B., and Goode, B.L. (2006) The yeast actin cytoskeleton: from cellular function to biochemical mechanism. *Microbiol Mol Biol Rev* **70**: 605–45

Munshi, R., Kandl, K. a, Carr-Schmid, a, Whitacre, J.L., Adams, a E.M., and Kinzy, T.G. (2001) Overexpression of translation elongation factor 1A affects the organization and function of the actin cytoskeleton in yeast. *Genetics* **157**: 1425–36

Murthi, A., Shaheen, H.H., Huang, H., Preston, M.A., Lai, T., Phizicky, E.M., and Hopper, A.K. (2010) Regulation of tRNA bidirectional nuclear-cytoplasmic trafficking in saccharomyces cerevisiae. *Mol Biol Cell* **21**: 639–649.

Naithani, S., Saracco, S.A., Butler, C.A., and Fox, T.D. (2003) Interactions among COX1, COX2, and COX3 mRNA-specific translational activator proteins on the inner surface of the mitochondrial inner membrane of Saccharomyces cerevisiae. *Mol Biol Cell* **14**: 324–33

Nakajima, J., Okamoto, N., Tohyama, J., Kato, M., Arai, H., Funahashi, O., *et al.* (2014) De novo EEF1A2 mutations in patients with characteristic facial features, intellectual disability, autistic behaviors and epilepsy. *Clin Genet* 1–6

Newbery, H.J., Loh, D.H., O'Donoghue, J.E., Tomlinson, V. a L., Chau, Y.-Y., Boyd, J. a, *et al.* (2007) Translation elongation factor eEF1A2 is essential for post-weaning survival in mice. *J Biol Chem* **282**: 28951–9

Owen, C.H., Derosier, D.J., and Condeelis, J. (1992) Actin crosslinking protein EF-1 a of Dictyostelium discoideum has a unique bonding rule that allows square-packed bundles. *J Struct Biol* **109**: 248–254

Ozcan, S., Dover, J., and Johnston, M. (1998) Glucose sensing and signaling by two glucose receptors in the yeast Saccharomyces cerevisiae. *EMBO J* **17**: 2566–73

Ozcan, S., Dover, J., Rosenwald, a G., Wölfl, S., and Johnston, M. (1996) Two glucose transporters in Saccharomyces cerevisiae are glucose sensors that generate a signal for induction of gene expression. *Proc Natl Acad Sci U S A* **93**: 12428–32

Paalman, J.W.G., Verwaal, R., Slofstra, S.H., Verkleij, A.J., Boonstra, J., and Verrips, C.T. (2003) Trehalose and glycogen accumulation is related to the duration of the G1 phase of Saccharomyces cerevisiae. *FEMS Yeast Res* **3**: 261–8

Palecek, J., Hasek, J., and Ruis, H. (2001) Rpg1p/Tif32p, a subunit of translation initiation factor 3, interacts with actin-associated protein Sla2p. *Biochem Biophys Res Commun* **282**: 1244–50

Paschal, B.M., Holzbaur, E.L., Pfister, K.K., Clark, S., Meyer, D.I., and Vallee, R.B. (1993) Characterization of a 50-kDa polypeptide in cytoplasmic dynein preparations reveals a complex with p150GLUED and a novel actin. *J Biol Chem* **268**: 15318–23

Pincheira, R., Chen, Q., Huang, Z., and Zhang, J.T. (2001) Two subcellular localizations of eIF3 p170 and its interaction with membrane-bound microfilaments: implications for alternative functions of p170. *Eur J Cell Biol* **80**: 410–8

Pinke, D.E., Kalloger, S.E., Francetic, T., Huntsman, D.G., and Lee, J.M. (2008) The prognostic significance of elongation factor eEF1A2 in ovarian cancer. *Gynecol Oncol* **108**: 561–8

Pinto, I., Ware, D.E., and Hampsey, M. (1992) The yeast SUA7 gene encodes a homolog of human transcription factor TFIIB and is required for normal start site selection in vivo. *Cell* **68**: 977–88

Pinto, I., Wu, W.H., Na, J.G., and Hampsey, M. (1994) Characterization of sua7 mutations defines a domain of TFIIB involved in transcription start site selection in yeast. *J Biol Chem* **269**: 30569–73

Pollard, T.D. (1986) Rate constants for the reactions of ATP- and ADP-actin with the ends of actin filaments. *J Cell Biol* **103**: 2747–54

Pollard, T.D. (2000) Molecular mechanisms controlling actin filament dynamics in nonmuscle cells. *Annu Rev Biophys Biomol Struct* **29:** 545-76

Quintyne, N.J., Gill, S.R., Eckley, D.M., Crego, C.L., Compton, D. a, and Schroer, T.A. (1999) Dynactin is required for microtubule anchoring at centrosomes. *J Cell Biol* **147**: 321–34

Ramaekers, F.C.S., Benedetti, E.L., Dunia, I., Vorstenbosch, P., and Bloemendal, H. (1983) Polyribosomes associated with microfilaments in cultured lens cells. *Biochim Biophys Acta - Gene Struct Expr* **740**: 441–448

Riehemann, K., and Sorg, C. (1993) Sequence homologies between four cytoskeleton-associated proteins. *Trends Biochem Sci* **18**: 82–83

Ruest, L.-B., Marcotte, R., and Wang, E. (2002) Peptide elongation factor eEF1A-2/S1 expression in cultured differentiated myotubes and its protective effect against caspase-3-mediated apoptosis. *J Biol Chem* **277**: 5418–25

Salina, D., Bodoor, K., Eckley, D.M., Schroer, T. a, Rattner, J.B., and Burke, B. (2002) Cytoplasmic dynein as a facilitator of nuclear envelope breakdown. *Cell* **108**: 97–107

Sasikumar, A., Perez, W., and Kinzy, T.G. (2012) The many roles of the eukaryotic elongation factor 1 complex. *Wiley Interdiscip Rev RNA* **3**: 543–555

Schafer, D. a, Gill, S.R., Cooper, J. a, Heuser, J.E., and Schroer, T. a (1994) Ultrastructural analysis of the dynactin complex: an actin-related protein is a component of a filament that resembles F-actin. *J Cell Biol* **126**: 403–12

Scheper, G.C., Knaap, M.S. van der, and Proud, C.G. (2007) Translation matters: protein synthesis defects in inherited disease. *Nat Rev Genet* **8**: 711–23

Schirmaier, F., and Philippsen, P. (1984) Identification of two genes coding for the translation elongation factor EF-1 alpha of S. cerevisiae. *EMBO J* **3**: 3311–5

Scrideli, C. a, Carlotti, C.G., Okamoto, O.K., Andrade, V.S., Cortez, M. a a, Motta, F.J.N., *et al.* (2008) Gene expression profile analysis of primary glioblastomas and non-neoplastic brain tissue: identification of potential target genes by oligonucleotide microarray and real-time quantitative PCR. *J Neurooncol* **88**: 281–91

Selga, E., Oleaga, C., Ramírez, S., Almagro, M.C. de, Noé, V., and Ciudad, C.J. (2009) Networking of differentially expressed genes in human cancer cells resistant to methotrexate. *Genome Med* **1**: 83

Shestakova, E., Motuz, L., Minin, A., Gelfand, V., and Gavrilova, L. (1991) Some of eukaryotic elongation factor 2 is colocalized with actin microfilament bundles in mouse embryo fibroblasts. *Cell Biol Int Rep* **15**: 75–84

Shortle, D., Haber, J., and Botstein, D. (1982) Lethal disruption of the yeast actin gene by integrative DNA transformation. *Science (80- )* **217**: 371–373

Shultz, L.D., Sweet, H.O., Davisson, M.T., and Coman, D.R. (1982) “Wasted”, a new mutant of the mouse with abnormalities characteristic of ataxia telangiectasia. *Nature* **297**: 402–404

Siddiq, A., Couch, F.J., Chen, G.K., Lindström, S., Eccles, D., Millikan, R.C., *et al.* (2012) A meta-analysis of genome-wide association studies of breast cancer identifies two novel susceptibility loci at 6q14 and 20q11. *Hum Mol Genet* **21**: 5373–84

Siegel, R., Naishadham, D., and Jemal, A. (2013) Cancer Statistics , 2013. *CA Cancer J Clin* **63**: 11–30.

Singer, M. a, and Lindquist, S. (1998) Thermotolerance in Saccharomyces cerevisiae: the Yin and Yang of trehalose. *Trends Biotechnol* **16**: 460–8

Skop, a R., and White, J.G. (1998) The dynactin complex is required for cleavage plane specification in early Caenorhabditis elegans embryos. *Curr Biol* **8**: 1110–6

Soares, D.C., Barlow, P.N., Newbery, H.J., Porteous, D.J., and Abbott, C.M. (2009) Structural models of human eEF1A1 and eEF1A2 reveal two distinct surface clusters of sequence variation and potential differences in phosphorylation. *PLoS One* **4**: e6315

Spellman, P.T., Sherlock, G., Zhang, M.Q., Iyer, V.R., Anders, K., Eisen, M.B., *et al.* (1998) Comprehensive identification of cell cycle-regulated genes of the yeast Saccharomyces cerevisiae by microarray hybridization. *Mol Biol Cell* **9**: 3273–97

Stapulionis, R., Kolli, S., and Deutscher, M.P. (1997) Efficient mammalian protein synthesis requires an intact F-actin system. *J Biol Chem* **272**: 24980–6

Starr, D. a, Williams, B.C., Hays, T.S., and Goldberg, M.L. (1998) ZW10 helps recruit dynactin and dynein to the kinetochore. *J Cell Biol* **142**: 763–74

Suda, M., Fukui, M., Sogabe, Y., Sato, K., Morimatsu, a, Arai, R., *et al.* (1999) Overproduction of elongation factor 1alpha, an essential translational component, causes aberrant cell morphology by affecting the control of growth polarity in fission yeast. *Genes Cells* **4**: 517–27

Sun, Y., Du, C., Wang, B., Zhang, Y., Liu, X., and Ren, G. (2014) Up-regulation of eEF1A2 promotes proliferation and inhibits apoptosis in prostate cancer. *Biochem Biophys Res Commun* **450:** 1-6

Sundstrom, P., Smith, D., Sypherd, P.S., Sundstrom, P., Smith, D., and Sypherd, P.S. (1990) Genes for elongation factor 1 alpha from the sequence analysis and expression of the two genes for elongation factor lot from the dimorphic yeast Candida albicans. *J Bacteriol* **172**: 2036-45

Sze, J.Y., Woontner, M., Jaehning, J.A., and Kohlhaw, G.B. (1992) In vitro transcriptional activation by a metabolic intermediate: activation by Leu3 depends on alpha-isopropylmalate. *Science* **258**: 1143–5

Tai, A.W., Chuang, J., Bode, C., Wolfrum, U., Sung, C., and Gutenberg-universita, J. (1999) Rhodopsin ' s carboxy-terminal cytoplasmic tail acts as a membrane receptor for cytoplasmic dynein by binding to the dynein light chain Tctex-1. **97**: 877–87.

Talapatra, S., Wagner, J.D.O., and Thompson, C.B. (2002) Elongation factor-1 alpha is a selective regulator of growth factor withdrawal and ER stress-induced apoptosis. *Cell Death Differ* **9**: 856–61

Teixeira, M.C., Monteiro, P.T., Guerreiro, J.F., Gonçalves, J.P., Mira, N.P., Santos, S.C. Dos, *et al.* (2014) The YEASTRACT database: an upgraded information system for the analysis of gene and genomic transcription regulation in Saccharomyces cerevisiae. *Nucleic Acids Res* **42**: D161–6

Teyssier, E., Hirokawa, G., Tretiakova, A., Jameson, B., Kaji, A., and Kaji, H. (2003) Temperature-sensitive mutation in yeast mitochondrial ribosome recycling factor (RRF). *Nucleic Acids Res* **31**: 4218–26

Thornton, S., Anand, N., Purcell, D., and Lee, J.M. (2003) Not just for housekeeping: protein initiation and elongation factors in cell growth and tumorigenesis. *J Mol Med (Berl)* **81**: 536–48

Tkach, J.M., Yimit, A., Lee, A.Y., Riffle, M., Costanzo, M., Jaschob, D., *et al.* (2012) Dissecting DNA damage response pathways by analysing protein localization and abundance changes during DNA replication stress. *Nat Cell Biol* **14**: 966–76

Tomlinson, V. a L., Newbery, H.J., Wray, N.R., Jackson, J., Larionov, A., Miller, W.R., *et al.* (2005) Translation elongation factor eEF1A2 is a potential oncoprotein that is overexpressed in two-thirds of breast tumours. *BMC Cancer* **5**: 113-

Torres, E.M., Sokolsky, T., Tucker, C.M., Chan, L.Y., Boselli, M., Dunham, M.J., and Amon, A. (2007) Effects of aneuploidy on cellular physiology and cell division in haploid yeast. *Science* **317**: 916–24

Valetti, C., Wetzel, D.M., Schrader, M., Hasbani, M.J., Gill, S.R., Kreis, T.E., and Schroer, T.A. (1999) Role of dynactin in endocytic traffic: effects of dynamitin overexpression and colocalization with CLIP-170. *Mol Biol Cell* **10**: 4107–20

Valouev, I.A., Kushnirov, V. V, and Ter-Avanesyan, M.D. (2002) Yeast polypeptide chain release factors eRF1 and eRF3 are involved in cytoskeleton organization and cell cycle regulation. *Cell Motil Cytoskeleton* **52**: 161–73

Varadi, A., Johnson-Cadwell, L.I., Cirulli, V., Yoon, Y., Allan, V.J., and Rutter, G.A. (2004) Cytoplasmic dynein regulates the subcellular distribution of mitochondria by controlling the recruitment of the fission factor dynamin-related protein-1. *J Cell Sci* **117**: 4389–400

Vaughan, K.T., and Vauee, R.B. (1995) Cytoplasmic dynein binds dynactin through a direct interaction between the intermediate chains and p150. **131**: 1507–16.

Vaughan, P.S., Miura, P., Henderson, M., Byrne, B., and Vaughan, K.T. (2002) A role for regulated binding of p150(Glued) to microtubule plus ends in organelle transport. *J Cell Biol* **158**: 305–19

Veeramah, K.R., Johnstone, L., Karafet, T.M., Wolf, D., Sprissler, R., Salogiannis, J., *et al.* (2013) Exome sequencing reveals new causal mutations in children with epileptic encephalopathies. *Epilepsia* **54**: 1270–81

Vranken, W.F., Boucher, W., Stevens, T.J., Fogh, R.H., Pajon, A., Llinas, M., *et al.* (2005) The CCPN data model for NMR spectroscopy: development of a software pipeline. *Proteins* **59**: 687–96

Water, R., Pringle, J., and Kleinsmith, L. (1980) Identification of an actin-like protein and of its messenger ribonucleic acid in Saccharomyces cerevisiae. *J Bacteriol* **144:** 1143-51

Waterman-Storer, C.M., Karki, S., and Holzbaur, E.L. (1995) The p150Glued component of the dynactin complex binds to both microtubules and the actin-related protein centractin (Arp-1). *Proc Natl Acad Sci U S A* **92**: 1634–8

Wettenhall, J.M., Simpson, K.M., Satterley, K., and Smyth, G.K. (2006) affylmGUI: a graphical user interface for linear modeling of single channel microarray data. *Bioinformatics* **22**: 897–9

Willett, M., Flint, S.A., Morley, S.J., and Pain, V.M. (2006) Compartmentalisation and localisation of the translation initiation factor (eIF) 4F complex in normally growing fibroblasts. *Exp Cell Res* **312**: 2942–53

Williams, G.T., and Farzaneh, F. (2012) Are snoRNAs and snoRNA host genes new players in cancer? *Nat Rev Cancer* **12**: 84–8

Wilson, C.L., Pepper, S.D., Hey, Y., and Miller, C.J. (2004) Amplification protocols introduce systematic but reproducible errors into gene expression studies. *Biotechniques* **36**: 498–506

Wintermeyer, W., Savelsbergh, A., Semenkov, Y.P., Katunin, V.I., and Rodnina, M.V. (2001) Mechanism of Elongation Factor G Function in tRNA Translocation on the Ribosome. *Cold Spring Harb Symp Quant Biol* **66**: 449–458

Wolosewick, J.J., and Porter, K.R. (1976) Stereo high-voltage electron microscopy of whole cells of the human diploid line, WI-38. *Am J Anat* **147**: 303–23

Xie, Y., and Varshavsky, A. (2001) RPN4 is a ligand, substrate, and transcriptional regulator of the 26S proteasome: a negative feedback circuit. *Proc Natl Acad Sci U S A* **98**: 3056–61

Yang, F., Demma, M., and Warren, V. (1990) Identification of an actin-binding protein from Dictyostelium as elongation factor 1a. *Nature* **374**: 494–6

Yeh, T.-Y., Quintyne, N.J., Scipioni, B.R., Eckley, D.M., and Schroer, T. a (2012) Dynactin's pointed-end complex is a cargo-targeting module. *Mol Biol Cell* **23**: 3827–37

Zähringer, H., Burgert, M., Holzer, H., and Nwaka, S. (1997) Neutral trehalase Nth1p of Saccharomyces cerevisiae encoded by the NTH1 gene is a multiple stress responsive protein. *FEBS Lett* **412**: 615–20

Zhu, H., Lam, D.C.L., Han, K.C., Tin, V.P.C., Suen, W.S., Wang, E., *et al.* (2007) High resolution analysis of genomic aberrations by metaphase and array comparative genomic hybridization identifies candidate tumour genes in lung cancer cell lines. *Cancer Lett* **245**: 303–14

# Appendix

# Appendix Chapter 2

| | 1 | 2 | 3 | 4 | 5 | 6 | 7 | 8 | 9 | 10 | 11 | 12 | 13 | 14 | 15 | 16 | 17 | 18 | 19 | 20 | 21 |
|---|---|---|---|---|---|---|---|---|---|---|---|---|---|---|---|---|---|---|---|---|---|
| *A* | BY4741 (WT) | | | Δarc18 | | | Δbit2 | | | Δcap2 | | | Δjnm1 | | | Δsac7 | | | Δvrp1 | | |
| *B* | BY4741 + Tef1 | | | Δarc18 + Tef1 | | | Δbit2 + Tef1 | | | Δcap2 + Tef1 | | | Δjnm1 + Tef1 | | | Δsac7 + Tef1 | | | Δvrp1 + Tef1 | | |
| *C* | Δabp140 | | | Δark1 | | | Δbit61 | | | Δcrn1 | | | Δlsb6 | | | Δscp1 | | | Δyke2 | | |
| *D* | Δabp140 +Tef1 | | | Δark1 + Tef1 | | | Δbit61 + Tef1 | | | Δcrn1 + Tef1 | | | Δlsb6 + Tef1 | | | Δscp1 + Tef1 | | | Δyke2 + Tef1 | | |
| *E* | Δacf4 | | | Δbni1 | | | Δarp1 | | | Δcyk3 | | | Δmsb3 | | | Δsla1 | | | Δysc84 | | |
| *F* | Δacf4 + Tef1 | | | Δbni1 + Tef1 | | | Δarp + Tef1 | | | Δcyk3 + Tef1 | | | Δmsb3 + Tef1 | | | Δsla1 + Tef1 | | | Δysc84 + Tef1 | | |
| *G* | Δaim21 | | | Δarp5 | | | Δbnr1 | | | Δend3 | | | Δmyo4 | | | Δslo1 | | | Δsiw14 | | |
| *H* | Δaim21 + Tef1 | | | Δarp5 + Tef1 | | | Δbnr1 + Tef1 | | | Δend3 + Tef1 | | | Δmyo4 + Tef1 | | | Δslo1 + Tef1 | | | Δsiw14 + Tef1 | | |
| *I* | Δaim3 | | | Δarp6 | | | Δbsp1 | | | Δent1 | | | Δplp1 | | | Δspa2 | | | | | |
| *J* | Δaim3 + Tef1 | | | Δarp6 + Tef1 | | | Δbsp1 + Tef1 | | | Δent1 + Tef1 | | | Δplp1 + Tef1 | | | Δspa2 + Tef1 | | | | | |
| *K* | Δaim7 | | | Δarp8 | | | Δbud6 | | | Δent2 | | | Δrgd1 | | | Δtpm2 | | | | | |
| *L* | Δaim + Tef1 | | | Δarp8 + Tef1 | | | Δbud6 + Tef1 | | | Δent2 + Tef1 | | | Δrgd1 + Tef1 | | | Δtpm2 + Tef1 | | | | | |
| *M* | Δaip1 | | | Δbag7 | | | Δbzz1 | | | Δgea1 | | | Δrvs167 | | | Δtsc11 | | | | | |
| *N* | Δaip1 + Tef1 | | | Δbag7 + Tef1 | | | Δbzz1 + Tef1 | | | Δgea1 + Tef1 | | | Δrvs167 + Tef1 | | | Δtsc11 + Tef1 | | | | | |
| *O* | Δadp1 | | | Δbbc1 | | | Δcap1 | | | Δgip3 | | | Δsac6 | | | Δtwf1 | | | | | |
| *P* | Δadp1 + Tef1 | | | Δbbc1 + Tef1 | | | Δcap1 + Tef1 | | | Δgip3 + Tef1 | | | Δsac6 + Tef1 | | | Δtwf1 + Tef1 | | | | | |

***App.1 Layout of strains from App.2***

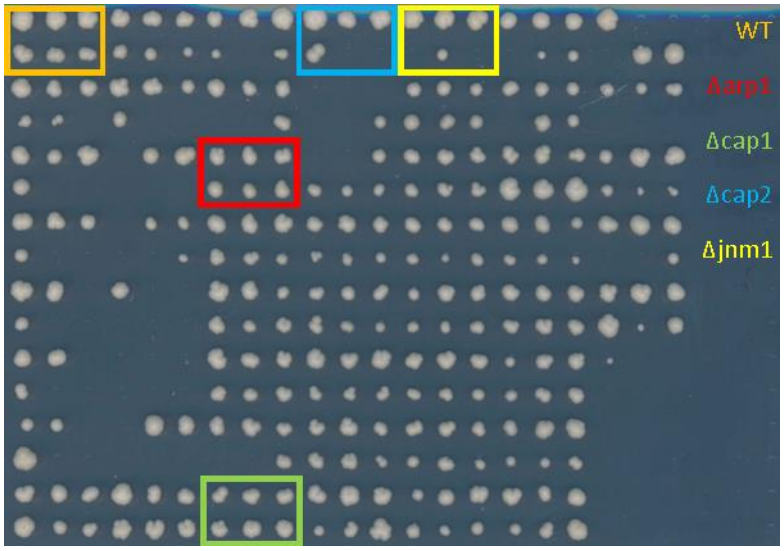


***App.2 Array of viable actin mutant strains with TEF1 overexpressed.*** *Strains that had been deleted for genes known to interact with, or control the function of actin were assayed for synthetic interactions with eEF1A. Strains were arranged horizontally in biological triplicate. Cells containing the control plasmid were in the upper row, with the TEF1 overexpression vector in the row below*

# Appendix Chapter 6

***App 3, table of complete microarray data set.*** *This shows the complete set of up and down regulated genes found in this study.*

| Genes up regulated | | | | Genes down regulated | |
|---|---|---|---|---|---|
| YAL001C | YEL052W | YJL090C | YMR244W | YDL037C | YLR333C |
| YAL002W | YEL053C | YJL092W | YMR247C | YNR072W | YCR095C |
| YAL005C | YEL055C | YJL093C | YMR247W-A | YMR230W-A | YDL166C |
| YAL009W | YEL056W | YJL094C | YMR250W | YOL141W | YOR381W-A |
| YAL010C | YEL057C | YJL095W | YMR251W | YGR035C | YHR085W |
| YAL011W | YEL058W | YJL097W | YMR251W-A | YIL046W-A | YDR471W |
| YAL012W | YEL059C-A | YJL098W | YMR252C | YHR022C-A | YOR080W |
| YAL013W | YEL060C | YJL099W | YMR255W | YNR075W | YHL001W /// YKL006W |
| YAL014C | YEL061C | YJL100W | YMR257C | YJR151W-A | YBL041W |
| YAL015C | YEL062W | YJL101C | YMR258C | YLR412C-A | YIL090W |
| YAL016C-B | YEL063C | YJL102W | YMR259C | YBR298C-A | YGR174W-A |
| YAL017W | YEL065W | YJL103C | YMR261C | YDR545W /// YEL076C | YJR010C-A |
| YAL020C | YEL066W | YJL106W | YMR262W | YML123C | YNL067W-B |
| YAL021C | YEL069C | YJL108C | YMR263W | YBL013W | YOR293W |
| YAL023C | YEL070W /// YNR073C | YJL110C | YMR264W | YMR063W | YGL050W |
| YAL024C | YEL071W | YJL112W | YMR265C | YKL095W | YGL030W |
| YAL026C | YEL075C /// YER189W | YJL116C | YMR266W | YGL258W | YGR027C |
| YAL027W | YER001W | YJL118W | YMR267W | YMR030W-A | YFL061W /// YNL335W |

| YAL028W | YER003C | YJL121C | YMR268C | YLR047C | YMR228W |
|---|---|---|---|---|---|
| YAL029C | YER004W | YJL122W | YMR270C | YPR119W | YBR111W-A |
| YAL030W | YER007C-A | YJL123C | YMR271C | YHR136C | YGR215W |
| YAL031C | YER007W | YJL124C | YMR272C | YOR204W | YPL227C |
| YAL032C | YER008C | YJL126W | YMR273C | YML058W-A | YDR303C |
| YAL033W | YER010C | YJL128C | YMR275C | YMR101C | YBR282W |
| YAL034C | YER011W | YJL129C | YMR276W | YMR117C | YNL331C |
| YAL034W-A | YER013W | YJL130C | YMR277W | YDR320C-A | YDL240W |
| YAL035W | YER014C-A | YJL131C | YMR278W | YHR189W | YBR175W |
| YAL036C | YER014W | YJL132W | YMR280C | YOL136C | YFL053W |
| YAL037C-A | YER016W | YJL133C-A | YMR281W | YLR363W-A | YJL047C-A |
| YAL037W | YER017C | YJL133W | YMR287C | YGR006W | YDR454C |
| YAL038W | YER018C | YJL134W | YMR289W | YER153C | YLR403W |
| YAL041W | YER019W | YJL136C | YMR291W | YJR153W | YBR252W |
| YAL042W | YER020W | YJL137C | YMR293C | YHL018W | YCR020W-B |
| YAL043C | YER023W | YJL138C /// YKR059W | YMR295C | YBR090C | YER051W |
| YAL044C | YER024W | YJL139C | YMR296C | YKL125W | YGR103W |
| YAL044W-A | YER027C | YJL141C | YMR297W | YGR040W | snR73 /// YMR013W-A |
| YAL046C | YER028C | YJL147C | YMR298W | YJR154W | YMR161W |
| YAL047C | YER032W | YJL149W | YMR299C | YLR030W | YHR197W |
| YAL049C | YER033C | YJL151C | YMR300C | YGR174W-A | YHR064C |
| YAL051W | YER034W | YJL154C | YMR301C | YMR032W | YER031C |
| YAL053W | YER035W | YJL158C | YMR302C | YPR094W | YER048W-A |
| YAL054C | YER037W | YJL159W | YMR303C | YFR032C | YIL138C |
| YAL058W | YER040W | YJL160C | YMR304W | YPL166W | YDL210W |
| YAL060W | YER041W | YJL161W | YMR305C | YIL027C | YPR151C |
| YAL061W | YER045C | YJL163C | YMR306W | YAL048C | YER127W |

| | | | | | |
|---|---|---|---|---|---|
| YAL062W | YER047C | YJL164C | YMR307W | YHR105W | YOR369C |
| YAL063C /// YAR050W | YER048C | YJL165C | YMR308C | YPR158W | YJL156C |
| YAL065C | YER049W | YJL167W | YMR310C | YOR387C | YMR002W |
| YAL067C | YER052C | YJL171C | YMR311C | YML108W | YIL004C |
| YAL067W-A | YER053C | YJL172W | YMR312W | YOR210W | YLR063W |
| YAL068C | YER053C-A | YJL174W | YMR313C | YOL101C | YDL232W |
| YAL068C /// YBL108C-A | YER054C | YJL176C | YMR314W | YLR393W | YJR051W |
| YAR007C | YER055C | YJL177W | YMR315W | YER087C-B | YPL027W |
| YAR009C /// YBL005W-B | YER059W | YJL178C | YMR316W | YFL031W | YKL100C |
| YAR014C | YER060W | YJL181W | YMR317W | YGR272C | YPR060C |
| YAR015W | YER061C | YJL184W | YMR318C | YGL029W | YML129C |
| YAR019C | YER062C | YJL185C | YMR322C /// YOR391C | YHL048C-A | YLR369W |
| YAR020C | YER063W | YJL186W | YMR323W /// YOR393W | YML003W | YPR052C |
| YAR027W | YER064C | YJL187C | YNL001W | YNL147W | YDR524C-B |
| YAR028W | YER066W | YJL191W | YNL003C | YPL130W | YGR154C |
| YAR029W | YER067W | YJL192C | YNL004W | YLR275W | YNL275W |
| YAR031W | YER068W | YJL193W | YNL005C | YMR272W-B | YKL006W |
| YAR033W /// YGL051W | YER069W | YJL196C | YNL007C | YOL002C | YPR043W |
| YAR035W | YER070W | YJL197W | YNL008C | YPL201C | YKL143W |
| YAR042W | YER071C | YJL198W | YNL011C | YPR108W-A | YER065C |
| YAR050W | YER073W | YJL200C | YNL012W | YJR135W-A | YMR090W |

| | | | | | |
|---|---|---|---|---|---|
| YAR062W /// YHR213W | YER075C | YJL201W | YNL014W | YBR152W | YHR116W |
| YAR064W /// YHR213W-B | YER076C | YJL203W | YNL015W | YDL157C | YOR186W |
| YAR068W /// YHR214W-A | YER077C | YJL204C | YNL016W | YLR264C-A | YPL019C |
| YAR070C /// YHR214C-E | YER079W | YJL206C | YNL018C | YKR083C | YGL220W |
| YAR071W /// YHR215W | YER081W | YJL207C | YNL018C /// YNL034W | YDR492W | YBR143C |
| YAR075W | YER082C | YJL212C | YNL019C /// YNL033W | YML017W | YDR318W |
| YAR075W /// YHR216W | YER083C | YJL213W | YNL020C | YBR120C | YGR106C |
| YBL001C | YER088C | YJL217W | YNL021W | YPL162C | YJL127C-B |
| YBL002W | YER089C | YJL218W | YNL023C | YPR201W | YER074W /// YIL069C |
| YBL003C | YER090W | YJL219W | YNL027W | YOR180C | YOR232W |
| YBL003C /// YDR225W | YER091C | YJL219W /// YOL156W | YNL031C | YER046W | YGR049W |
| YBL004W | YER093C | YJR001W | YNL032W | YER085C | YKL104C |
| YBL005W | YER094C | YJR003C | YNL034W | YBL100W-C | YKL217W |
| YBL005W-B /// YBR012W-B | YER095W | YJR005W | YNL035C | YBR257W | YNL133C |
| YBL005W-B /// YBR012W-B | YER096W | YJR006W | YNL037C | YGR105W | YMR060C |
| YBL005W-B /// YDR261C-D | YER099C | YJR007W | YNL039W | YOR315W | YNR043W |
| YBL006C | YER101C | YJR008W | YNL040W | YGR079W | YPL257W |
| YBL007C | YER102W | YJR013W | YNL041C | YER039C | YCL011C |

| YBL009W | YER103W | YJR014W | YNL042W | YLR068W | YNL062C |
|---|---|---|---|---|---|
| YBL010C | YER104W | YJR015W | YNL042W-B /// YOL013W-A | YOR243C | YLR146C |
| YBL011W | YER105C | YJR016C | YNL045W | YDR523C | YBL107W-A /// YER138W-A |
| YBL015W | YER106W | YJR017C | YNL049C | YOR313C | YLR019W |
| YBL016W | YER107C | YJR019C | YNL050C | YNL162W-A | YML073C |
| YBL017C | YER109C | YJR021C | YNL051W | YHR081W | YNL308C |
| YBL019W | YER110C | YJR024C | YNL053W | YHR196W | YPL043W |
| YBL021C | YER111C | YJR025C | YNL054W | YNL024C-A | YMR084W |
| YBL022C | YER113C | YJR030C | YNL055C | YEL048C | YJL190C |
| YBL024W | YER114C | YJR031C | YNL056W | YLR435W | YBR291C |
| YBL027W | YER115C | YJR032W | YNL058C | YMR188C | YHR084W |
| YBL029C-A | YER116C | YJR033C | YNL059C | YGR046W | YAR008W |
| YBL029W | YER118C | YJR035W | YNL061W | YLR204W | YGR024C |
| YBL030C | YER119C | YJR039W | YNL063W | YLR408C | YJL143W |
| YBL031W | YER120W | YJR040W | YNL065W | YAR023C | YJL179W |
| YBL032W | YER122C | YJR042W | YNL066W | YOL154W | YNR032W |
| YBL033C | YER123W | YJR043C | YNL067W | YLR346C | YKL184W |
| YBL034C | YER124C | YJR044C | YNL068C | YMR286W | YGR155W |
| YBL037W | YER125W | YJR045C | YNL069C | YGL247W | YJL117W |
| YBL042C | YER128W | YJR046W | YNL071W | YBL111C /// YDR545W | YOR189W |
| YBL043W | YER129W | YJR047C | YNL072W | YHL020C | YMR274C |
| YBL045C | YER130C | YJR048W | YNL073W | YIL099W | YDL098C |
| YBL046W | YER132C | YJR049C | YNL074C | YDR536W | YLR438C-A |
| YBL047C | YER134C | YJR050W | YNL076W | YJL144W | YMR212C |
| YBL049W | YER137C | YJR052W | YNL080C | YOR060C | YOR026W |

| | | | | | |
|---|---|---|---|---|---|
| YBL050W | YER141W | YJR054W | YNL082W | YHR072W-A | YIL106W |
| YBL051C | YER143W | YJR057W | YNL085W | YGR271C-A | YDR167W |
| YBL052C | YER144C | YJR058C | YNL086W | YLR262C | YOR075W |
| YBL055C | YER145C | YJR059W | YNL087W | YDR524W-C | YPL108W |
| YBL056W | YER146W | YJR060W | YNL088W | YPR046W | YEL054C |
| YBL058W | YER147C | YJR061W | YNL090W | YMR040W | YDR381C-A |
| YBL059C-A | YER149C | YJR064W | YNL091W | YLR037C | YIL014W |
| YBL059W | YER150W | YJR065C | YNL092W | YCR028C | YHR153C |
| YBL061C | YER151C | YJR066W | YNL093W | YJL194W | YMR177W |
| YBL063W | YER152C | YJR067C | YNL094W | YLR254C | YBL023C |
| YBL064C | YER154W | YJR069C | YNL095C | YOR021C | YER060W-A |
| YBL066C | YER155C | YJR070C | YNL096C | YDR496C | YAL022C |
| YBL067C | YER156C | YJR072C | YNL097C-B | YML119W | YKL074C |
| YBL069W | YER157W | YJR073C | YNL098C | YDR256C | YLR426W |
| YBL071C-B | YER158C | YJR074W | YNL099C | YER039C-A | YDL130W |
| YBL071W-A | YER159C | YJR075W | YNL100W | YGR108W | YBR191W |
| YBL072C | YER162C | YJR076C | YNL102W | YBR065C | YGL106W |
| YBL075C | YER163C | YJR077C | YNL103W | YLR145W | YOR346W |
| YBL076C | YER164W | YJR078W | YNL104C | YLR051C | YBL039C |
| YBL078C | YER165W | YJR079W | YNL106C | YPR153W | YDL136W /// YDL191W |
| YBL079W | YER166W | YJR080C | YNL108C | YDR432W | YNL302C /// YOL121C |
| YBL080C | YER167W | YJR083C | YNL115C | YNL307C | YPL051W |
| YBL081W | YER169W | YJR085C | YNL116W | YPR166C | YJL072C |
| YBL084C | YER170W | YJR088C | YNL117W | YDR191W | YEL069C |
| YBL085W | YER171W | YJR090C | YNL118C | YFR001W | YGL263W |
| YBL086C | YER172C | YJR091C | YNL123W | YGR204C-A | YDR375C |
| YBL087C | YER175C | YJR092W | YNL124W | YER002W | YNL197C |

| | | | | | |
|---|---|---|---|---|---|
| YBL088C | YER176W | YJR093C | YNL125C | YBR211C | YGR038W |
| YBL089W | YER177W | YJR094C | YNL126W | YMR253C | YBR195C |
| YBL091C | YER178W | YJR095W | YNL127W | YJR097W | YLR276C |
| YBL091C-A | YER179W | YJR096W | YNL128W | YIL040W | YJL058C |
| YBL093C | YER182W | YJR098C | YNL130C | YML037C | YNL075W |
| YBL095W | YER183C | YJR099W | YNL130C-A | YIL071C | YIL069C |
| YBL098W | YER184C | YJR100C | YNL132W | YCR100C | YDL081C |
| YBL100W-A /// YBL100W-B | YER188C-A | YJR103W | YNL135C | YKR034W | YLR196W |
| YBL100W-B /// YCL019W | YFL002C | YJR104C | YNL136W | YDR075W | YGR273C |
| YBL101C | YFL003C | YJR105W | YNL137C | YOR025W | YGL112C |
| YBL102W | YFL004W | YJR107W | YNL138W | YGR030C | YKL195W |
| YBL103C | YFL008W | YJR108W | YNL139C /// YNL140C | YPL113C | YBR173C |
| YBL104C | YFL009W | YJR109C | YNL141W | YKL068W-A | YOR272W |
| YBL105C | YFL010C | YJR110W | YNL142W | YDL243C | YLR064W |
| YBL106C | YFL010W-A | YJR111C | YNL144C | YKL058W | YDR014W |
| YBL109W /// YDR544C | YFL012W | YJR112W | YNL146C-A | YER142C | YBL036C |
| YBL111C /// YDR545W | YFL013C | YJR112W-A | YNL146W | YCL056C | YGR057C |
| YBL111C /// YDR545W | YFL014W | YJR113C | YNL152W | YML041C | YLR312W-A |
| YBL112C /// YBL113C | YFL016C | YJR114W | YNL154C | YMR015C | YJL166W |
| YBL113C /// YDR545W | YFL018C | YJR115W | YNL156C | YPL038W-A | YDR082W |
| YBL113W-A /// YDR545C-A | YFL020C | YJR116W | YNL159C | YER044C | YPL234C |

| | | | | | |
|---|---|---|---|---|---|
| YBR001C | YFL020C | YJR117W | YNL160W | YNL038W | YPR137W |
| YBR003W | YFL021W | YJR119C | YNL161W | YER006W | YIR018C-A |
| YBR004C | YFL022C | YJR120W | YNL163C | YGL127C | YDR361C |
| YBR005W | YFL023W | YJR121W | YNL165W | YIL016W | YMR159C |
| YBR007C | YFL024C | YJR122W | YNL166C | YOR344C | YDR519W |
| YBR008C | YFL025C | YJR125C | YNL167C | YIL127C | YML100W-A |
| YBR010W | YFL026W | YJR126C | YNL168C | YGL041C-B | YEL073C |
| YBR011C | YFL027C | YJR127C | YNL172W | YLR456W | YAL064W |
| YBR013C | YFL028C | YJR129C | YNL173C | YGR211W | YOR312C |
| YBR014C | YFL029C | YJR130C | YNL175C | YNL222W | YMR294W |
| YBR015C | YFL030W | YJR131W | YNL176C | YDR071C | YNL265C |
| YBR017C | YFL033C | YJR132W | YNL178W | YGR236C | YIR024C |
| YBR018C | YFL034C-A | YJR133W | YNL180C | YKL055C | YNL029C |
| YBR020W | YFL034C-B | YJR134C | YNL181W | YGL246C | YOR056C |
| YBR022W | YFL034W | YJR135C | YNL182C | YER015W | YDL070W |
| YBR023C | YFL036W | YJR137C | YNL183C | YIL158W | YPR107C |
| YBR025C | YFL037W | YJR138W | YNL185C | YLR168C | YNL254C |
| YBR026C | YFL038C | YJR139C | YNL186W | YOL077W-A | YKL119C |
| YBR028C | YFL039C | YJR140C | YNL187W | YLL009C | YPR020W |
| YBR030W | YFL041W | YJR142W | YNL189W | YDR184C | YDR362C |
| YBR031W /// YDR012W | YFL042C | YJR144W | YNL190W | YBR091C | YGR118W |
| YBR035C | YFL044C | YJR147W | YNL191W | YCR024C-B | YMR284W |
| YBR036C | YFL045C | YJR148W | YNL192W | YGL054C | YDR402C |
| YBR037C | YFL047W | YJR149W | YNL193W | YDL205C | YGL129C |
| YBR039W | YFL048C | YJR150C | YNL194C | YGR126W | YER043C |
| YBR040W | YFL050C | YJR151C | YNL195C | YNR020C | YDL042C |
| YBR041W | YFL052W | YJR155W | YNL196C | YBL028C | YOR167C |

| YBR042C | YFL054C | YKL002W | YNL199C | YPL146C | YGL008C |
|---|---|---|---|---|---|
| YBR043C | YFL059W /// YNL333W | YKL006C-A | YNL200C | YMR269W | YDR012W |
| YBR045C | YFL060C /// YNL334C | YKL007W | YNL201C | YLR220W | YPL249C-A |
| YBR046C | YFL062W /// YGR295C /// YNL336W | YKL008C | YNL202W | YGL240W | YDR508C |
| YBR047W | YFL067W | YKL010C | YNL204C | YJR055W | YKL116C |
| YBR048W | YFR002W | YKL012W | YNL206C | YPL225W | YCR031C |
| YBR049C | YFR003C | YKL013C | YNL208W | YJL214W | YJR143C |
| YBR052C | YFR006W | YKL014C | YNL209W | YGR036C | YOR340C |
| YBR053C | YFR007W | YKL015W | YNL210W | YBR196C-A | YMR071C |
| YBR054W | YFR008W | YKL017C | YNL214W | YDR042C | YML099C |
| YBR055C | YFR009W | YKL019W | YNL215W | YJL035C | YDR339C |
| YBR056W | YFR010W | YKL020C | YNL217W | YPL211W | YFL055W |
| YBR058C | YFR012W | YKL022C | YNL221C | YBL026W | YBL044W |
| YBR059C | YFR012W-A | YKL023W | YNL224C | YKL050C | YDR228C |
| YBR060C | YFR013W | YKL024C | YNL227C | YHR086W-A | YOR245C |
| YBR061C | YFR014C | YKL025C | YNL229C | YNR062C | YKL185W |
| YBR063C | YFR015C | YKL026C | YNL230C | YOR183W | YML026C |
| YBR067C | YFR016C | YKL027W | YNL233W | YDR078C | YKR009C |
| YBR068C | YFR017C | YKL028W | YNL236W | YOL163W | YPL119C |
| YBR070C | YFR018C | YKL029C | YNL237W | YBR153W | YAR002C-A |
| YBR071W | YFR019W | YKL032C | YNL238W | YGR092W | YGL044C |
| YBR072C-A | YFR021W | YKL033W | YNL239W | YLR462W | YHR004C |
| YBR072W | YFR022W | YKL034W | YNL240C | YBL040C | YOR153W |
| YBR073W | YFR023W | YKL035W | YNL241C | YMR003W | YDR030C |
| YBR074W | YFR024C-A | YKL038W | YNL242W | YER058W | YPL070W |

| | | | | | |
|---|---|---|---|---|---|
| YBR076W | YFR025C | YKL042W | YNL243W | YMR155W | YPR138C |
| YBR077C | YFR026C | YKL047W | YNL245C | YBR271W | YGL171W |
| YBR079C | YFR027W | YKL048C | YNL246W | YOR083W | YBR016W |
| YBR080C | YFR028C | YKL051W | YNL247W | YNL277W-A | YLR359W |
| YBR081C | YFR029W | YKL052C | YNL248C | YGR183C | YMR098C |
| YBR082C | YFR030W | YKL054C | YNL250W | YOR032C | YDR083W |
| YBR083W | YFR031C | YKL057C | YNL255C | YLR421C | YNL084C |
| YBR084C-A | YFR031C-A /// YIL018W | YKL059C | YNL257C | YOL059W | YDR348C |
| YBR084W | YFR032C-A | YKL060C | YNL258C | YDR031W | YBR009C /// YNL030W |
| YBR085W | YFR032C-B | YKL061W | YNL260C | YCR102C | YER175W-A |
| YBR086C | YFR033C | YKL063C | YNL261W | YPL165C | YBR164C |
| YBR087W | YFR034C | YKL064W | YNL263C | YIL098C | YLR264W |
| YBR089C-A /// YBR090C | YFR035C | YKL067W | YNL264C | YDR383C | YKL065C |
| YBR097W | YFR036W | YKL068W | YNL267W | YPR101W | YLR074C |
| YBR101C | YFR038W | YKL069W | YNL268W | YNL112W | YDR120C |
| YBR102C | YFR039C | YKL070W | YNL269W | YMR056C | YDR322W |
| YBR103W | YFR040W | YKL071W | YNL270C | YBR180W | YKL192C |
| YBR104W | YFR041C | YKL072W | YNL271C | YBL039W-B | YLR038C |
| YBR105C | YFR043C | YKL073W | YNL273W | YBR255C-A | YAL055W |
| YBR106W | YFR044C | YKL075C | YNL274C | YIL103W | YCL038C |
| YBR107C | YFR045W | YKL079W | YNL277W | YDR086C | YCR054C |
| YBR108W | YFR046C | YKL080W | YNL278W | YDL121C | YDR450W |
| YBR109C | YFR047C | YKL081W | YNL280C | YNR032C-A | YPR133C |
| YBR110W | YFR048W | YKL084W | YNL281W | YMR239C | YHR021W-A |
| YBR111C | YFR049W | YKL085W | YNL283C | YML043C | YNL299W |

| | | | | | |
|---|---|---|---|---|---|
| YBR112C | YFR051C | YKL086W | YNL284C | YPR100W | YFR057W |
| YBR115C | YFR053C | YKL087C | YNL287W | YKL001C | YDL175C |
| YBR117C | YFR055W | YKL088W | YNL288W | YCL042W | YPL118W |
| YBR118W /// YPR080W | YGL001C | YKL089W | YNL289W | YFL051C | YIL139C |
| YBR119W | YGL002W | YKL091C | YNL291C | YHL039W | YJL170C |
| YBR121C | YGL003C | YKL092C | YNL292W | YDR201W | YMR225C |
| YBR123C | YGL004C | YKL093W | YNL293W | YDR033W | YLL012W |
| YBR126C | YGL006W | YKL094W | YNL294C | YOR045W | YLR133W |
| YBR128C | YGL007C-A | YKL096C-B | YNL295W | YJL136W-A | YKL039W |
| YBR130C | YGL009C | YKL096W | YNL297C | YLR108C | YLR453C |
| YBR132C | YGL011C | YKL099C | YNL298W | YBR268W | YGR263C |
| YBR133C | YGL012W | YKL101W | YNL300W | YNL119W | YDR345C |
| YBR135W | YGL013C | YKL103C | YNL301C | YIL170W /// YOL156W | YGL086W |
| YBR136W | YGL014W | YKL105C | YNL301C /// YOL120C | YFL056C | YCL031C |
| YBR137W | YGL015C | YKL106C-A | YNL304W | YGR230W | YMR140W |
| YBR139W | YGL016W | YKL106W | YNL305C | YAR073W /// YHR216W | YDL155W |
| YBR140C | YGL017W | YKL108W | YNL306W | YOR158W | YGR071C |
| YBR141C | YGL018C | YKL109W | YNL309W | YBR258C | YLR060W |
| YBR142W | YGL019W | YKL110C | YNL310C | YEL020W-A | YEL034W |
| YBR145W | YGL020C | YKL112W | YNL311C | YHR152W | YLR287C |
| YBR146W | YGL022W | YKL114C | YNL312W | YBL008W-A | YPR056W |
| YBR147W | YGL023C | YKL117W | YNL314W | YKL170W | YBR089C-A |
| YBR148W | YGL025C | YKL120W | YNL315C | YOR262W | YNL212W |
| YBR149W | YGL026C | YKL121W | YNL316C | YMR130W | YBL072C /// YER102W |

| | | | | | |
|---|---|---|---|---|---|
| YBR150C | YGL027C | YKL124W | YNL317W | YOR258W | YAR069C /// YHR214C-D |
| YBR151W | YGL028C | YKL126W | YNL318C | YPL119C-A | YCR028C-A |
| YBR157C | YGL031C | YKL127W | YNL321W | YOL142W | YGR060W |
| YBR159W | YGL032C | YKL128C | YNL322C | YKL009W | YPL005W |
| YBR160W | YGL033W | YKL129C | YNL323W | YLR401C | YJL189W |
| YBR161W | YGL035C | YKL132C | YNL325C | YPL179W | YOR224C |
| YBR166C | YGL036W | YKL133C | YNL326C | YNL113W | YKL041W |
| YBR168W | YGL037C | YKL134C | YNL327W | YDR021W | YPL267W |
| YBR169C | YGL039W | YKL135C | YNL329C | YER019C-A | YLR154C |
| YBR170C | YGL040C | YKL139W | YNL330C | YKL130C | YPR082C |
| YBR172C | YGL043W | YKL140W | YNR001C | YNL110C | YNL079C |
| YBR176W | YGL045W | YKL141W | YNR002C | YGR142W | YNL225C |
| YBR177C | YGL047W | YKL142W | YNR003C | YDL248W /// YJR161C | YPL094C |
| YBR179C | YGL049C | YKL145W | YNR006W | YNL002C | YDL088C |
| YBR182C | YGL051W | YKL146W | YNR007C | YIR031C | YKR023W |
| YBR182C-A | YGL053W | YKL148C | YNR008W | YDR399W | YPR041W |
| YBR183W | YGL056C | YKL149C | YNR009W | YDR249C | YGR278W |
| YBR185C | YGL058W | YKL150W | YNR010W | YLR104W | YDR529C |
| YBR186W | YGL059W | YKL151C | YNR011C | YGR177C | YDL083C |
| YBR187W | YGL062W | YKL152C | YNR012W | YDR512C | YNR074C |
| YBR193C | YGL065C | YKL154W | YNR013C | YDL160C | YOR281C |
| YBR194W | YGL066W | YKL155C | YNR014W | YBL020W | YEL026W |
| YBR196C | YGL067W | YKL157W | YNR015W | YPL036W | YJL051W |
| YBR197C | YGL071W | YKL159C | YNR016C | YJL052C-A | YKL156W |
| YBR199W | YGL073W | YKL161C | YNR017W | YHR151C | YML065W |

| | | | | | |
|---|---|---|---|---|---|
| YBR200W | YGL076C /// YPL198W | YKL168C | YNR018W | YHR168W | YDR013W |
| YBR201W | YGL078C | YKL171W | YNR019W | YPL018W | YOL127W |
| YBR204C | YGL079W | YKL172W | YNR021W | YPL245W | YDR285W |
| YBR205W | YGL081W | YKL173W | YNR023W | YHL024W | YDR121W |
| YBR207W | YGL082W | YKL174C | YNR026C | YGL209W | YHR053C /// YHR055C |
| YBR208C | YGL083W | YKL180W | YNR027W | YPR200C | YOR117W |
| YBR212W | YGL085W | YKL181W | YNR029C | YOR166C | YLR085C |
| YBR213W | YGL087C | YKL182W | YNR030W | YNL244C | YOR003W |
| YBR214W | YGL090W | YKL183W | YNR031C | YAL040C | YIR022W |
| YBR215W | YGL091C | YKL186C | YNR033W | YDR091C | YDR115W |
| YBR216C | YGL092W | YKL188C | YNR034W | YOR349W | YLR061W |
| YBR218C | YGL093W | YKL189W | YNR034W-A | YDR275W | YDR370C |
| YBR219C /// YBR220C | YGL094C | YKL191W | YNR035C | YDR072C | YNL122C |
| YBR220C | YGL095C | YKL193C | YNR036C | YBL090W | YLR226W |
| YBR221C | YGL096W | YKL194C | YNR037C | YER026C | YJL125C |
| YBR221W-A | YGL097W | YKL197C | YNR038W | YCR003W | YKL176C |
| YBR222C | YGL100W | YKL198C | YNR039C | YMR077C | YML082W |
| YBR223C | YGL101W | YKL201C | YNR040W | YHR157W | YOL019W-A |
| YBR225W | YGL104C | YKL203C | YNR041C | YNL169C | YCL036W |
| YBR227C | YGL105W | YKL204W | YNR044W | YDL038C | YGR072W |
| YBR228W | YGL107C | YKL205W | YNR045W | YBR233W-A | YDR300C |
| YBR229C | YGL108C | YKL206C | YNR046W | YOR190W | YML126C |
| YBR230C | YGL110C | YKL207W | YNR047W | YKR075C | YDR441C |
| YBR230W-A | YGL111W | YKL208W | YNR049C | YHR052W | YOR172W |
| YBR233W | YGL114W | YKL209C | YNR050C | YBL038W | YML088W |
| YBR234C | YGL115W | YKL210W | YNR051C | YOR039W | --- |

| YBR235W | YGL117W | YKL211C | YNR052C | YJR011C | YGR209C |
|---|---|---|---|---|---|
| YBR236C | YGL119W | YKL212W | YNR054C | YOR150W | YJR082C |
| YBR239C | YGL121C | YKL213C | YNR055C | YNL213C | YDR387C |
| YBR240C | YGL122C | YKL214C | YNR056C | YBR098W | YLR285W |
| YBR241C | YGL124C | YKL215C | YNR057C | YKL166C | YDR528W |
| YBR242W | YGL125W | YKL218C | YNR058W | YJL115W | YLR107W |
| YBR243C | YGL126W | YKL219W | YNR059W | YDR437W | YNL253W |
| YBR245C | YGL128C | YKR001C | YNR060W | YKL122C | YJL104W |
| YBR246W | YGL130W | YKR002W | YNR064C | YIL160C | YBR293W |
| YBR248C | YGL131C | YKR003W | YNR065C | YIR021W | YCR002C |
| YBR249C | YGL133W | YKR007W | YNR066C | YMR256C | YJR094W-A |
| YBR251W | YGL134W | YKR008W | YNR067C | YMR180C | YKR057W |
| YBR254C | YGL136C | YKR010C | YNR068C | YBR210W | YMR319C |
| YBR255W | YGL137W | YKR011C | YNR069C | YBR129C | YDR511W |
| YBR256C | YGL138C | YKR013W | YOL003C | YPL226W | YLR395C |
| YBR260C | YGL139W | YKR014C | YOL004W | YDR280W | YDR146C |
| YBR261C | YGL140C | YKR015C | YOL005C | YDR196C | YOL038W |
| YBR262C | YGL141W | YKR016W | YOL006C | YML048W | YDR062W |
| YBR265W | YGL143C | YKR018C | YOL007C | YPL013C | YMR030W |
| YBR269C | YGL144C | YKR019C | YOL008W | YDR079W | YGL064C |
| YBR270C | YGL145W | YKR020W | YOL013C | YER139C | YBR298C |
| YBR272C | YGL146C | YKR021W | YOL013W-A | YDL179W | YDL128W |
| YBR273C | YGL148W | YKR022C | YOL015W | YER140W | YAR018C |
| YBR274W | YGL150C | YKR025W | YOL016C | YJR062C | YLR125W |
| YBR275C | YGL151W | YKR026C | YOL017W | YOL010W | YHR021C |
| YBR276C | YGL153W | YKR027W | YOL020W | YGL192W | YGL226W |
| YBR278W | YGL154C | YKR028W | YOL021C | YNL153C | YGR220C |
| YBR279W | YGL155W | YKR029C | YOL022C | YHR143W-A | YML085C |

| | | | | | |
|---|---|---|---|---|---|
| YBR281C | YGL156W | YKR031C | YOL025W | YDR195W | YOR089C |
| YBR284W | YGL157W | YKR036C | YOL026C | YIL037C | YEL044W |
| YBR285W | YGL158W | YKR037C | YOL027C | YER180C-A | YOR038C |
| YBR286W | YGL159W | YKR038C | YOL028C | YLR190W | YDL247W |
| YBR287W | YGL160W | YKR041W | YOL029C | YDL085W | YIL091C |
| YBR289W | YGL162W | YKR042W | YOL030W | YOR009W | YLR370C |
| YBR290W | YGL163C | YKR043C | YOL031C | YIL008W | YML102W |
| YBR295W | YGL164C | YKR044W | YOL032W | YHR066W | YPL191C |
| YBR296C-A | YGL166W | YKR045C | YOL033W | YNL107W | YDR404C |
| YBR297W | YGL167C | YKR046C | YOL034W | YLR221C | YHR132W-A |
| YBR299W /// YGR292W | YGL168W | YKR048C | YOL036W | YML077W | YIL101C |
| YBR302C /// YML132W | YGL170C | YKR049C | YOL040C | YLR154W-E | YDR302W |
| YCL001W-A | YGL172W | YKR050W | YOL043C | YML054C | YFL017C |
| YCL001W-B | YGL173C | YKR052C | YOL044W | YBR200W-A | YIL118W |
| YCL002C | YGL174W | YKR054C | YOL047C | YLL054C | YGR059W |
| YCL004W | YGL176C | YKR055W | YOL048C | YPL242C | YER186C |
| YCL008C | YGL178W | YKR058W | YOL049W | YBR021W | YHL011C |
| YCL009C | YGL179C | YKR061W | YOL051W | YKL090W | YHL026C |
| YCL010C | YGL180W | YKR062W | YOL052C | YDR045C | YLR167W |
| YCL014W | YGL181W | YKR063C | YOL052C-A | YBR066C | YIL035C |
| YCL016C | YGL183C | YKR066C | YOL053W | YML046W | YOR044W |
| YCL017C | YGL184C | YKR067W | YOL054W | YMR080C | YLR353W |
| YCL018W | YGL185C | YKR069W | YOL055C | YOL038C-A | YDR227W |
| YCL021W-A | YGL186C | YKR070W | YOL056W | YBR162W-A | YPR061C |
| YCL024W | YGL187C | YKR071C | YOL058W | YHR194W | YIL148W |
| YCL025C | YGL188C-A | YKR072C | YOL060C | YMR223W | YMR230W |

| YCL026C-A | YGL189C | YKR076W | YOL062C | YJR022W | YML009C |
|---|---|---|---|---|---|
| YCL026C-B | YGL191W | YKR077W | YOL063C | YOR147W | YOR351C |
| YCL027W | YGL194C | YKR078W | YOL064C | YGL038C | YER056C |
| YCL028W | YGL195W | YKR079C | YOL065C | YIL166C | YKL018W |
| YCL029C | YGL196W | YKR080W | YOL066C | YIL064W | YOR386W |
| YCL030C | YGL197W | YKR082W | YOL068C | YMR134W | YOR237W |
| YCL032W | YGL198W | YKR084C | YOL069W | YHR148W | YOR063W |
| YCL033C | YGL200C | YKR086W | YOL070C | YDL212W | YOR274W |
| YCL035C | YGL201C | YKR087C | YOL071W | YHR175W-A | YIL146C |
| YCL037C | YGL202W | YKR089C | YOL072W | YER112W | YDL008W |
| YCL039W | YGL203C | YKR090W | YOL073C | YDL153C | YDR494W |
| YCL040W | YGL205W | YKR091W | YOL075C | YDR386W | YOR141C |
| YCL043C | YGL206C | YKR092C | YOL076W | YGR016W | YLR172C |
| YCL044C | YGL207W | YKR093W | YOL078W | YER009W | YOL098C |
| YCL045C | YGL208W | YKR095W | YOL081W | YHR139C | YGR283C |
| YCL047C | YGL211W | YKR095W-A | YOL082W | YFR037C | YNL251C |
| YCL048W | YGL212W | YKR096W | YOL083W | YIL143C | YMR093W |
| YCL049C | YGL215W | YKR097W | YOL084W | YIL049W | YNL010W |
| YCL050C | YGL216W | YKR098C | YOL087C | YHR159W | YDR192C |
| YCL051W | YGL219C | YKR099W | YOL088C | YCR068W | YGR148C |
| YCL052C | YGL221C | YKR100C | YOL089C | YMR292W | YDL059C |
| YCL057W | YGL222C | YKR101W | YOL090W | YGL010W | YER098W |
| YCL058C | YGL223C | YKR102W | YOL091W | YPL064C | YDL015C |
| YCL059C | YGL224C | YKR103W | YOL093W | YHR038W | YOL149W |
| YCL061C | YGL227W | YKR104W | YOL095C | YBR202W | YNL231C |
| YCL063W | YGL228W | YLL001W | YOL096C | YAR003W | YGR205W |
| YCL064C | YGL229C | YLL002W | YOL097C | YKL082C | YPL030W |
| YCL068C /// YCR038C | YGL230C | YLL003W | YOL100W | YOR279C | YML024W |

| | | | | | |
|---|---|---|---|---|---|
| YCL069W /// YKR105C | YGL232W | YLL005C | YOL102C | YAR066W /// YHR214W | YDR418W |
| YCL073C /// YKR106W | YGL233W | YLL006W | YOL103W | YNL009W | YDR525W-A |
| YCR004C | YGL235W | YLL006W-A | YOL104C | YDR366C | YMR072W |
| YCR005C | YGL236C | YLL007C | YOL107W | YKR017C | YMR171C |
| YCR007C | YGL237C | YLL008W | YOL108C | YDR412W | YHR141C /// YNL162W |
| YCR008W | YGL241W | YLL010C | YOL109W | YML053C | YBR217W |
| YCR009C | YGL242C | YLL011W | YOL110W | YDL069C | YPR073C |
| YCR010C | YGL243W | YLL013C | YOL111C | YGL262W | YJL111W |
| YCR011C | YGL244W | YLL015W | YOL112W | YGR076C | YOL086C |
| YCR012W | YGL245W | YLL018C | YOL113W | YHR005C-A | YKL222C |
| YCR017C | YGL248W | YLL018C-A | YOL114C | YOR212W | YDL183C |
| YCR018C | YGL249W | YLL019C | YOL116W | YPL052W | YDR064W |
| YCR019W | YGL250W | YLL021W | YOL117W | YDR502C | YDR173C |
| YCR020C | YGL251C | YLL022C | YOL119C | YBR122C | YDR221W |
| YCR021C | YGL252C | YLL023C | YOL120C | YAL059W | YLR114C |
| YCR023C | YGL254W | YLL024C | YOL121C | YER074W-A | YNL025C |
| YCR024C | YGL257C | YLL025W | YOL122C | YDR276C | YBR237W |
| YCR026C | YGL258W-A | YLL025W | YOL123W | YEL003W | YDR067C |
| YCR030C | YGL259W | YLL026W | YOL125W | YNL234W | YGR055W |
| YCR032W | YGR001C | YLL027W | YOL126C | YMR079W | YBL097W |
| YCR033W | YGR004W | YLL029W | YOL128C | YLL034C | YDR182W-A |
| YCR034W | YGR005C | YLL031C | YOL129W | YOR043W | YNL328C |
| YCR036W | YGR007W | YLL032C | YOL131W | YBR296C | YGL238W |
| YCR037C | YGR008C | YLL033W | YOL132W | YDR364C | YER021W |
| YCR038C | YGR009C | YLL036C | YOL133W | YML007W | YOL105C |

| | | | | | |
|---|---|---|---|---|---|
| YCR042C | YGR012W | YLL038C | YOL135C | YJL173C | YDL215C |
| YCR043C | YGR013W | YLL039C | YOL138C | YJL107C | YPL209C |
| YCR044C | YGR014W | YLL040C | YOL139C | YLR307W | YHR010W |
| YCR046C | YGR015C | YLL041C | YOL140W | YLL014W | YHL013C |
| YCR048W | YGR017W | YLL043W | YOL143C | YLR002C | YER131W |
| YCR051W | YGR019W | YLL048C | YOL144W | YER072W | YGR082W |
| YCR052W | YGR020C | YLL050C | YOL145C | YLR385C | YDR427W |
| YCR053W | YGR021W | YLL051C | YOL146W | YGL070C | YGL068W |
| YCR059C | YGR023W | YLL052C | YOL147C | YGR234W | YIL074C |
| YCR060W | YGR026W | YLL053C | YOL148C | YDL045W-A | YOR305W |
| YCR061W | YGR028W | YLL055W | YOL151W | YER042W | YIR015W |
| YCR063W | YGR029W | YLL056C | YOL152W | YLR154C-H /// YLR156C-A | YDL241W |
| YCR065W | YGR032W | YLL057C | YOL155C | YKR068C | YKL221W |
| YCR067C | YGR033C | YLL058W | YOL155W-A | YJR102C | YJL162C |
| YCR069W | YGR035W-A | YLL061W | YOL158C | YOR268C | YOR031W |
| YCR071C | YGR041W | YLL062C | YOL159C | YOR148C | YML018C |
| YCR073C | YGR042W | YLL063C | YOL159C-A | YBR058C-A | YGR002C |
| YCR073W-A | YGR043C | YLL064C /// YNR076W | YOL162W | YAL056W | YPR165W |
| YCR075C | YGR044C | YLL066W-B | YOL164W | YCR020C-A | YJR056C |
| YCR076C | YGR047C | YLR001C | YOL164W-A | YGL077C | YBR131W |
| YCR077C | YGR052W | YLR004C | YOL166W-A | YMR065W | YOR390W /// YPL279C |
| YCR079W | YGR053C | YLR006C | YOR001W | YOL057W | YKL033W-A |
| YCR081W | YGR054W | YLR007W | YOR002W | YER044C-A | YGR010W |
| YCR083W | YGR056W | YLR010C | YOR005C | YOR032W-A | YPR179C |
| YCR084C | YGR058W | YLR012C | YOR007C | YDR287W | YML120C |

| | | | | | |
|---|---|---|---|---|---|
| YCR086W | YGR061C | YLR013W | YOR008C | YNL024C | YNL157W |
| YCR088W | YGR062C | YLR014C | YOR008C-A | YDR243C | YMR321C /// YPL273W |
| YCR089W | YGR065C | YLR015W | YOR010C | YPL172C | YJL155C |
| YCR091W | YGR066C | YLR016C | YOR011W | YGL084C | YER148W |
| YCR092C | YGR067C | YLR017W | YOR011W-A | YER126C | YLR180W |
| YCR093W | YGR068C | YLR018C | YOR012W | YLR262C-A | YOR114W |
| YCR094W | YGR075C | YLR020C | YOR016C | YBR138C | YGL021W |
| YCR099C | YGR078C | YLR021W | YOR017W | YCL034W | YDR060W |
| YCR104W /// YIR041W | YGR080W | YLR022C | YOR018W | YOL045W | YCR027C |
| YCR106W | YGR081C | YLR023C | YOR019W | YEL015W | YDR273W |
| YCR107W | YGR083C | YLR024C | YOR022C | YBL074C | YMR288W |
| YCR107W | YGR085C | YLR026C | YOR023C | YCR097W | YLR066W |
| YCR107W /// YOL165C | YGR085C /// YPR102C | YLR027C | YOR027W | YCR075W-A | YPL218W |
| YCR108C | YGR086C | YLR028C | YOR028C | YMR279C | YGR261C |
| YDL002C | YGR088W | YLR029C | YOR030W | YLR008C | YJR084W |
| YDL005C | YGR089W | YLR032W | YOR033C | YKR024C | YIL104C |
| YDL007W | YGR090W | YLR034C | YOR034C | YHR060W | YAR061W /// YHR212W-A |
| YDL010W | YGR091W | YLR035C | YOR034C-A | YOR365C | YGL063W |
| YDL012C | YGR093W | YLR037C | YOR035C | YLR367W | YHR002W |
| YDL013W | YGR094W | YLR039C | YOR037W | YNR063W | YPL024W |
| YDL014W | YGR095C | YLR042C | YOR040W | YKR005C | YHL003C |
| YDL017W | YGR096W | YLR044C | YOR042W | YLR298C | YPL099C |
| YDL018C | YGR097W | YLR045C | YOR046C | YLR003C | YNL006W |
| YDL019C | YGR098C | YLR046C | YOR048C | YGR045C | YLR325C |

| | | | | | |
|---|---|---|---|---|---|
| YDL021W | YGR099W | YLR048W | YOR049C | YBR301W | YMR158W |
| YDL022W | YGR100W | YLR050C | YOR051C | YNL083W | YJR005C-A |
| YDL024C | YGR102C | YLR052W | YOR054C | YJR002W | YGR077C |
| YDL025C | YGR104C | YLR053C | YOR057W | YDR299W | YLL049W |
| YDL027C | YGR109C | YLR055C | YOR059C | YLR466C-B | YGL080W |
| YDL028C | YGR109W-A /// YGR109W-B /// YIL080W /// YIL082W /// YIL082W-A | YLR056W | YOR061W | YGR275W | YOR129C |
| YDL029W | YGR109W-B /// YIL080W | YLR057W | YOR065W | YGR262C | YLR268W |
| YDL031W | YGR109W-B /// YIL080W /// YIL082W-A | YLR058C | YOR066W | YBR294W | YDR458C |
| YDL033C | YGR110W | YLR059C | YOR068C | YOL023W | YHR170W |
| YDL035C | YGR111W | YLR067C | YOR069W | YPL053C | YJR004C |
| YDL036C | YGR112W | YLR069C | YOR070C | YPL271W | YBR092C |
| YDL039C | YGR116W | YLR070C | YOR071C | YJR106W | YOR095C |
| YDL040C | YGR117C | YLR071C | YOR072W-B | YGL055W | YPL202C |
| YDL045C | YGR119C | YLR072W | YOR073W | YER036C | YNL138W-A |
| YDL046W | YGR120C | YLR073C | YOR074C | YBR033W | YLR163C |
| YDL047W | YGR121C | YLR075W | YOR076C | YLR147C | YPR048W |
| YDL048C | YGR122W | YLR077W | YOR077W | YBR056W-A | YJR123W |
| YDL053C | YGR124W | YLR078C | YOR078W | YLR117C | YJR068W |
| YDL054C | YGR125W | YLR079W | YOR079C | YDL020C | YJR053W |
| YDL055C | YGR127W | YLR080W | YOR081C | YDR183W | YMR022W |
| YDL056W | YGR129W | YLR081W | YOR084W | YOL014W | YDR023W |
| YDL057W | YGR130C | YLR084C | YOR086C | YDL147W | YLR185W |

| YDL058W | YGR132C | YLR086W | YOR087W | YLR423C | YGL255W |
|---|---|---|---|---|---|
| YDL060W | YGR133W | YLR087C | YOR090C | YLR225C | YDR212W |
| YDL064W | YGR134W | YLR088W | YOR091W | YJL157C | YGL006W-A |
| YDL066W | YGR136W | YLR089C | YOR092W | YER173W | YGR143W |
| YDL072C | YGR138C | YLR090W | YOR093C | YER180C | YLR283W |
| YDL073W | YGR138C /// YPR156C | YLR091W | YOR097C | YMR290C | YDL219W |
| YDL074C | YGR140W | YLR092W | YOR098C | YOL077C | YML069W |
| YDL076C | YGR141W | YLR093C | YOR099W | YOR004W | YAR035C-A |
| YDL077C | YGR144W | YLR095C | YOR104W | YDR281C | YMR061W |
| YDL078C | YGR146C | YLR096W | YOR108W | YCR101C | YML038C |
| YDL079C | YGR146C-A | YLR097C | YOR109W | YDR087C | YMR194W |
| YDL080C | YGR150C | YLR098C | YOR110W | YBR167C | YLR418C |
| YDL082W | YGR153W | YLR099C | YOR111W | YHR089C | YBR095C |
| YDL086W | YGR156W | YLR099W-A | YOR112W | YOR067C | YER093C-A |
| YDL087C | YGR157W | YLR100W | YOR113W | YBR247C | YBL025W |
| YDL089W | YGR158C | YLR102C | YOR115C | YGL005C | YDL067C |
| YDL091C | YGR161C | YLR105C | YOR118W | YGR128C | YDR382W |
| YDL093W | YGR162W | YLR106C | YOR119C | YHR079C-A | YKL056C |
| YDL095W | YGR163W | YLR109W | YOR120W | YJR136C | YPL145C |
| YDL099W | YGR165W | YLR113W | YOR122C | YJL006C | YKL179C |
| YDL100C | YGR166W | YLR115W | YOR123C | YMR033W | YOR194C |
| YDL101C | YGR167W | YLR116W | YOR124C | YNL111C | YMR235C |
| YDL102W | YGR169C | YLR119W | YOR125C | YGR084C | YBL035C |
| YDL103C | YGR169C-A | YLR121C | YOR126C | YOR260W | YDR283C |
| YDL104C | YGR170W | YLR126C | YOR127W | YPR187W | YJL183W |
| YDL105W | YGR172C | YLR127C | YOR128C | YER078W-A | YPL260W |
| YDL106C | YGR173W | YLR128W | YOR130C | YCL055W | YOR131C |
| YDL108W | YGR175C | YLR129W | YOR132W | YNL220W | YDL090C |

| | | | | | |
|---|---|---|---|---|---|
| YDL109C | YGR178C | YLR130C | YOR134W | YDR111C | YFL007W |
| YDL110C | YGR179C | YLR131C | YOR136W | YOR107W | YJL069C |
| YDL111C | YGR180C | YLR132C | YOR137C | YHR187W | YCL054W |
| YDL113C | YGR181W | YLR134W | YOR138C | YNL077W | YDR162C |
| YDL115C | YGR184C | YLR135W | YOR140W | YBR238C | YDR174W |
| YDL116W | YGR185C | YLR136C | YOR142W | YHR037W | YMR039C |
| YDL117W | YGR186W | YLR137W | YOR144C | YDL160C-A | YNR071C |
| YDL119C | YGR187C | YLR138W | YOR151C | YMR010W | YIR012W |
| YDL120W | YGR188C | YLR139C | YOR152C | YDR179C | YDR125C |
| YDL122W | YGR189C | YLR141W | YOR154W | YGL116W | YCL005W-A |
| YDL123W | YGR191W | YLR142W | YOR155C | YLR165C | YEL069C /// YNR072W |
| YDL124W | YGR192C | YLR143W | YOR156C | YNR004W | YBR171W |
| YDL125C | YGR193C | YLR144C | YOR160W | YNL070W | YBL068W |
| YDL126C | YGR194C | YLR148W | YOR161C | YBR219C | YCR087C-A |
| YDL127W | YGR195W | YLR149C | YOR161C-C | YLR036C | YJR089W |
| YDL129W | YGR196C | YLR150W | YOR162C | YCL057C-A | YAL008W |
| YDL130W-A | YGR199W | YLR151C | YOR163W | YDL065C | YLR120C |
| YDL131W | YGR200C | YLR152C | YOR164C | YCL001W | YOL166W-A |
| YDL132W | YGR201C | YLR153C | YOR168W | YMR282C | YIL076W |
| YDL134C | YGR203W | YLR154W-F | YOR173W | YML081C-A | YBR288C |
| YDL135C | YGR204W | YLR155C /// YLR157C /// YLR158C /// YLR160C | YOR174W | YPL042C | YOR294W |
| YDL138W | YGR207C | YLR156W /// YLR157W-E /// YLR159W /// YLR161W | YOR175C | YJL003W | YOR116C |

| | | | | | |
|---|---|---|---|---|---|
| YDL139C | YGR208W | YLR157W-E | YOR176W | YNL148C | YOR385W |
| YDL140C | YGR213C | YLR162W | YOR177C | YBL054W | YBR184W |
| YDL141W | YGR214W | YLR162W-A | YOR179C | YGR212W | YOL080C |
| YDL142C | YGR217W | YLR164W | YOR181W | YNL121C | YOL011W |
| YDL144C | YGR218W | YLR166C | YOR184W | YJL096W | YGR087C |
| YDL145C | YGR221C | YLR170C | YOR185C | YER012W | YFR011C |
| YDL146W | YGR223C | YLR173W | YOR187W | YGR121W-A | YJL145W |
| YDL149W | YGR225W | YLR174W | YOR188W | YFR004W | YBR191W /// YPL079W |
| YDL150W | YGR226C | YLR175W | YOR191W | YLR049C | YBR188C |
| YDL154W | YGR227W | YLR176C | YOR192C | YPL071C | YBR263W |
| YDL156W | YGR229C | YLR177W | YOR192C-C | YOR269W | YJL146W |
| YDL159W | YGR231C | YLR178C | YOR193W | YDL063C | YGR135W |
| YDL159W-A | YGR233C | YLR179C | YOR195W | YBR165W | YLL046C |
| YDL161W | YGR235C | YLR181C | YOR196C | YDL247W /// YJR160C | YML118W |
| YDL164C | YGR237C | YLR182W | YOR197W | YAL025C | YOR062C |
| YDL165W | YGR238C | YLR183C | YOR201C | YKR056W | YOL115W |
| YDL168W | YGR239C | YLR186W | YOR202W | YPR169W | YFL046W |
| YDL169C | YGR240C | YLR187W | YOR205C | YKR051W | YKL162C |
| YDL170W | YGR240C-A | YLR188W | YOR207C | YER168C | YAL003W |
| YDL171C | YGR244C | YLR189C | YOR208W | YGL226C-A | YBR125C |
| YDL173W | YGR245C | YLR192C | YOR209C | YBR264C | YDR498C |
| YDL174C | YGR246C | YLR193C | YOR211C | YHR191C | YGR171C |
| YDL176W | YGR247W | YLR194C | YOR213C | YML005W | YPR040W |
| YDL177C | YGR248W | YLR195C | YOR214C | YGR123C | YMR145C |
| YDL178W | YGR249W | YLR199C | YOR215C | YFL040W | YOL092W |
| YDL180W | YGR250C | YLR201C | YOR216C | YCR090C | YPL002C |

| | | | | | |
|---|---|---|---|---|---|
| YDL181W | YGR251W | YLR203C | YOR217W | YDR139C | YPR199C |
| YDL182W | YGR252W | YLR206W | YOR219C | YGR063C | YOR178C |
| YDL185W | YGR253C | YLR207W | YOR220W | YGL256W | YMR309C |
| YDL186W | YGR254W | YLR208W | YOR221C | YLR415C | YMR028W |
| YDL188C | YGR255C | YLR209C | YOR222W | YDR346C | YBR078W |
| YDL189W | YGR256W | YLR210W | YOR223W | YJL012C | YLR292C |
| YDL190C | YGR257C | YLR211C | YOR226C | YGR284C | YMR203W |
| YDL193W | YGR258C | YLR214W | YOR227W | YPR104C | YFR031C-A |
| YDL194W | YGR260W | YLR215C | YOR228C | YPL017C | YBL107C |
| YDL195W | YGR266W | YLR216C | YOR230W | YNL081C | YNL272C |
| YDL197C | YGR268C | YLR219W | YOR231W | YJR036C | YOR339C |
| YDL198C | YGR270W | YLR222C | YOR233W | YDR469W | YDL061C |
| YDL199C | YGR271W | YLR223C | YOR236W | YOR143C | YPL263C |
| YDL200C | YGR274C | YLR227C | YOR238W | YJL023C | YNL097C |
| YDL202W | YGR276C | YLR228C | YOR239W | YNL131W | YFR052W |
| YDL203C | YGR277C | YLR231C | YOR241W | YKL167C | YDR177W |
| YDL204W | YGR279C | YLR234W | YOR244W | YNL052W | YPL104W |
| YDL206W | YGR281W | YLR237W | YOR246C | YHR138C | YPL193W |
| YDL207W | YGR282C | YLR238W | YOR247W | YMR183C | YPL047W |
| YDL216C | YGR285C | YLR239C | YOR250C | YHR167W | YLR368W |
| YDL217C | YGR287C | YLR240W | YOR251C | YDR377W | YHR005C |
| YDL218W | YGR288W | YLR242C | YOR253W | YLR094C | YMR152W |
| YDL220C | YGR289C | YLR244C | YOR254C | YDL003W | YCR057C |
| YDL222C | YHL002W | YLR246W | YOR255W | YCL067C /// YCR039C /// YCR096C | YLL035W |
| YDL223C | YHL004W | YLR247C | YOR256C | YLR065C | YHR076W |
| YDL224C | YHL006C | YLR248W | YOR264W | YOR145C | YOR308C |
| YDL225W | YHL007C | YLR249W | YOR266W | YMR138W | YOR276W |

| | | | | | |
|---|---|---|---|---|---|
| YDL226C | YHL008C | YLR250W | YOR267C | YDL049C | YBR158W |
| YDL227C | YHL009C | YLR251W | YOR270C | YFL017W-A | YMR217W |
| YDL229W | YHL009W-A /// YHL009W-B /// YJL113W /// YJL114W /// YPL060C-A | YLR253W | YOR271C | YGR101W | YNL282W |
| YDL229W /// YNL209W | YHL009W-B /// YJL113W | YLR256W | YOR273C | YHR100C | YGL099W |
| YDL230W | YHL010C | YLR257W | YOR275C | YJL030W | YIL065C |
| YDL231C | YHL014C | YLR258W | YOR278W | YBR231C | YLR191W |
| YDL233W | YHL015W-A | YLR259C | YOR280C | YBR029C | YOL061W |
| YDL234C | YHL017W | YLR260W | YOR284W | YDR309C | YOR316C-A |
| YDL235C | YHL019C | YLR263W | YOR285W | YOR376W-A | YLR350W |
| YDL236W | YHL021C | YLR265C | YOR286W | YER056C-A | YML105C |
| YDL237W | YHL023C | YLR266C | YOR288C | YLR229C | YPR109W |
| YDL238C | YHL025W | YLR267W | YOR289W | YIL011W | YIL105C |
| YDL239C | YHL027W | YLR270W | YOR290C | YOL067C | YNL320W |
| YDL244W /// YFL058W /// YJR156C /// YNL332W | YHL028W | YLR271W | YOR291W | YBR192W | YKL216W |
| YDL246C /// YJR159W | YHL029C | YLR272C | YOR292C | YDR161W | YDR410C |
| YDR001C | YHL030W | YLR273C | YOR293C-A | YBR038W | YKR035W-A |
| YDR003W | YHL031C | YLR277C | YOR295W | YOR036W | YGR149W |
| YDR003W-A | YHL032C | YLR278C | YOR296W | YKR039W | YCR015C |
| YDR004W | YHL033C | YLR281C | YOR297C | YDR328C | YLR284C |
| YDR005C | YHL033C /// YLL045C | YLR285C-A | YOR298C-A | YLR241W | YMR074C |
| YDR006C | YHL034C | YLR286C | YOR298W | YOR058C | YNR048W |

| | | | | | |
|---|---|---|---|---|---|
| YDR009W | YHL035C | YLR288C | YOR299W | YLR103C | YER092W |
| YDR011W | YHL036W | YLR289W | YOR301W | YKL003C | YLR372W |
| YDR016C | YHL038C | YLR290C | YOR302W | YHR039C-A | YKL021C |
| YDR017C | YHL040C | YLR291C | YOR303W | YDR101C | YLR406C |
| YDR018C | YHL042W | YLR293C | YOR304W | YCR082W | YPR102C |
| YDR019C | YHL043W | YLR295C | YOR306C | YDR497C | YDL148C |
| YDR020C | YHL044W | YLR297W | YOR307C | YHL012W | YPR155C |
| YDR022C | YHL047C | YLR299W | YOR310C | YAR033W | YMR146C |
| YDR025W | YHL048W | YLR300W | YOR311C | YCR066W | YOR352W |
| YDR026C | YHR001W | YLR301W | YOR316C | YER074W | YML001W |
| YDR027C | YHR001W-A | YLR303W | YOR317W | YOR159C | YNL134C |
| YDR028C | YHR003C | YLR304C | YOR320C | YER136W | YNL216W |
| YDR032C | YHR006W | YLR305C | YOR321W | YGR286C | YEL019C |
| YDR034C | YHR007C | YLR306W | YOR322C | YHR035W | YNL046W |
| YDR034W-B | YHR007C-A | YLR307C-A | YOR323C | YMR233W | YAL064W-B |
| YDR035W | YHR008C | YLR308W | YOR324C | YPL187W | YLR452C |
| YDR036C | YHR009C | YLR309C | YOR326W | YOL124C | YBL014C |
| YDR037W | YHR011W | YLR310C | YOR327C | YDL243C /// YFL057C | YDR098C |
| YDR038C | YHR012W | YLR312C | YOR328W | YNL259C | YMR137C |
| YDR038C /// YDR039C /// YDR040C | YHR013C | YLR313C | YOR329C | YHL016C | YNL232W |
| YDR041W | YHR015W | YLR313C | YOR330C | YDR267C | YLR213C |
| YDR043C | YHR016C | YLR314C | YOR332W | YLL066W-B | YLR243W |
| YDR044W | YHR017W | YLR315W | YOR334W | YHL001W | YGL161C |
| YDR046C | YHR018C | YLR316C | YOR335C | YOL018C | YEL013W |
| YDR047W | YHR019C | YLR318W | YOR336W | YJL127C | YJL168C |
| YDR049W | YHR020W | YLR319C | YOR337W | YOR242C | YCR014C |

| | | | | | |
|---|---|---|---|---|---|
| YDR050C | YHR022C | YLR320W | YOR338W | YPL210C | YJL208C |
| YDR051C | YHR023W | YLR321C | YOR341W | YBR044C | YGL060W |
| YDR052C | YHR024C | YLR323C | YOR347C | YER038C | YLR212C |
| YDR054C | YHR025W | YLR324W | YOR350C | YHR045W | YJR010W |
| YDR055W | YHR026W | YLR326W | YOR353C | YNL218W | YKL220C |
| YDR056C | YHR027C | YLR327C | YOR354C | YPR018W | YHR057C |
| YDR057W | YHR028C | YLR328W | YOR355W | YGR222W | YBR019C |
| YDR058C | YHR029C | YLR329W | YOR356W | YHR123W | YGL057C |
| YDR059C | YHR030C | YLR330W | YOR357C | YER078C | YLR118C |
| YDR061W | YHR031C | YLR332W | YOR358W | YPR068C | YER174C |
| YDR063W | YHR032W | YLR335W | YOR359W | YBL060W | YGR264C |
| YDR065W | YHR033W | YLR336C | YOR360C | YNL149C | YKL049C |
| YDR066C | YHR034C | YLR337C | YOR363C | YPL239W | YLR274W |
| YDR069C | YHR036W | YLR340W | YOR367W | YNL256W | YDL061C |
| YDR070C | YHR039C | YLR341W | YOR370C | YPL156C | YGL210W |
| YDR073W | YHR040W | YLR342W | YOR371C | YER187W | YPR057W |
| YDR074W | YHR041C | YLR342W-A | YOR372C | YBR050C | YPL096C-A |
| YDR076W | YHR042W | YLR343W | YOR373W | YIL029C | YAL016W |
| YDR077W | YHR043C | YLR344W | YOR374W | YMR122W-A | YNR022C |
| YDR080W | YHR043C /// YHR044C | YLR345W | YOR375C | YPR024W | YDR244W |
| YDR081C | YHR044C | YLR347C | YOR378W | YEL030W | YGL234W |
| YDR084C | YHR046C | YLR348C | YOR380W | YML080W | YLR054C |
| YDR085C | YHR047C | YLR351C | YOR381W | YHR121W | YOR259C |
| YDR088C | YHR048W | YLR352W | YOR382W | YLR156W /// YLR157W-D /// YLR159W /// YLR161W | YHR193C |

| | | | | | |
|---|---|---|---|---|---|
| YDR089W | YHR049W | YLR354C | YOR383C | YKL018C-A | YAL019W |
| YDR090C | YHR050W | YLR355C | YOR388C /// YPL275W | YDR254W | YGR224W |
| YDR092W | YHR050W-A | YLR356W | YOR389W | YPL243W | YGL135W /// YPL220W |
| YDR093W | YHR051W | YLR357W | YOR389W /// YPL277C | YLR200W | YNR028W |
| YDR096W | YHR054C /// YHR056C | YLR360W | YOR389W /// YPL278C | YNL211C | YCL005W |
| YDR097C | YHR058C | YLR362W | YOR394C-A | YNL078W | YNL252C |
| YDR099W | YHR061C | YLR364W | YPL003W | YLR388W | YML086C |
| YDR100W | YHR062C | YLR371W | YPL004C | YDL209C | YFL011W |
| YDR103W | YHR063C | YLR373C | YPL006W | YDL043C | YIL002W-A |
| YDR104C | YHR068W | YLR375W | YPL007C | YJL011C | YOR342C |
| YDR105C | YHR069C | YLR377C | YPL008W | YJR063W | YKL163W |
| YDR106W | YHR070W | YLR378C | YPL009C | YER133W | YPL244C |
| YDR108W | YHR071W | YLR380W | YPL011C | YER050C | YDL213C |
| YDR109C | YHR072W | YLR381W | YPL012W | YOL042W | YIL024C |
| YDR110W | YHR073W | YLR382C | YPL014W | YDL192W | YDR123C |
| YDR113C | YHR074W | YLR383W | YPL015C | YPR182W | YGL147C |
| YDR116C | YHR077C | YLR384C | YPL016W | YOL039W | YPR019W |
| YDR117C | YHR078W | YLR386W | YPL020C | YDL211C | YMR135C |
| YDR118W | YHR079C | YLR387C | YPL021W | YAR010C /// YBR012W-A | YOR361C |
| YDR119W | YHR080C | YLR389C | YPL022W | YDR322C-A | YDR379W |
| YDR122W | YHR082C | YLR390W | YPL023C | YCL066W /// YCR040W | YFL001W |
| YDR126W | YHR083W | YLR390W-A | YPL026C | YGR197C | YLR413W |

| | | | | | |
|---|---|---|---|---|---|
| YDR127W | YHR087W | YLR394W | YPL028W | YKR030W | YHR147C |
| YDR128W | YHR088W | YLR396C | YPL029W | YNL151C | YLR218C |
| YDR129C | YHR092C | YLR397C | YPL031C | YMR260C | YDR240C |
| YDR130C | YHR094C | YLR398C | YPL032C | YDL133C-A /// YDL184C | YDR107C |
| YDR131C | YHR096C | YLR399C | YPL033C | YDR373W | YNL249C |
| YDR132C | YHR097C | YLR404W | YPL034W | YGL169W | YML115C |
| YDR135C | YHR098C | YLR405W | YPL037C | YKL043W | YGR145W |
| YDR137W | YHR099W | YLR406C-A | YPL038W | YGR152C | YDR337W |
| YDR140W | YHR101C | YLR407W | YPL039W | YKR053C | YMR013C |
| YDR141C | YHR102W | YLR410W | YPL040C | YNL313C | YKL077W |
| YDR142C | YHR104W | YLR414C | YPL041C | YDR465C | YJL019W |
| YDR143C | YHR106W | YLR419W | YPL045W | YDR447C /// YML024W | YGL189C |
| YDR144C | YHR107C | YLR420W | YPL046C | YHR075C | YMR241W |
| YDR145W | YHR108W | YLR422W | YPL048W | YHR124W | YDL097C |
| YDR148C | YHR109W | YLR424W | YPL049C | YPR103W | YCR045C |
| YDR150W | YHR110W | YLR425W | YPL050C | YDL133W | YML022W |
| YDR152W | YHR111W | YLR427W | YPL055C | YKL160W | YER161C |
| YDR153C | YHR112C | YLR429W | YPL056C | YLR224W | YGL103W |
| YDR155C | YHR113W | YLR430W | YPL057C | YGL225W | YDL001W |
| YDR156W | YHR114W | YLR431C | YPL058C | YJR086W | YOR047C |
| YDR158W | YHR115C | YLR432W | YPL059W | YMR242C /// YOR312C | YHR205W |
| YDR159W | YHR117W | YLR436C | YPL060W | YLR205C | YBR114W |
| YDR160W | YHR118C | YLR437C | YPL061W | YPL254W | YMR211W |
| YDR163W | YHR119W | YLR438W | YPL063W | YDR138W | YLR040C |

| YDR164C | YHR120W | YLR439W | YPL065W | YGR118W /// YPR132W | YPR173C |
|---|---|---|---|---|---|
| YDR166C | YHR122W | YLR440C | YPL066W | YDL030W | YDL201W |
| YDR168W | YHR126C | YLR441C | YPL067C | YFR042W | YKL165C |
| YDR169C | YHR127W | YLR442C | YPL068C | YGL142C | YDR513W |
| YDR169C-A | YHR128W | YLR443W | YPL072W | YOR362C | YLR361C |
| YDR170C | YHR129C | YLR445W | YPL074W | YPL266W | YER087W |
| YDR171W | YHR132C | YLR446W | YPL075W | YOR287C | YLR033W |
| YDR176W | YHR133C | YLR447C | YPL076W | YLR083C | YJR034W |
| YDR178W | YHR134W | YLR448W | YPL077C | YDL137W | YLR361C-A |
| YDR179W-A | YHR135C | YLR449W | YPL078C | YNL207W | YHR190W |
| YDR180W | YHR137W | YLR450W | YPL079W | YEL021W | YGR295C |
| YDR181C | YHR140W | YLR451W | YPL081W | YPR001W | YHR181W |
| YDR182W | YHR142W | YLR454W | YPL082C | YCR072C | YML064C |
| YDR186C | YHR143W | YLR455W | YPL083C | YKL098W | YBL092W |
| YDR188W | YHR146W | YLR457C | YPL084W | YOL041C | YNL188W |
| YDR189W | YHR149C | YLR459W | YPL085W | YJL036W | YOR096W |
| YDR190C | YHR150W | YLR461W /// YOL161C | YPL086C | YBR196C-B | YGL120C |
| YDR194C | YHR154W | YML004C | YPL087W | YDR151C | YLR411W |
| YDR194W-A | YHR155W | YML006C | YPL088W | YMR285C | YKL187C |
| YDR197W | YHR156C | YML007C-A | YPL089C | YDR333C | YDR514C |
| YDR198C | YHR158C | YML008C | YPL091W | YLR388W | YMR184W |
| YDR200C | YHR161C | YML010W | YPL092W | YLR409C | YKL062W |
| YDR202C | YHR162W | YML011C | YPL093W | YDR308C | YIR021W-A |
| YDR204W | YHR163W | YML013W | YPL096W | YNL262W | YMR133W |
| YDR205W | YHR164C | YML014W | YPL097W | YOL019W | YBL099W |
| YDR206W | YHR165C | YML015C | YPL098C | YOR265W | YKL046C |

| YDR207C | YHR166C | YML016C | YPL100W | YLL004W | YPR078C |
|---|---|---|---|---|---|
| YDR208W | YHR169W | YML019W | YPL101W | YKL037W | YDR316W |
| YDR211W | YHR171W | YML021C | YPL103C | YKL096W-A | YEL064C |
| YDR213W | YHR172W | YML023C | YPL105C | YDR210W | YGR198W |
| YDR214W | YHR174W | YML025C | YPL106C | YKR088C | YGR003W |
| YDR216W | YHR176W | YML027W | YPL107W | YKR081C | YBR024W |
| YDR217C | YHR178W | YML028W | YPL109C | YNL155W | YKR006C |
| YDR218C | YHR179W | YML029W | YPL110C | YER029C | YMR208W |
| YDR219C | YHR182W | YML030W | YPL111W | YGL231C | YFL005W |
| YDR222W | YHR183W | YML031W | YPL112C | YOR304C-A | YLR376C |
| YDR223W | YHR184W | YML032C | YPL115C | YMR315W-A | YDL114W |
| YDR224C | YHR185C | YML034W | YPL116W | YNL145W | YLR245C |
| YDR225W | YHR186C | YML035C | YPL117C | YGR267C | YBR093C |
| YDR226W | YHR188C | YML042W | YPL120W | YOR103C | YER080W |
| YDR229W | YHR192W | YML047C | YPL121C | YIR028W | YML116W |
| YDR231C | YHR195W | YML049C | YPL122C | YKL137W | YOR384W |
| YDR232W | YHR198C | YML050W | YPL123C | YOR020C | YOR368W |
| YDR233C | YHR199C | YML051W | YPL124W | YGR243W | YHR144C |
| YDR234W | YHR200W | YML052W | YPL125W | YJL027C | YLR110C |
| YDR235W | YHR201C | YML056C | YPL126W | YKR085C | YBR259W |
| YDR236C | YHR202W | YML057W | YPL127C | YPR161C | YGR037C |
| YDR237W | YHR203C /// YJR145C | YML059C | YPL129W | YJL216C | YNL064C |
| YDR238C | YHR204W | YML060W | YPL132W | YJL209W | YGL048C |
| YDR239C | YHR206W | YML061C | YPL133C | YKL138C-A | YER100W |
| YDR242W | YHR207C | YML062C | YPL134C | YHR059W | YPL148C |
| YDR245W | YHR208W | YML063W | YPL135W | YOL137W | YBR094W |
| YDR246W | YHR209W | YML066C | YPL137C | YCR047C | YBL082C /// YBL083C |
| YDR246W-A | YHR210C | YML067C | YPL138C | YNR053C | YDR312W |

| YDR247W | YHR216W | YML070W | YPL139C | YLR009W | YOR085W |
|---|---|---|---|---|---|
| YDR248C | YIL001W | YML071C | YPL140C | YPL237W | YHL015W |
| YDR251W | YIL002C | YML072C | YPL141C | YKL196C | YMR132C |
| YDR252W | YIL003W | YML074C | YPL143W | YBR002C | YKL138C |
| YDR253C | YIL005W | YML075C | YPL144W | YGL175C | YKL190W |
| YDR255C | YIL007C | YML076C | YPL147W | YOL009C | YNL048W |
| YDR257C | YIL009C-A | YML078W | YPL149W | YPR133W-A | YEL037C |
| YDR258C | YIL010W | YML079W | YPL150W | YIR005W | YIR042C |
| YDR259C | YIL013C | YML081W | YPL152W | YBR162C | YJR124C |
| YDR260C | YIL014C-A | YML083C | YPL152W-A | YPL213W | YHR199C-A |
| YDR261C | YIL015W | YML087C | YPL153C | YGR206W | YOL130W |
| YDR263C | YIL017C | YML091C | YPL154C | YIL033C | YDR533C |
| YDR264C | YIL018W | YML092C | YPL158C | YOL086W-A | YDL044C |
| YDR265W | YIL020C | YML093W | YPL160W | YNL164C | YDL052C |
| YDR266C | YIL021W | YML094W | YPL161C | YLR197W | YER057C |
| YDR268W | YIL022W | YML095C | YPL163C | YCR016W | YER086W |
| YDR270W | YIL023C | YML096W | YPL164C | YBR155W | YAL018C |
| YDR272W | YIL026C | YML097C | YPL167C | YGR048W | YMR185W |
| YDR277C | YIL030C | YML098W | YPL168W | YJR141W | YDR319C |
| YDR282C | YIL031W | YML100W | YPL169C | YOR229W | YPL186C |
| YDR284C | YIL034C | YML101C | YPL170W | YOR206W | YGL123W |
| YDR288W | YIL036W | YML103C | YPL174C | YPL095C | YNL158W |
| YDR289C | YIL038C | YML104C | YPL175W | YBL018C | YDR391C |
| YDR291W | YIL039W | YML106W | YPL176C | YDR034C-A | YDR435C |
| YDR292C | YIL041W | YML107C | YPL177C | YML055W | YDR532C |
| YDR293C | YIL042C | YML109W | YPL180W | YIL009W | YPR186C |
| YDR295C | YIL043C | YML110C | YPL181W | YPR143W | YMR031C |
| YDR296W | YIL044C | YML111W | YPL183C | YKR074W | YOR064C |

| YDR297W | YIL045W | YML112W | YPL183W-A | YMR059W | YML012W |
|---|---|---|---|---|---|
| YDR298C | YIL046W | YML113W | YPL188W | YDR363W-A | YJL109C |
| YDR301W | YIL047C /// YIL047C-A | YML114C | YPL189C-A | YBR250W | YJL153C |
| YDR304C | YIL048W | YML117W | YPL190C | YHR091C | YMR283C |
| YDR305C | YIL050W | YML121W | YPL194W | YLR287C-A /// YOR182C | YEL017C-A |
| YDR306C | YIL051C | YML124C | YPL195W | YKL178C | YMR242C |
| YDR307W | YIL053W | YML125C | YPL196W | YPL159C | YMR153W |
| YDR310C | YIL055C | YML127W | YPL199C | YPL189W | YML002W |
| YDR311W | YIL056W | YML128C | YPL200W | YPR113W | YHR131C |
| YDR313C | YIL057C | YML130C | YPL203W | YMR001C | YKL011C |
| YDR314C | YIL060W | YML131W | YPL204W | YER025W | YNL022C |
| YDR315C | YIL061C | YMR001C-A | YPL206C | YPR112C | YHR014W |
| YDR317W | YIL062C | YMR004W | YPL207W | YJL038C | YBR088C |
| YDR320C | YIL063C | YMR005W | YPL208W | YDR447C | YBR198C |
| YDR321W | YIL066C | YMR006C | YPL212C | YGR031W | YJL050W |
| YDR323C | YIL067C | YMR008C | YPL215W | YDR079C-A | YGL213C |
| YDR325W | YIL068C | YMR009W | YPL216W | YDL167C | YDR347W |
| YDR326C | YIL070C | YMR012W | YPL217C | YDR147W | YPL128C |
| YDR329C | YIL072W | YMR014W | YPL219W | YLR005W | YKL045W |
| YDR331W | YIL073C | YMR016C | YPL221W | YER117W | YNL036W |
| YDR332W | YIL075C | YMR017W | YPL222W | YIL019W | YDL112W |
| YDR334W | YIL077C | YMR018W | YPL223C | YPR098C | YNR061C |
| YDR335W | YIL078W | YMR019W | YPL224C | YML068W | YER005W |
| YDR336W | YIL079C | YMR020W | YPL228W | YPL001W | YOR014W |
| YDR338C | YIL083C | YMR021C | YPL229W | YDL006W | YHR065C |
| YDR342C /// YDR343C | YIL085C | YMR023C | YPL230W | YLL060C | YBR244W |

| | | | | | |
|---|---|---|---|---|---|
| YDR349C | YIL087C | YMR024W | YPL231W | YOR020W-A | YMR157C |
| YDR350C | YIL088C | YMR025W | YPL232W | YDL085C-A | YIL133C |
| YDR351W | YIL089W | YMR026C | YPL233W | YKL005C | YJL001W |
| YDR352W | YIL092W | YMR027W | YPL235W | YGL098W | YDL084W |
| YDR353W | YIL093C | YMR029C | YPL236C | YIL052C | YMR246W |
| YDR354W | YIL094C | YMR035W | YPL240C | YBR069C | YLR392C |
| YDR356W | YIL095W | YMR036C | YPL241C | YDR002W | YPR121W |
| YDR357C | YIL097W | YMR037C | YPL246C | YOR171C | YPL069C |
| YDR358W | YIL102C | YMR038C | YPL247C | YIL144W | YGR113W |
| YDR359C | YIL107C | YMR041C | YPL249C | YPR132W | YDR477W |
| YDR363W | YIL108W | YMR042W | YPL250C | YOR101W | YKL113C |
| YDR365C | YIL109C | YMR043W | YPL252C | YOR257W | YNL047C |
| YDR367W | YIL110W | YMR044W | YPL253C | YDR450W /// YML026C | YOR234C |
| YDR368W | YIL111W | YMR047C | YPL255W | YPL155C | YDL004W |
| YDR369C | YIL112W | YMR048W | YPL256C | YJL180C | YML054C-A |
| YDR374C | YIL113W | YMR049C | YPL258C | YKL183C-A | YGR241C |
| YDR378C | YIL114C | YMR052W | YPL259C | YLR363C | YHR103W |
| YDR379C-A | YIL115C | YMR053C | YPL262W | YCR024C-A | YNL290W |
| YDR380W | YIL116W | YMR054W | YPL264C | YDR376W | YDR279W |
| YDR381W | YIL117C | YMR055C | YPL265W | YJL010C | YDL107W |
| YDR384C | YIL119C | YMR058W | YPL268W | YOR149C | YPL054W |
| YDR385W /// YOR133W | YIL120W | YMR062C | YPL269W | YDR500C | YPL178W |
| YDR388W | YIL121W | YMR064W | YPL270W | YLR412W | YBL057C |
| YDR389W | YIL122W | YMR067C | YPL272C | YLR031W | YFR050C |
| YDR390C | YIL123W | YMR068W | YPL273W | YIL084C | YNL101W |
| YDR392W | YIL124W | YMR069W | YPL274W | YHR160C | YDR185C |

| YDR393W | YIL125W | YMR070W | YPL277C | YNL044W | YJL049W |
|---|---|---|---|---|---|
| YDR394W | YIL126W | YMR073C | YPL279C | YPR028W | YNL279W |
| YDR395W | YIL128W | YMR076C | YPR002W | YKL053C-A | YML020W |
| YDR397C | YIL129C | YMR078C | YPR003C | YHR175W | YPR108W |
| YDR398W | YIL130W | YMR081C | YPR004C | YBR057C | YBR280C |
| YDR400W | YIL131C | YMR083W | YPR005C | YBR253W | YDR462W |
| YDR403W | YIL132C | YMR085W | YPR006C | YDL092W | YGR070W |
| YDR405W | YIL134C-A | YMR086W | YPR008W | YEL072W | YNL286W |
| YDR406W | YIL134W | YMR087W | YPR009W | YPL192C | YDR262W |
| YDR407C | YIL135C | YMR088C | YPR010C | YDL075W | YDL143W |
| YDR408C | YIL136W | YMR089C | YPR011C | YCR098C | YAR002W |
| YDR409W | YIL137C | YMR091C | YPR013C | YLR043C | YLR433C |
| YDR411C | YIL140W | YMR092C | YPR015C | YKL144C | YNR075C-A |
| YDR414C | YIL142W | YMR094W | YPR016C | YDR515W | YBR085C-A |
| YDR415C | YIL145C | YMR095C | YPR017C | YMR143W | YMR193W |
| YDR416W | YIL147C | YMR096W | YPR021C | YGR159C | YDL245C /// YJR158W |
| YDR419W | YIL149C | YMR097C | YPR022C | YDL208W | YBR267W |
| YDR420W | YIL150C | YMR099C | YPR023C | YMR143W | YGL061C |
| YDR421W | YIL151C | YMR100W | YPR025C | YBR034C | YGR280C |
| YDR422C | YIL152W | YMR102C | YPR026W | YDR449C | YNL219C |
| YDR423C | YIL153W | YMR104C | YPR027C | YBR006W | YOR394W /// YPL282C |
| YDR425W | YIL154C | YMR105C | YPR029C | YLL028W | YGR210C |
| YDR428C | YIL155C | YMR105W-A | YPR030W | YMR075W | YOR319W |
| YDR429C | YIL156W | YMR106C | YPR031W | YKL040C | YJL044C |
| YDR430C | YIL157C | YMR107W | YPR032W | YGL089C | YPR007C |
| YDR434W | YIL159W | YMR108W | YPR033C | YMR244C-A | YNL026W |

| YDR436W | YIL161W | YMR109W | YPR034W | YOR249C | YDR341C |
|---|---|---|---|---|---|
| YDR439W | YIL162W | YMR110C | YPR035W | YML058W | YPR159C-A |
| YDR440W | YIL164C | YMR111C | YPR036W | YGR131W | YLR011W |
| YDR443C | YIL165C | YMR112C | YPR036W-A | YFR005C | YBR283C |
| YDR444W | YIL169C | YMR113W | YPR037C | YGR147C | YKL164C |
| YDR446W | YIL169C /// YOL155C | YMR114C | YPR042C | YIR011C | YNL177C |
| YDR448W | YIL172C /// YJL221C /// YOL157C | YMR115W | YPR045C | YDR324C | YBR048W /// YDR025W |
| YDR451C | YIL173W /// YJL222W | YMR116C | YPR047W | YAL063C-A | YJR041C |
| YDR452W | YIL176C /// YJL223C | YMR118C | YPR049C | YPL173W | YOL094C |
| YDR453C | YIR001C | YMR119W | YPR051W | YGR232W | YAL064C-A |
| YDR456W | YIR002C | YMR120C | YPR054W | YGR202C | YOR106W |
| YDR457W | YIR003W | YMR121C | YPR055W | YNR070W | YKR060W |
| YDR459C | YIR004W | YMR123W | YPR058W | YOL001W | YBR181C /// YPL090C |
| YDR460W | YIR006C | YMR124W | YPR062W | YDR175C | YGR216C |
| YDR463W | YIR007W | YMR125W | YPR063C | YER030W | YDR286C |
| YDR464W | YIR008C | YMR126C | YPR065W | YJL140W | YEL032W |
| YDR466W | YIR009W | YMR127C | YPR066W | YOL024W | YPL131W |
| YDR468C | YIR010W | YMR128W | YPR067W | YJL148W | YLR082C |
| YDR470C | YIR013C | YMR129W | YPR069C | YBR127C | YPL171C |
| YDR472W | YIR014W | YMR131C | YPR070W | YNL129W | YKL078W |
| YDR473C | YIR016W | YMR136W | YPR071W | YBR096W | YDR294C |
| YDR475C | YIR017C | YMR139W | YPR072W | YMR011W | YAL007C |
| YDR476C | YIR018W | YMR142C | YPR074C | YBL008W | YKR094C |
| YDR478W | YIR019C | YMR144W | YPR075C | YPL157W | YKR064W |
| YDR479C | YIR023W | YMR148W | YPR079W | YJL205C | YPL214C |
| YDR480W | YIR025W | YMR149W | YPR081C | YOR094W | YGL190C |
| YDR481C | YIR026C | YMR150C | YPR083W | YOR283W | YPR147C |

| YDR482C | YIR027C | YMR154C | YPR084W | YOR377W | YJR152W |
|---|---|---|---|---|---|
| YDR483W | YIR029W | YMR156C | YPR085C | YOR100C | YGL113W |
| YDR484W | YIR030C | YMR158C-A | YPR086W | YBL005W-A /// YBL005W-B | YKL004W |
| YDR485C | YIR032C | YMR160W | YPR088C | YMR209C | YJL073W |
| YDR486C | YIR033W | YMR162C | YPR089W | YNR024W | YJL043W |
| YDR487C | YIR034C | YMR163C | YPR091C | YOR006C | YGR168C |
| YDR488C | YIR035C | YMR164C | YPR093C | YCL012C | YHR067W |
| YDR489W | YIR036C | YMR165C | YPR095C | YDR461W | YBR062C |
| YDR490C | YIR037W | YMR166C | YPR097W | YBR163W | YJL091C |
| YDR493W | YIR038C | YMR167W | YPR105C | YAL039C | YHR213W-A |
| YDR495C | YIR039C | YMR168C | YPR106W | YMR066W | YDL214C |
| YDR499W | YJL002C | YMR169C | YPR110C | YDR371W | YOR261C |
| YDR501W | YJL004C | YMR170C | YPR111W | YHR090C | YDR330W |
| YDR503C | YJL005W | YMR172W | YPR114W | YKR004C | YEL023C |
| YDR504C | YJL008C | YMR173W /// YMR173W-A | YPR115W | YJR118C | YJL210W |
| YDR505C | YJL013C | YMR174C | YPR116W | YML036W | YMR034C |
| YDR506C | YJL014W | YMR175W | YPR117W | YPL151C | YOR348C |
| YDR507C | YJL016W | YMR175W-A | YPR118W | YBR189W | YKL107W |
| YDR510W | YJL020C | YMR176W | YPR120C | YIL096C | YBR156C |
| YDR516C | YJL024C | YMR178W | YPR122W | YOR293W | YNL042W-B |
| YDR517W | YJL025W | YMR181C | YPR124W | YDR172W | YMR179W |
| YDR518W | YJL026W | YMR182C | YPR125W | YOL012C | YMR147W |
| YDR520C | YJL029C | YMR182W-A | YPR127W | YGL075C | |
| YDR522C | YJL031C | YMR186W | YPR128C | YDR068W | |
| YDR524C | YJL033W | YMR187C | YPR129W | YJL105W | |
| YDR527W | YJL034W | YMR189W | YPR131C | YFL041W-A | |

| | | | | |
|---|---|---|---|---|
| YDR530C | YJL037W | YMR190C | YPR134W | YLR025W |
| YDR531W | YJL039C | YMR191W | YPR135W | YBR203W |
| YDR534C | YJL041W | YMR192W | YPR139C | YLR233C |
| YDR538W | YJL042W | YMR194C-B | YPR140W | YPL184C |
| YDR539W | YJL045W | YMR195W | YPR141C | YHL022C |
| YDR540C | YJL046W | YMR196W | YPR144C | YIL006W |
| YDR541C | YJL047C | YMR197C | YPR145W | YGL253W |
| YDR545W /// YEL076C-A | YJL048C | YMR198W | YPR148C | YJR101W |
| YEL001C | YJL052W | YMR199W | YPR149W | YKR065C |
| YEL002C | YJL053W | YMR200W | YPR152C | YCR035C |
| YEL004W | YJL054W | YMR201C | YPR154W | YDR124W |
| YEL005C | YJL055W | YMR202W | YPR156C | YPL010W |
| YEL006W | YJL056C | YMR204C | YPR157W | YDR165W |
| YEL007W | YJL057C | YMR205C | YPR159W | YGR174C |
| YEL009C | YJL059W | YMR206W | YPR160W | YOR198C |
| YEL011W | YJL060W | YMR207C | YPR162C | YDR372C |
| YEL012W | YJL061W | YMR210W | YPR163C | YKL175W |
| YEL016C | YJL062W | YMR213W | YPR164W | YLL045C |
| YEL017W | YJL062W-A | YMR214W | YPR167C | YHR086W |
| YEL018W | YJL063C | YMR215W | YPR168W | YER185W |
| YEL020C | YJL065C | YMR216C | YPR171W | YLR417W |
| YEL022W | YJL066C | YMR218C | YPR172W | YDL051W |
| YEL024W | YJL068C | YMR219W | YPR174C | YCR105W |
| YEL025C | YJL070C | YMR220W | YPR175W | YLR460C |
| YEL027W | YJL071W | YMR221C | YPR176C | YLR466C-B |
| YEL029C | YJL074C | YMR222C | YPR178W | YDR424C |
| YEL031W | YJL076W | YMR224C | YPR180W | YOR052C |

| | | | | |
|---|---|---|---|---|
| YEL035C | YJL077C | YMR226C | YPR181C | YGR074W |
| YEL036C | YJL077W-B | YMR227C | YPR183W | YOR165W |
| YEL038W | YJL078C | YMR229C | YPR184W | YKL016C |
| YEL039C | YJL079C | YMR230W | YPR185W | YLL042C |
| YEL040W | YJL080C | YMR231W | YPR188C | YHR177W |
| YEL041W | YJL081C | YMR232W | YPR189W | YOR252W |
| YEL042W | YJL082W | YMR234W | YPR190C | YDR438W |
| YEL043W | YJL083W | YMR236W | YPR191W | YBR154C |
| YEL046C | YJL084C | YMR237W | YPR192W | YNL223W |
| YEL047C | YJL085W | YMR238W | YPR193C | YOL097W-A |
| YEL049W | YJL087C | YMR240C | YPR194C | YOR157C |
| YEL050C | YJL088W | YMR242W-A | YPR196W | YNL302C |
| YEL051W | YJL089W | YMR243C | YPR198W | YFL049W |

# Appendix Chapter 7

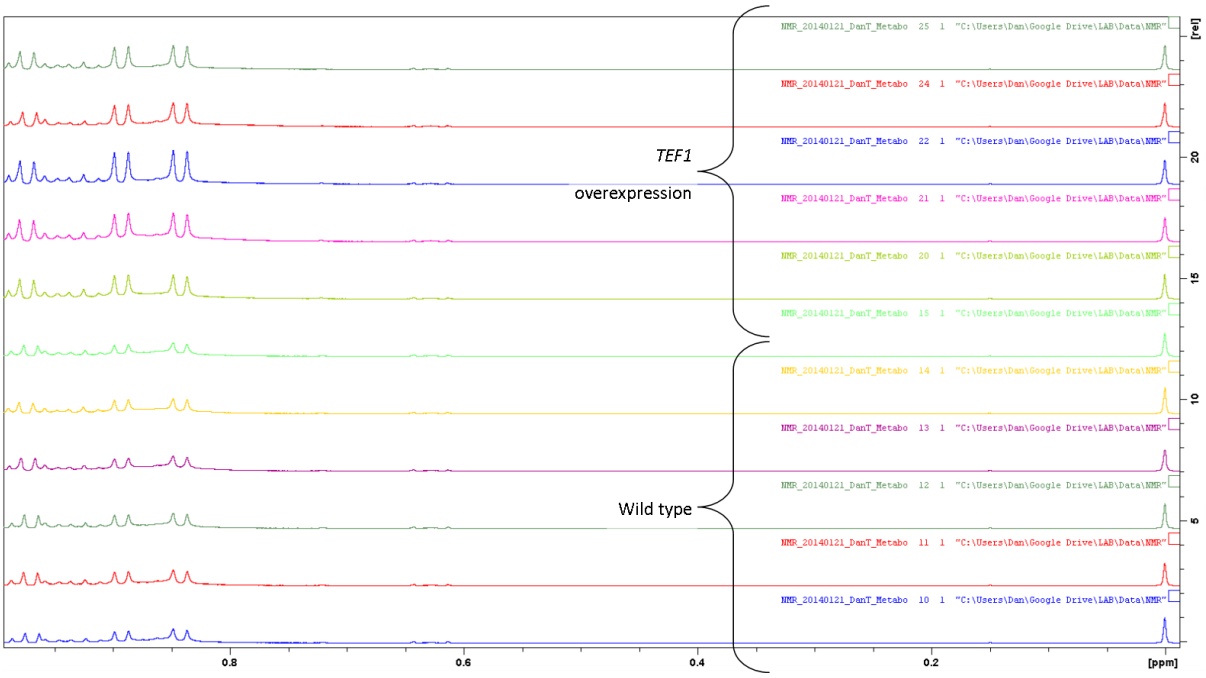


***App.4-a, A comparison of 0-1ppm of 1D proton spectra of wild type and TEF1 overexpression cells.***

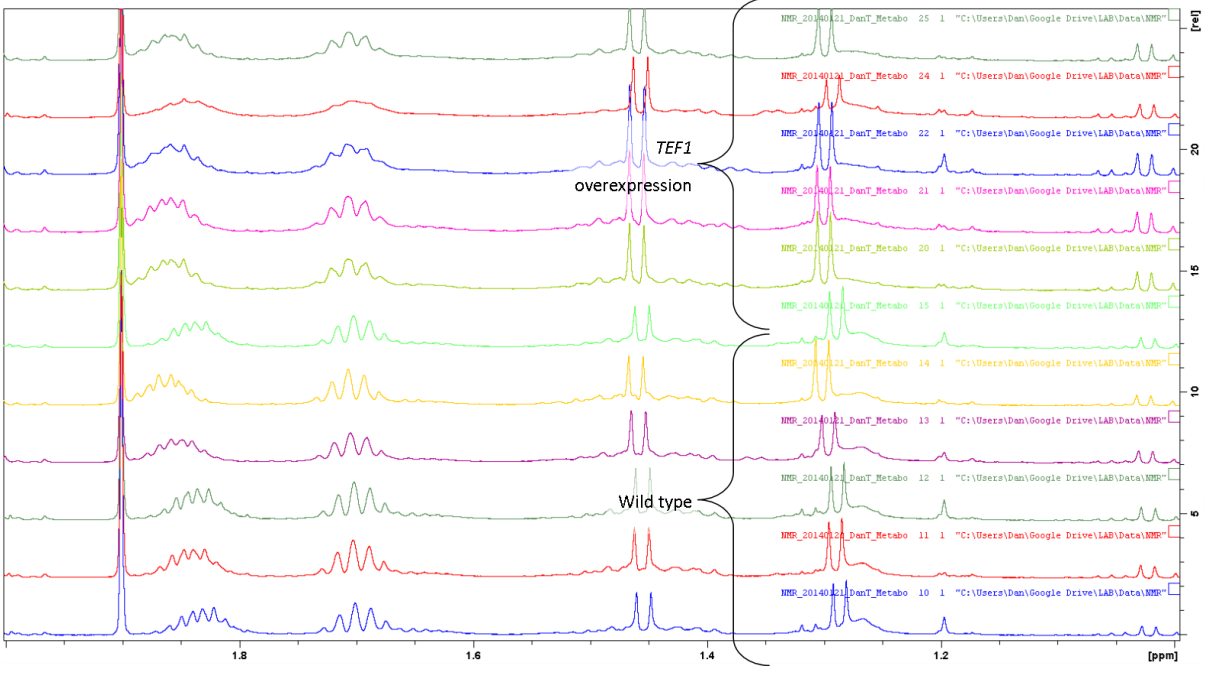


***App.4-b, A comparison of 1-2ppm of 1D proton spectra of wild type and TEF1 overexpression cells.***

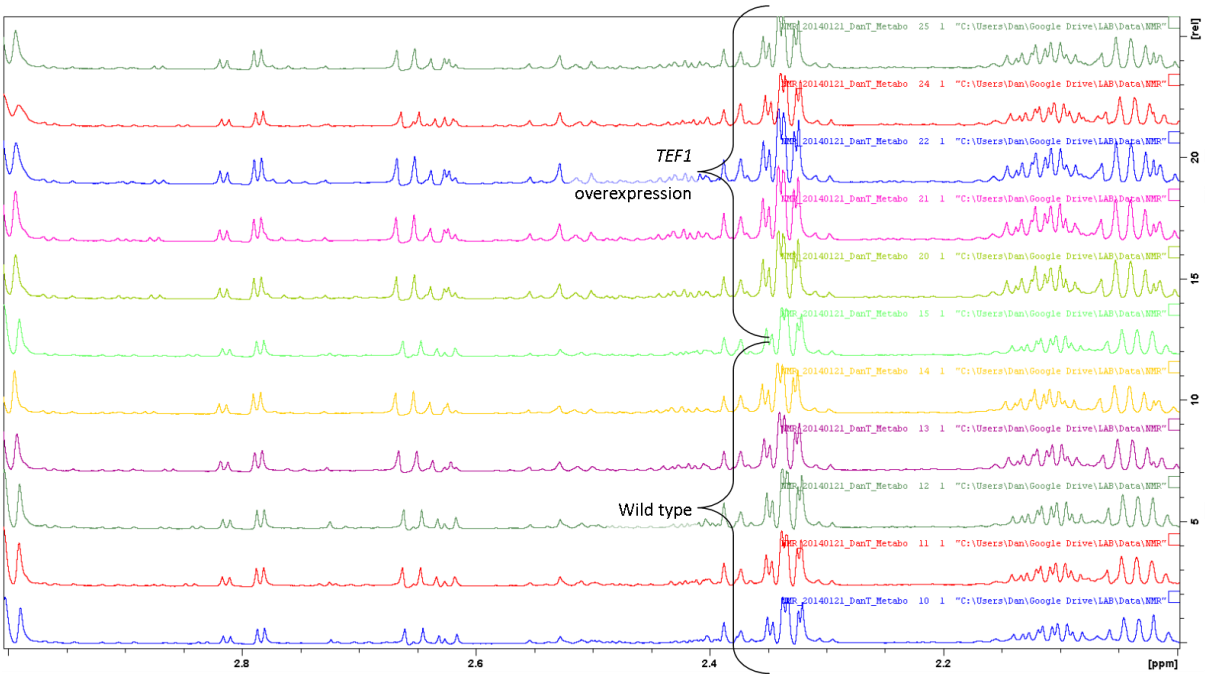


***App.4-c, A comparison of 2-3ppm of 1D proton spectra of wild type and TEF1 overexpression cells.***

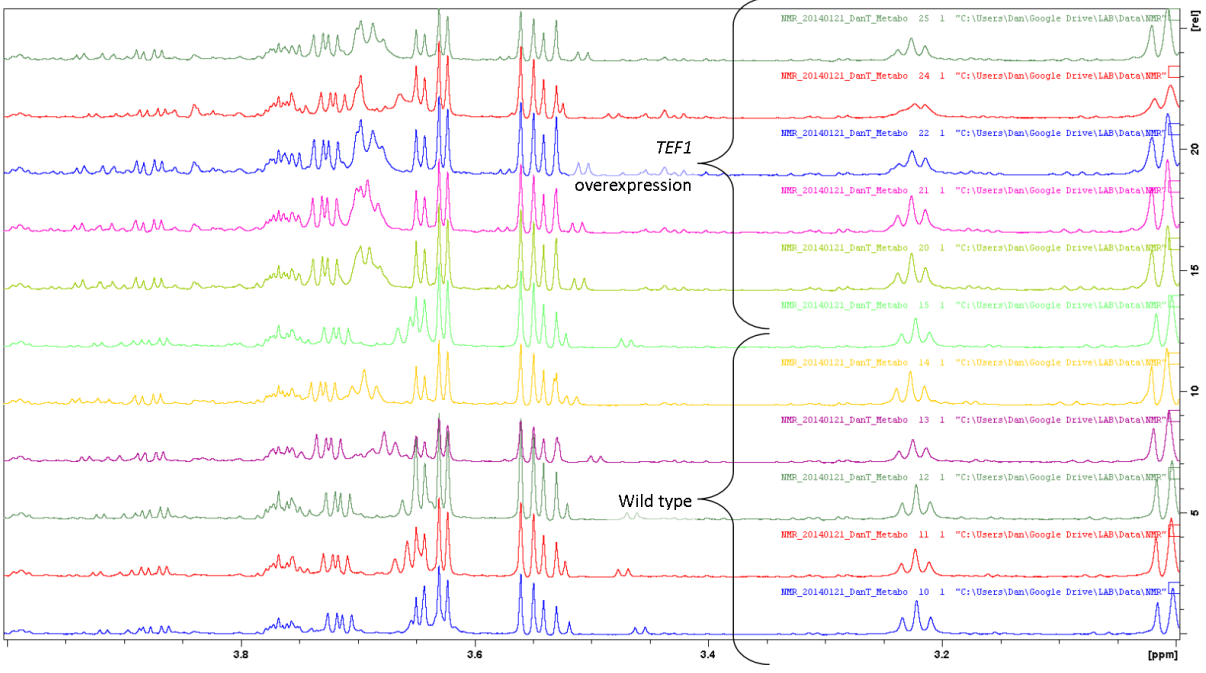


***App.4-d, A comparison of 3-4ppm of 1D proton spectra of wild type and TEF1 overexpression cells.***

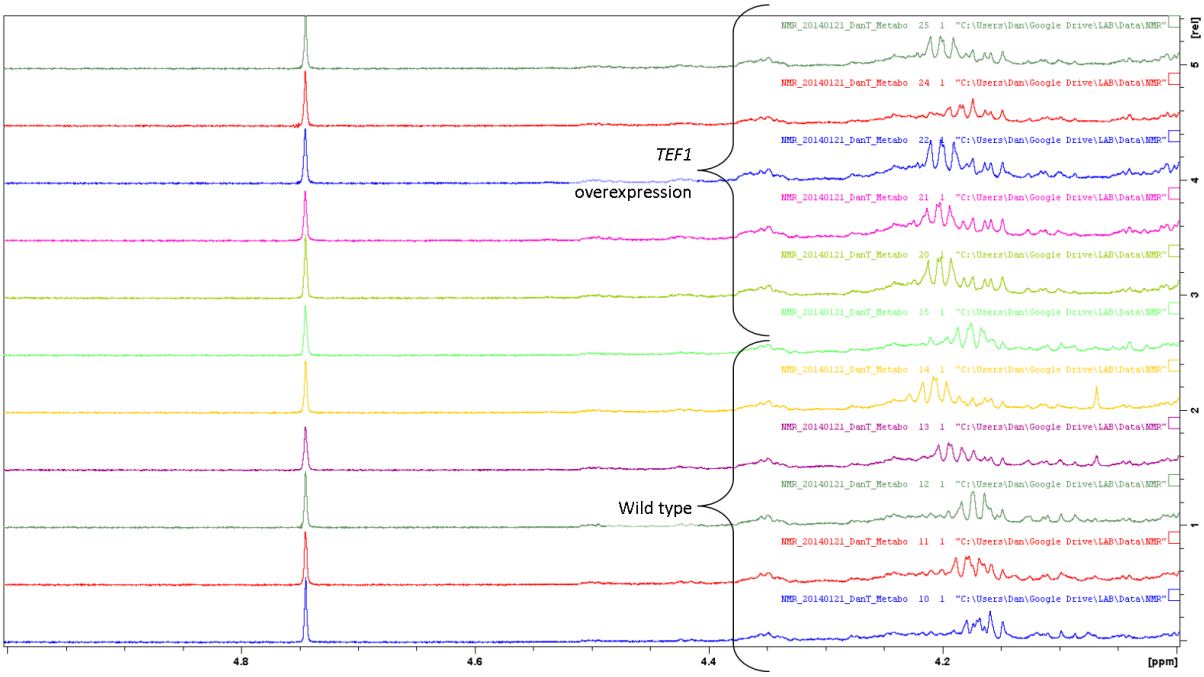


***App.4-e, A comparison of 4-5ppm of 1D proton spectra of wild type and TEF1 overexpression cells.***

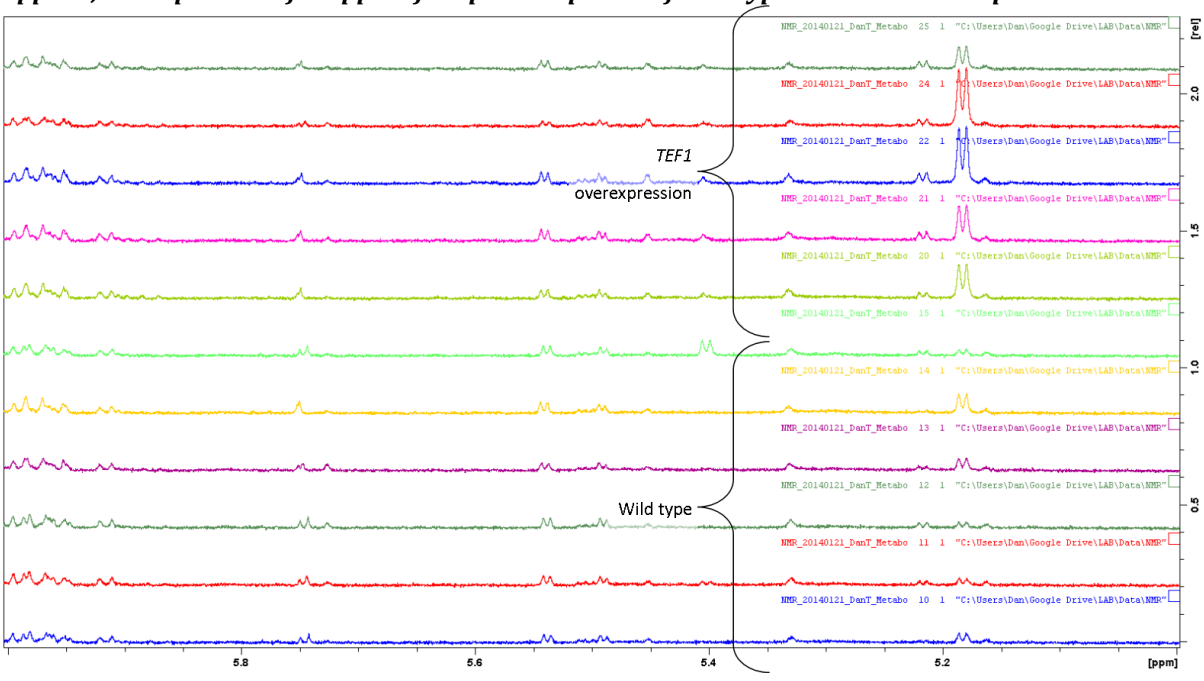


***App.4-f, A comparison of 5-6ppm of 1D proton spectra of wild type and TEF1 overexpression cells.***

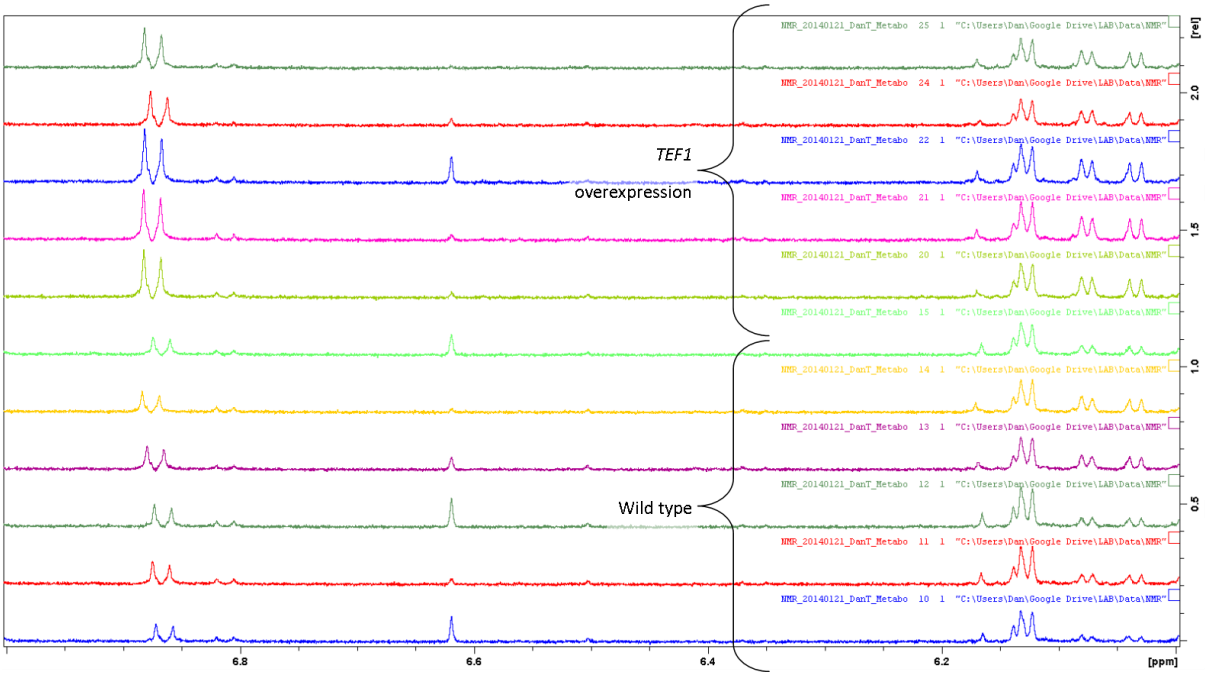


***App.4-g, A comparison of 6-7ppm of 1D proton spectra of wild type and TEF1 overexpression cells.***

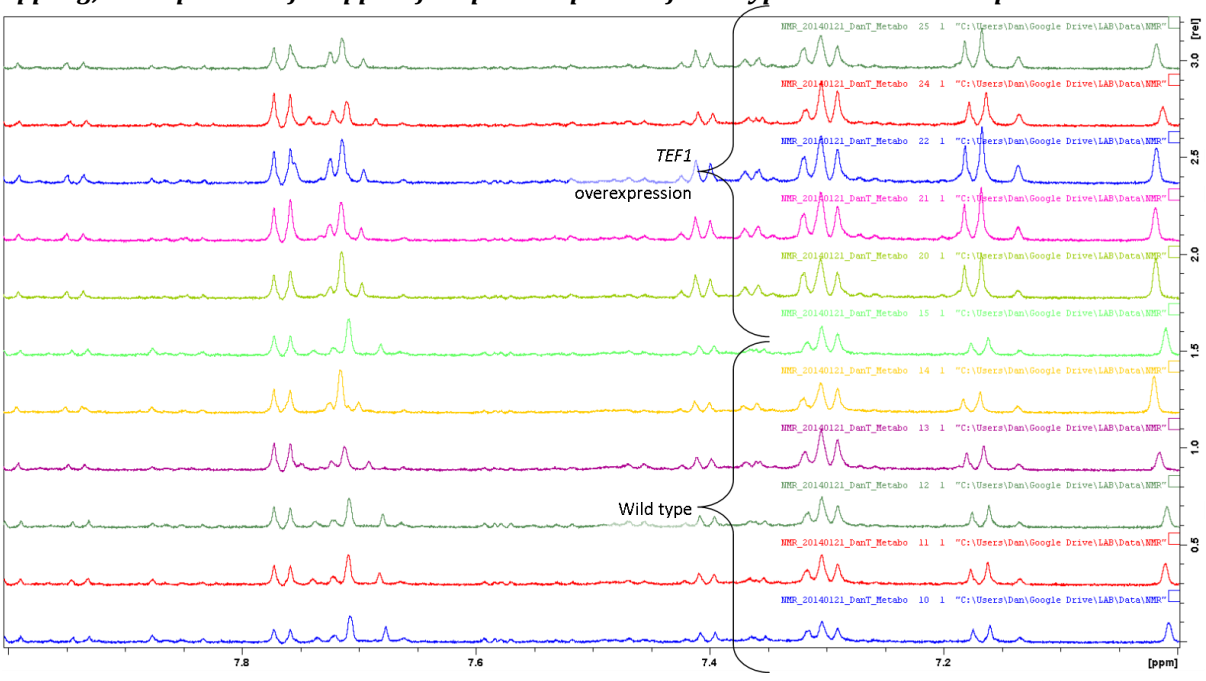


***App.4-h, A comparison of 7-8ppm of 1D proton spectra of wild type and TEF1 overexpression cells.***

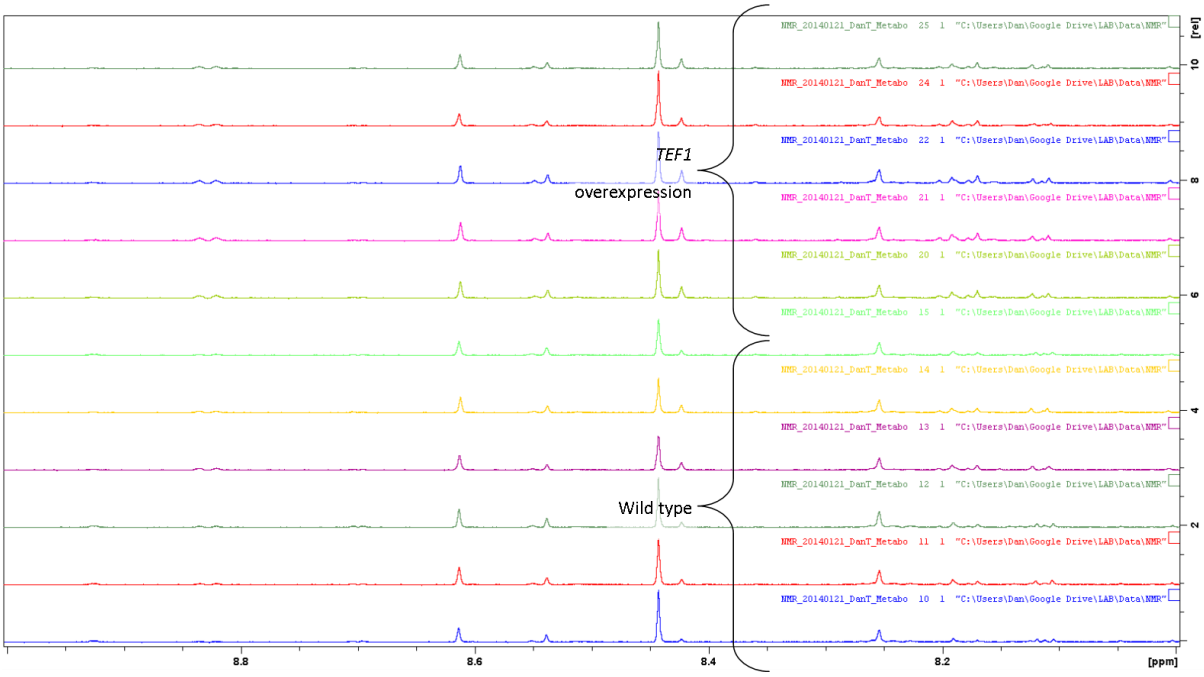


***App.4-i, A comparison of 8-9ppm of 1D proton spectra of wild type and TEF1 overexpression cells.***

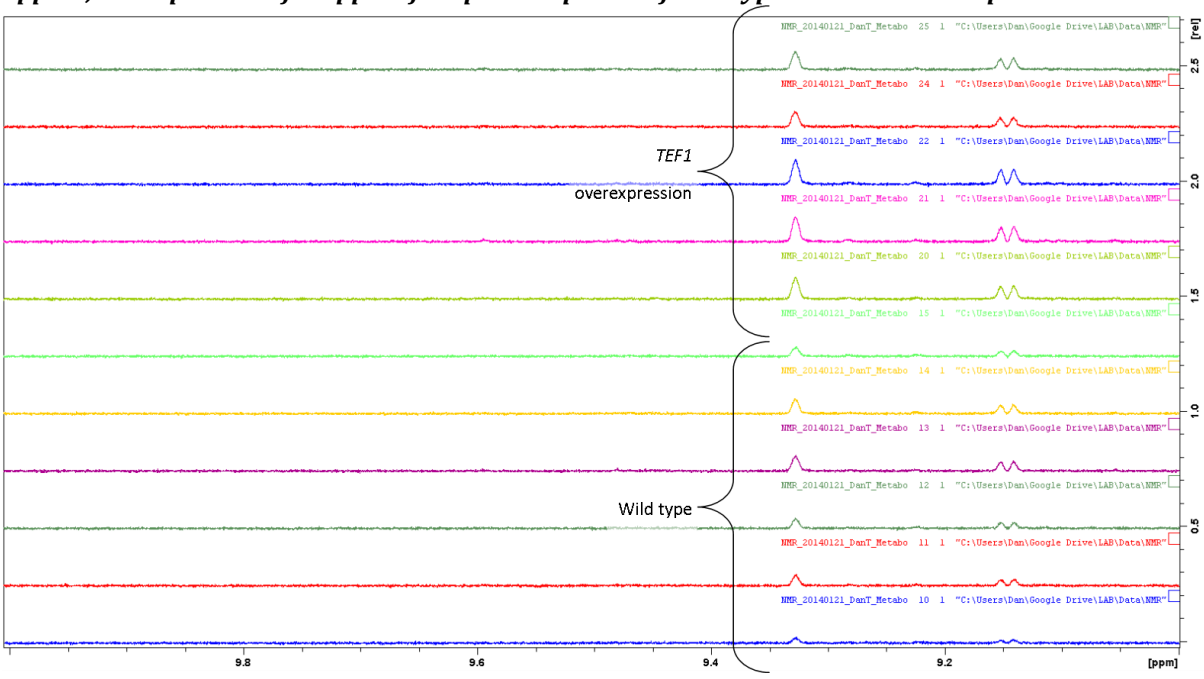


***App.4-j, A comparison of 9-10ppm of 1D proton spectra of wild type and TEF1 overexpression cells.***

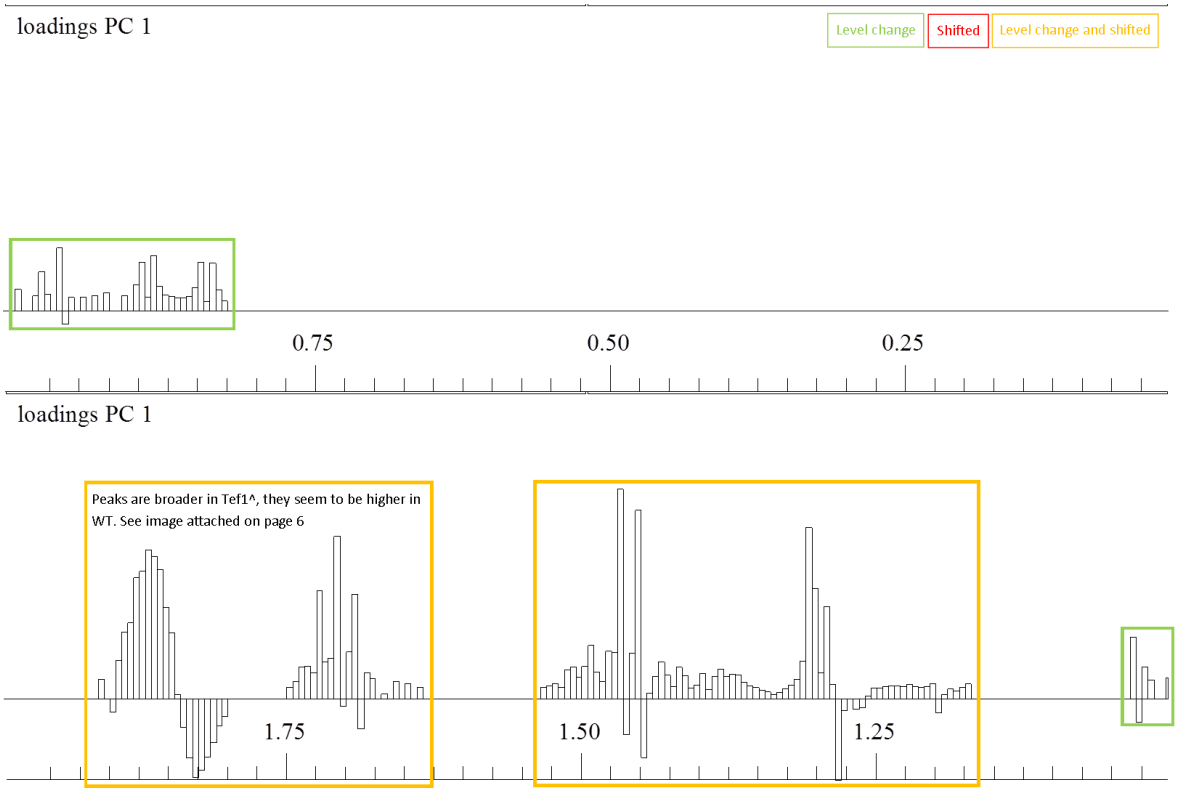


***App.5-a, Loading difference of 0-2ppm of wild type and TEF1 overexpression cells.***

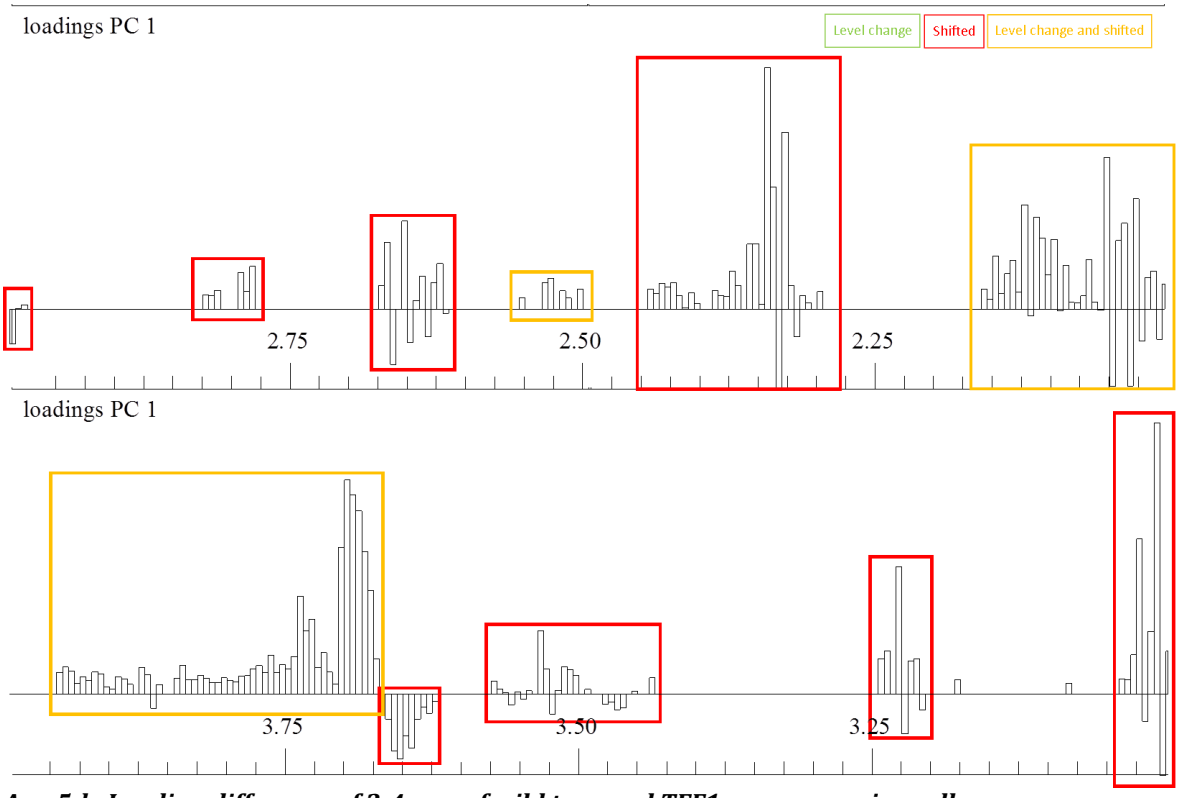


***App.5-b, Loading difference of 2-4ppm of wild type and TEF1 overexpression cells.***

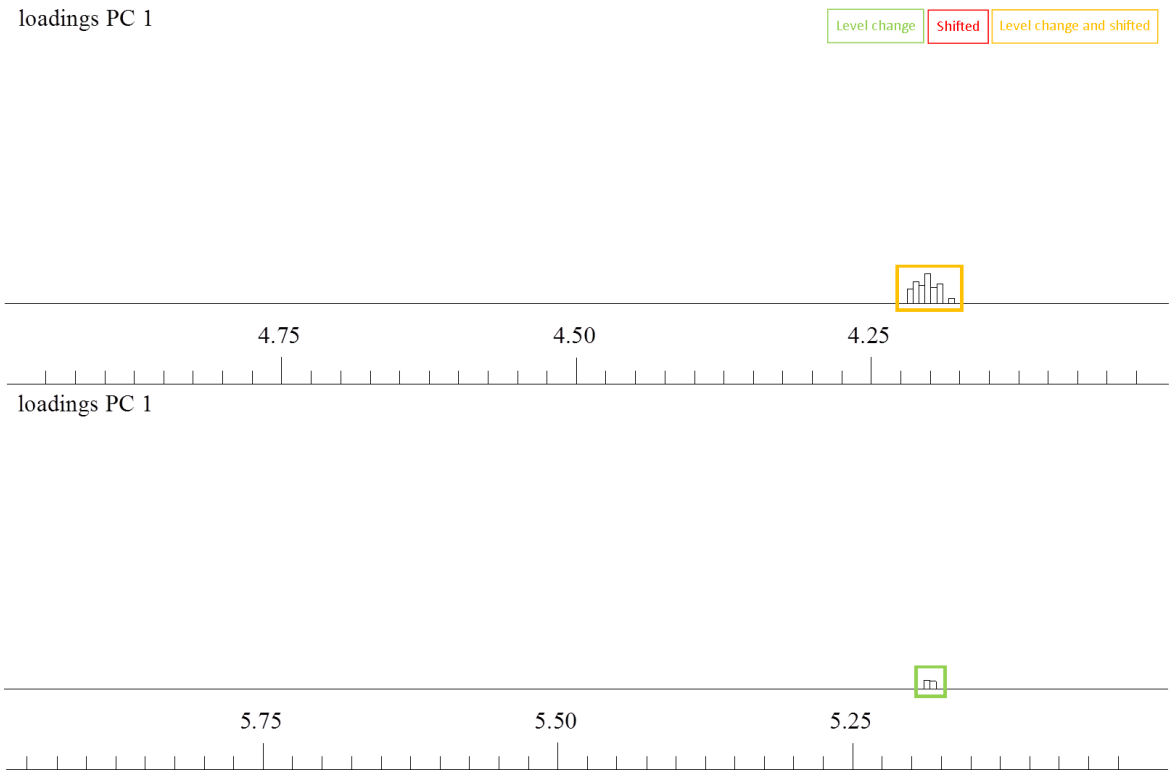


***App.5-c, Loading difference of 4-6ppm of wild type and TEF1 overexpression cells.***

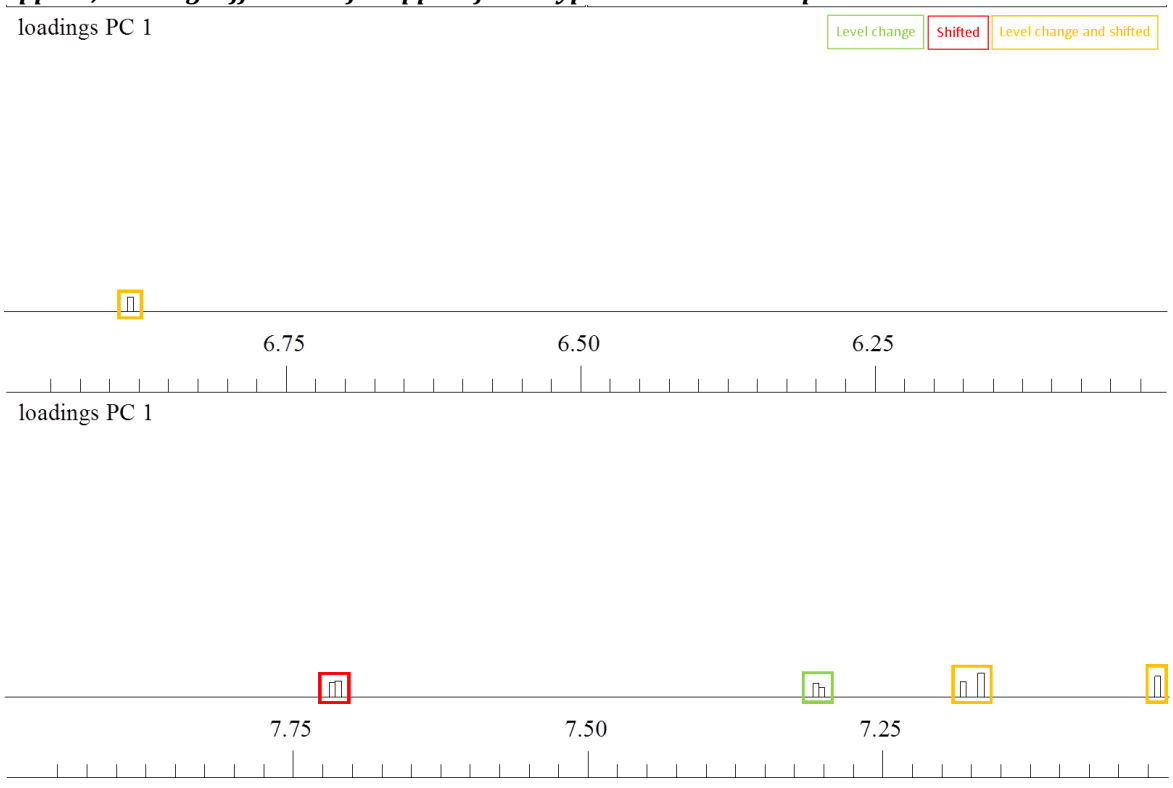


***App.5-d, Loading difference of 6-8ppm of wild type and TEF1 overexpression cells.***

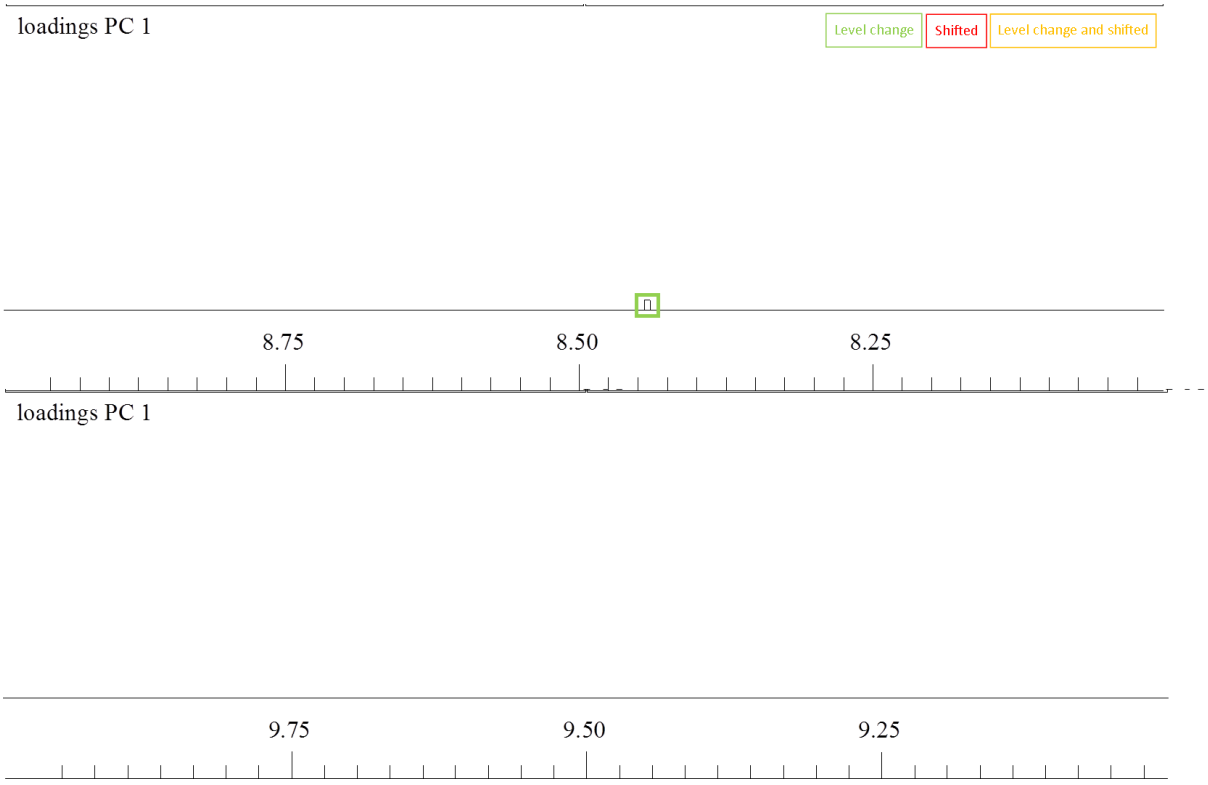


***App.5-e, Loading difference of 8-10ppm of wild type and TEF1 overexpression cells.***

| Asparagine | Methionine |
|---|---|
| Citrate | Nicotinamide |
| Cysteine | Phenylalanine |
| Glucose | Proline |
| Glutamine | Pyruvate |
| Histidine | Serine |
| Inosine | Uracil |
| Lactate | |

***App.6,List of 15 tentative assignments from metabolite analysis***

| | | | | | |
|---|---|---|---|---|---|
| 3-hydroxybutyrate | Acetate | Alanine | Arginine | Asparagine | Aspartate |
| ATP | cAMP | Choline chloride | Citric acid | Creatine | Creatinine |
| Cysteine | Dihydroxyacetone | Fructose-6-phosphate | Glucose | Glucose-6-phosphate | Glutamate |
| Glutamine | Glycine | GMP | Histidine | Isocitrate | Isoleucine |
| Leucine | Lysine | Malic acid | Maltose | Mannose | Methionine |
| NAD | NADH | NADPH | Oxaloacetic acid | Phenylalanine | Phosphoenolpyruvate |
| Proline | Serine | Succinate | Succinyl CoA | Sucrose | Threonine |
| Tryptophan | Tyrosine | UDP GlcNAC | Valine | A-ketoglutarate | |

***App.7, list of 47 compounds available in our metabolite database***

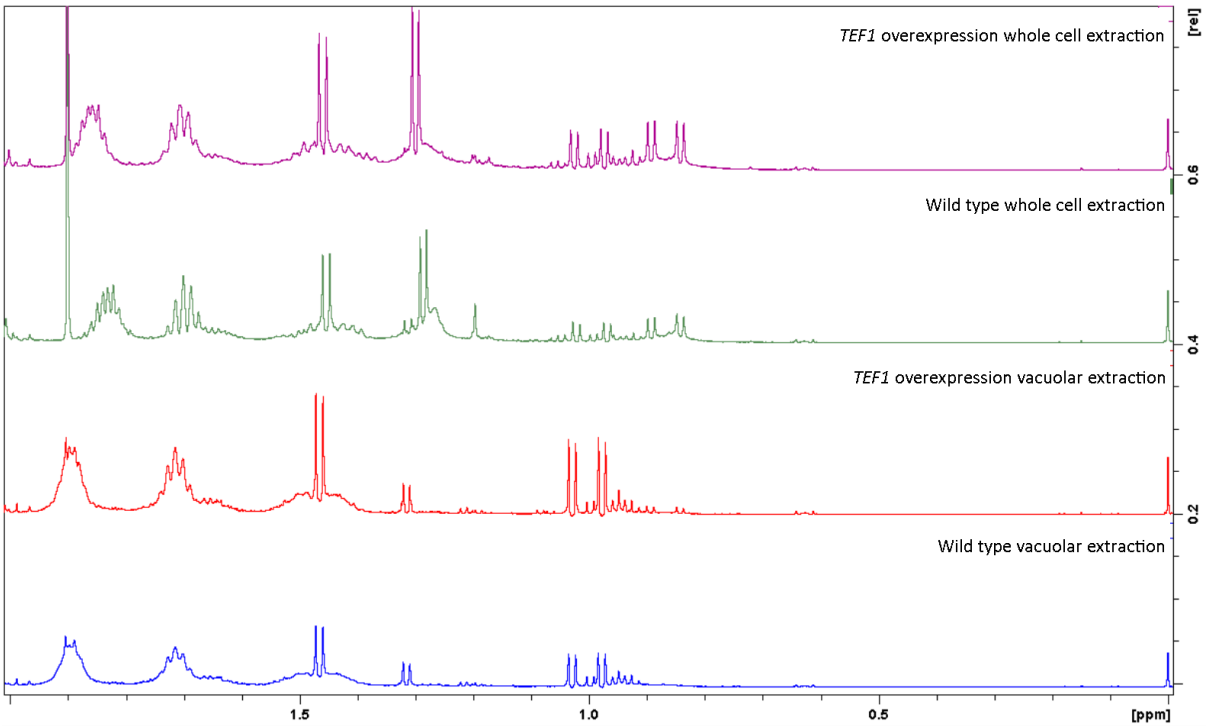


***App.8-a, Comparison of 0-2ppm of whole cell and vacuolar metabolite extractions***

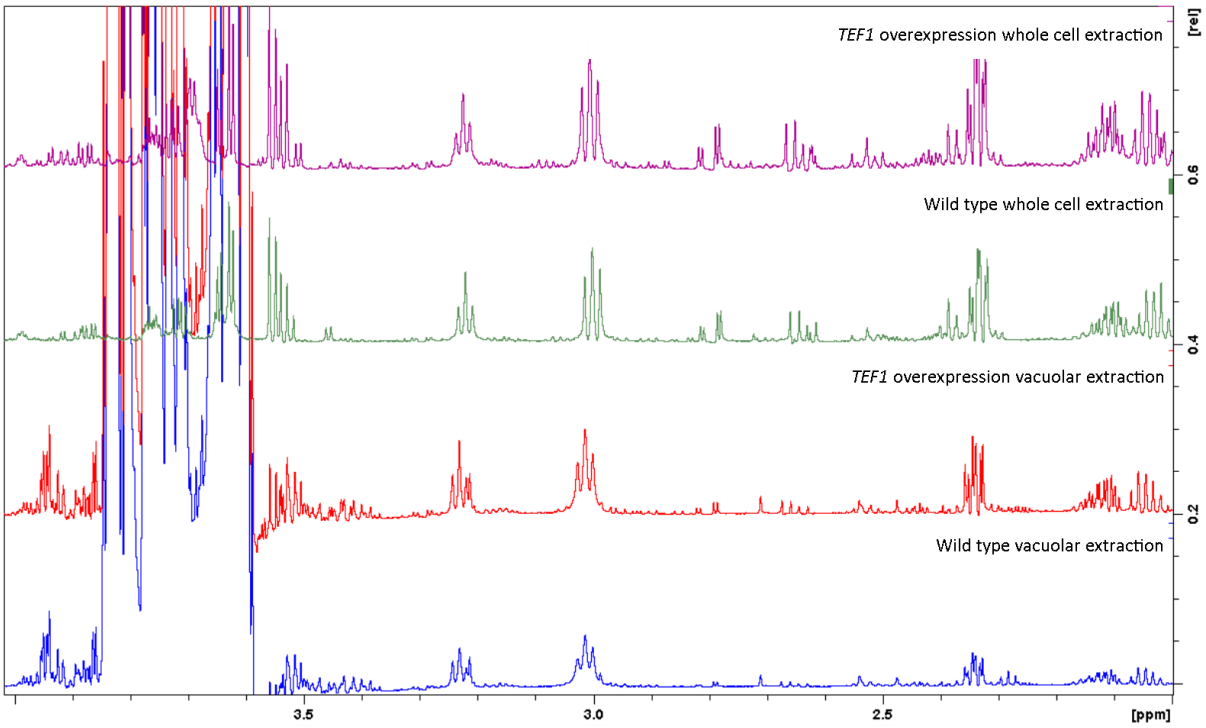


***App.8-b, Comparison of 2-4ppm of whole cell and vacuolar metabolite extractions***

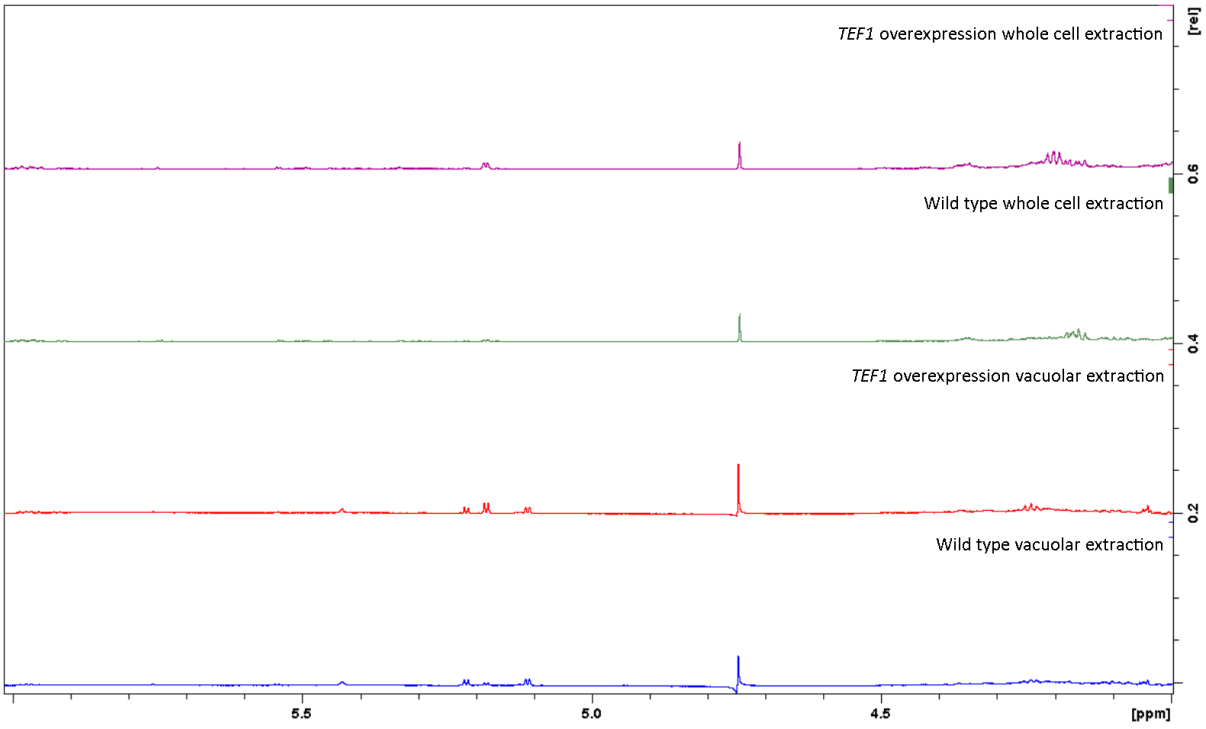


***App.8-c, Comparison of 4-6ppm of whole cell and vacuolar metabolite extractions***

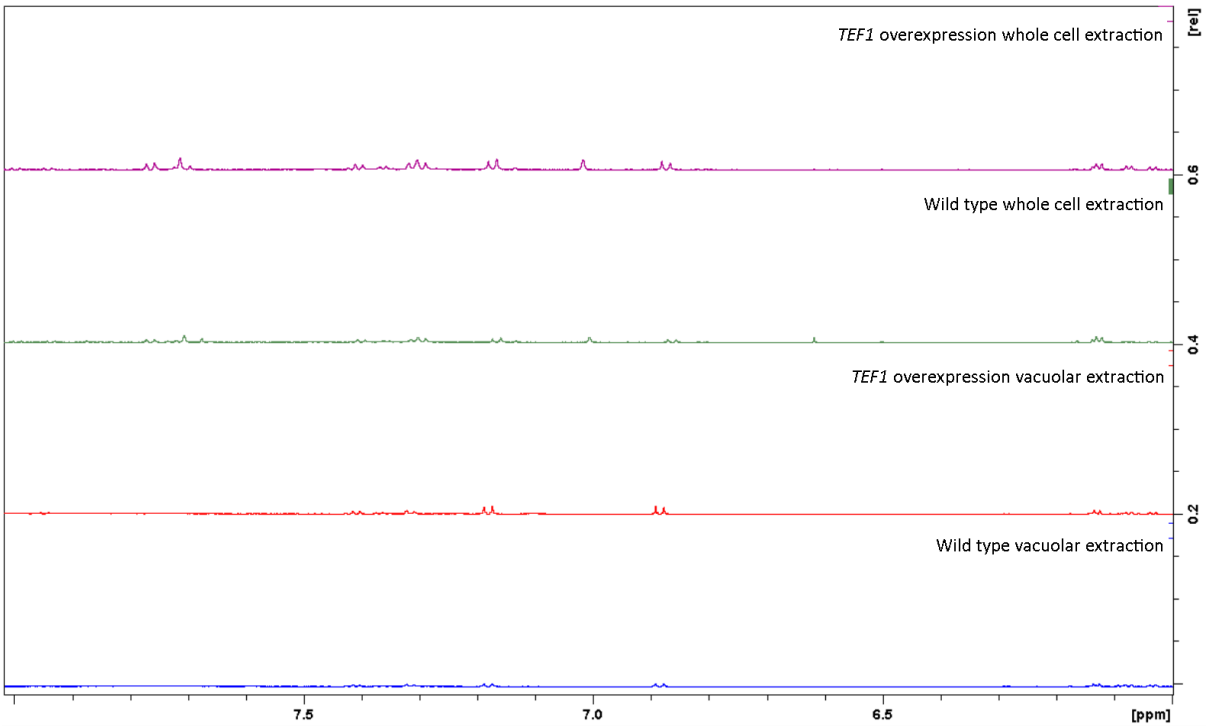


***App.8-d, Comparison of 6-8ppm of whole cell and vacuolar metabolite extractions***

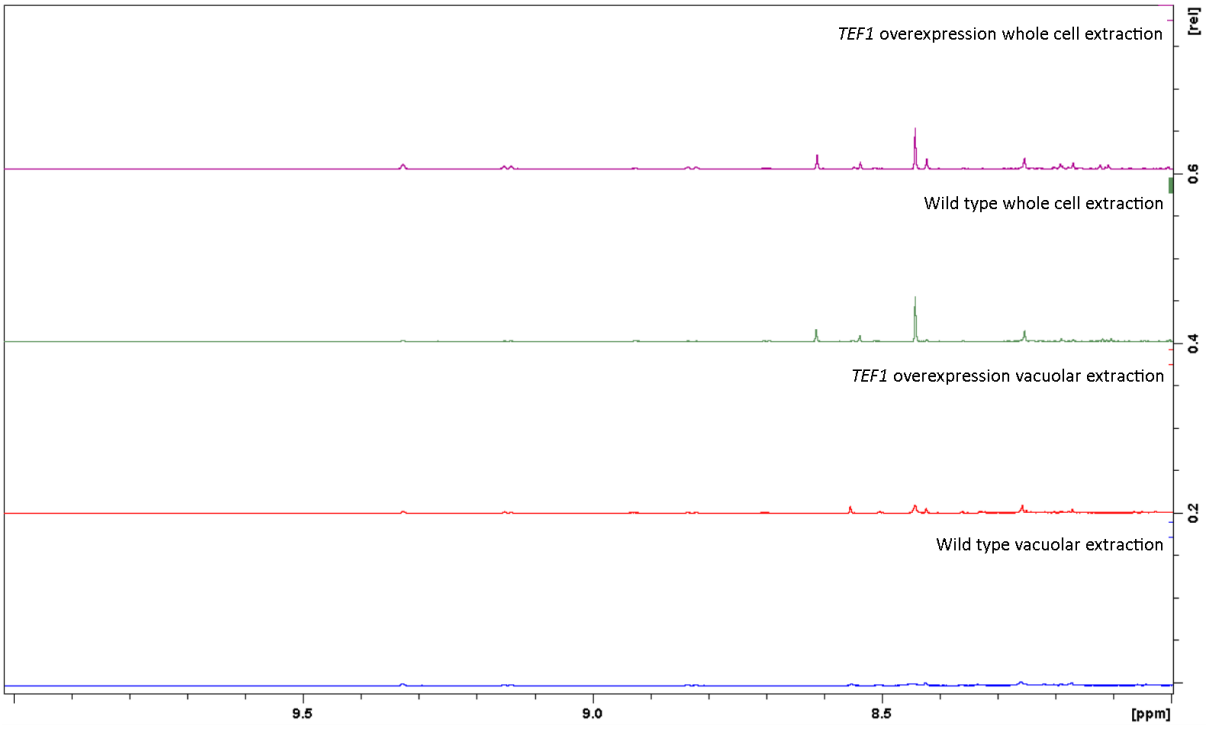


***App.8-e, Comparison of 8-10ppm of whole cell and vacuolar metabolite extractions***